



Life Utilization Criteria Identification in Design (LUCID)

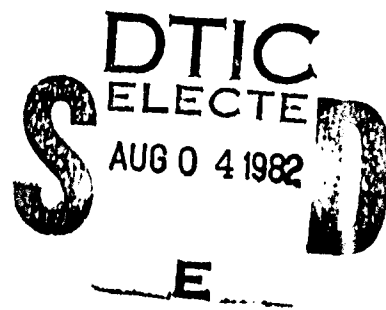
Detroit Diesel Allison
Division of General Motors
P. O. Box 894
Indianapolis, Indiana 46206

June 1982

Final Report for Period September 1978 to December 1981

Approved for public release
Distribution unlimited

Aero Propulsion Laboratory
Air Force Wright Aeronautical Laboratories
Air Force Systems Command
Wright-Patterson Air Force Base, Ohio 45433



AD A 117807

DTIC FILE COPY

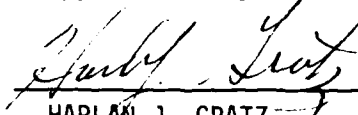
When Government drawings, specifications, or other data are used for any purpose other than in connection with a definitely related Government procurement operation, the United States Government thereby incurs no responsibility nor any obligation whatsoever; and the fact that the government may have formulated, furnished, or in any way supplied the said drawings, specifications, or other data, is not to be regarded by implication or otherwise as in any manner licensing the holder or any other person or corporation, or conveying any rights or permission to manufacture use, or sell any patented invention that may in any way be related thereto.

This report has been reviewed by the Office of Public Affairs (ASD/PA) and is releasable to the National Technical Information Service (NTIS). At NTIS, it will be available to the general public, including foreign nations.

This technical report has been reviewed and is approved for publication.



MARK D. REITZ
Project Engineer



HARLAN J. GRATZ
Tech Area Manager

FOR THE COMMANDER



JACK RICHENS
Acting Director
Turbine Engine Division

"If your address has changed, if you wish to be removed from our mailing list, or if the addressee is no longer employed by your organization please notify AFWAL/POTA W-PAFB, OH 45433 to help us maintain a current mailing list".

Copies of this report should not be returned unless return is required by security considerations, contractual obligations, or notice on a specific document.

Unclassified

SECURITY CLASSIFICATION OF THIS PAGE (When Data Entered)

REPORT DOCUMENTATION PAGE		READ INSTRUCTIONS BEFORE COMPLETING FORM
1. REPORT NUMBER AFWAL-TR-82-2039	2. GOVT ACCESSION NO. AD-A117867	3. RECIPIENT'S CATALOG NUMBER
4. TITLE (and Subtitle) Life Utilization Criteria Identification in Design (LUCID) Final Report		5. TYPE OF REPORT & PERIOD COVERED Final report September 1978-December 1981
		6. PERFORMING ORG. REPORT NUMBER EDR 10982
7. AUTHOR(s) J. E. Holmes		8. CONTRACT OR GRANT NUMBER(s) F33615-78-C-2072
9. PERFORMING ORGANIZATION NAME AND ADDRESS Detroit Diesel Allison P. O. Box 894 Indianapolis, Indiana 46206		10. PROGRAM ELEMENT, PROJECT, TASK AREA & WORK UNIT NUMBERS 30661138
11. CONTROLLING OFFICE NAME AND ADDRESS Aero Propulsion Laboratory (AFWAL/POTA) Wright-Patterson AFB, Ohio 45433		12. REPORT DATE June 1982
		13. NUMBER OF PAGES 150
14. MONITORING AGENCY NAME & ADDRESS (if different from Controlling Office) Air Force Wright Aeronautical Laboratories		15. SECURITY CLASS. (of this report) Unclassified
		15a. DECLASSIFICATION DOWNGRADING SCHEDULE
16. DISTRIBUTION STATEMENT (of this Report) Approved for public release, distribution unlimited		
17. DISTRIBUTION STATEMENT (of the abstract entered in Block 20, if different from Report)		
18. SUPPLEMENTARY NOTES		
19. KEY WORDS (Continue on reverse side if necessary and identify by block number) Engine utilization prediction Structural life prediction Conceptual design selection		
20. ABSTRACT (Continue on reverse side if necessary and identify by block number) LUCID has developed and demonstrated the capability to predict realistic engine usage during the conceptual design phase of a gas turbine design cycle. A method has also been developed and demonstrated to include life and usage considerations as well as performance aspects in the process of selecting the optimal engine and aircraft definitions for an advanced military high performance application. This process also defines usage and life data for subsequent design and development efforts on the selected engine. These LUCID techniques (cont)		

Unclassified

SECURITY CLASSIFICATION OF THIS PAGE (When Data Entered)

20. ABSTRACT (cont)

allow trade-offs of engine life and performance parameters to be identified.

Unclassified

SECURITY CLASSIFICATION OF THIS PAGE (When Data Entered)

FOREWORD

This final report was produced in accordance with Life Utilization Criteria Identification in Design Contract No. F33615-78-C-2072, under the direction of Mr. Mark D. Reitz, POTA of the Air Force Wright Aeronautical Laboratories, Aero Propulsion Laboratory. It presents the work conducted by Detroit Diesel Allison Division (DDA) of General Motors Corporation and Boeing Military Aircraft Company as a subcontractor. Created in accordance with Sequence 7 of Attachment No. 1, Contract Data Requirements List (Form 1423) of the contract, the work under the contract was performed under Jim Holmes and Jack Gill of DDA and Steve Kyle and Larry Winslow of Boeing.

TABLE OF CONTENTS

<u>Section</u>	<u>Title</u>	<u>Page</u>
	Summary	1
I	Introduction	3
II	Task 3.1.1--Life Capability/Installed Life Model Development .	5
III	Task 3.1.2--Mission/Performance Definition	35
IV	Task 3.1.3--Utilization Prediction Procedure Development . . .	51
V	Task 3.1.4--Engine/Aircraft Initial Screening.	67
VI	Task 3.1.5--Region of Interest Development	81
VII	Task 3.1.6--Vane/TLCF Sensitivity Study	95
VIII	Task 3.2.1--Effects of Life Capability	103
IX	Task 3.2.2--Reference Utilization Procedure.	113
X	Task 3.2.3--Define Reference Aircraft Utilization and Sensitivities.	117
XI	Task 3.2.4--Engine Component Life Capability	119
XII	Task 3.2.5--System Performance Sensitivity	131
XIII	Task 3.2.6--Engine and Aircraft Design Selection	143
XIV	Task 3.2.8--Data and Data Format Definition.	145
XV	Conclusions and Recommendations.	149



Accession For	
NTIS GRA&I	<input checked="" type="checkbox"/>
DTIC TAB	<input type="checkbox"/>
Unannounced	<input type="checkbox"/>
Justification	
By _____	
Distribution/ _____	
Availability Codes	
Dist	Avail and/or Special
A	

LIST OF ILLUSTRATIONS

<u>Figure</u>	<u>Title</u>	<u>Page</u>
1	Mechanical LCF sensitivity to life capability levels.	6
2	Logic used to determine installed life of components subject to mechanically induced LCF.	8
3	Airfoil stress rupture/LCF model methodology.	10
4	Initial cycle radial stress comparison at midfoil section--one-dimensional thermal stress/strain analysis versus three-dimensional plate finite element analysis	12
5	Go-and-go endurance test cycle.	13
6	Accelerated mission test cycle.	14
7	Reference analytical cycle used in severity index calculation .	15
8	TF41 HPT-1 vane comparison of predicted and test installed life for leading-edge transverse cracks.	16
9	TF41 HPT-1 cast blade comparison of calculated installed life and test results in post region	17
10	TF41 HPT-2 blade--comparison of calculated installed life and test results.	17
11	TF41 HPT-1 disk bore calculated reference life capability compared with test results.	18
12	Turbine airfoil LCF model methodology	19
13	Strain regression data base	20
14	Turbine airfoil temperature gradient definitions.	21
15	Blade strain regression equation form	21
16	Vane strain regression equation form.	22
17	Blade regression critical locations	22
18	Vane regression critical locations.	23
19	Turbine blade life capability comparison.	26
20	Turbine blade installed life prediction comparison.	27
21	Turbine blade relative installed life prediction comparison .	28
22	Turbine vane life capability comparison	29
23	Turbine vane installed life prediction comparison	30
24	Turbine vane relative installed life prediction comparison. .	31
25	Turbine blade stress rupture model methodology.	32
26	HPC-1 wheel MLCF damage map	32
27	Combustor case MLCF damage map.	33
28	HPT-1 wheel MLCF damage map	33
29	Base-line HPT-1 blade thermal LCF critical locations.	34
30	Base-line HPT-1 vane critical locations	34
31	Model 987-354 aircraft general arrangement.	37
32	LUCID design mission definition	39
33	Stick mission aircraft utilization--subsonic weapons delivery/initial training.	43
34	Stick mission aircraft utilization--air combat/initial training.	44
35	Stick mission aircraft utilization--supersonic weapons delivery/initial training	45
36	Stick mission aircraft utilization--navigation/familiarization/initial training.	46
37	Stick mission aircraft utilization--subsonic weapons delivery/proficiency training.	47
38	Stick mission aircraft utilization--air combat/proficiency training.	48

<u>Figure</u>	<u>Title</u>	<u>Page</u>
39	Stick mission aircraft utilization--supersonic weapons delivery/proficiency training	49
40	Stick mission aircraft utilization--navigation/familiarization/ proficiency training.	50
41	Utilization prediction procedure.	51
42	Dynamic usage procedure	54
43	Example of editing A-7 IECMS data	55
44	Example of filtering A-7 IECMS data	56
45	Parameter tolerance for F-14 approach	58
46	Raw flight PLA comparison to PSD-generated PLA.	59
47	Wing cruise PSD buildup	61
48	Approach/GCA PSD representation	62
49	Mission usage definition.	64
50	Sample dynamic overlay for subsonic weapons delivery/proficiency training mission.	65
51	Preliminary engine general arrangement.	69
52	Wing parametric planform variation for LUCID model 987-354. . .	71
53	Optimum system definition for supersonic cruise Mach number variations for 550-nmi mission radius	73
54	Impact of constraints with supersonic cruise Mach number. . . .	74
55	Performance data trends with supersonic cruise Mach number. . .	75
56	Initial LUCID screening--OPR and Mach number carpet plot. . . .	76
57	Initial LUCID screening--OPR and RIT carpet plot.	77
58	Initial LUCID screening--OPR and THETAB carpet plot	77
59	Initial LUCID screening--T/W and W/S carpet plot.	78
60	Independent variable sensitivity for constrained 2.2 M_N optimum design.	78
61	Independent variable sensitivity for constrained 2.2 M_N optimum design.	79
62	Independent variable sensitivity for constrained 1.6 M_N optimum design.	79
63	Initial screening--aspect ratio (AR15)-wing loading (W/S) relationship.	80
64	ROI data cases.	82
65	ROI engine data altitude/Mach matrix.	83
66	ROI minimum airplane size trends with engine cycle variables. .	85
67	ROI data set optimization for minimum TOGW.	86
68	ROI data set optimization for minimum TOGW.	86
69	Time history--subsonic weapons delivery/proficiency training mission	87
70	Time history--air combat/proficiency training mission	88
71	Time history--supersonic weapons delivery/proficiency training mission	89
72	Time history--navigation/familiarization/proficiency training mission	90
73	Time history--subsonic weapons delivery/initial training mission	91
74	Time history--air combat/initial training mission	92
75	Time history--supersonic weapons delivery/initial training mission	93
76	Time history--navigation/familiarization/initial training mission	94

<u>Figure</u>	<u>Title</u>	<u>Page</u>
77	Vane heat transfer design point	96
78	Case 34 installed life trends for HPT-1 vane.	98
79	Case 35 installed life trends for HPT-1 vane.	99
80	Heat transfer mechanisms.	100
81	Axial channel region section.	100
82	Surface temperatures in suction surface channel region.	101
83	Surface temperatures in pressure surface channel region	101
84	Engine characteristic adjustment.	104
85	BA54 compressor rotor optimization model.	105
86	Compressor rotor weight trends.	106
87	HP compressor rotor weight effect with changing LCF requirements.	107
88	Burner/diffuser outer case.	107
89	Turbine weight estimation	108
90	HP turbine wheel effects on engine weight of changing LCF requirements.	108
91	HPT-1 blade effects on engine weight of changing stress rupture requirements.	110
92	Rotor airfoils: Cooling flow trends with metal temperature change.	110
93	Vane airfoils: Cooling flow trends with metal temperature change.	111
94	Basic F-4 training requirements.	114
95	Sample F-4 training details	115
96	Current TAC aircraft usage summary.	116
97	Training mission mix for reference aircraft utilization	118
98	Wartime mission sensitivity to engine weight and SFC--Configuration 34	118
99	Severity index reference cycles	120
100	HPT-1 blade nominal designs	124
101	HP compressor severity index regressions.	132
102	Combustor case severity index regressions	133
103	HPT wheel severity index regressions.	133
104	HPT blade severity index regressions.	134
105	Blade failure mode severity index regressions	134
106	HPT vane severity index regressions	135
107	Comparison of predicted versus actual severity index levels	136
108	Engine component life consumption versus training mission-- OPR=9, RIT=3000°F	137
109	Engine component life consumption versus training mission-- OPR=15, RIT=3000°F.	138
110	Engine component life consumption versus training mission-- OPR=15, RIT=3400°F.	139
111	ROI mission performance regressions	139
112	ROI engine cycle impact on TOGW	140
113	Comparison of optimum THETAB.	140
114	Minimum TOGW versus engine OPR and RIT.	141
115	Regression of engine life parameters.	141

LIST OF TABLES

<u>Table</u>	<u>Title</u>	<u>Page</u>
1	Parts examined for the LUCID program and associated failure mechanisms	6
2	TF41 failure mode analysis verification.	13
3	Turbine airfoil TLCF strain regression accuracy.	23
4	Effect of creep relaxation on installed life prediction for turbine airfoils	23
5	Engine definitions	24
6	Turbine blade stress rupture/TLCF life capability summary.	25
7	Turbine vane TLCF life capability summary.	26
8	Simplified model versus original model without creep turbine airfoil stress rupture	27
9	Component materials.	29
10	Steady-state mission segment buildup for design (combat) mission.	36
11	Design mission performance constraints.	36
12	Current TAC training buildup (Syllabus).	41
13	Flight data segment breakdown.	57
14	Wing cruise segment validation comparison.	63
15	Approach/GCA segment validation comparison	63
16	Dependent variable regression accuracy for initial screening	71
17	Initial screening unconstrained optimal system definitions	72
18	Initial screening constrained optimal system definitions	72
19	ROI dependent variable regression (R^2) statistic	83
20	Range of ROI variables	84
21	DDA-defined engine utilization parameters for LUCID.	85
22	Vane local strain regression accuracy.	97
23	Combustor case thickness changes with LCF requirements	106
24	Turbine cycle definitions.	109
25	PD422 parametric deck life index inputs.	111
26	Installed life goals	119
27	HPC-1, HPT-1 wheel/MLCF results.	121
28	Severity index summary HPC-1 wheel/MLCF.	121
29	Severity index summary HPT-1 wheel/MLCF.	122
30	Severity index summary combustor case/MLCF	123
31	Combustor case ΔP -case 34 (9/3400/1.18).	123
32	HPT-1 blade/TLCF + SR results.	125
33	Severity index summary HPT-1 blade/combined TLCF + SR.	126
34	HPT-1 blade failure mode ratio summary	127
35	HPT-1 vane/TLCF results.	128
36	Severity index summary HPT-1 vane/TLCF	128
37	PD422 parametric deck input summary for consistent installed life level	129

SUMMARY

The Life Utilization Criteria Identification in Design (LUCID) program was structured in two phases. Phase I involved the technique development and data base generation; Phase II applied the techniques to an advanced tactical fighter for the 1990s.

In Phase I, Detroit Diesel Allison (DDA) has adapted existing models to use in predicting engine characteristics (performance, weight, and dimensions) for life capability variations. In addition, component/failure mode analysis models have been developed to predict life capability and installed life levels for key components in a dry, variable geometry turbojet. These models have been verified with TF41 experience. Boeing has developed a process to predict aircraft utilization for an advanced tactical fighter based on realistic mission and pilot throttle movement definitions. These definitions resulted from observation of current USAF training procedures and from analysis of existing data from continuously recorded flights on current combat aircraft in the field.

During Phase I, an initial screening of a family of aircraft and engines for an advanced tactical fighter was performed. A smaller region of interest (ROI) was defined resulting from this initial screening.

Phase II focused on the aircraft and engines within this ROI to address the impact of utilization with a consistent installed life definition for the engines. During Phase II, a reference utilization was adopted for an advanced tactical fighter. Seventeen engine/aircraft systems were examined for this reference utilization, and life capability requirements were determined to address a consistent set of installed life goals. Representative engine characteristic trends with changing life capability levels were generated in the form of sensitivity data. The sensitivity data were used to redefine each engine's characteristic in the ROI. Airplanes were then resized with the revised engine characteristics. The effect of a consistent life assessment did influence the selection of the optimal engine/aircraft system definition as well as increase the figure of merit (aircraft takeoff gross weight--TOGW) by 3%. In addition for the optimal system, both realistic utilization data and life capability requirements were defined.

A discussion of the type of data and its format has been prepared for LUCID application to enable the USAF to consider engine structural life as well as system performance for future studies of military applications. This is especially important for aircraft where a wide diversity of utilizations is anticipated.

The following recommendations for potential follow-on programs are appropriate for conceptual engine design incorporating utilization and life capability considerations. These represent expansions of the basic LUCID approach.

- o Update turbine airfoil/thermal low cycle fatigue (TLCF) models with revised methodology for Lamilly currently under development
- o Increase number of indicator components examined at preliminary design level (i.e., combustor liner/TLCF)

- o Expand turbine airfoil/TLCF model input to cover designs with different cooling schemes
- o Expand aircraft utilization prediction capability via review and analysis of continuously recorded engine data from Project Red Flag exercises
- o Examine impact of new engine technology on critical components with varying life capability
- o Assess impact of reference mission selection (least damaging or most damaging) on optimal engine/aircraft definition
- o Expand region-of-interest to address an aircraft parameter (such as thrust loading) and assess impact of engine life and utilization on optimal airplane/engine definition
- o Assess sensitivity of an engine/airframe definition to types of changes typically encountered during a development program (such as aircraft weight growth requiring higher steady-state power settings)

I. INTRODUCTION

This report covers the work done by Detroit Diesel Allison (DDA) and Boeing Military Aircraft Company during the Life Utilization Criteria Identification in Design (LUCID) contract under USAF funding. This effort began in September 1978 and continued through December 1981. The objective of this contract was to develop and demonstrate a technique for determining the impact of realistic vehicle usage on optimum system selection while taking into consideration a consistent engine installed life definition. This allows tradeoffs of performance and life goals during conceptual design and the definition of realistic, usage-dependent structural design requirements for initiation of engine detail design. Boeing, as a subcontractor for this contract, has performed aircraft conceptual design studies and predicted training mission utilization data.

In the conceptual design phase, an engine designer does not know how his engine will be used when it reaches the field. LUCID attempts to utilize the training experience of current military aircraft in projecting usage for conceptual design where the designer has the most flexibility to address it. For similar type aircraft, confidence is fairly high in predicting representative usage data. For cases where no similar aircraft are involved, confidence in usage syntheses is not as high. Only where there exists some insight into training objectives and functions can usage be reasonably well predicted.

Throttle movements during a flight are as important as mission type and frequency. Interpreting continuously recorded engine flight data can be very difficult, and pilot debriefings are very helpful in data interpretation. By reviewing data of this type, insight can be gained into various maneuvers and formations with their attendant throttle movements. This insight is invaluable when projecting usage for a new airplane.

LUCID employed usage projections in the conceptual design process of selecting the optimum engine and aircraft definition to perform a given task. In an iterative sequence, each engine and aircraft was addressed individually. Engine design was tailored to specific usage-dependent structural design criteria. After each engine design had been altered to address its usage, the aircraft were resized; and the resulting data provided the basis for selecting a system with minimum aircraft takeoff gross weight. Thus, each engine reflected a design that incorporated a consistent installed life (for a reference usage), and the system selection was examined to observe whether the optimal engine/aircraft definition was affected by this life/usage bias.

Models have been developed and verified that predict life capability/installed life consistent with conceptual design level of information. Components and their respective failure modes have been selected to indicate what life capability levels are sufficient to address installed life goals. Based on these indications, techniques have been devised to tailor the entire gas turbine design for differences in usage-dependent requirements (specifically low cycle fatigue and stress rupture).

During Phase I, the LUCID techniques were defined and developed using new and existing computer models where appropriate. During the last part of Phase I, a data base of aircraft and engines was created with which to begin Phase II. For Phase II, these techniques were applied to an advanced tactical fighter aircraft powered by dry, variable geometry turbojets for a 1995 initial operating capability (IOC). Aircraft takeoff gross weight (TOGW) served as the figure of merit for these evaluations.

This report is organized according to the program structure. Each task is discussed individually.

II. TASK 3.1.1--LIFE CAPABILITY/INSTALLED LIFE MODEL DEVELOPMENT

DDA has developed and verified with TF41 experience simplified component/failure mode models for some of the important components in a dry, variable geometry turbojet. These models were used in Phase II to determine life capability requirements to achieve component installed life goals for a given utilization. In addition, the models were used to compute relative life consumption rates (severity indexes) for each individual training mission relative to a time history chosen for reference purposes, i.e., an engine start/ stop cycle at sea level static (SLS). Thus, severity indexes are a measure of relative mission severity for that component and failure mode.

The installed life model methodology requires definition of the component material's properties, life capability level (stress, operating temperature, etc.), and a procedure to determine stress/metal temperature for different operating conditions. Damage is assessed for each mission time segment for stress rupture or pertinent cycle for low cycle fatigue (LCF) and is accumulated using Miner's rule for the entire mission. For a given mission, the component life consumption rates vary with life capability. An example of this trend is shown in Figure 1 for a typical turbine wheel/LCF for a usage representative of current engine trim pad operation. For this case, increasing LCF life capability by lowering the peak bore stress decreases the life consumption rate for a given utilization. This trend is acknowledged when determining life capability requirements for a desired installed life level over a given utilization.

A dry, variable turbine geometry turbojet contains many structural members. Mechanical design criteria include yield/burst, stiffness, high cycle fatigue (HCF), oxidation/erosion, creep/rupture, and LCF requirements for structural integrity for engine operation over the flight/maneuvering envelope. Generally, the last three criteria are utilization dependent. The components selected for evaluation in LUCID fall into one of three categories: 1) safety critical items--items that are not contained, the loss of which would lead to engine failure and possible aircraft loss; 2) short-lived engine components--hot section components whose life capability, experience has shown, determine the time between overhaul; and 3) parts that are critical in defining size and weight of the engine and associated performance and for which a later redesign might cause a performance or weight penalty.

Safety critical components may be standard rotating components, such as compressor or turbine rotors, or, as in current lightweight high-performance engines, such as the F100, components such as high-pressure engine cases. These high-pressure engine cases can fail rapidly, after initial fatigue cracking, and rupture fuel lines. Explosions result that will destroy even multiple engine aircraft.

Short-lived engine parts, such as turbine blades or vanes, determine the engine time between overhauls (TBO). If the TBO can be extended, the weapon system will enjoy greater availability and the cost of engine maintenance will be reduced because of reduction in parts usage and reduction in costly tear-downs.

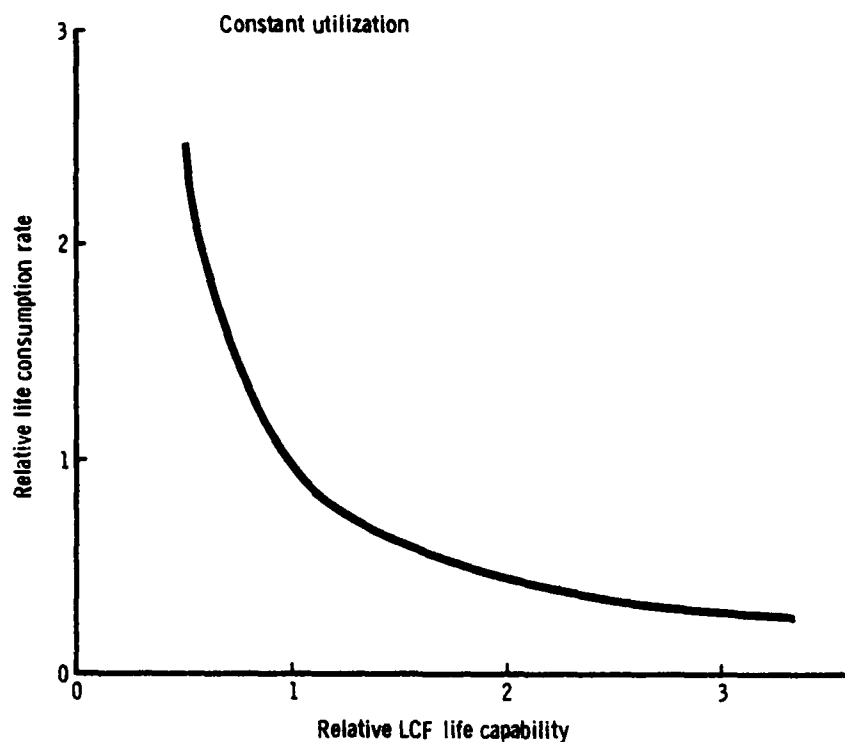


Figure 1. Mechanical LCF sensitivity to life capability levels.

On the other hand, substantial weight or performance penalties would be imposed upon an engine if large and heavy rotating components, such as turbine disks, require redesign during engine development or production phases. Upon examining potential engine components, it is quickly obvious that in the preliminary design phase only a few critical (or representative) parts can be examined. The parts chosen are those that experience has shown are most critical and are generally representative for a component. The parts and the failure modes assessed in this effort are shown in Table 1.

Table 1.
Parts examined for the LUCID program and associated failure mechanisms.

<u>Component</u>	<u>Part</u>	<u>Failure mechanism and location</u>
Turbine rotor	First-stage turbine wheel	Mechanical LCF at bore stress rupture/ thermal fatigue at meanline section
	First-stage turbine blade	
Turbine vane	First-stage turbine vane	Thermal fatigue at meanline section
Compressor rotor	First-stage compressor wheel	Mechanical LCF at bore
Combustor case	Combustor case	Mechanical LCF at weld

After determination of the parts to be considered, definition of the most sensitive locations to a particular failure mode follows.

The failure mode and locations must satisfy the following criteria: 1) the location should be in an area that experience and analysis have indicated is a candidate for failure--a turbine blade meanline section, for example, where the hottest gas and metal temperatures typically exist; 2) the location must be in an area well enough defined in the preliminary design phase to render the analysis accurate; and, finally, 3) locations should be examined where failures could be catastrophic in nature and/or require extensive engine redesign to correct with attendant weight/performance penalties. One such area is a wheel bore. The locations to be considered for each of the components are also found in Table 1.

The criteria for the selection of failure modes are not difficult to define. First, the failure mode must be significant in limiting the life of the part analyzed, and, second, it must be amenable to analysis in the preliminary design phase. Failure modes that normally would not be detected until late in engine model development testing must be addressed. This is easily illustrated with the following examples.

a. Experience with turbine wheels, as in the TF41 engine, has shown that mechanically induced LCF may cause cracking at the drive flange holes or in wheel lugs that attach the blades to the disk. Yet this type of failure is readily detected during the detailed design analysis phase and eliminated prior to engine development testing, and subsequent redesign would rarely result in a severe weight penalty. Moreover, during preliminary design, the geometry is rarely well enough defined for these areas to be analyzed in sufficient detail. However, a mechanically and/or thermally induced LCF failure in a wheel bore would be a catastrophic failure requiring significant increases in wheel size and weight to eliminate the problem. These increases in weight would require increasing the size of the static structure, and the result would be a reduction in the thrust-to-weight of the engine.

b. All blades and vanes are subject to HCF failures induced by excessive vibratory excitation. These failures are not yet completely amenable to analysis in the preliminary design phase. (The magnitude of excitation cannot be calculated.) While known responsive excitations are avoided in the earliest design phases, a few hours of diagnostic or development testing would detect these potential failures. Small changes in blade geometry with little impact to stage weight normally eliminate the resonance.

If, on the other hand, a blade is subject to stress rupture or thermally induced LCF failures, these go undetected until later in the detailed design phase or in the testing associated with an engine development program. Redesign requires a complete new blade with new cooling flows and geometry, changes that affect performance both directly (cooling flows) and indirectly (increases in attachment and wheel weight).

FAILURE MODE MODEL METHODOLOGIES

Three important failure modes are quantified in the installed life analyses. These modes are mechanically induced LCF, thermally induced LCF, and stress rupture.

Mechanically Induced LCF

Once realistic throttle movements have been predicted for a mission, a performance analysis of the simulated engine predicts the engine operating parameters. These parameters, such as rotor speed or internal gas pressure loadings, vary with time and thereby create mechanically induced fluctuating stresses in a component. If this stress is primarily a function of only one mechanical operating parameter, the governing failure mode in this component will be LCF.

The level of stress in rotating components (wheels) is proportional to the square of the rotor speed. The level of stress in the combustor case is proportional to the internal pressure. (The ensuing explanation of mechanically induced LCF methodology will also apply to the combustor case with pressure as the driving load instead of the square of the rotor speed. For simplicity, the combustor case will not again be specifically referenced in this section.)

Because rotor speed can be determined from a performance analysis, the relationship between speed, stress, and flight time can be established for each rotating component. Combining this information with a knowledge of the fatigue life analysis of the component, or part, leads to the predicted installed component life. The manner in which this is accomplished is explained in this subsection. Figure 2 shows the flow diagram for the generation and transfer of information.

The nature of the integrated airframe and engine behavior for a system in the region of interest, along with the associated dynamic missions, or mission mix, provides a time history of engine rotor speeds. This rotor speed history is input to a rainflow cycle count routine. This cycle counting technique identifies full and partial cycles in the rotor speed history necessary for

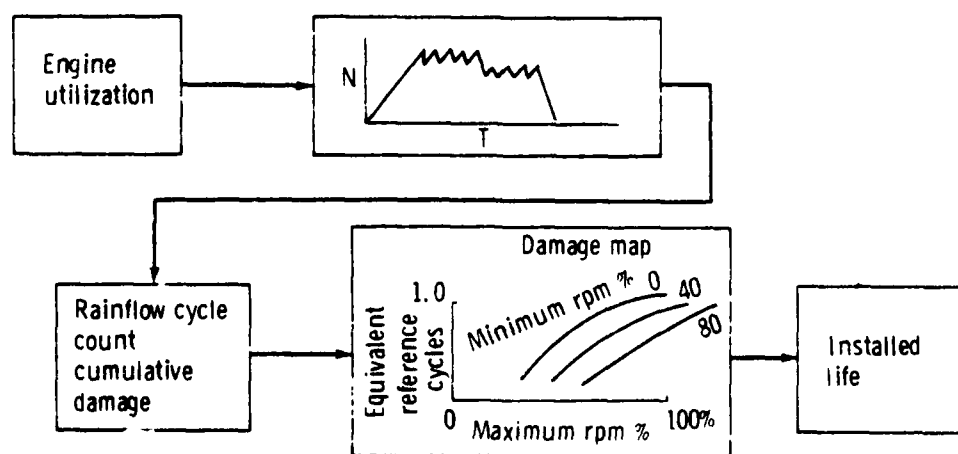


Figure 2. Logic used to determine installed life of components subject to mechanically induced LCF.

interacting with a damage map for a given component. The output of the damage map is the life usage rate, which, factored into the predicted life capability, results in the predicted component installed life.

The rainflow method of cycle counting was utilized to count all closed strain cycles, as well as partial cycles in a complex strain time history (Ref. 1).

The analysis of rotor components is simplified by considering only loading effects proportional to the square of the rotor speed since other effects as temperature and pressure are generally negligible in comparison. Thus, applying the cycle counting technique to the rotor speed history is as valid as applying it to a strain time history.

One exception to this simplification may occur during aircraft takeoff. Thermal gradients cause axial compressive stresses in the bore of a thick turbine wheel. This results in an increased equivalent stress and a corresponding increase in the cycle damage. When analyzing thick turbine disks, this additional damage will be accounted for by estimating the additional thermal axial stress during takeoff.

Thermally Induced LCF

The components subject to thermally induced LCF are hot turbine components such as blades or vanes, which must endure large thermal gradients for both transient and steady state operation.

Figure 3 is a schematic of the logic used to determine the predicted installed life of components subjected to thermally induced LCF.

Although thermally induced LCF and stress rupture are separate failure modes (and discussed separately), both are failure modes in the turbine blades, and our damage analysis must consider them as additive damages.

Furthermore, the information required for a stress rupture calculation is an included subset of the information required in thermally induced LCF calculations. As a result, stress rupture and thermally induced LCF life calculations are conducted simultaneously.

The logic required for assessing thermal LCF damage is more complex than that for mechanically induced LCF because stresses that introduce damage to a part are a function of temperature distribution as well as mechanical loading. In addition, the material fatigue properties are highly temperature sensitive as well as dependent upon mean stress and strain range. This added complexity eliminates the ability to compute cumulative fatigue damage accurately through the use of a damage map.

The performance analysis of the engine utilization simulation results in real time traces of engine parameters important to the thermal fatigue analysis. Parameters--such as the high-pressure rotor speed N_H , the low-pressure rotor speed N_L , the compressor discharge pressure P_3 , the burner outlet pressure P_4 , and the engine mass flow rate \dot{M} --are time traces used in an internal aerodynamics routine to compute centrifugal force and gas bending

1. F. D. Richards, N. R. LaPointe, and R. M. Wetzel, "A Cycle Counting Algorithm for Fatigue Damage Analysis," SAE paper 740278, 1974.

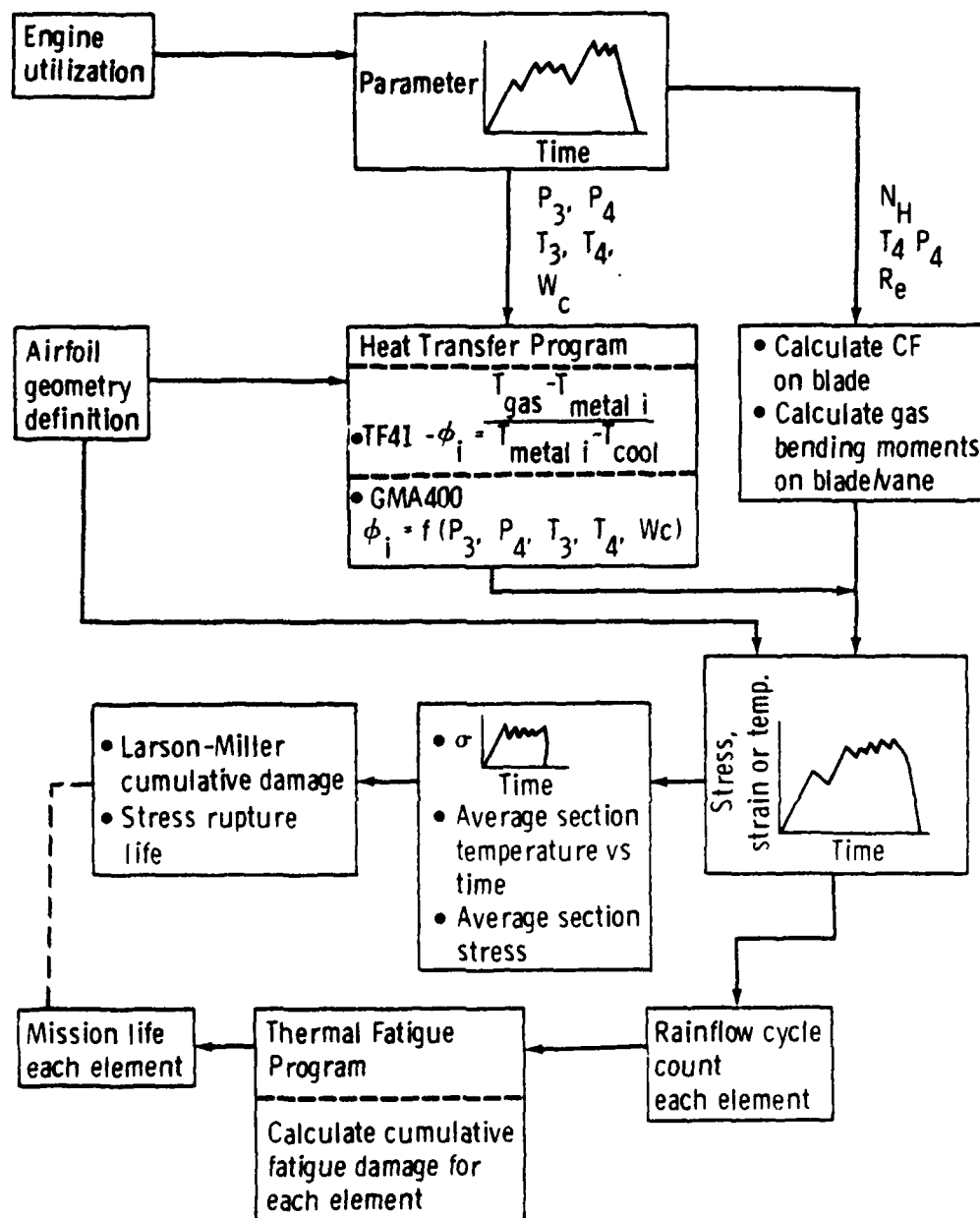


Figure 3. Airfoil stress rupture/LCF model methodology.

Parameters--such as P_3 , P_4 , the compressor discharge temperature T_3 , the burner discharge temperature T_4 , and cooling mass flow--are used in a heat transfer routine. This routine will calculate vane or blade local temperatures. Temperatures calculated are chordwise inner and outer wall metal temperatures, as well as temperatures at the structural strut-Lamilloy® sheet

*Lamilloy is a registered trademark of the General Motors Corporation.

interface. These temperatures are calculated for a single vane or blade section at the same time "slice" as the mechanical loading. To facilitate handling of the large amount of data that must be produced for the TLCF analysis, the blade/vane coordinates, as defined by aerodynamics, along with surface temperatures, defined by heat transfer, enter a mesh generator. This mesh generator defines elements in terms of area, coordinates, and temperatures for input into the one-dimensional stress/strain program.

The one-dimensional stress/strain program converts mechanical loadings such as rotor speed and gas bending moments, as well as chordwise thermal loadings, into radial stresses and strains for each element. This program is the heart of the thermally induced LCF calculation and will be briefly elaborated upon.

Any program that will handle the quantity of information available from the engine utilization for a complete mission must be simple and inexpensive to run on the computer. This eliminates any consideration of three-dimensional finite element techniques.

The program must also yield accurate results. Fatigue calculations are quite sensitive to stress levels. Comparisons of the results of the one-dimensional thermal creep program with three-dimensional elastic finite element calculations show excellent agreement on radial stress before creep has had time to occur. Figure 4 illustrates this for the air-cooled TF41 HPT-1 kit blade. Obviously, after creep begins, the one-dimensional program will be more accurate than the elastic program. Finally the program must handle loads resulting from gas bending moments and centrifugal forces as well as temperature gradients. The program accomplishes this.

The program output will define stresses and strains for each element at each time slice that represents a significant change in mechanical or thermal loading. This information will enter the cycle counting procedure as before and exit as a definition of cycles and half cycles for each element. This information, with the associated element cycle temperature, will enter the LCF program. This program will do a cumulative damage analysis, which results in a mission life for each element.

Stress Rupture

The third failure mechanism that is of concern is stress rupture. This damage mechanism will be applicable only to turbine blades in the LUCID program.

Stress rupture life, as previously indicated, is computed in the same pass as the thermally induced low cycle fatigue. The damage incurred by a component for this mechanism, however, is the result of continuous high stress at temperature, rather than a cycling of stress. To minimize cost, several simplifications have been incorporated into the stress rupture logic. The stresses are assumed to be the average stresses of the blade section. The associated temperature is the area weighted average section temperature at the same time slice.

As a time trace (at discrete time slices) of average stress is generated in the one-dimensional thermal stress/strain program, the corresponding value of the material Larson-Miller stress rupture parameter is found. This parameter, along with the average section temperature, enables a computation of a stress rupture life, L_R , in hours. Knowing the length of the time interval t during

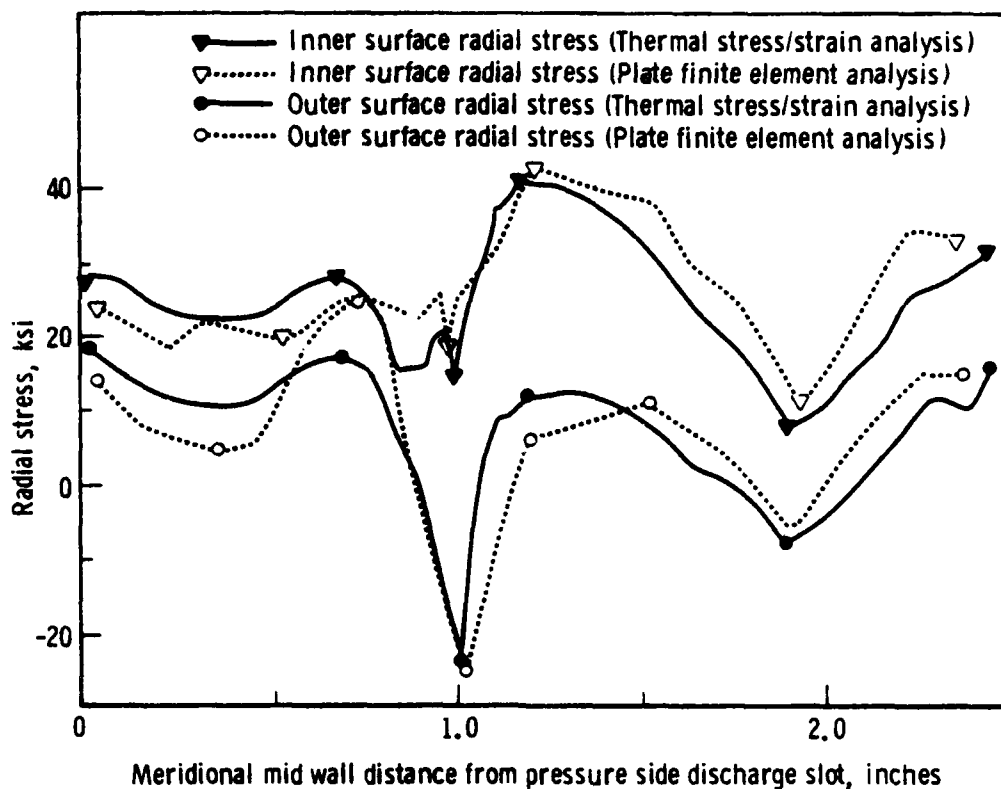


Figure 4. Initial cycle radial stress comparison at midfoil section--one-dimensional thermal stress/strain analysis versus three-dimensional plate finite element analysis.

which the stress was held (essentially) constant, a damage fraction (t/L_R) is calculated. All of these "damage fractions" are summed for a given utilization. The reciprocal of this fraction is the section stress rupture installed life.

Damage resulting from stress rupture may be added to thermally induced LCF damage via Miner's rule. The reciprocal of this damage sum will be the installed life with damage from both mechanisms considered.

FAILURE MODEL VERIFICATION

TF41 turbine section experience for known test histories has been used to verify the life analysis. Table 2 lists the TF41 components used for this verification effort along with the failure mode, critical location on the component, and the mission time histories analyzed. Development engine test histories for the go-go test cycle and the accelerated mission test (AMT) cycle are shown in Figures 5 and 6, respectively. A reference cycle used analytically for the severity index calculation is shown in Figure 7. The severity index for a component/failure mode is defined as follows:

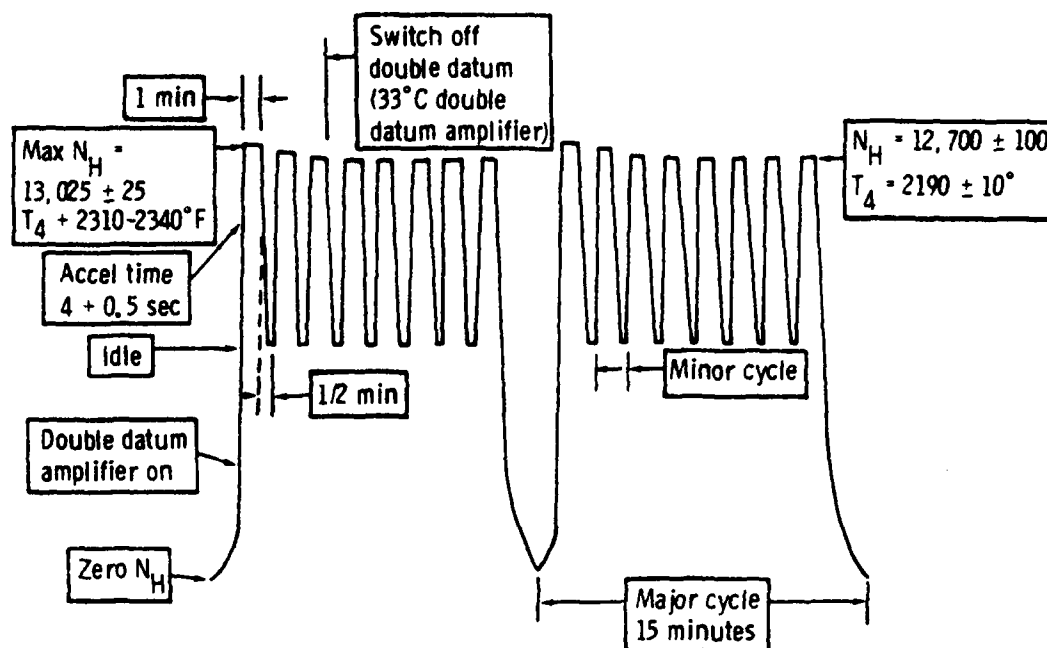
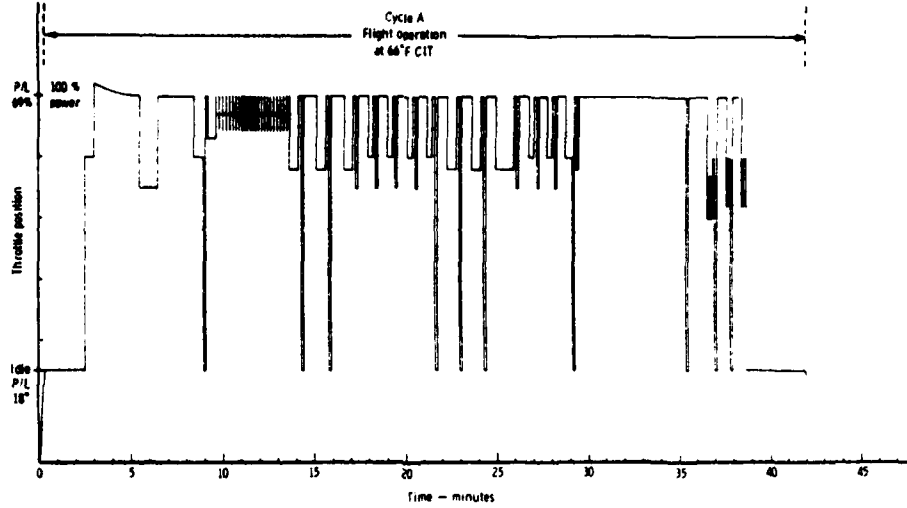


Figure 5. Go-and-go endurance test cycle.

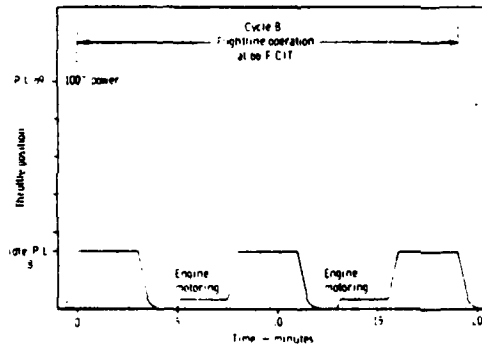
Table 2.
TF41 failure mode analysis verification.

<u>Component</u>	<u>Failure mode/ location</u>	<u>Mission</u>
TF41 standard HPT-1 vane triplet	Thermal LCF, leading edge transverse crack initiation at meanline section	AMT Go-go Ref cycle
TF41 cast HPT-1 blade	Thermal LCF, lower post crack initiated at meanline section	AMT Go-go Ref cycle
TF41 solid HPT-2 forged blade pair	Stress rupture, meanline section	Go-go Ref cycle
TF41 HPT-1 forged wheel	Mechanical LCF, bore crack initiation	Spin pit Ref cycle

20 Cycle A's (Right test cycle)



4 Cycle B's (Rightline test cycle)



1 Cycle C (Ground start/check test cycle)

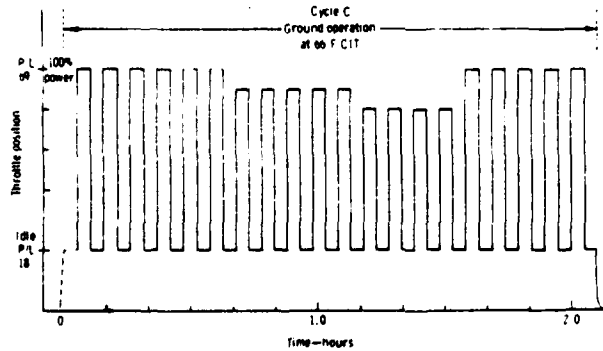


Figure 6. Accelerated mission test cycle.

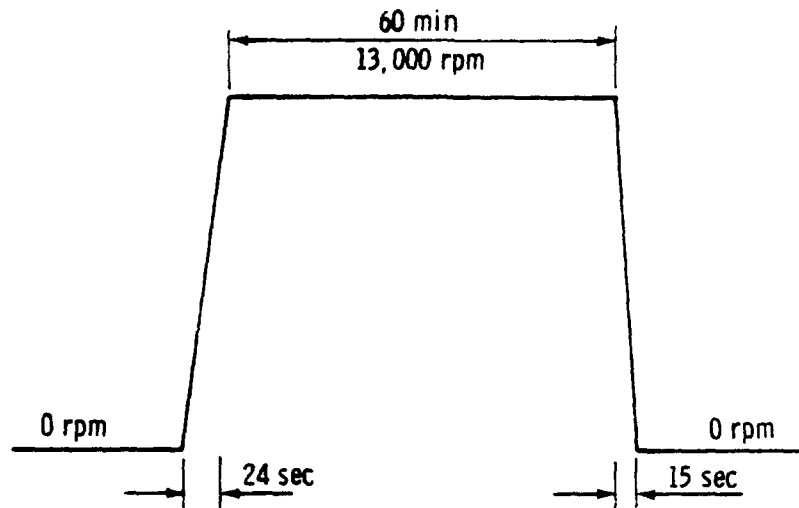


Figure 7. Reference analytical cycle used in severity index calculation.

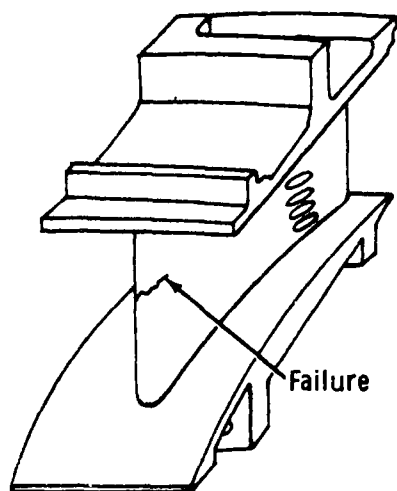
Severity index (SI)

$$\text{Severity index (SI)} = \frac{\text{Predicted life usage rate for mission of interest}}{\text{Predicted life usage rate for reference cycle}}$$

The severity index or relative life usage rate gives a quick comparison of mission severity for that component/failure mode. Although the failure mode analyses have been used to predict absolute mission life and relative life usage rates, the inherent simplifications in these analyses, which ignore transient temperature overshoots, would be expected to result in overprediction of absolute mission life. At the same time, since the simplifications are used in the same manner for two missions to compute a severity index, the mission life ratio might be expected to agree quite well with test experience. Both of these trends have been observed and are presented individually in the following discussion.

HPT-1 Cast Vane

The vane of Stellite 31 material was analyzed for the two test missions and the reference cycle at a meanline airfoil section independent of the other two airfoils in one vane segment. The vane metal temperatures used in the analysis corresponded to a vane located at the peak temperature burner hotspot. Since a vane sits in one spot of the circumferential burner profile, metal temperature levels vary from vane to vane. In the TF41 engine, typically only a few vane airfoils out of the set of 60 are exposed to the highest burner outlet temperatures. Sufficient testing has not been done to establish a failure history distribution (typical and -3σ vane life). Results for transverse cracking on the leading edge are compared in Figure 8. For the transverse cracking, predicted mission lives exceed test experience by 25 to 40%. However, the life usage rate of the go-and-go test cycle relative to the AMT cycle calculated at 2.75 agreed well with the test result of 2.42. It should be noted that frequent cracking in the vane in the radial direction also occurs. However, the simplified airfoil/TLCF model methodology does not consider failures in the radial direction. This approach is considered reasonable for conceptual design.



Mission	Calculated life (hr)		Typical test life (hr)	Ratio calculated/test
	Typical	-3 σ		
Go-go	62.5	47.2	50.0	1.25
AMT	172.0	123.0	121.0	1.40
Reference	867.0	653.0	—	—

Mission	Calculated SI = $\frac{\text{Ref hr}}{\text{Mission hr}}$		Test SI = $\frac{\text{Ref hr}}{\text{Mission hr}}$	Ratio test / calculated
	Typical	-3 σ	Typical	Typical
Go-go	13.9	13.8	17.3	1.25
AMT	5.0	5.3	7.2	1.40
Ratio = $\frac{\text{Go-go}}{\text{AMT}}$	2.75	2.61	2.42	0.88

Figure 8. TF41 HPT-1 vane comparison of predicted and test installed life for leading edge transverse cracks.

HPT-1 Cast Blade

The Mar-M246 cast blade was analyzed for the AMT and go-and-go test cycles along with the reference cycle for severity index purposes. The critical location is where the lower cast pin attaches internally to the suction surface. At that location, three-dimensional effects raise the peak equivalent stress. Analysis experience for this blade was used to relate two- to three-dimensional stress/strain levels on the appropriate element for the two-dimensional model used here. Predicted and test data for the AMT, go-and-go, and reference cycles are tabulated in Figure 9. Predicted lives are within 60% of the test lives, which is quite good. The relative life usage rates, as expected, are more accurate. They are within 5% of the test data for the -3 σ blade.

HPT-2 Forged Blade

This uncooled solid blade of the N118 material was analyzed for the go-and-go test cycle where the damage was almost entirely a result of stress rupture since the blade metal temperature could get as high as 1800°F (this includes a +35°F engine-to-engine metal temperature variation). The analysis procedure is based on average section stress and temperature. Since transient overshoots and non-steady-state metal temperatures are not considered in the analysis, some leading and trailing edge fatigue damage is neglected. (These regions would tend to heat and cool more rapidly than the surrounding material resulting in additional thermal stresses.) This additional damage causes all cracking to originate at the blade trailing edge. Even with this simplification, the predicted -3 σ blade life of 44.3 hr of go-and-go testing agrees well with the minimum observed life of 45 hr from two sets of 110 blades (see Figure 10).

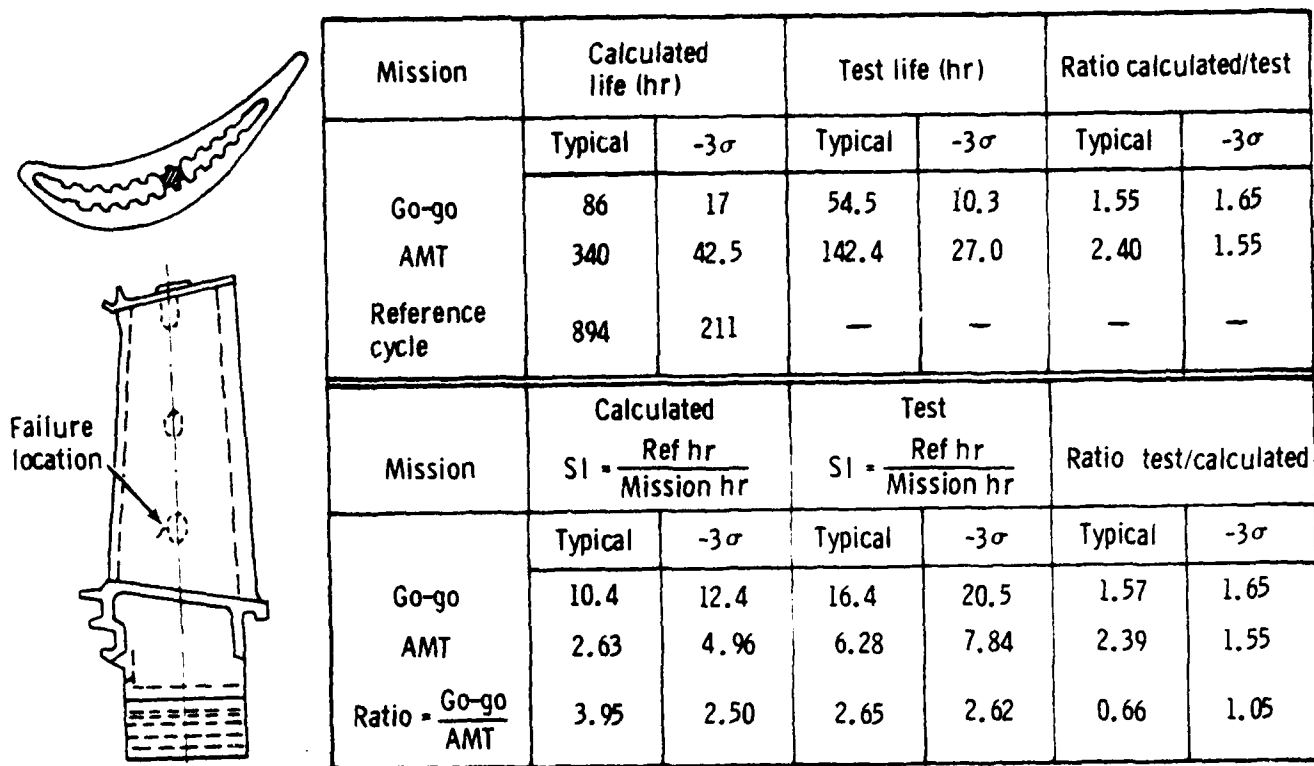


Figure 9. TF41 HPT-1 cast blade comparison of calculated installed life and test results in post region.

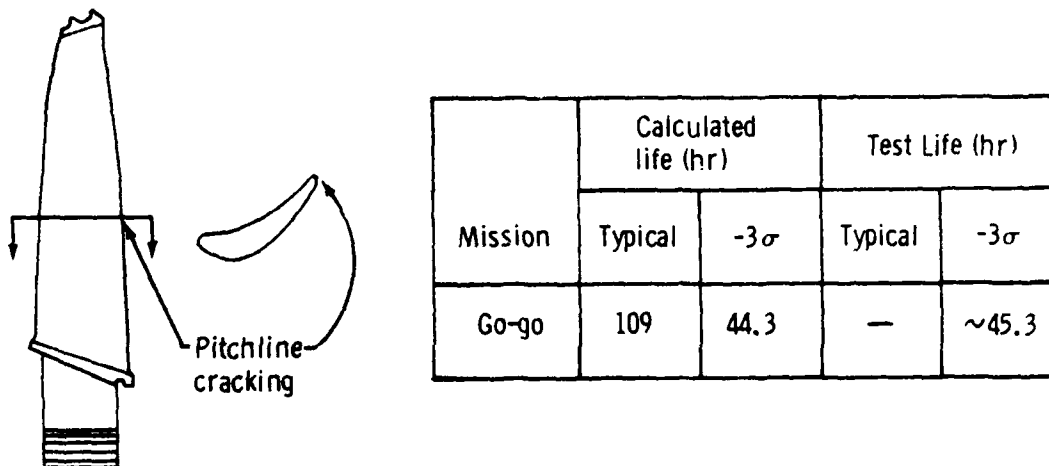


Figure 10. TF41 HPT-2 blade--comparison of calculated installed life and test results.

HPT-1 Disk

The disk of N901 material was analyzed for a spin pit cycle (0-13,000-0 rpm) and the reference cycle. Figure 11 displays the predicted typical and -3σ lives to 10,138 reference cycles and 4870 reference cycles, respectively. In addition, six cases of fatigue failures are shown where the test lives were converted to reference cycle lives with the calculated test life usage rates. The differences in disks 3 and 4 show potentially a great deal of scatter resulting from service life usage unknowns. Overall, the predicted results agree reasonably well with test failures.

For the blade and vane TLCF, the analysis procedures predict mission lives within a factor of two when compared to test data, whereas the analyses for wheels and stress rupture failure modes for blades predict failures very close to recorded test times. For all models verified herein, the predicted relative life usage rates agree very well with test data.

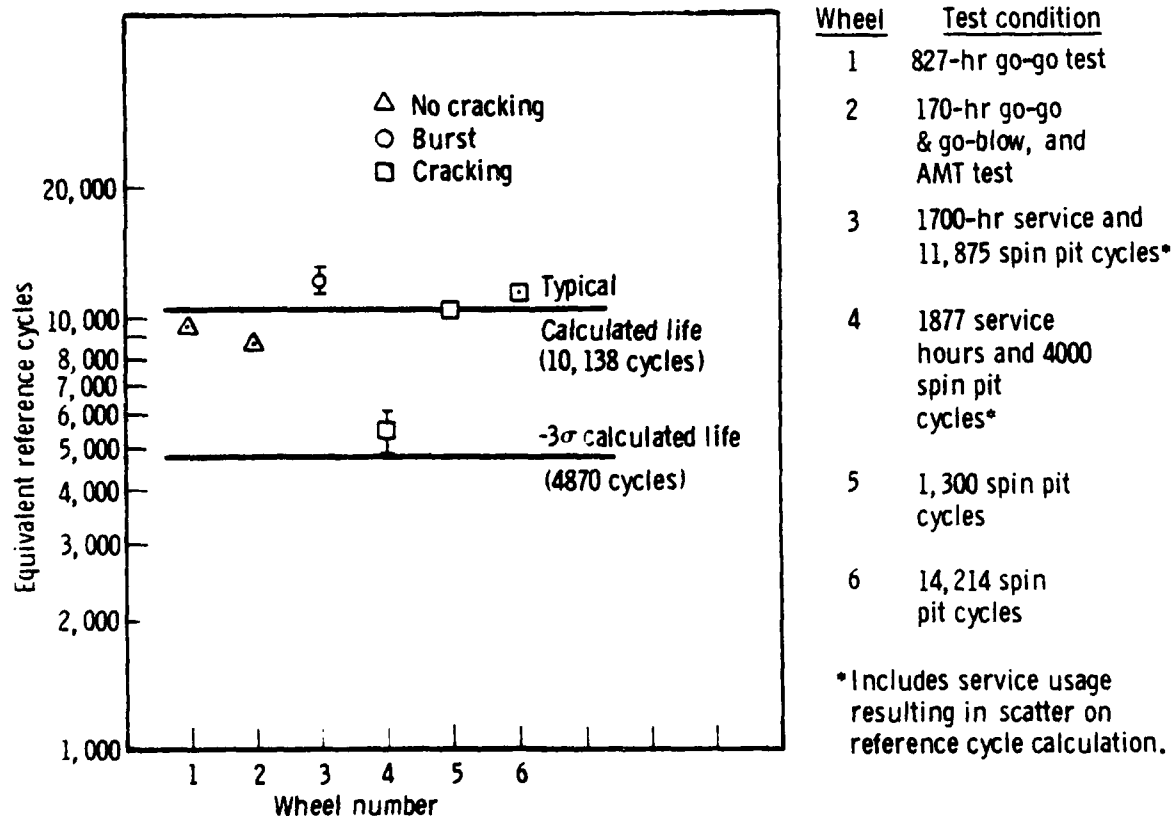


Figure 11. TF41 HPT-1 disk bore calculated reference life capability compared with test results.

TURBINE AIRFOIL TLCF MODEL SIMPLIFICATION

To address a large number of engines in conceptual design, DDA deemed it necessary to simplify the turbine airfoil/TLCF model methodology. The original model addressed the entire airfoil, considering creep relaxation to predict the local stress and strain history for the critical location. The simplification (see Figure 12) was based on observing the original model predictions for just this critical location and creating a regression equation to predict local strain for this critical location. This approach necessitated neglecting creep relaxation. The basic approach for verifying this simplification was by comparing it to original model predictions for four missions. These missions were picked to give a range in typical tactical fighter usage (super-cruiser, deep strike, battlefield interdiction, training missions). In addition, several turbines were examined to confirm the validity of the simplified approach.

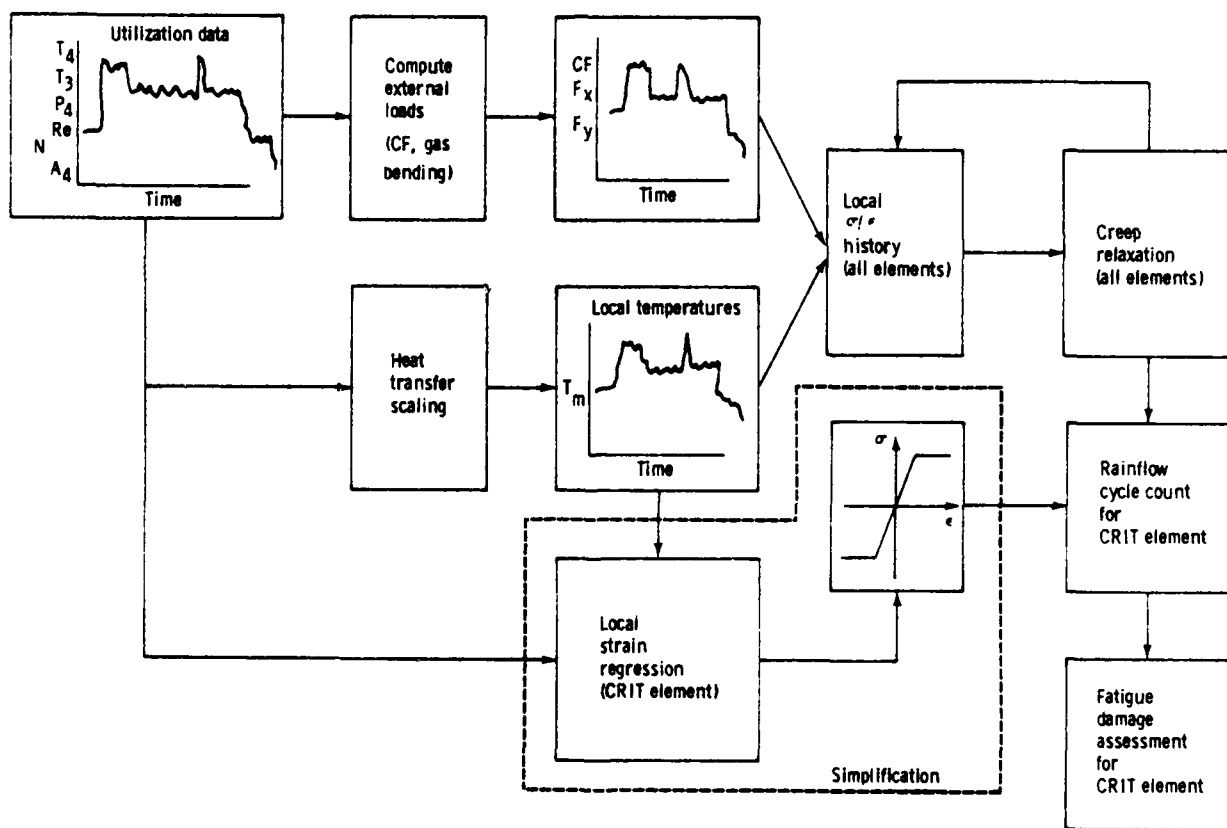


Figure 12. Turbine airfoil LCF model methodology.

A local strain data base was generated for a base-line turbine blade and vane from a series of flight (altitude and Mach) and power setting conditions (see Figure 13). The regression could then be used to compute local strain from knowledge of only rotor speed, a local metal temperature level and gradient, and turbine inlet total pressure. Since the local total strain has several contributing types of loading (centrifugal, gas bending, thermal), a consistent definition was adopted for metal temperature gradients and is shown in Figure 14 for the thermal strain component. An overall airfoil temperature gradient ΔT_c and a local temperature gradient ΔT_w were used for regression purposes for the thermal strain component. Figures 15 and 16 display the regression equation types used for the blade and vane, respectively. Since turbine airfoils have strains resulting from several sources (i.e., thermal, centrifugal, gas bending), each figure shows the equation form for each strain component and the total strain, which is a sum of the component strains. Regressions were generated for a base-line turbine blade and vane for three critical locations on each airfoil (see Figures 17 and 18). Table 3 displays the accuracy of the local total strain regressions for these different locations of each turbine airfoil. This accuracy is displayed in terms of R^2 , where the regression fit becomes better as R^2 approaches unity. The vane regression accuracy suffers in the trailing edge area because of local plastic deformation for some operating conditions.

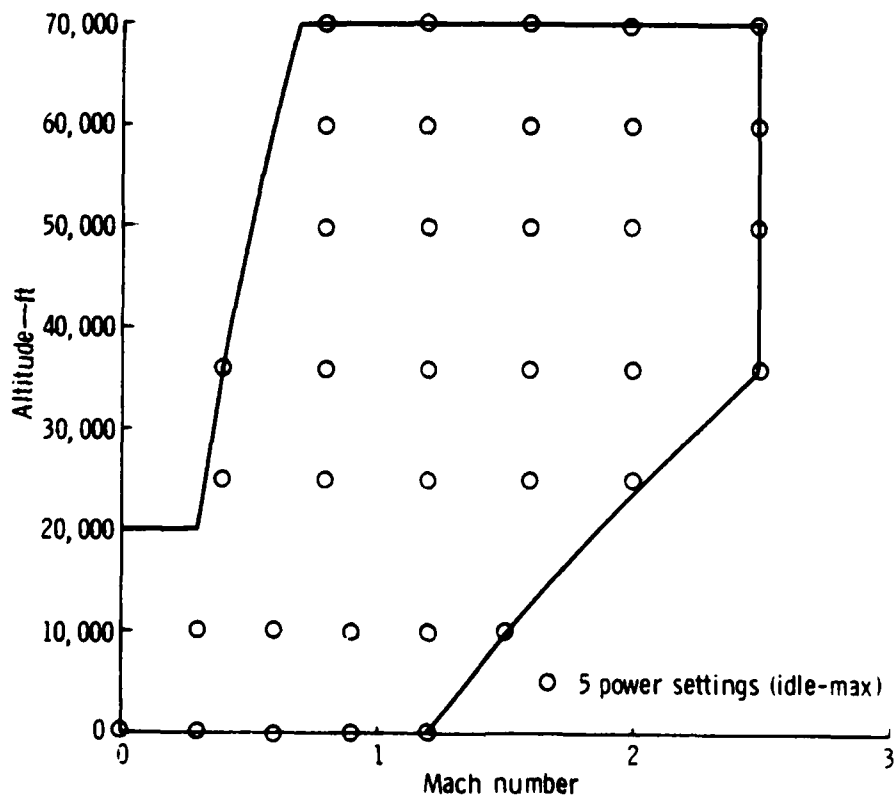


Figure 13. Strain regression data base.

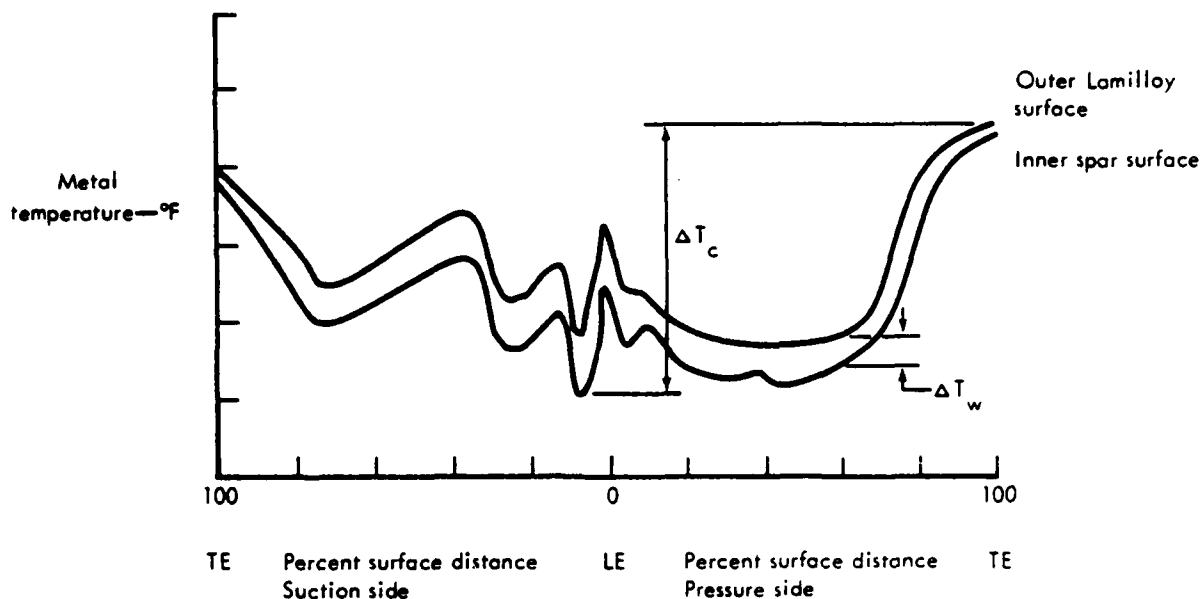


Figure 14. Turbine airfoil temperature gradient definitions.

Blade

Strain components

$$\epsilon_C = N^2 (A_0 + A_1 T_m + A_2 T_m^2)$$

Centrifugal

$$\epsilon_T = A_0 + A_1 \Delta T_c + A_2 \Delta T_c^2 + A_3 \Delta T_w + A_4 \Delta T_w^2$$

Thermal gradient

$$\epsilon_B = (T_m - 2000) (A_0 + A_1 T_m + A_2 T_m^2)$$

Bonding residual

Total strain

$$\epsilon = f(T_m, \Delta T_c, \Delta T_w, N) = \epsilon_C + \epsilon_T + \epsilon_B$$

$$\epsilon = A_1 T_m + A_2 \Delta T_c + A_3 \Delta T_w + A_4 T_m^2 + A_5 \Delta T_c^2 + A_6 \Delta T_w^2 + SA_7 N^2 + SA_8 T_m N^2 + AS_9 T_m^2 N^2 + A_{10}$$

s = Allows scaling for different centrifugal stress levels (life capability levels)

Figure 15. Blade strain regression equation form.

As part of the checkout of the simplified TLCF model, the significance of neglecting creep relaxation was reviewed for a blade stress rupture and TLF and a vane TLF. As shown in Table 4, original model predictions for the TLF failure mode show little effect from creep relaxation for the blade for all of the mission examined. The vane predictions are effected for two of the mis-

Vane

Strain components

$$\epsilon_G = P_4 (A_0 + A_1 T_m + A_2 T_m^2)$$

$$\epsilon_T = A_0 + A_1 \Delta T_c + A_2 \Delta T_c^2 + A_3 \Delta T_w + A_4 \Delta T_w^2$$

$$\epsilon_B = (T_m - 2000) (A_0 + A_1 T_m + A_2 T_m^2)$$

Gas bending

Thermal gradient

Bonding residual

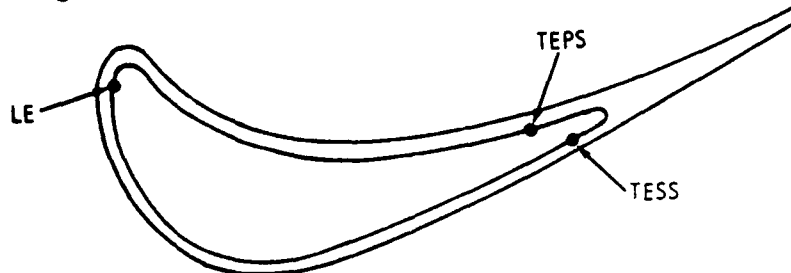
Total strain

$$\epsilon = f(T_m, \Delta T_c, \Delta T_w, P_4) = \epsilon_G + \epsilon_T + \epsilon_B$$

$$\epsilon = A_1 T_m + A_2 \Delta T_c + A_3 \Delta T_w + SA_4 P_4 + A_5 T_m^2 + A_6 \Delta T_c^2 + A_7 \Delta T_w^2 + SA_8 P_4 T_m + SA_9 P_4 T_m^2 + A_{10}$$

s = Allows scaling for different gas bending stress levels
(life capability levels)

Figure 16. Vane strain regression equation form.



LE = leading edge
TEPS = trailing edge, pressure side
TESS = trailing edge, suction side

Figure 17. Blade regression critical locations.

sions. The blade predictions for the stress rupture model are effected for two of the missions where a substantial amount of time is spent, high stresses and metal temperatures exist, and creep is important. However, inaccuracies resulting from neglecting creep relaxation have been judged acceptable because of the capability arising from the TLCF model simplification.

Four dry, variable geometry turbojets were selected for evaluation to compare original TLCF model predictions against simplified TLCF model predictions. These engine cycle definitions are shown in Table 5. PD422-12 was used as a base-line engine with the others having a variation in one performance cycle parameter from the base line. PD422-12 was used to form the regression for the blade and vane. This regression was then used to predict installed lives for all of the engines.

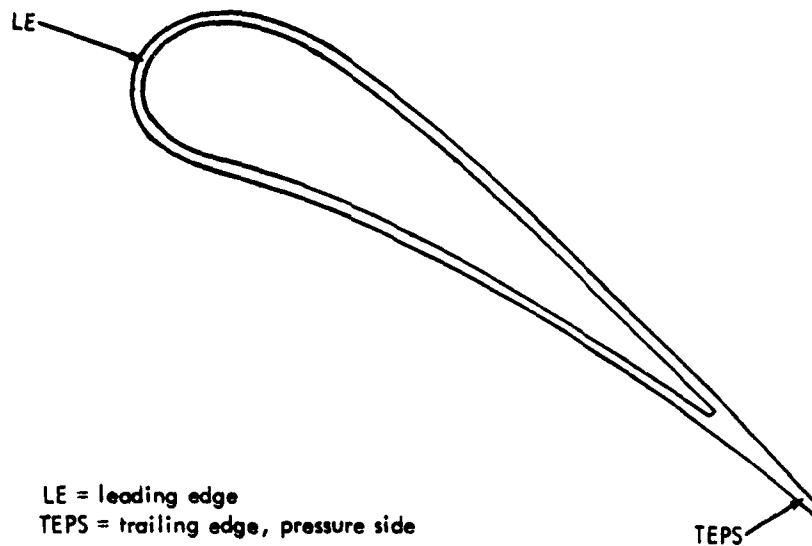


Figure 18. Vane regression critical locations.

Table 3.
Turbine airfoil TLCF strain regression and accuracy.

<u>Airfoil</u>	<u>Location*</u>	<u>Independent variables</u>	<u>Dependent variable</u>	<u>R²</u>
Blade	LE	$\Delta T_m, \Delta T_c, \Delta T_w, N$	total	0.9989
	TEPS			0.9987
	TESS			0.9988
Vane	LE	$\Delta T_m, \Delta T_c, \Delta T_w, P_4$	total	0.9843
	TEPS			0.9452
	TESS			0.9397

* LE--leading edge
TEPS--trailing edge, pressure side
TESS--Trailing edge, suction side

Table 4.
Effect of creep relaxation on installed life prediction for turbine airfoils.

	Installed life without creep/installed life with creep		
	Blade		Vane
<u>Mission</u>	<u>Stress rupture</u>	<u>TLCF</u>	<u>TLCF</u>
Supercruiser	1.32	1.05	0.97
Deep strike	1.28	1.06	0.99
Interdiction	1.04	1.02	0.84
Training	1.00	1.00	0.91

Table 5.
Engine definitions

<u>Designation</u>	<u>PD422-4</u>	<u>PD422-11</u>	<u>PD422-12</u>	<u>PD422-60</u>
R_c	9	15	15	15
θ_B	1.0	1.0	1.0	1.36
RIT--°F	3400	3050	3400	3400
W_a --lb/sec	200	200	200	200
Turbine stages	1	2	2	2

A summary of the blade life capability levels (original model predictions) is given in Table 6 for each of the blade designs evaluated. They all have a similar stress rupture life capability level expressed in terms of time at max power at M_N 2/60,000 ft. However, the TLCF life capability varies near the trailing edge on the pressure surface, which is the critical location. Figure 19 shows a comparison between original model and simplified model life capability predictions. The simplified model compares very well with the original model for the base-line engine (PD422-12). For the critical location (the trailing edge, pressure surface), the simplified model agrees reasonably well. In the leading edge area, some load redistribution is occurring in the other blade designs, which the regression does not accurately predict. In the trailing edge, suction surface region, the simplified model follows the same trend as the original model but inaccuracies were observed. Using the base-line blade regression, Figure 20 compares absolute levels of installed life predictions for the three locations for four different missions. For the critical location (trailing edge, pressure surface), the simplified model has some inaccuracies as a result of the simplification, but it is considered reasonable for conceptual design. The same trend in the leading edge area as for the life capability prediction was noted. Installed lives were not predicted for PD422-60 to reduce the work scope of this task since the results were expected to be similar because the average spar stress at the meanline section was virtually identical to that of the base line. Overall, absolute installed life predictions with the simplified model are considered accurate within 2:1. Figure 21 displays severity index comparisons for the simplified model relative to the detailed model. In general, the simplified model severity index predictions are more accurate than the absolute level of installed life predictions relative to the original model. However, inaccuracies are observed as a result of the simplification. For both models, the severity index predictions are using the supercruiser mission as the denominator to display damage rates relative to those for the supercruiser mission.

For the vanes, a summary of the life capability predictions from the original model for three different locations on each of the four vane designs is given in Table 7. The critical locations are on the trailing edge, pressure side. The life capabilities are expressed in terms of engine start/max/stop cycles at M_N 2/60,000 ft. A regression for the PD422-12 vane was developed. Figure 22 displays the predicted results using this regression versus the original model. The simplified model predictions agree fairly well with the original model although some inaccuracy results. Absolute and relative installed life predictions are shown in Figures 23 and 24, respectively, for four different missions and three locations each.

Table 6.
Turbine blade stress rupture/TLCF life capability summary.

	<u>Engine designation</u>			
	<u>PD422-4</u>	<u>PD422-11</u>	<u>PD422-12</u>	<u>PD422-60</u>
Stress rupture data				
Average spar				
Stress--psi	33680	17032	18499	18467
Temperature--°F	1442	1580	1568	1574
Max power life capability--hr*	2170	1376	1403	1179
TLCF data				
Leading edge				
Surface location--%	5.4	3.9	3.9	3.0
Stress--psi	41574	22152	24641	26189
Temperature--°F	1330	1504	1458	1475
Life capability--0-max-0--cycles*	7399	180762	109495	68244
Trailing edge, pressure surface				
Surface location--%	59.6	60.4	60.3	60.9
Stress--psi	59311	37463	43254	39840
Temperature--°F	1352	1504	1480	1503
Life capability--0-max-0--cycles*	820	6006	2900	4015
Trailing edge, suction surface				
Surface location--%	69.3	68.8	68.8	68.5
Stress--psi	44485	25821	30386	29985
Temperature--°F	1426	1571	1550	1553
Life capability--0-max-0--cycles*	3952	45582	16936	17833

*M_N 2/60,000 ft flight condition

Overall, the vane installed life predictions are considered accurate within 2.5-3:1 with the simplified model.

A simplified blade stress rupture model was developed because the original airfoil TLCF model also computed stress rupture damage. Figure 25 displays the original model methodology along with the simplified model. The heat transfer assessments in both models are identical. The simplified model computes average section stress via a speed proportionality since centrifugal force is the primary load. The original model computed local stresses/strains, considered creep relaxation, and determined the average section stress via area weighting. The effect of neglecting creep relaxation was discussed earlier and shown in Table 4. The differences in installed life predictions resulting from the average stress computations only is displayed in Table 8. The simplified model gives reasonably accurate results for conceptual design.

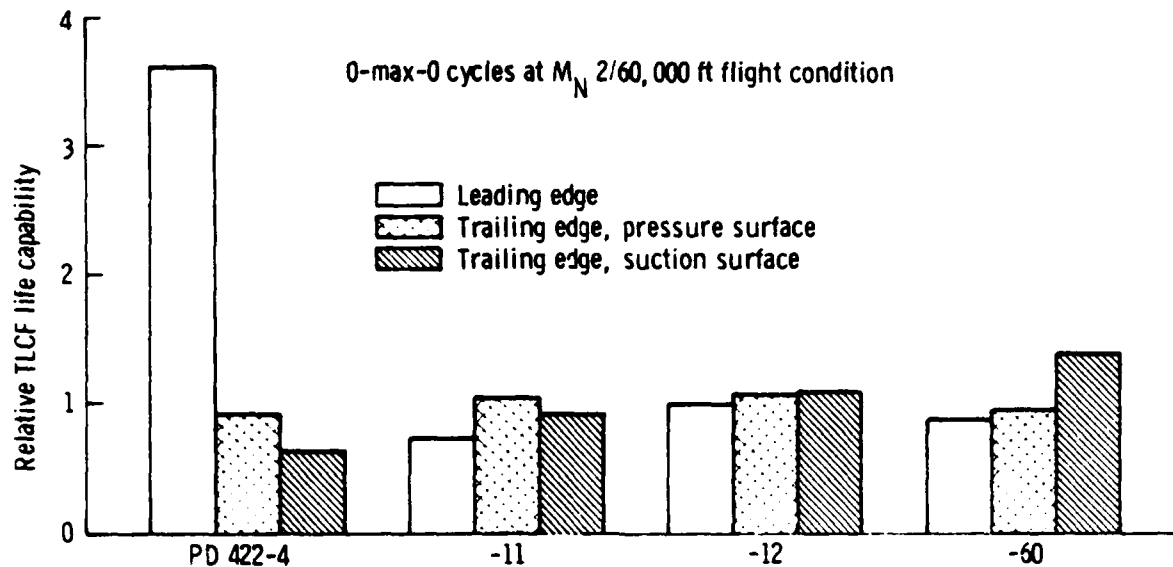


Figure 19. Turbine blade life capability comparison--simplified model relative to original model predictions.

Table 7.
Turbine vane TILCF life capability summary.

	Engine designation			
	PD422-4	PD422-11	PD422-12	PD422-60
Average spar	Max/min	Max/min	Max/min	Max/min
Stress--psi	1,466/489	1,393/540	1,380/379	1,342/-54
Temperature--°F	1,697/70	1,698/70	1,704/70	1,702/70
TLCF				
Leading edge				
Surface location--%	12.2	12.3	12.2	12.2
Stress--psi	-19,775/32,258	-22,332/22,921	-20,579/33,539	-21,495/30,499
Temperature--°F	1,870/70	1,847/70	1,863/70	1,854/70
Life capability--0-max-0--cycles*	470	708	444	500
Trailing edge, pressure surface				
Surface location--%	98.4	98.6	98.5	98.5
Stress--psi	-8,941/126,855	-12,500/96,797	-8,914/123,353	-10,769/99,652
Temperature--°F	2,028/70	1,959/70	2,018/70	1,986/70
Life capability--0-max-0--cycles*	82	95	108	118
Trailing edge, suction surface				
Surface location--%	98.4	98.6	98.5	98.5
Stress--psi	-9,213/126,855	-12,889/93,526	-9,318/118,953	-11,467/92,940
Temperature--°F	2,023/70	1,953/70	2,011/70	1,974/70
Life capability--0-max-0--cycles*	82	95	109	120

* M_N 2/60,000 ft flight condition

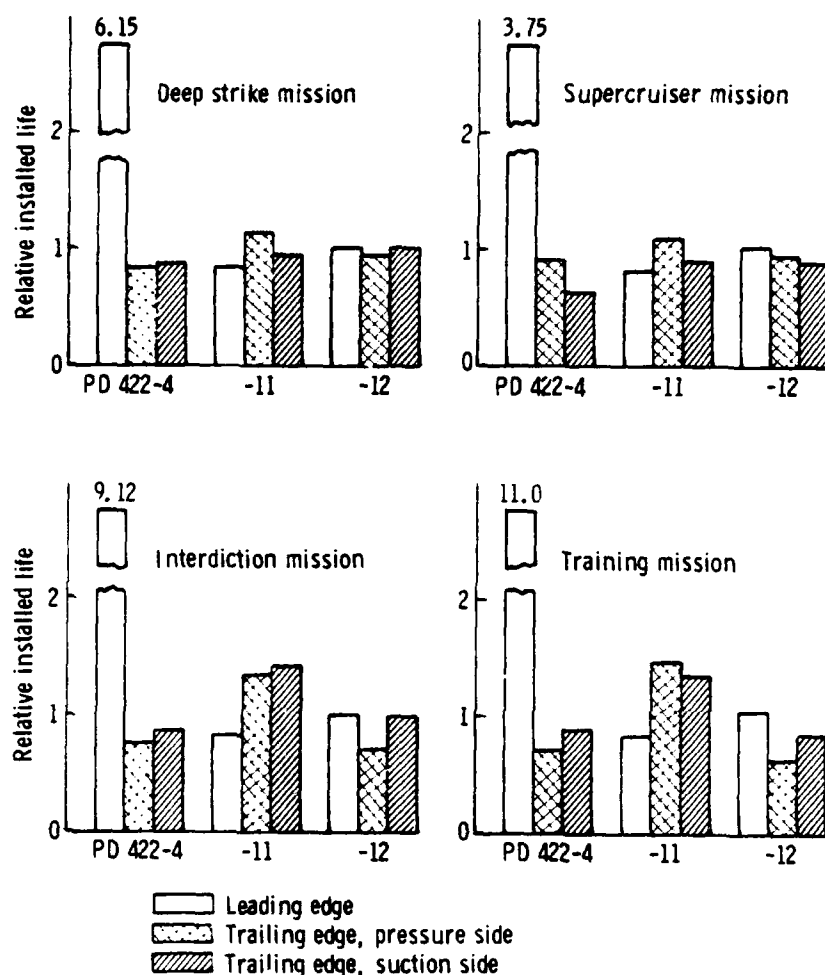


Figure 20. Turbine blade installed life comparison--simplified model relative to original model predictions.

Table 8.
Simplified model versus original model without creep turbine airfoil stress rupture.

<u>Mission</u>	<u>Relative installed life*</u>
Supercruiser	0.937
Deep strike	0.972
Interdiction	0.938
Training	1.080

*Simplified model/original model predictions.

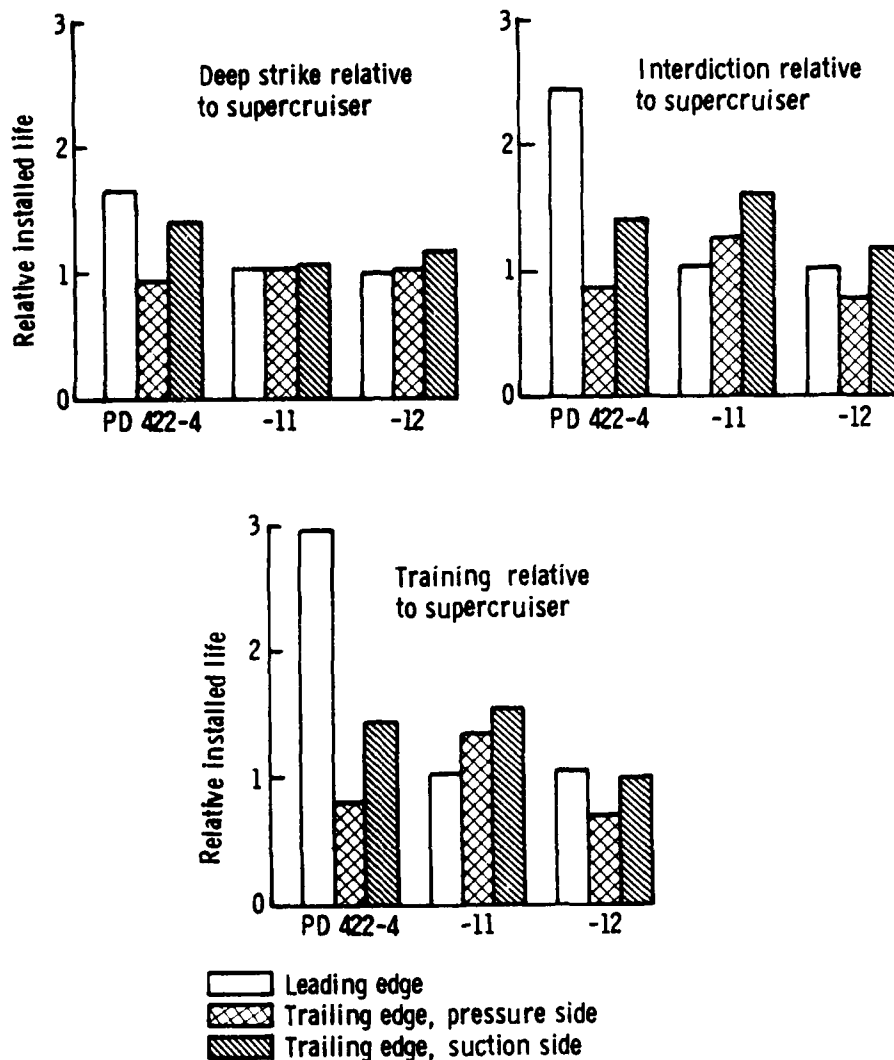


Figure 21. Turbine blade relative installed life comparison--simplified model relative to original model predictions.

COMPONENT INPUT DATA

Geometry, material properties, load, and temperature data were compiled for component designs incorporating similar technologies appropriate for use with the parametric PD422 series of gas turbines discussed in Task 3.1.4. These base-line component designs formed the basis for predicting life capability requirements in Task 3.2.4. The component materials are listed in Table 9 for the base-line designs.

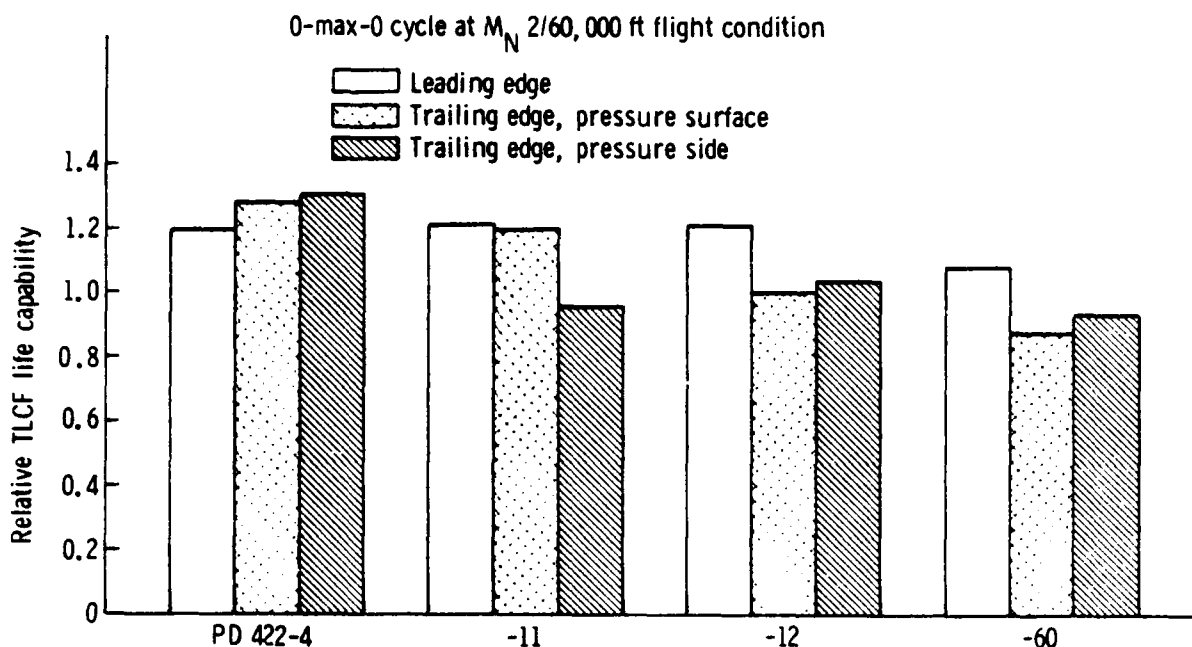


Figure 22. Turbine vane life capability comparison--simplified model relative to original model predictions.

Table 9.
Component materials.

<u>Component</u>	<u>Material</u>
HPC-1 wheel	AF95
Combustor case	IN706
HPT-1 wheel	AF95
HPT-1 vane	MA956 (Lamilloy)
	Mar-M246 (Spar)
HPT-1 Blade	HA188 (Lamilloy)
	Mar-M246 (Spar)

The mechanical low cycle fatigue (MLCF) damage map for the first-stage compressor wheel bore is shown in Figure 26 for a peak operating temperature of 390°F and a base-line life capability of 9,000 0-100-0% N cycles. The MLCF damage map for the outer combustor case is shown in Figure 27 for a peak operating temperature of 975°F and a base-line life capability of 34,000 0-max-0 ΔP cycles. The combustor case is nominally sized for burst considerations with twice the internal pressure at max power, Mach 1.2, sea level. The MLCF damage map for the HPT-1 wheel bore is depicted in Figure 28 for a peak temperature of 850°F and a base-line life capability of 18,000 0-100-0% N cycles. The damage maps cover a sufficient range to allow scaling for the anticipated life capability levels.

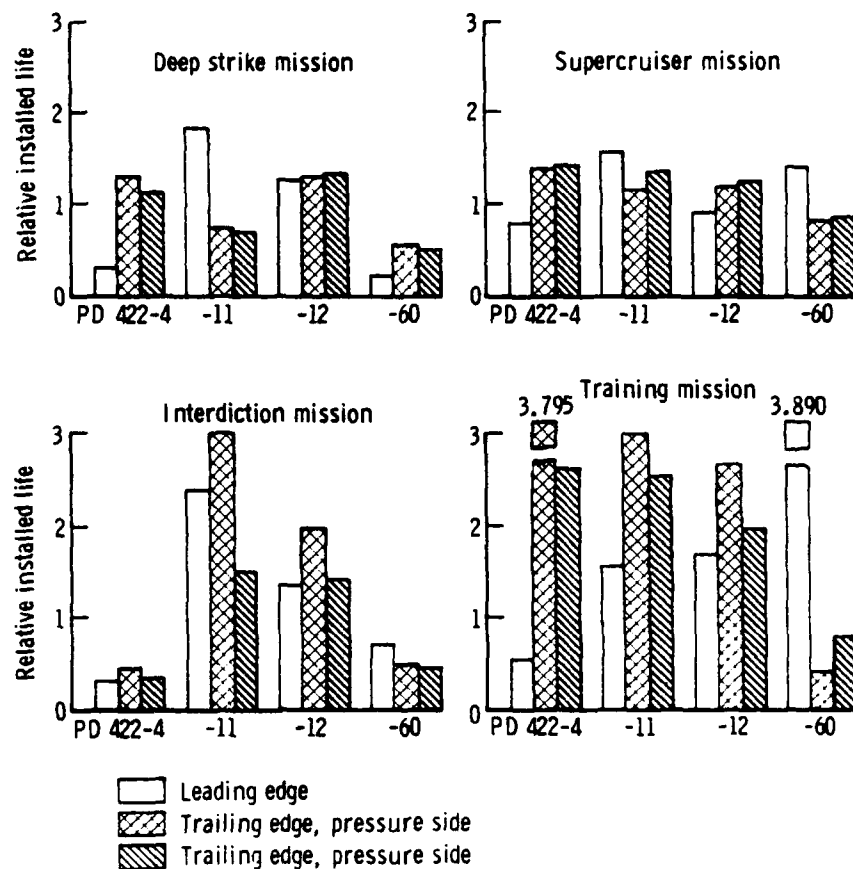


Figure 23. Turbine vane installed life comparison--simplified model relative to original model predictions.

Component characteristics were tabulated for a base-line first-stage turbine vane and blade. Both are cast spar construction with a Lamilloy bonded outer skin. The blade, shown in Figure 29, is made of Mar-M246 spar material and HA188 skin material. The TLCF limiting locations for the spar and skin are shown in the leading edge area. The vane is shown in Figure 30 and made of Mar-M246 spar material with an MA956 Lamilloy skin. The spar and skin critical locations for TLCF are shown in the trailing edge on the pressure side.

These base-line component designs were used as the basis for determining life capability requirements in Task 3.2.4. The base-line turbine vane design was modified in Task 3.1.6 to tailor it to the training mission mix for this advanced tactical fighter application.

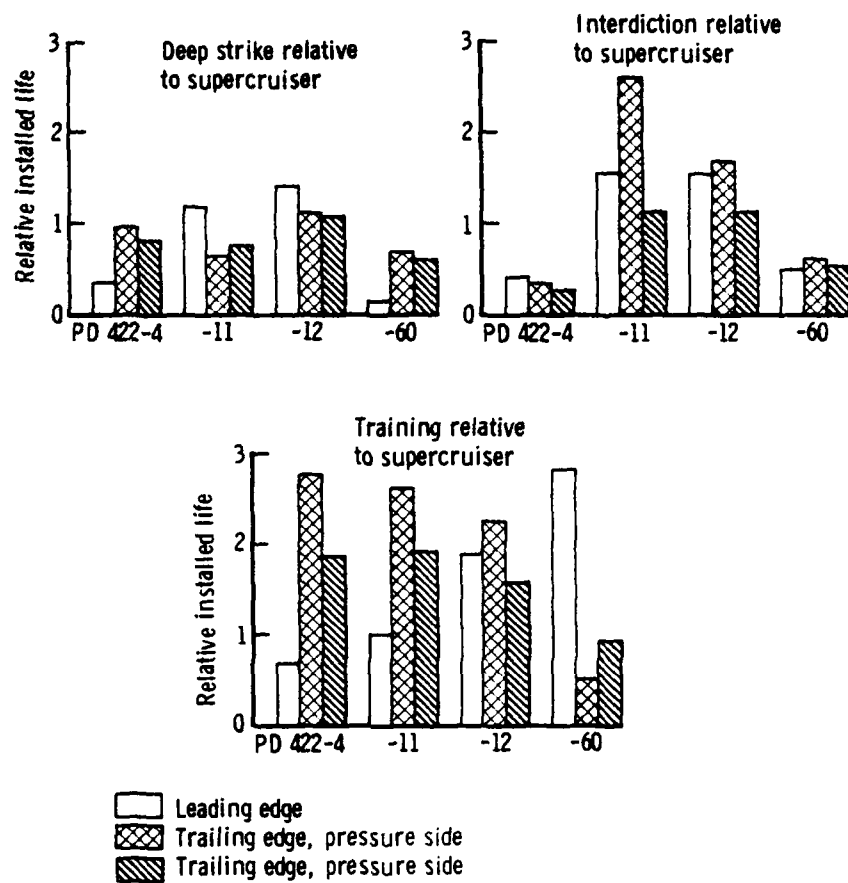


Figure 24. Turbine vane relative installed life comparison--simplified model relative to original model predictions.

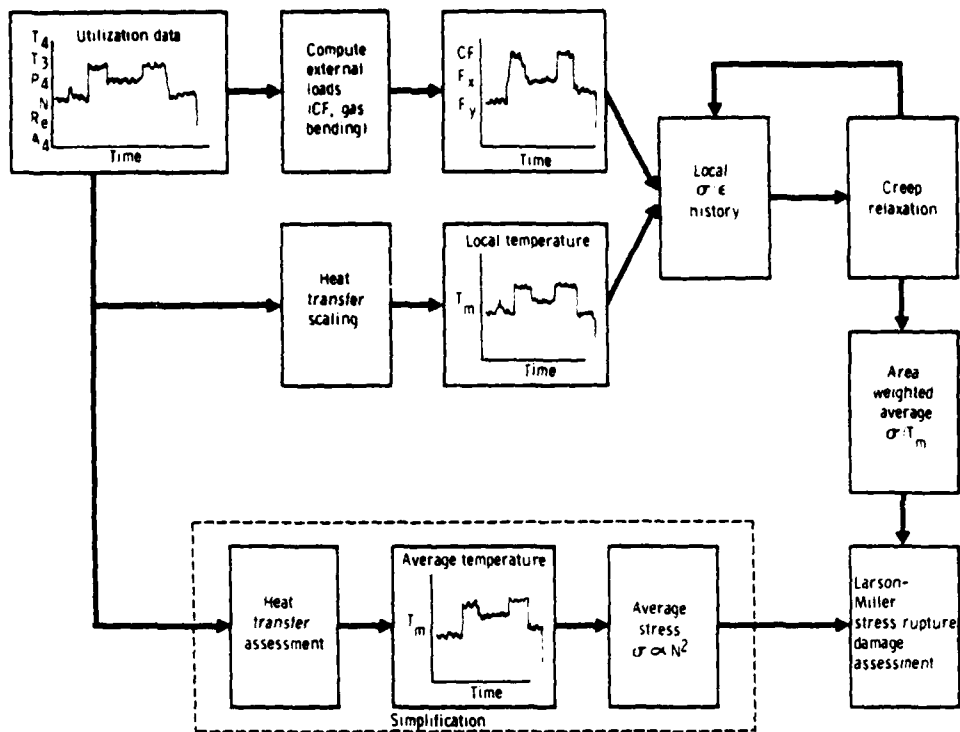


Figure 25. Turbine blade stress rupture model methodology.

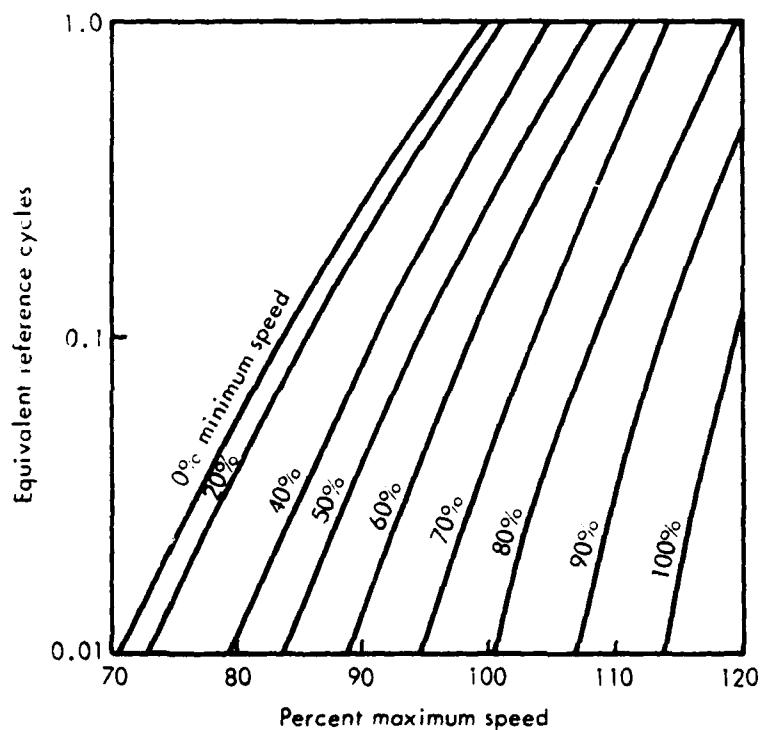


Figure 26. HPC-1 wheel MLCF damage map.

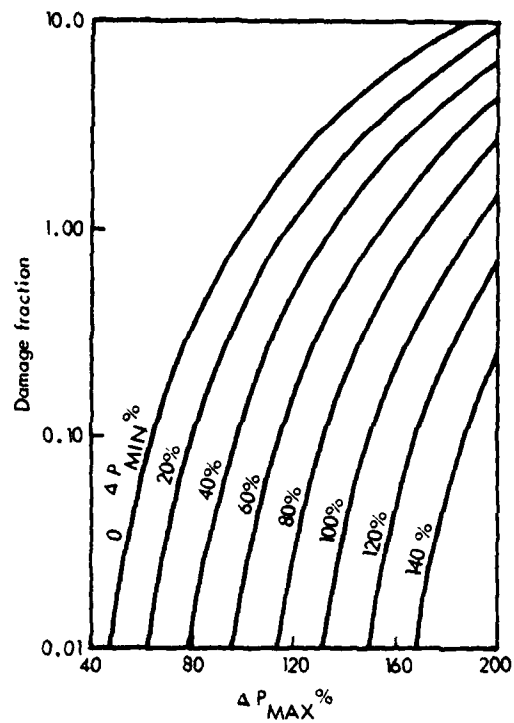


Figure 27. Combustor case MLCF damage map.

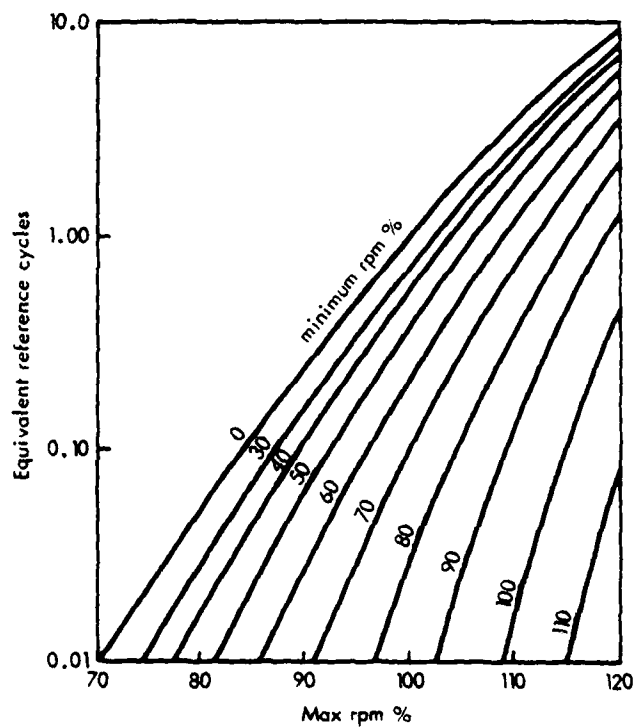


Figure 28. HPT-1 wheel MLCF damage map.

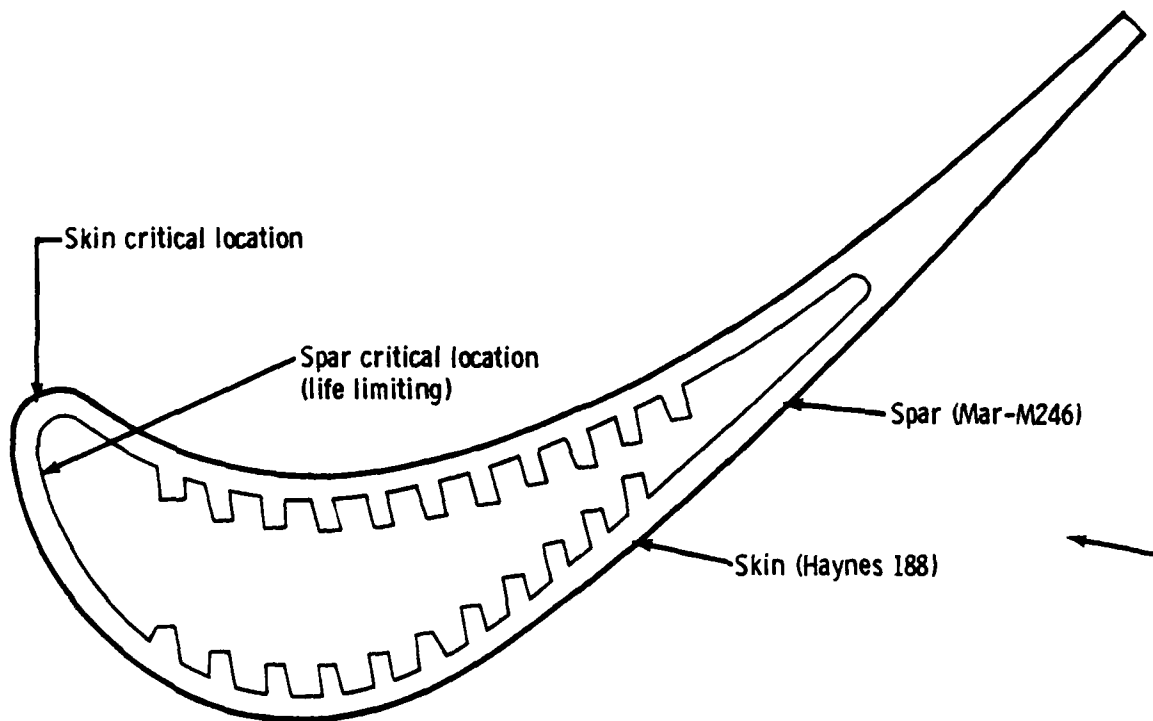


Figure 29. Base-line HPT-1 blade thermal LCF critical locations.

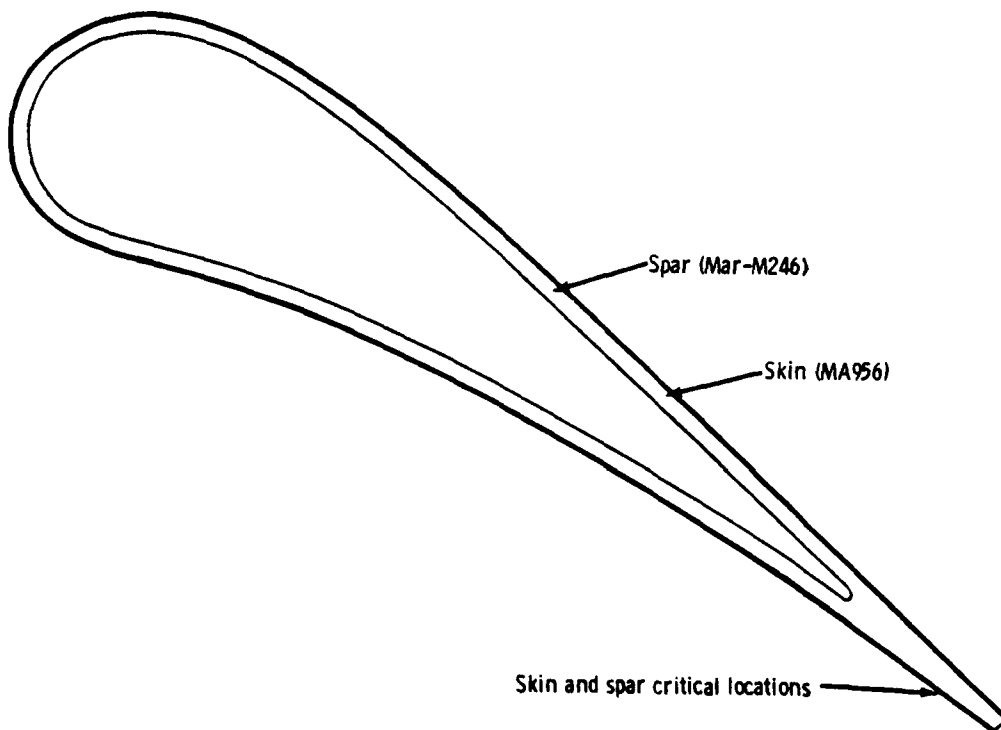


Figure 30. Base-line HPT-1 vane critical locations.

III. TASK 3.1.2--MISSION/PERFORMANCE DEFINITION

Boeing work in Task 3.1.2 covered selection and definition of the base-line airplane for use as a point-of-departure configuration in subsequent screening studies, definition of the wartime design mission flight profile and performance requirements, and definition of representative peacetime training missions based on current Tactical Air Command (TAC) practice.

A reevaluation of the proposed base-line configuration and wartime design mission was required after contract award because of customer deletions in the contract effort. Since only a dry, turbojet engine type was to be examined instead of the two proposed types (augmented turbofan and dry turbojet), an aircraft configuration and associated design mission more in line with this single engine type was desired. Review of several Boeing aircraft configurations being used for tactical applications showed a configuration (Model 987-350) that evolved from previous contract work (ATS) to be well suited for the LUCID contract. The aircraft configuration was a supercruiser design using underwing-mounted, podded engines, a delta wing planform, canards, and semi-submerged weapons.

The LUCID point of departure retained the basic planform and size of the Model 987-350 but incorporated Allison PD414-6 engines with axisymmetric flap nozzles. The resulting configuration is defined as the 987-354 and is shown in Figure 31. Also shown in this figure is a maximum thrust to weight (1.20)-sized version of the airplane. This version was examined to check for any configuration-oriented difficulties in incorporating the large engine size. From this study, no unworkable problems appear associated with the large engine size. The larger engine size was examined to ensure no difficulty in parametric studies to be conducted around the design in Tasks 3.1.4 and 3.1.5. The selected design mission was an all supersonic cruise strike mission. It is illustrated in Figure 32 and consists of a minimal time engine warmup followed by a maximum power takeoff and low level acceleration to a specified q (dynamic pressure) level for start of climb. A constant indicated air speed climb was maintained to the initial supersonic cruise altitude. After the supersonic cruise to the target, a 360-deg turn was made at full power for a maneuver fuel allowance, followed by delivery of the 4000-lb payload. A supersonic cruise back to the base was followed by a no range credit, no fuel burned, descent/decel to a 20-min loiter before landing. Fuel reserves on the mission consisted of 5% of total fuel, and a 5% military standard conservatism was applied to fuel consumption.

The discrete steady-state segments making up the mission are outlined in Table 10. The table shows, by segment, any prespecified features and notes any pertinent aspect of the segment.

The system performance requirements for this mission were selected to simulate a capability that might be expected of a 1995 advanced tactical fighter. These requirements were based on current studies and directly relate to operational or survival considerations.

The specific requirements are shown in Table 11.

Table 10.
Steady-state mission segment buildup for design (combat) mission.

<u>Mission segment</u>	<u>Flight condition</u>	<u>Flight time</u>	<u>Power setting</u>	<u>Comment</u>
Start/warmup	SLS	15 min	Idle	
Takeoff	SL	As reqd	Maximum	
Acceleration	Increased Mach, constant altitude	As reqd	Maximum	
Climb	Increased Mach and altitude	As reqd	Maximum	Constant q
Supersonic cruise	Design Mach, opt altitude	As reqd	As reqd	
Supersonic pen.	Design Mach, opt altitude	As reqd	As reqd	
Turn (maneuver)	Design Mach, opt altitude	As reqd	Maximum	
Weapon release	Design Mach, opt altitude	As reqd	As reqd	Offensive payload
Supersonic return	Design Mach, opt altitude	As reqd	As reqd	
Descent/decel	---	---	---	No fuel, no range
Loiter	Opt Mach SL	20 min	As reqd	No range credit
Landing	SL	---	---	No fuel allowance

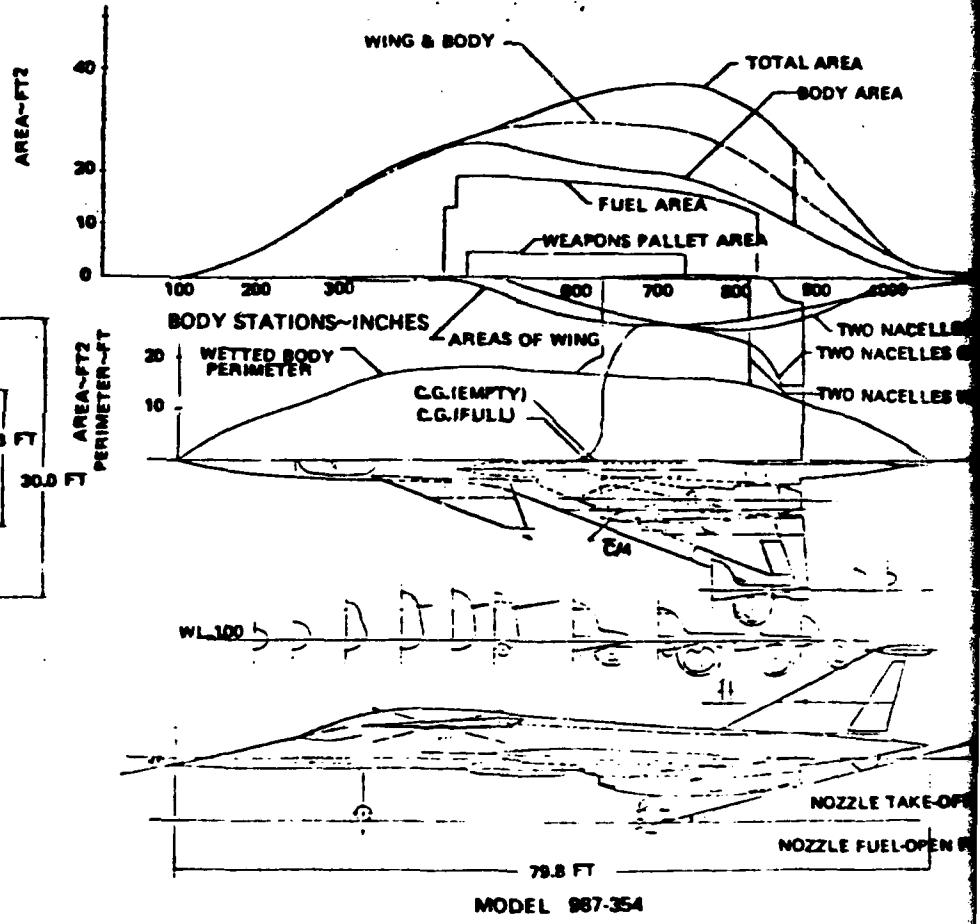
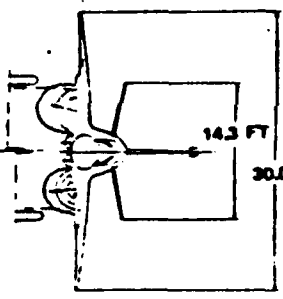
Table 11.
Design mission performance constraints.

<u>Constraint parameter</u>	<u>Required level</u>	<u>Operating condition</u>
Takeoff field length	3000 ft	SL, standard day, max power
Landing velocity	120 knots	SL, standard day, end mission weight
Subsonic maneuver	3.0 g	Mach = 0.90, altitude = 30,000 ft max power, 80% fuel
Supersonic maneuver	2.0-4.0 g's (Mach dependent)	Design Mach, altitude = 45,000 ft max power, 60% fuel
Maneuver fuel allowance (turn)	= 360-deg turn	Design Mach, penetration altitude, max power, with payload

Several of these requirements were determined during a no credit "size" segment in the mission simulator. A "size" segment allows assessment of various performance parameters without impact on the mission itself. Thus consistency of aircraft configuration and operating conditions was maintained for each design considered.

The takeoff and landing requirements were considered compatible with short airfield capability. Landing approach speeds were used in lieu of ground roll since the performance simulator was not set up to compute the latter. The 120-knot landing approach speed was found in other studies to yield approximately 3000 ft of ground roll at end-of-mission aircraft weight.

MODEL 987-346
MODEL 987-354



MODEL 987-354

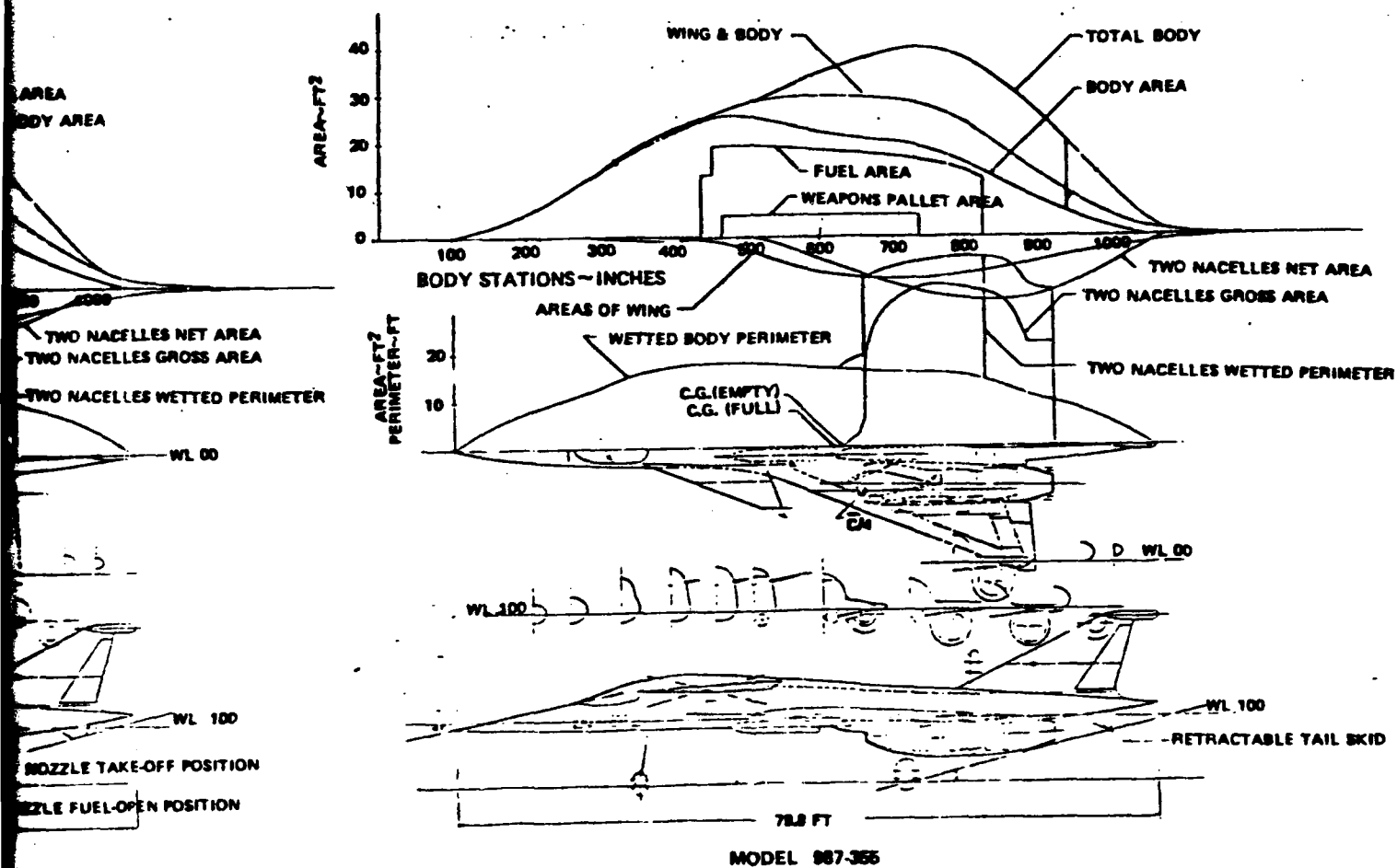


Figure 31. Model 987-354 aircraft general arrangement.

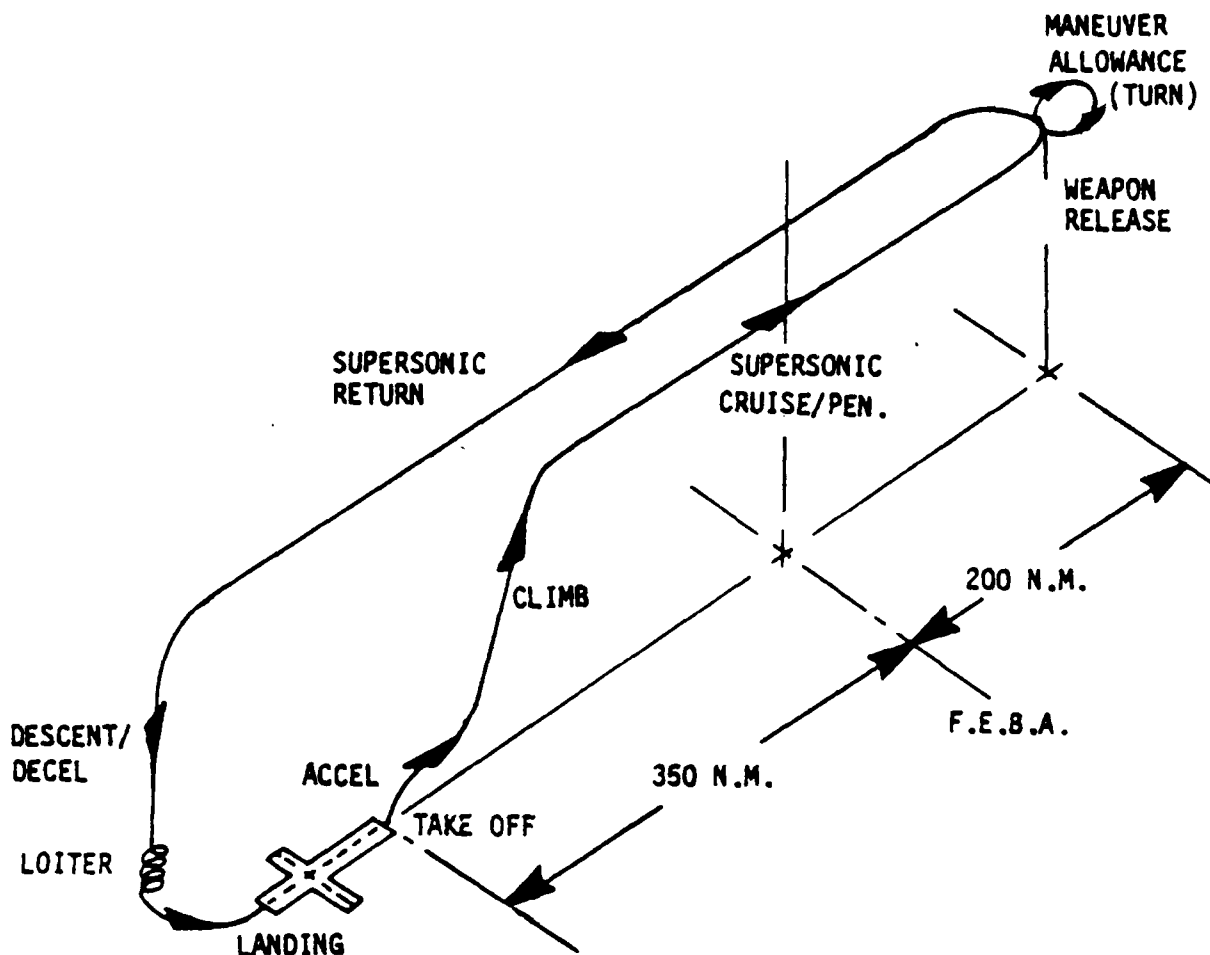


Figure 32. LUCID design mission definition.

These constraints were only applied during the design (combat) mission; they did not apply during training missions.

The wartime design mission provided the system performance definition for LUCID. The cyclic engine usage definition came from the peacetime training missions whereas the time at maximum power usage resulted from the wartime design mission.

The approach taken in defining training usage was to generate time histories of key parameters (Mach, altitude, power setting, etc.) showing both steady-state and dynamic (cyclic) characteristics for several representative mission types. Steady-state usage was derived using a detailed mission segment build-up in the mission simulation program. Dynamic overlays of key parameters on appropriate steady-state mission segments were accomplished by the procedure described under Task 3.1.3.

The development of training mission types and their buildup were guided by current USAF TAC training practices. Such guidance consisted of discussions with TAC pilots and personnel, aircraft training manuals (Syllabus, TAC 51-50 and TAC 55), and flight data from event recorders. Use of such data was tempered, however, as this contract was working at the conceptual design level for a new system and as such did not intend to delve too deeply into minute or specialized details of each current system's training practices.

The general approach used in developing these missions was to set up a base-line mission scenario, define appropriate details for each type of training objective for use within the scenario, and specify fundamental classifications of operation around which each mission type could be flown. Segments for the base-line scenario buildup consisted of the following:

- | | |
|--------------------------------|--|
| o Warmup and taxi | A fixed time segment |
| o Takeoff and initial climbout | Max power accel/climb to initial hold altitude--Altitude determined by mission classification |
| o Segment accel/climb | Stepped altitude climb to cruise--Intermediate altitudes determined by mission classification |
| o Formation cruise (lead) | Nonoptimum altitude/Mach cruise out to target range as flight leader |
| o Primary training objective | A repetitive set of several segments representing a type of training objective (e.g., subsonic weapons delivery) |
| o Formation cruise (wing) | A nonoptimum return cruise to base flying wing man position |
| o Descent/decel and approach | Conventional descent to a fixed altitude, airspeed, and time approach |
| o Touch and go and approach | A series of landings, takeoffs, and approach conditions |
| o Landing and taxi | A final landing and ground roll with a taxi to park aircraft |

The specific details (time, Mach number, altitudes, etc.) and individual mission program segments (accel, climb, hold, etc.) that actually made up these general segments were based on operating practices as summarized from TAC training manuals, pilot interviews, and event flight recorders for each mission type.

The basic mission types, which made up the primary training objective segments, were broken into four training categories. These categories were

- | | |
|-------------------------------|--|
| o Navigation/familiarization | Consists of basic flight maneuvers, navigation, and instrument practice |
| o Air combat maneuver | Consists of individual offensive and defensive air combat maneuvers and mock engagement |
| o Subsonic ground attack | Consists of repetitive target acquisition and subsonic weapons delivery |
| o Supersonic weapons delivery | Consists of supersonic target acquisition, weapons delivery, and missile avoidance maneuvers |

The first three categories represent composite missions from current USAF TAC practice. The major input for their definition was the TAC Syllabus manuals from which mission types, number of sorties, and flight hours were tabulated (see Table 12) and compressed into the three general categories. The fourth category represents training for the LUCID aircraft's primary design role--supersonic air-to-ground weapons delivery. Since the current TAC aircraft inventory does not have any supersonic cruise designed aircraft, no training procedures were available. Therefore, a completely hypothetical mission was developed. The resultant mission profile required that all supersonic operation be within the confines of the USAF "Red Flag" training area and that appropriate ground targets be available within the area. For each of these training categories, two training classifications for each were defined, thereby making up eight training mission profiles. The two training classifications on which these various mission types were flown were

o Initial training

Simulation of operation from a training Air Force base within close proximity to target/weapons range

o Proficiency training

Simulation of operation from an operational base located far from a weapons range--Such location was assumed to necessitate an air-to-air refuel prior to entering the range.

Table 12.
Current TAC training buildup (Syllabus).

Mission	F-4 Basic		F-4 NR		F-4 A/G		F-4 AA		RF-4		F-111A		F-111E		F-111F		F-15		A-10	
	SOR	HR	SOR	HR	SOR	HR	SOR	HR	SOR	HR	SOR	HR	SOR	HR	SOR	HR	SOR	HR	SOR	HR
Navigation	---	---	---	---	---	---	---	---	---	---	---	---	---	---	---	---	---	---	---	---
Evaluation	---	---	---	---	---	---	---	---	1	1.7	1	2.5	1	3.0	1	3.0	1	1.5	3	6.0
Transition	13	19.5	10	15.0	13	19.5	13	20.5	14	23.5	5	12.0	5	12.5	1	2.5	---	---	7	14.0
Formation	4	6.0	---	---	---	---	---	---	---	---	---	---	---	---	---	---	2.5	3.8	---	---
Air refuel	---	---	2	4.8	---	---	---	---	3	6.9	---	---	---	---	---	---	---	---	---	---
Familiarization	17	25.5	12	19.8	13	19.5	13	20.5	18	32.1	6	14.5	6	15.5	2	5.5	3.5	5.3	10	20.0
DACH	---	---	---	---	---	---	---	---	---	---	---	---	---	---	---	---	2	2.0	---	---
ACH	6	4.8	3	2.4	4	2.4	5	4.0	---	---	---	---	---	---	---	---	4	4.2	---	---
OACH	---	---	---	---	---	---	---	---	---	---	---	---	---	---	---	---	---	---	---	---
BFH	8	10.8	7	9.3	8	7.8	14	23.2	---	---	---	---	---	---	---	---	---	---	---	---
OBFH	---	---	---	---	---	---	---	---	---	---	---	---	---	---	---	---	3	3.6	---	---
DBFH	---	---	---	---	---	---	---	---	---	---	---	---	---	---	---	---	5	6.5	---	---
ACT	4	3.2	---	---	---	---	5	4.0	4	6.8	---	---	---	---	---	---	---	---	---	---
DACT	---	---	---	---	---	---	---	---	---	---	---	---	---	---	---	---	4	4.0	4	7.2
Intercept	---	---	---	---	---	---	---	---	---	---	---	---	---	---	---	---	3	5.0	---	---
Air combat	18	18.8	10	11.7	12	10.2	24	31.2	4	6.8	---	---	---	---	---	---	21	25.3	4	7.2
GA	11	15.4	7	13.1	15	25.5	6	7.8	---	---	4	10.0	3	7.5	3	8.5	---	---	---	---
GAT	5	6.5	5	6.5	8	10.4	---	---	---	---	---	---	---	---	---	---	---	---	8.5	19.8
GAM	4	5.2	---	3.9	---	---	---	---	---	---	---	---	---	---	---	---	---	---	---	---
GAR	---	---	3	5.1	5	7.5	3	4.5	---	---	---	---	---	---	---	---	---	---	---	---
SAD	---	---	---	---	---	---	---	---	---	---	10	28.0	7	19.0	4	11.5	---	---	6.0	19.8
SAR	---	---	---	---	---	---	---	---	---	---	6	16.5	4	10.5	3	8.0	---	---	---	---
Ground attack	20	27.1	18	28.6	28	43.4	9	12.3	---	---	20	54.5	14	37.0	10	28.0	---	---	14.5	39.6

The predominant effects of proficiency versus initial classification on training were to reduce the time (fuel) available for repetitive sets of the primary training objective, by virtue of the cruise range required to get home from the target area; provide nonoptimum Mach, altitude subsonic cruise segments from and to the target area; and change the level of engine operation during maneuvers. Also, by varying the ratio of initial to proficiency training, which makes up the total usage definition, various stages of aircraft maturity could be simulated.

Stick (steady-state condition) mission definitions of these eight training uses were done through detailed segment (e.g., climb, accel, turn, cruise, etc) buildups in the mission simulation computer program. The large number of segment parameter definitions (e.g., rates of change, altitude, and Mach) needed necessitated very extensive computer simulation. In general, these missions required six to eight times the number of segments used to define the wartime design mission. A sample of the stick mission output of Mach, altitude, and power setting for each mission is shown in Figures 33 through 40. Development and generation of the dynamic component to be added to appropriate steady-state segments for definition of the complete usage are discussed under Task 3.1.3.

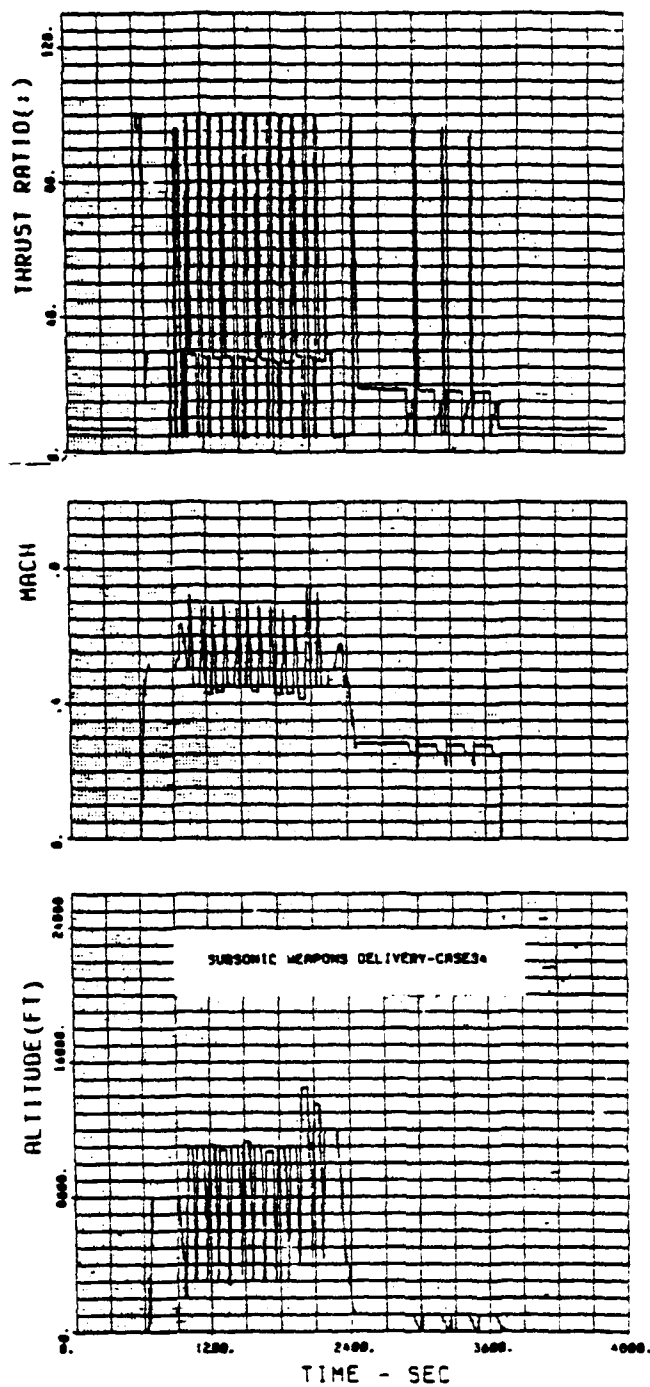


Figure 33. Stick mission aircraft utilization--subsonic weapons delivery/initial training.

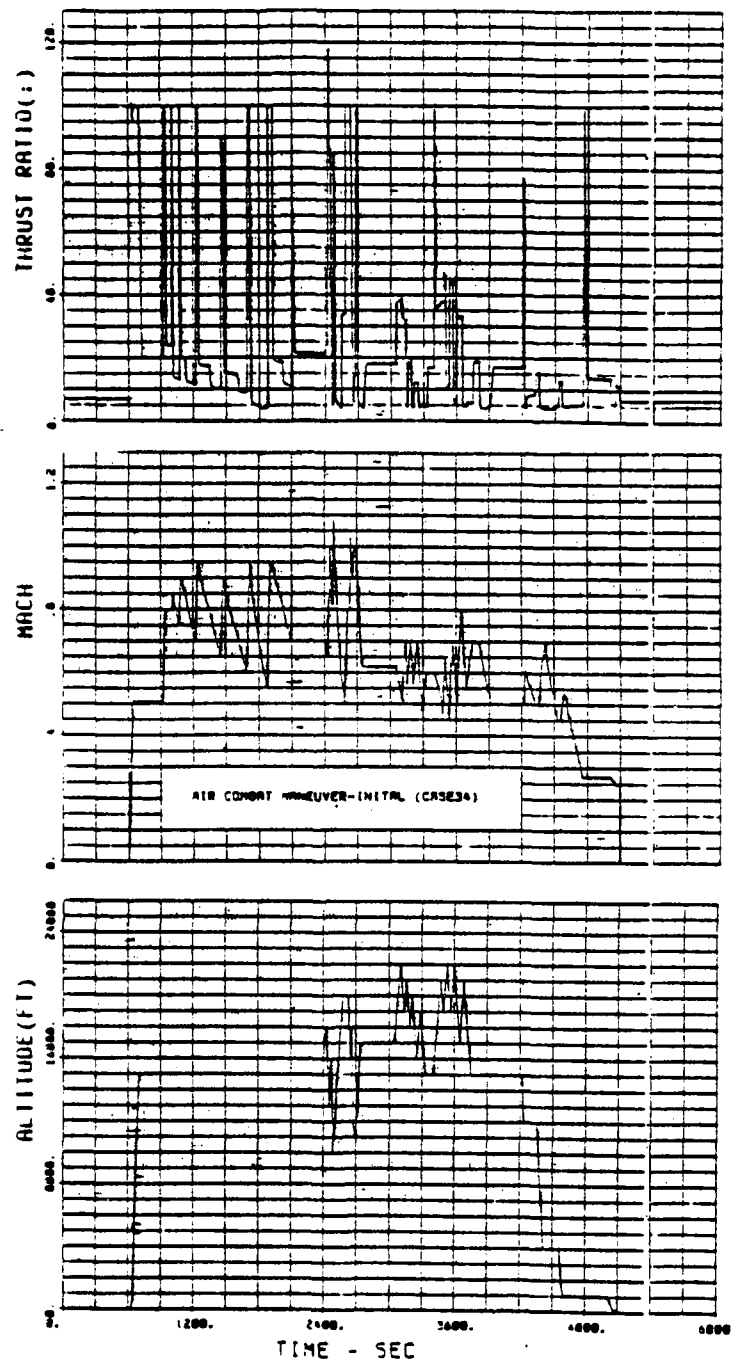


Figure 34. Stick mission aircraft utilization--air combat/initial training.

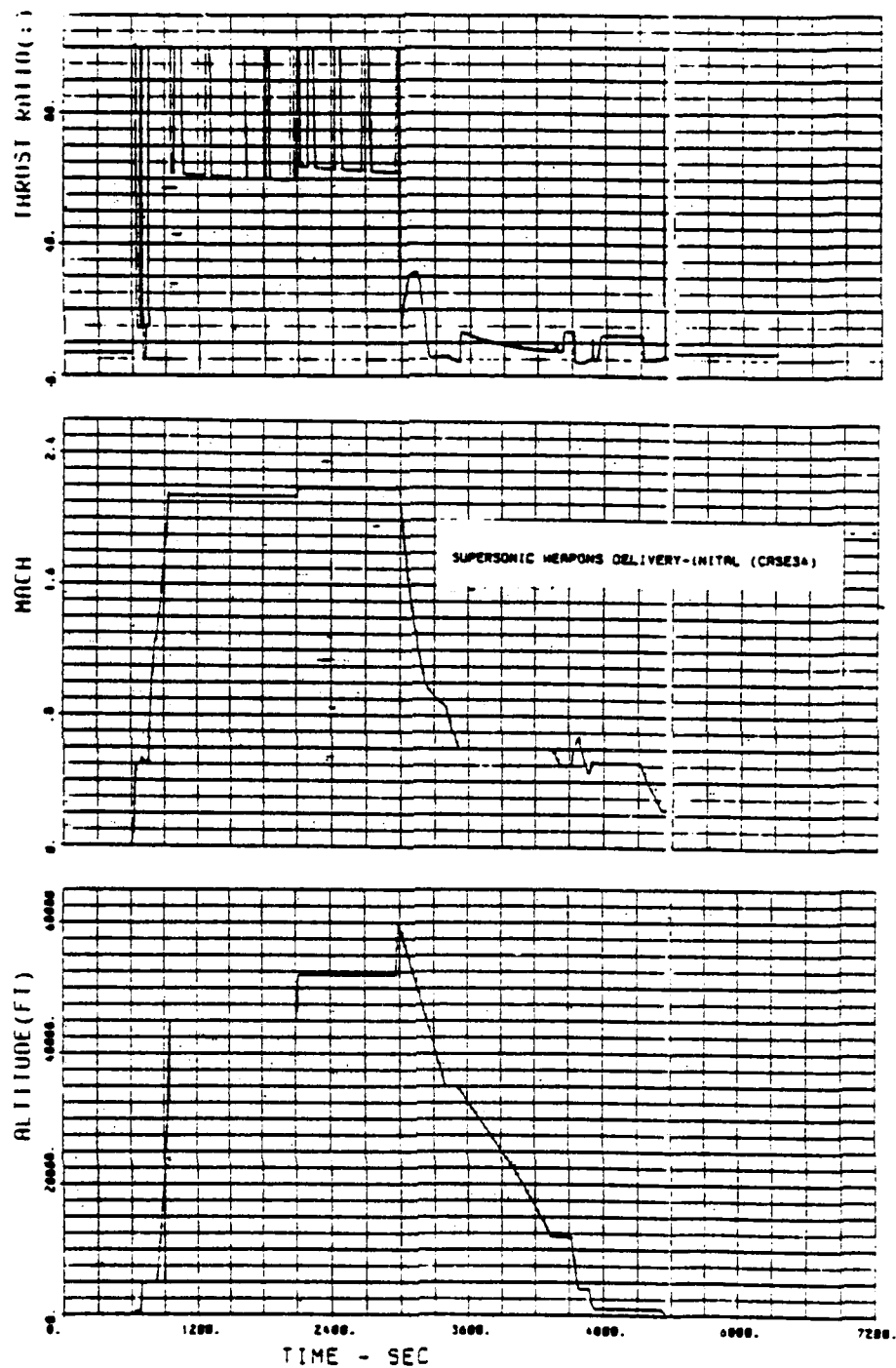


Figure 35. Stick mission aircraft utilization--supersonic weapons delivery/initial training.

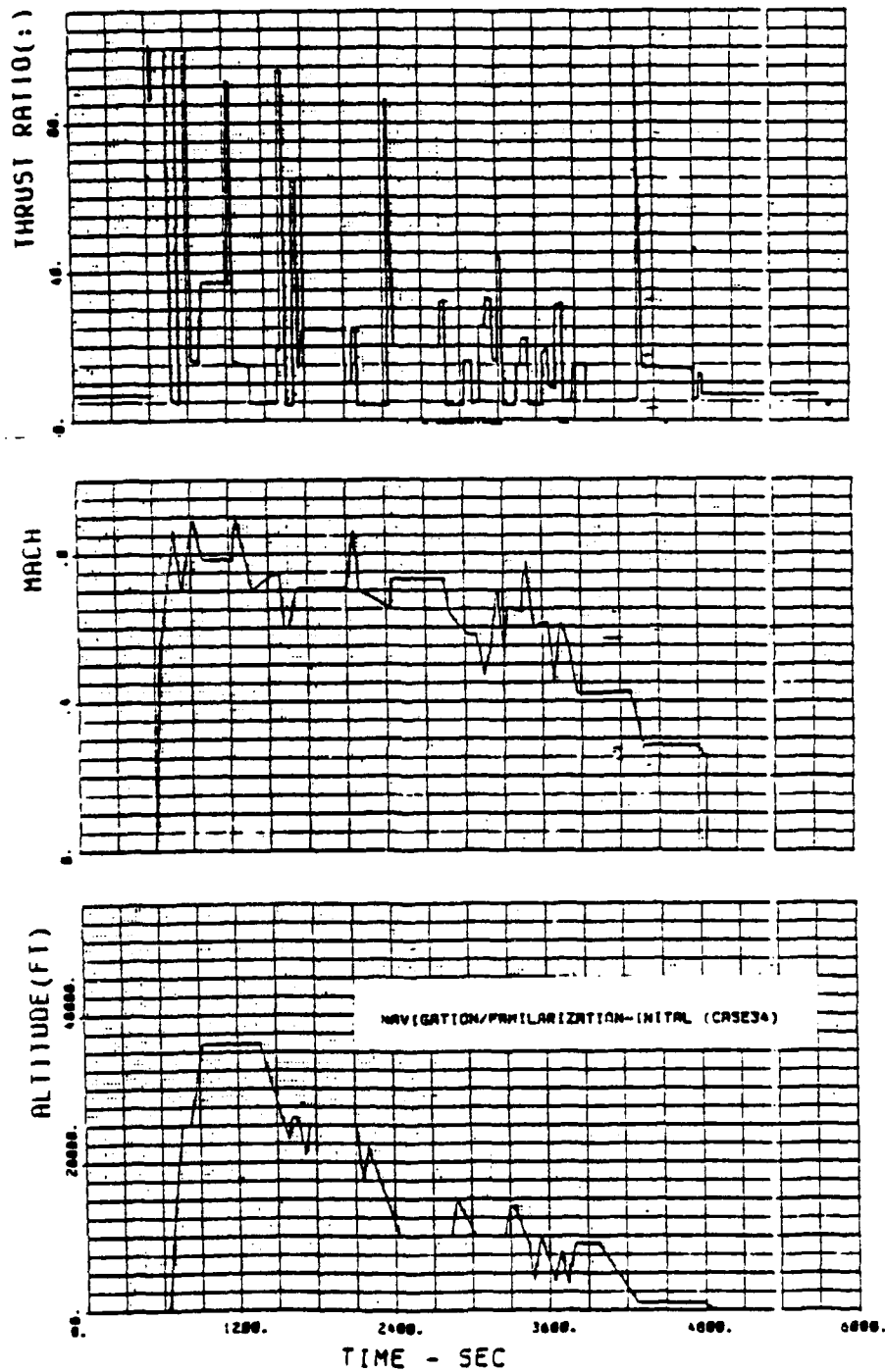


Figure 36. Stick mission aircraft utilization--navigation/familiarization/initial training.

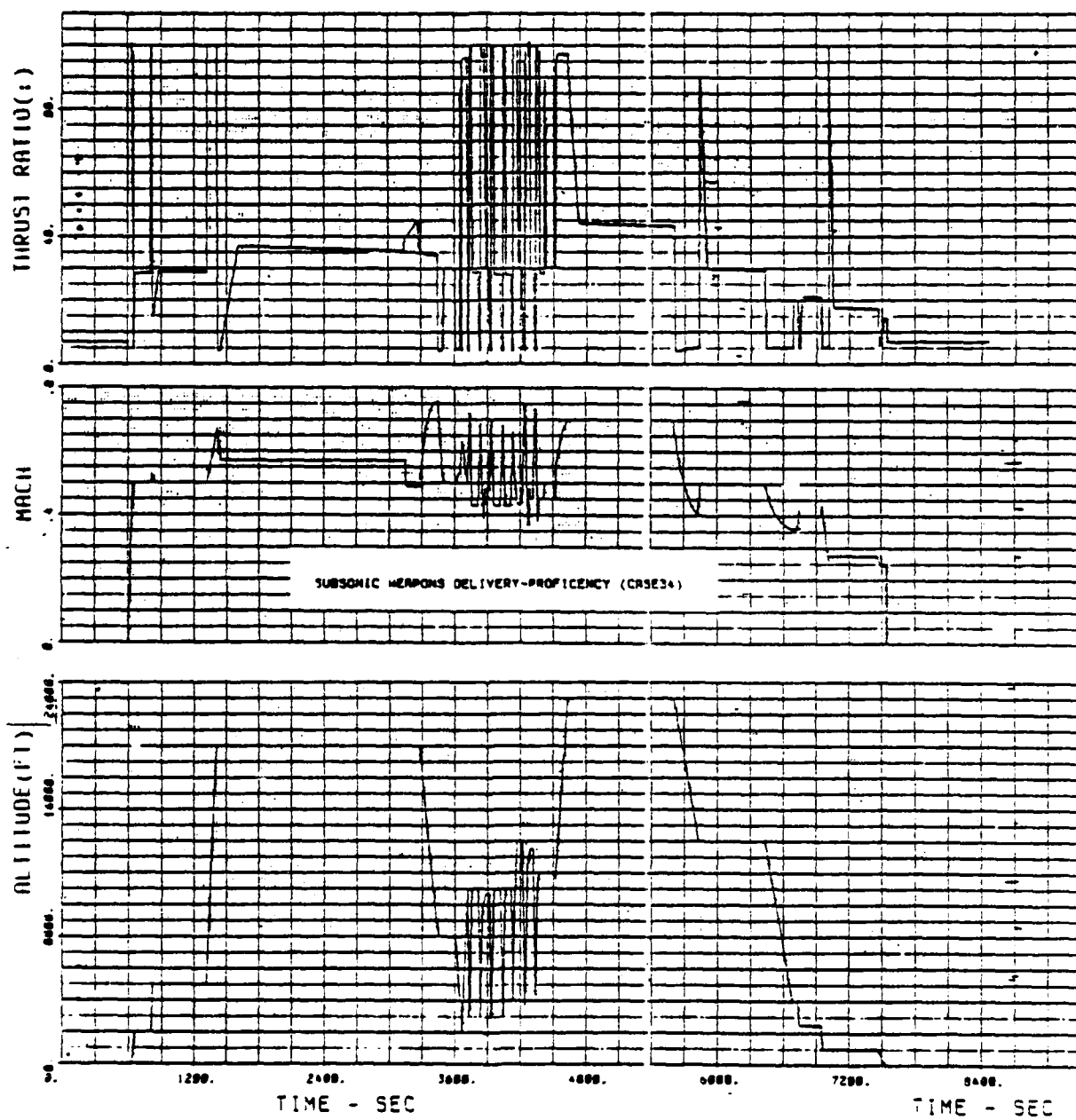


Figure 37. Stick mission aircraft utilization--subsonic weapons delivery/ proficiency training.

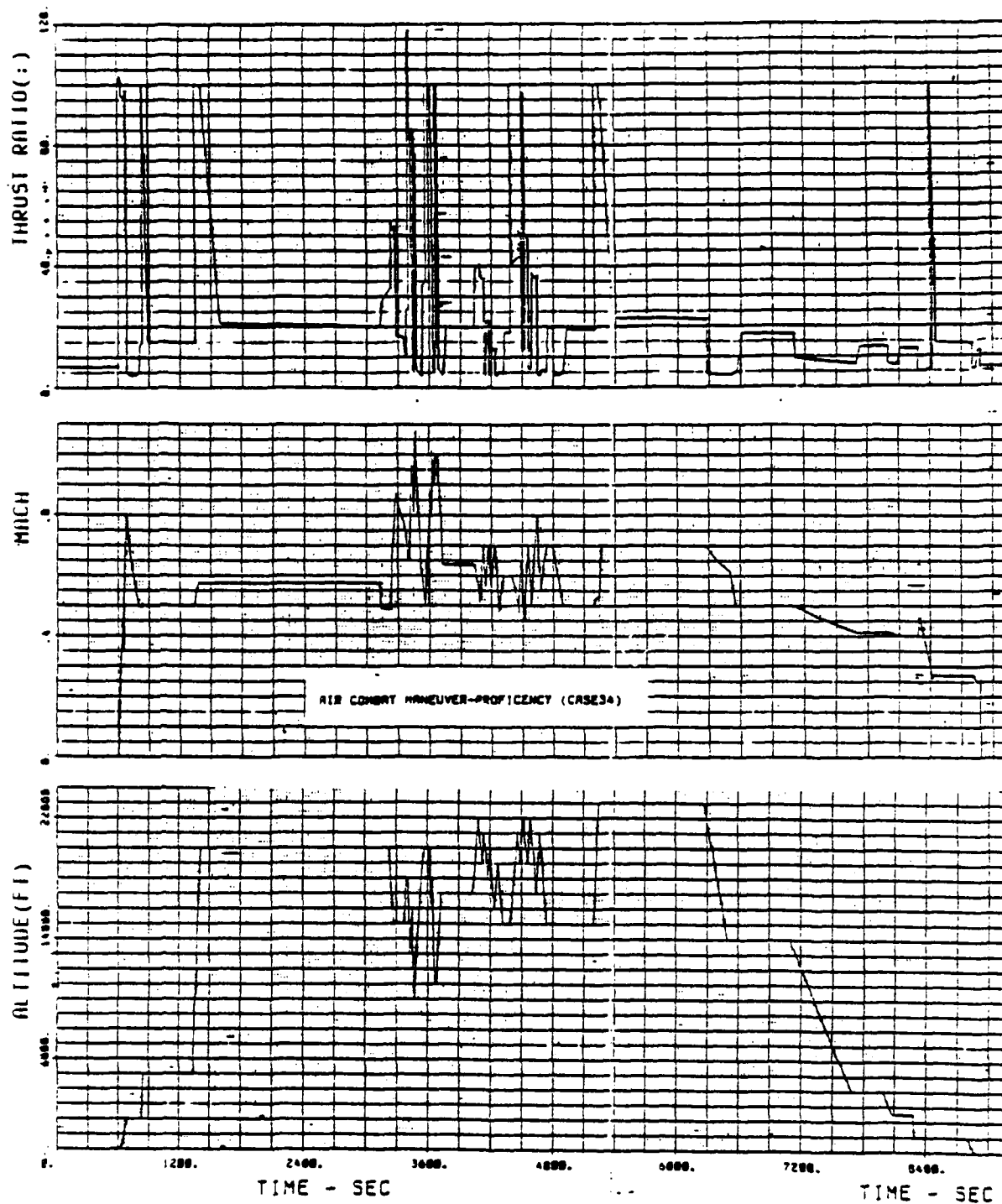


Figure 38. Stick mission aircraft utilization--air combat/proficiency training.

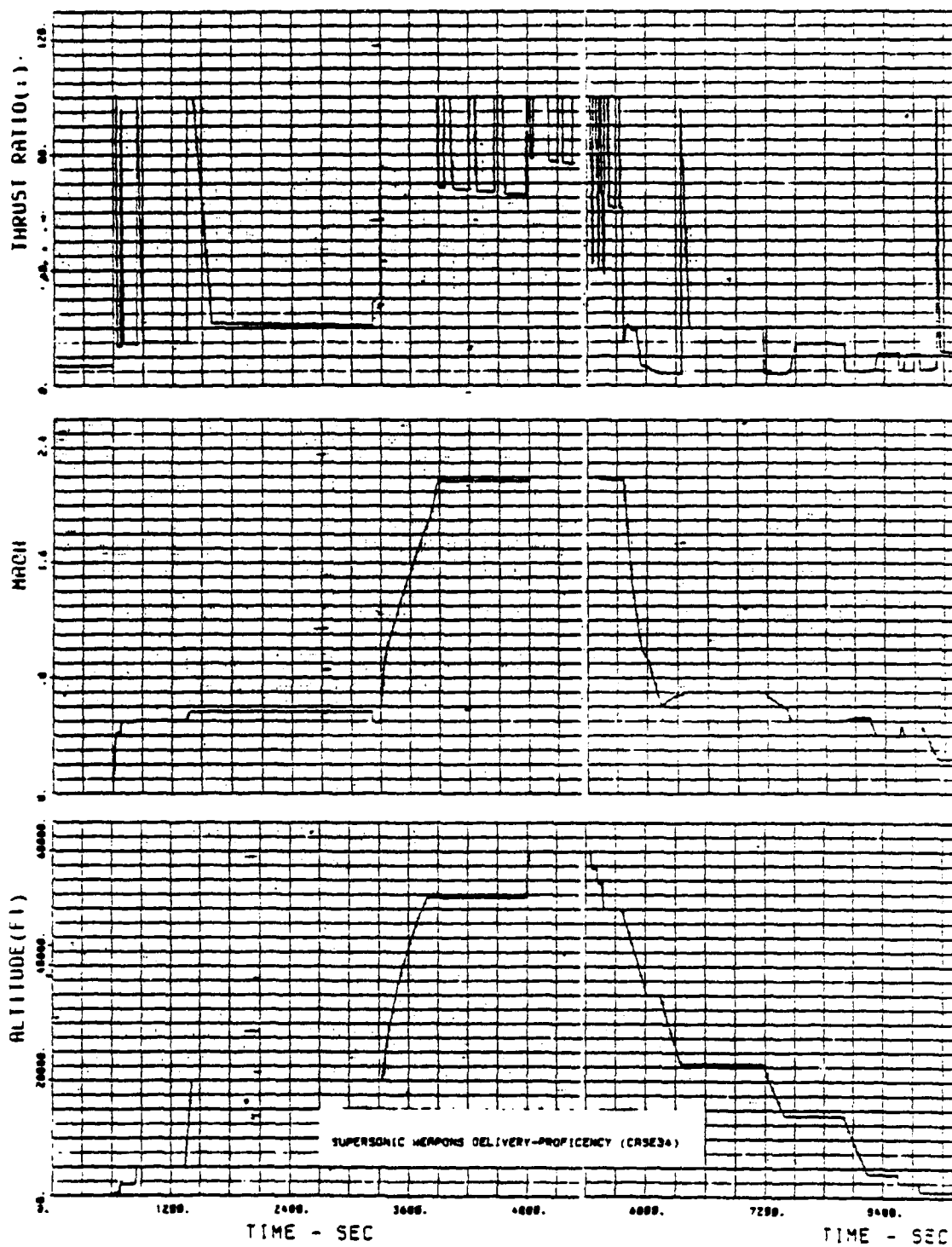


Figure 39. Stick mission aircraft utilization--supersonic weapons delivery/proficiency training.

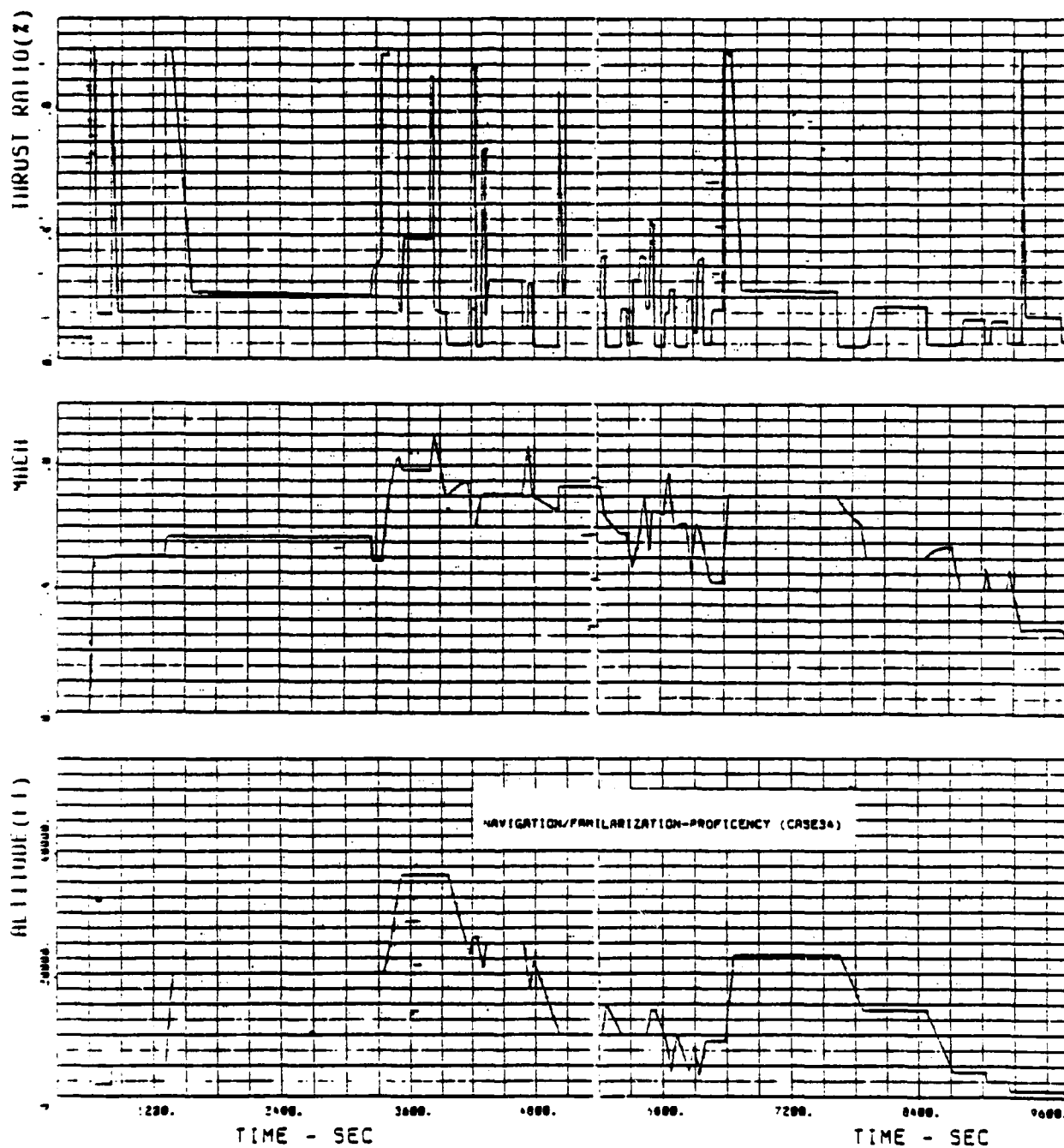


Figure 40. Stick mission aircraft utilization--navigation/familiarization/proficiency training.

IV. TASK 3.1.3--UTILIZATION PREDICTION PROCEDURE DEVELOPMENT

The purpose of this task was to develop a procedure to predict how an advanced, high-performance vehicle was utilized. This utilization information would then be used to assess the cyclic and creep/rupture distress upon the engine structure. The utilization procedure addresses the various training objectives, initial pilot training, and pilot proficiency maintenance, via different mission types, including throttle movements that are typical of pilot throttle activity during a flight. Boeing developed a capability to predict time-varying aircraft usage for different mission types, and DDA developed a technique to convert this data to an engine time history of internal engine parameters. These are graphically depicted in Figure 41. In Phase II Boeing addressed a mission mix to determine the frequency for each training mission. This section describes first DDA's contribution and then Boeing's effort in this task.

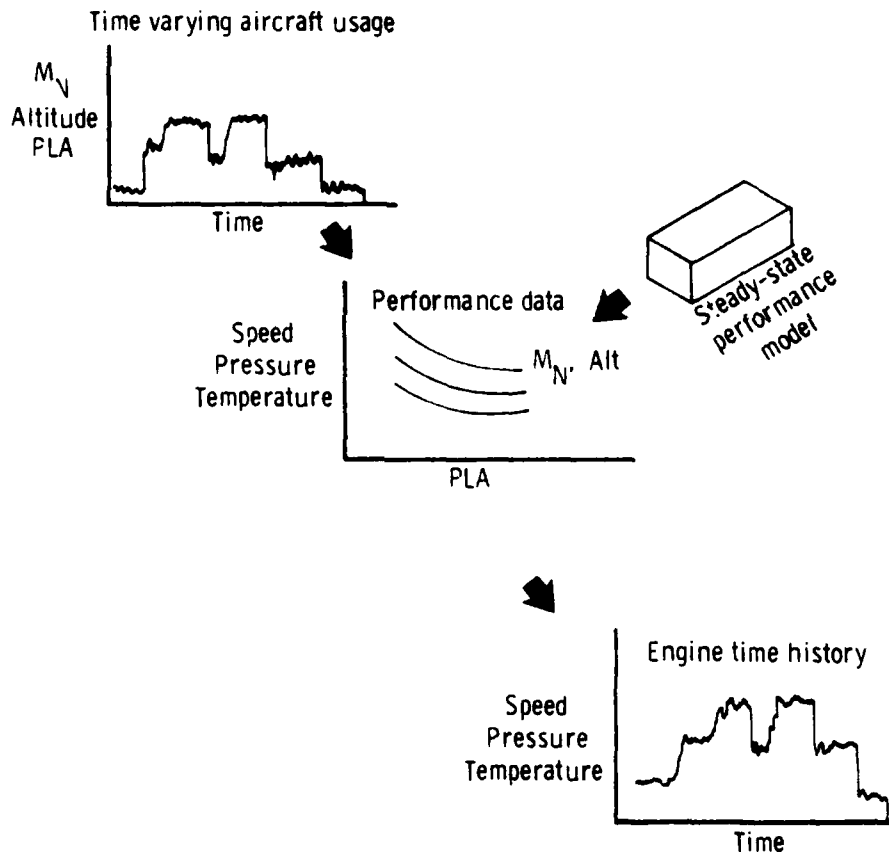


Figure 41. Utilization prediction procedure.

The primary objective that DDA addressed was to predict time-varying histories of internal engine parameters that could be used to predict component damage for this time history. Component damage is sensitive to the time-varying loads and environments. Thus, it was necessary to predict appropriate internal engine parameters to be used for load and environment definition in time. In examining available Inflight Engine Condition Monitoring System (IECMS) data for the A-7 aircraft/TF41 engine, internal engine parameters such as speed and turbine temperatures respond to Mach, altitude, and power setting inputs. This response is dependent upon the engine control system and the engine response characteristics (i.e., inertias). Because this prediction procedure is to be applied during conceptual design, tools are available to predict steady-state loads and operating temperatures at a level of effort compatible with conceptual design. Therefore, the engine response characteristics have been ignored to simplify the time history definition process. Advanced electronic controls, which can handle complex control algorithms, tend to significantly reduce overshoot problems that exist with today's hydro-mechanical control systems. In addition, the necessity for trimming the engine control system in the field will be decreased by the electronic control capability to self trim. Therefore, the time history definition process is judged reasonable for conceptual design using steady-state assumptions. The technique for converting time-varying aircraft usage to engine time histories was to develop a table of performance data with a steady-state performance model and interpolate with Mach, altitude, and power setting at each instant in time (see Figure 41). The internal engine parameters were then limited to spool speeds and component inlet/exist conditions (pressures and temperatures). The damage models then were developed to address loads and operating temperatures for these data. For the dry, variable geometry turbojets and components/failure modes addressed for LUCID, the following data were required for each instant in time:

N	Rotor speed
CDP	Compressor discharge total pressure
CDT	Compressor discharge total temperature
RIT	Turbine rotor inlet total temperature
P _a	Ambient static pressure
P ₁	Engine inlet total pressure
A ₄	Turbine variable geometry setting

Because Boeing had to predict the required power setting for each aircraft maneuver, this technique was utilized by Boeing to predict engine time history data for each mission. DDA supplied guidelines to Boeing for them to determine how frequently engine time history data were required. The basis for these guidelines was a $\pm 10^\circ\text{F}$ change in turbine blade metal temperature. Since metal temperature changes with M_N and altitude at both constant power settings as well as varying power settings, the following guidelines were transmitted to Boeing:

o Climbs (constant M_N and power setting)

Altitude	
0-20,000	2000-ft intervals
20,000-36,089	1500-ft intervals
36,089-50,000	600-ft intervals
50,000-70,000	500-ft intervals

o Accelerations (constant altitude and power setting)
0.03 M_N intervals

o Cruises (constant M_N and altitude)
2% max thrust interval

These guidelines were to be used to determine the time frequency of data in the aircraft time-varying usage and also to form judgments about significance of dynamic variations in altitude, Mach number, and power setting. The primary Boeing objective in this task was to develop and verify a unique method that used actual flight data to define the dynamic operation of an aircraft and engine. The method considered only the dynamic component of a parameter (e.g., power lever angle--PLA), over a recognized segment type (e.g., approach, wingman cruise, etc.). Such data were mathematically reduced to display the distribution of amplitudes with frequency, i.e., its power spectral density (PSD) distribution. Comparison of PSDs from several flights of the same aircraft allowed definition of an average PSD for that aircraft. Doing the same for several aircraft provided an average segment PSD for a generalized class of aircraft. This PSD could then be converted back into a representative dynamic variation of the specific parameter with time. A schematic representation of this procedure is shown in Figure 42.

The primary steps that this task encompassed were collect, review, sort, and edit available flight recorded data; select and modify existing spectral analysis programs to accomplish the data reduction; and, finally, verify that the approximations provide acceptable representations of usage as judged by resultant engine component damage.

Availability of continuous flight recorded data for tactical aircraft on training missions was found to be quite limited. The primary sources for such data were DDA IECMS (A-7 aircraft), NAPC (S-3A, AV-8A, and F-14 aircraft), and AFWAL-POTA (A-10 aircraft). Although other potential sources were found, no usable data materialized. Without exception, all of the available data required some degree of filtering, correcting, and/or editing of the time-dependent signals. Two examples of such data modifications are shown in Figures 43 and 44. In Figure 43, the data had two different signals of the same parameter (PLA) covering the same time span. In this case, one signal was found to be from a different flight so it was edited out. In Figure 44, spurious signals, possibly recording noise or vibration, were part of the PLA time trace. By setting a filter to remove data whose rate-of-change in PLA was greater than possible on the aircraft, the majority of bad data was removed. However, some questionable spikes, which required closer examination, can still be seen to exist. Other typical difficulties encountered consisted of repetition of a time trace sequence at different intervals within the flight, "hiccups" or step jumps in one or more parameters intermittently or rhythmically during a flight, "dead bands" in one or more parameters where either no data or a constant level of data was recorded, and out-of-range data that apparently were limited in value because of recorder/sensor abnormal operation. All these problems made the flight data reduction very tedious and time consuming.

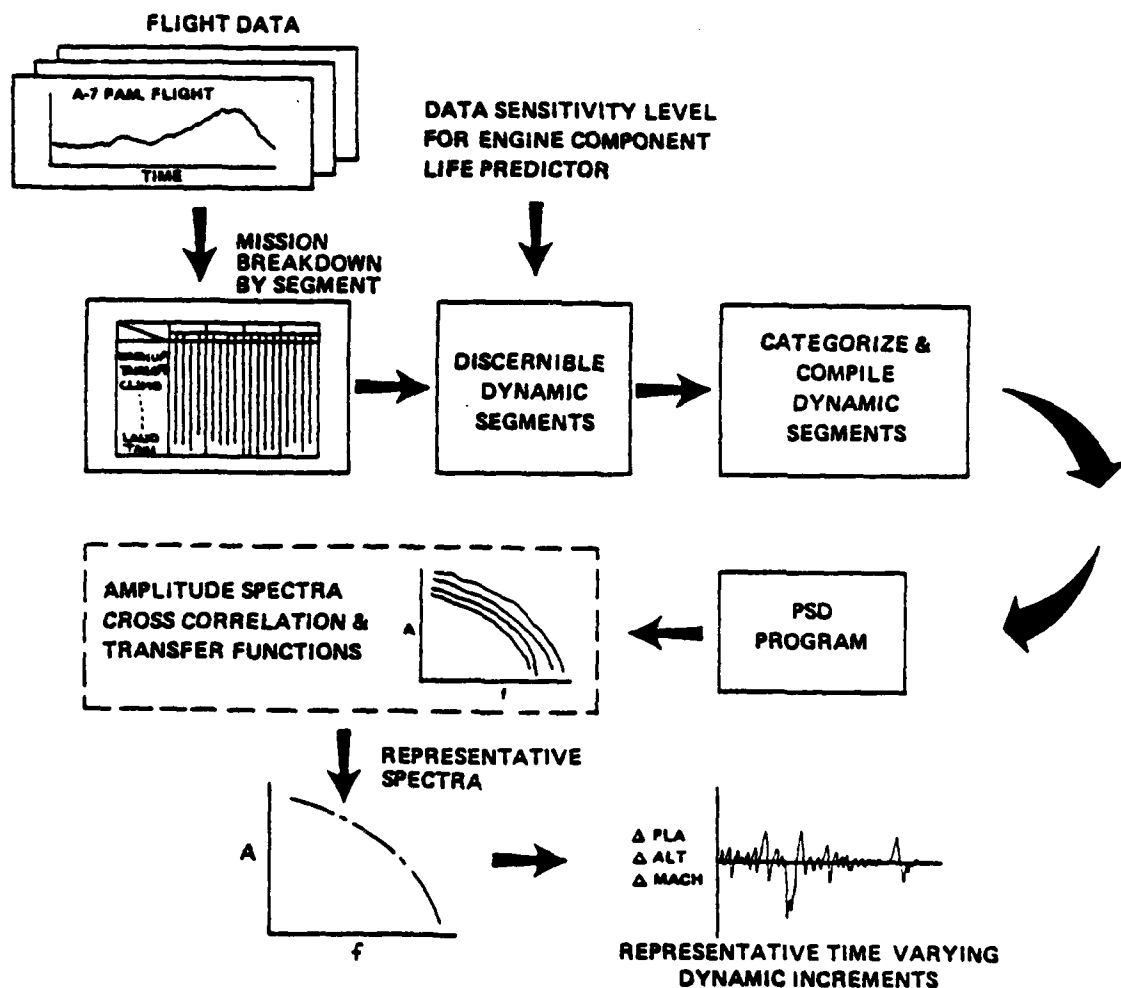


Figure 42. Dynamic usage procedure.

Another very slow and unfruitful task was breaking down each flight into consistent segment types. Since no definition of aircraft operation with time was provided for much of the data, cross correlation of parameters (altitude, Mach, PLA, g) was the only way to attempt to classify segments. Initially, it was attempted to break the flights down into very basic definable operations (e.g., climb, accel, cruise, etc.) as shown in Table 13. This proved to be too tedious and left too much to guesswork. Also, it showed that much of the engine usage, as defined by PLA, was either step function or transient, not dynamic (cyclic).

Thus, a more expedient approach was taken of breaking out only obvious dynamic segments. In conjunction with this, DDA defined accuracy bands to the primary parameters of interest for their engine life models. These tolerance levels showed that the primary parameter to work on was engine thrust, which was best correlated to PLA. An example of the tolerance band for altitude, air speed,

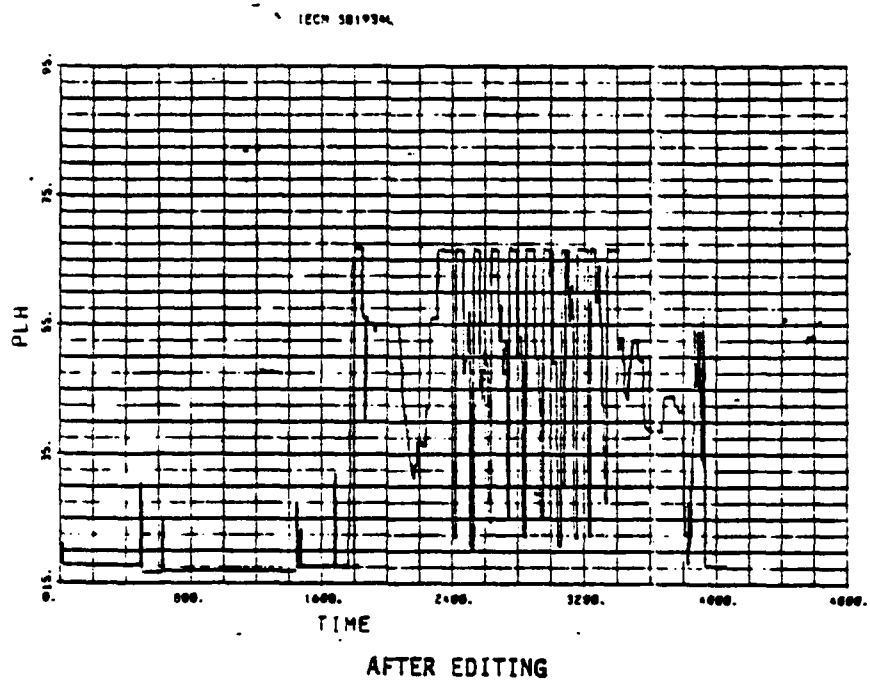
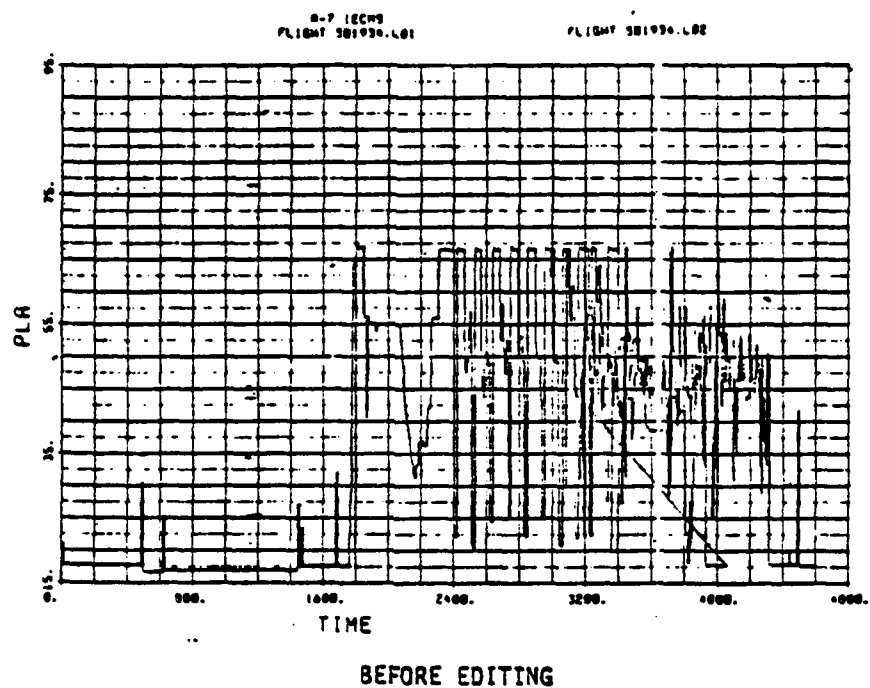


Figure 43. Example of editing A-7 IECMS data.

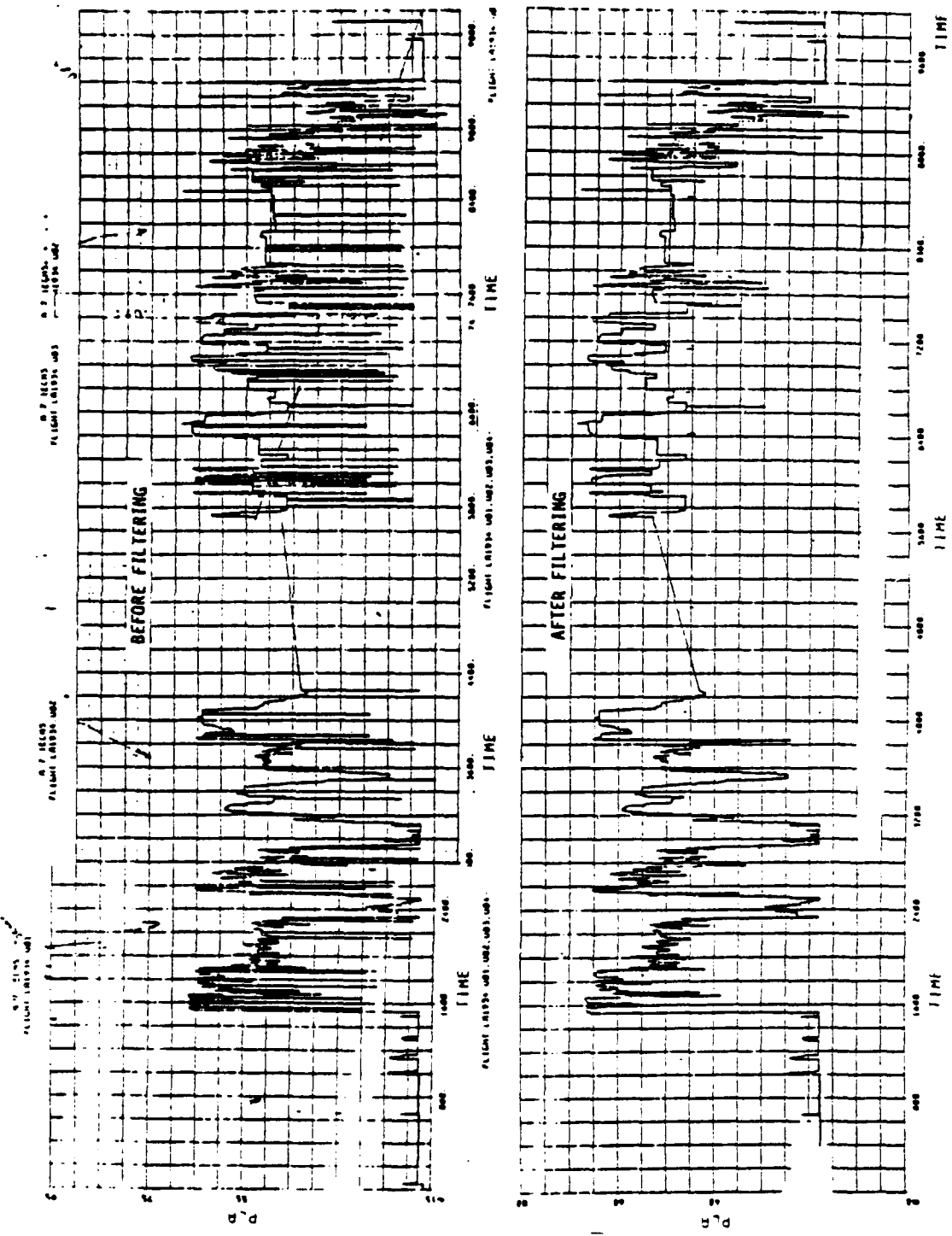


Figure 44. Example of filtering A-7 IECMS data.

Table 13.
Flight data segment breakdown.

Mission/segment	Mission segmented flight data												A-10 1-16													
	F-14A						S-3A							AV-8B						A-7						
	1	2	3	4	5	6	1	2	3	4	5	6	7	1	2	3	4	5	6	7	8	9	10	11	12	
Warmup/taxi		1	1	1	1				1	1	1		1				1	1	1	1	1	1	1	1	1	
Take-off/climbout		1	1	1	1				1	1	1		1				1	1	1	1	1	1	1	1	1	
Hold		1	1	1	1					2	1						1		1			1				
Accel/climb			1	1	1					1	1						1	1	1	2	1	1	1	1	1	
Accel										2	2									2	1	1	1	2		
Climb		1			1				1	2	1		2				1									
Climb/decel		1				1					1		1													
Cruise (solo)																	1				2	1	1		3	2
Const alt A/S		2			1	1	1				2	3	4	8		1										
Const alt											1	1														
Const A/S		1																								
Cruise (wing)											2													2		
Const alt A/S						2											1							1		
Const alt																										
Const A/S																										
Decel											2	2									1					
Descent			1	1	1	3			1	3	1	1	2							1					2	
Descent/decel		2									2		2			1	1				3	2			1	
Descent/accel		1											1							1						
Approach		3	3	3	3	4					4	2	4							1				1		
Descent/touch		3	3	3	3	4					27	4	2	4						1	1	1	14	1	1	1
Touch/climbout		2	2	2	2	3					3	1	3													
Landing/taxi		1	1	1	1	1					2	1	1	1						1	1	1	1	1	1	1
Unknown		1	1								1	4		1		1	2									
RFD data		2	2	1		2					1		2	1		1	1	1	2				3	2		5
Air-air				2																						
Ground attack, H			1												2						2	11				3
Ground attack, L																										
Checkout						1									1		1									

38 pass

38 passes

and thrust (percent low rotor speed used as it is proportional to thrust and was a recorded parameter) is shown in Figure 45 for an approach segment of an F-14. From review of the available flight data, only two truly dynamic segments were defined--wingman cruise and approach/ground controlled approach (GCA). Other segment types were defined but were found to have insufficient data or were more like step functions in engine operation. In this latter category were the following segment types: ground operation--transient, low level throttle spikes; ground attack (subsonic dive bombing only)--large amplitude step function throttle; air combat maneuver, air-to-air refuel, ground attack (strafing or pop-up)--insufficient data.

Although many segment types were not used for PSD representation, the insight into how they were flown provided valuable assistance in the stick mission computer simulation.

Initial attempts to generate spectral distributions of selected flight data showed severe shortcomings in available computer programs. This was corrected through outside development of a tailored PSD computer program. Some of the features required in the PSD program were capability to combine several single flight segment spectra into one composite spectrum; combine spectra generated from different time increments and time spans; generate a representative time trace from a spectrum; include a random or definitive phase angle; and limit the frequency band (clip) of a spectrum when converting back to a time trace.

In addition to the PSD program, several peripheral computer programs were also developed. These programs allowed conversion of raw flight data into data sets for spectral analysis and on-line display of dynamic components from inputs (raw) and output (PSD-generated) time trace plus the PSD distribution.

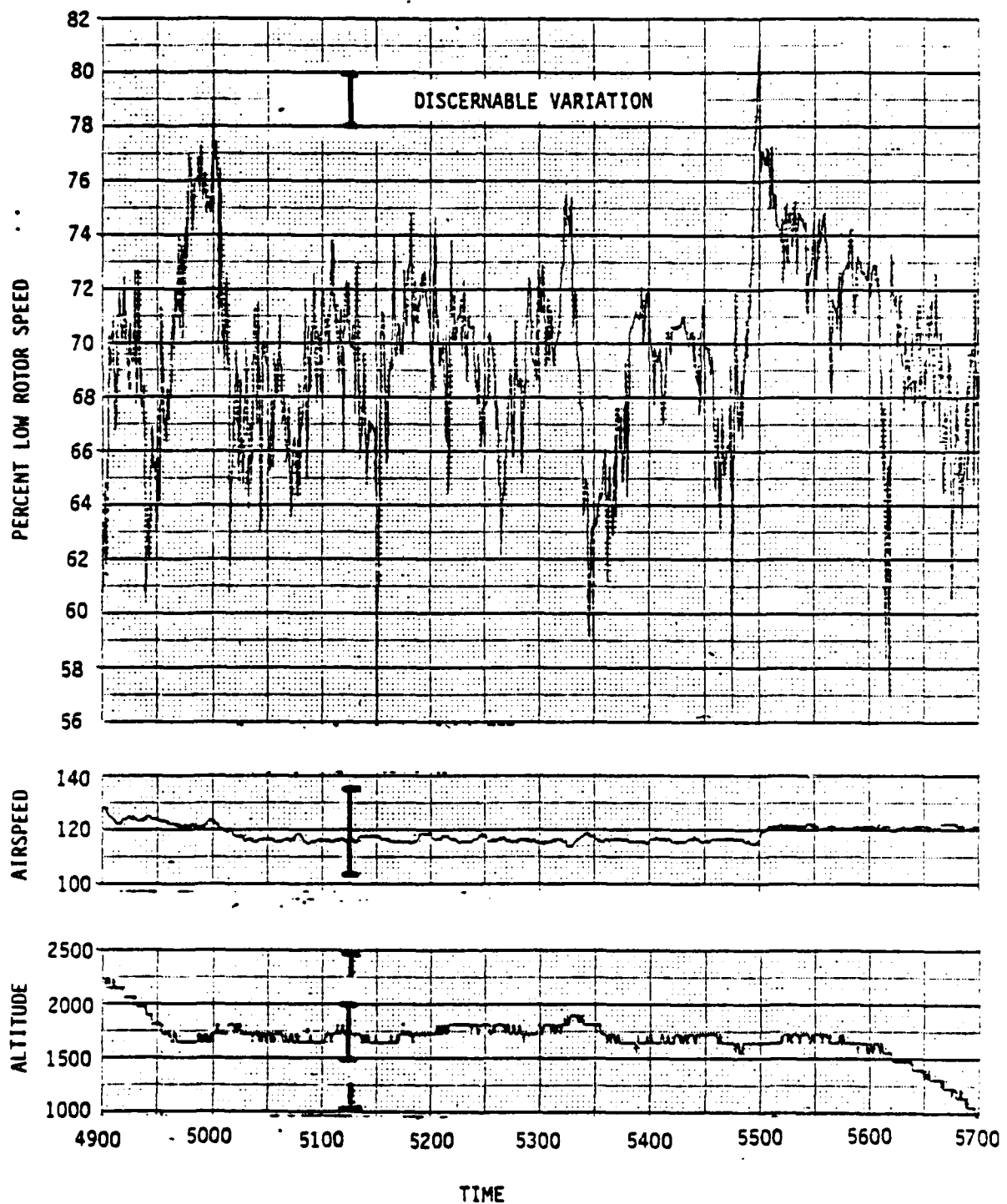


Figure 45. Parameter tolerance for F-14 approach.

Using several wingman cruise raw flight segments from an A-7 aircraft, the conversion of each raw signal to an isolated PSD and back to a representative dynamic time trace is shown in Figure 46. The parameter being examined is PLA. It can be seen in this figure that the representative histories contain the same peak overall excursion, single-cycle excursion, and cyclic distribution of the raw PLA signal. While the PSD-generated signal cannot duplicate precise square wave steps as seen in the raw signal, the general form of the resultant trace is felt to be quite representative of the original signal. Although this conclusion is subjective in nature, the same conclusion was reached by more objective validations, which are discussed later in this section.

Generation of the composite representative PSD and its time trace for a given flight segment involved the following procedure. Using the PSDs from several flight segments of the same time span (a requirement of the PSD program) for a given aircraft type, an average, composite PSD was generated.

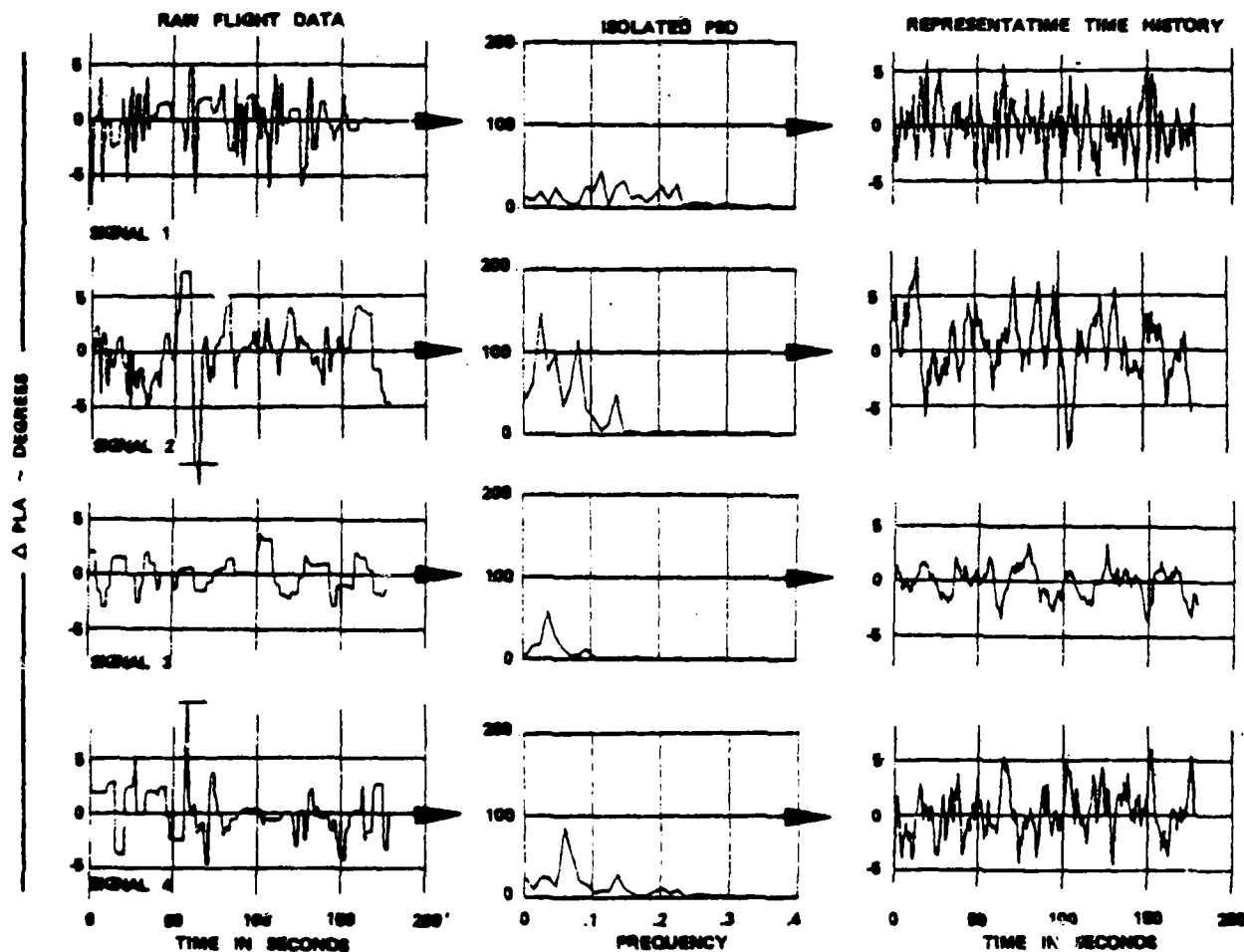


Figure 46. Raw flight PLA comparison to PSD-generated PLA.

This was repeated for each different time span set of data. Next, an average PSD was created from all the different time span PSDs for that aircraft type. If a given segment type had available data from several aircraft types, the final PSD for each aircraft was compared. If the individual aircraft PSDs showed a high similarity, an average composite PSD was generated. If the individual aircraft PSDs showed dissimilar results, the intent was to find a normalizing parameter(s) basic to each aircraft type. Such parameters as aircraft thrust to weight, wing loading, or engine cycle were the potential candidates. However, for the two types of segments considered, the latter problem did not arise; therefore, definition and inclusion of a normalizing parameter was not attempted. From the final composite PSD of a given segment type, dynamic time traces of any time span could then be generated for integration into the complete mission time history.

The results of this process are shown for PLA on the two considered segment types--wingman cruise and approach--in Figures 47 and 48, respectively. The wingman results were based on only one aircraft type (A-7) but utilized 16 separate flight segments. The approach results used data from three different aircraft (F-14, A-7, S-3A), which had a total of 44 separate flight segments. In both figures, the representative PLA time history is shown for an arbitrary 180-sec time span. The PSD program can compute with any time span and uses appropriate phase angles to ensure no repetition of the time trace.

Validation of the PSD-generated time traces was based on their ability to give consistent results in DDA-provided engine component severity index models (SIM) when compared to answers from raw (actual) flight data. Two SIMs were provided. One considered high-pressure turbine blade stress rupture levels; the other considered high-pressure turbine wheel mechanical LCF. Both models derive relative component life usage rates.

In the validation exercise, the following process was used for each segment type. Several raw flight segments were selected as base cases. Each was run through the SIMs to define their severity index level (SIL). For each base case the mean PLA, altitude, and air speed were determined. These mean levels were required, since the PSD-defined time trace only establishes a Δ PLA. Also the altitude and air speed levels were required inputs to the SIMs. Using these mean levels ensured consistent SIL comparisons between the base cases and the PSD traces. SILs were then generated based on the isolated (single flight) PSD trace, the first average (all constant time flights) PSD trace, and the final composite PSD trace. By stepping through the various PSDs, a feel for any smoothing due to averaging could be observed. In order to compare SIL answers for the various steps, it was found that the mechanical severity level had to be normalized by the specific time span used. This was required since the various PSD traces were not always produced for the exact base case time span and because the typical mechanical severity levels were near unity in value. The same normalizing was not done for the stress rupture severity level since these values were an order of magnitude sensitive and, therefore, not noticeably affected by time differences of two or less.

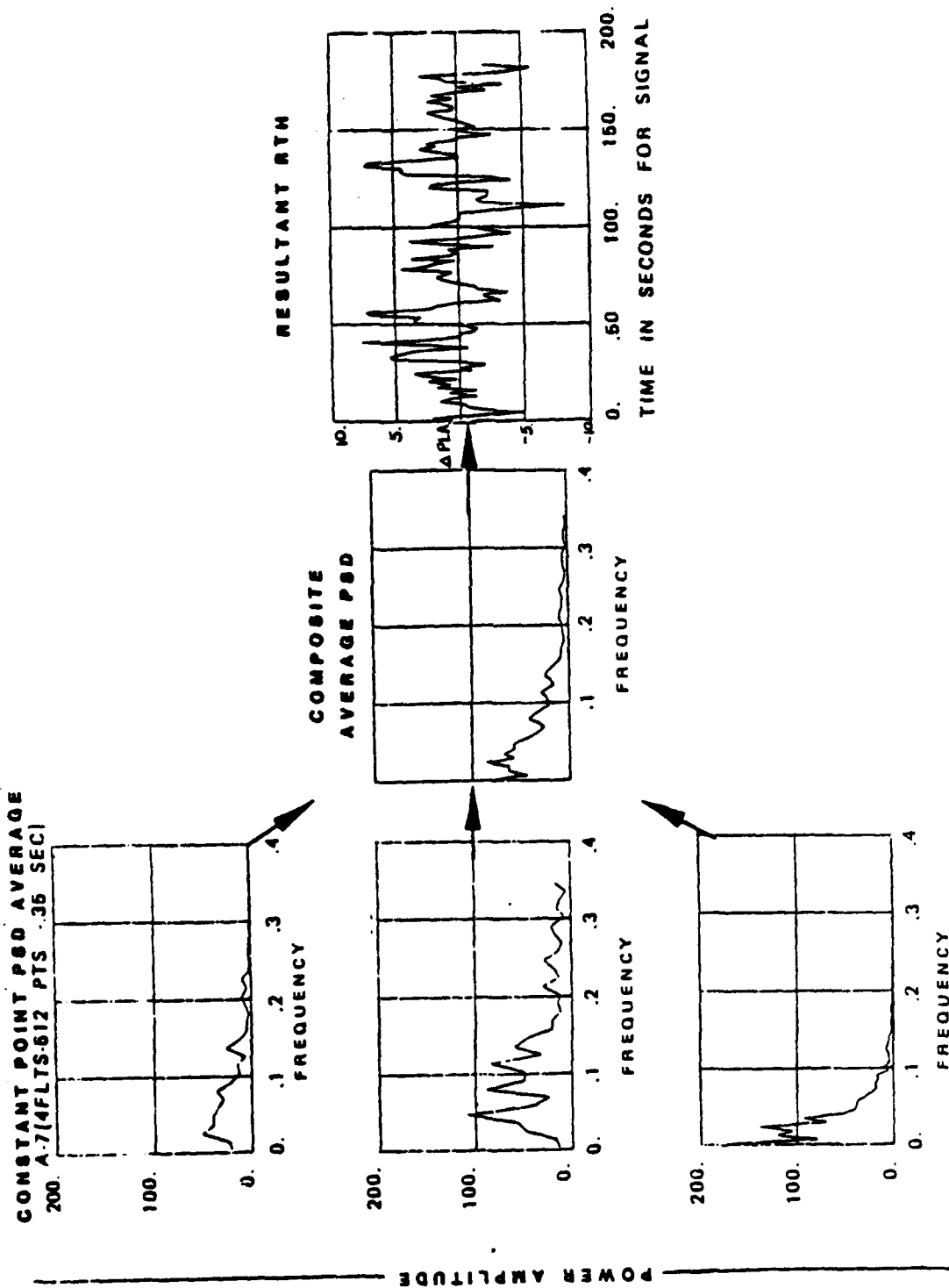


Figure 47. Wing cruise PSD buildup.

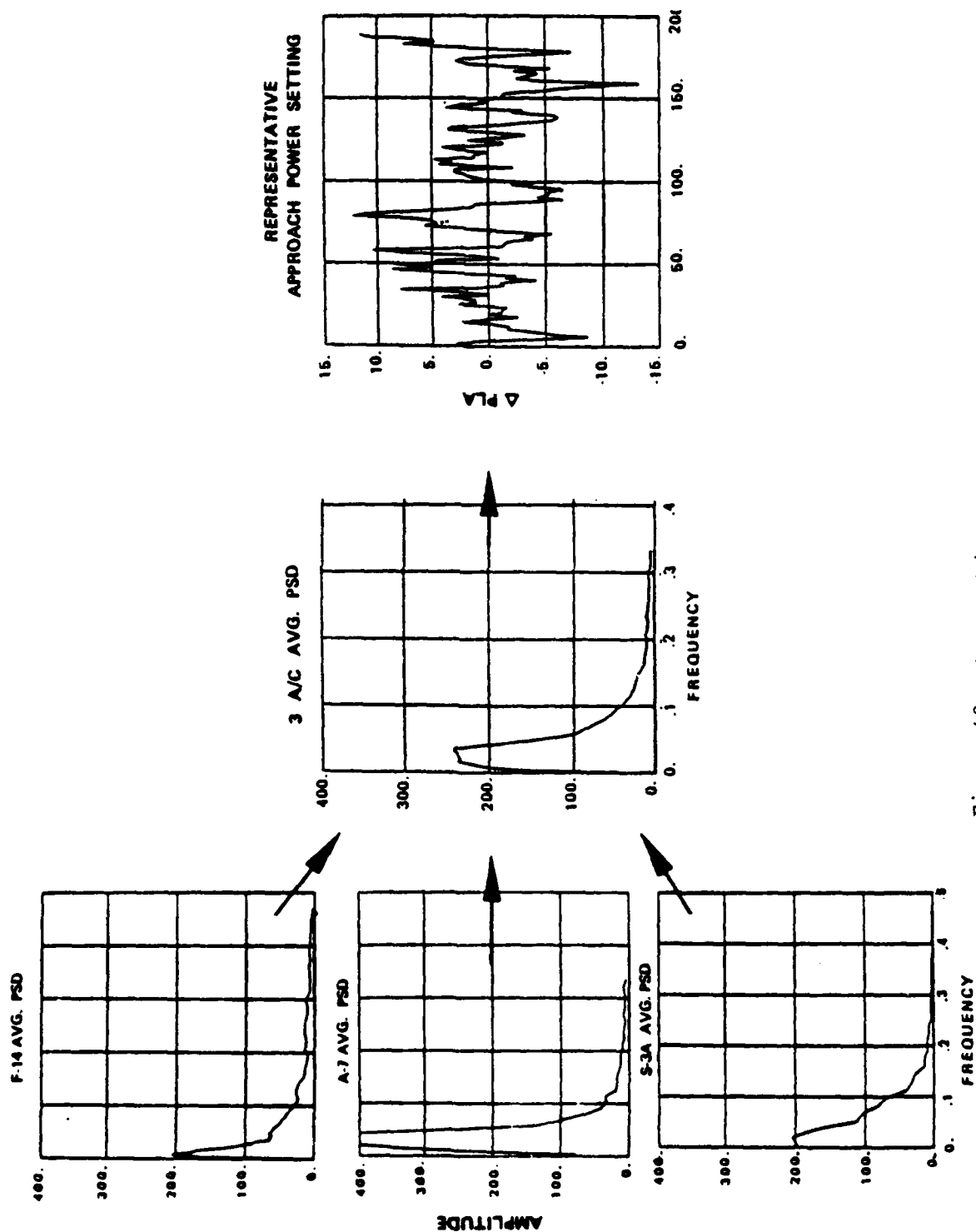


Figure 48. Approach/GCA PSD representation.

The results of these validation comparisons are shown in Tables 14 and 15 for the wingman cruise and approach segments, respectively. From these comparisons, the final composite (avg/avg) representative time history (RTH) values of stress rupture severity (SRSI) were generally consistent with the high order of magnitude raw flight case levels (10^{-5} , 10^{-6} , 10^{-7}) and overpredicted by 10% to 20% the lower valued (10^{-15} , 10^{-16} , 10^{-17}) cases. For mechanical severity (represented by ETC in Tables 14 and 15), the avg/avg RTH again gave generally close agreement with high-valued raw flight cases and overpredicted the lower-valued cases.

Table 14.
Wing cruise segment validation comparison.

Mission type and flight number	Isolated raw flight data				Severity index levels Isolated RTH			Average RTH			Average/average RTH			
	Flight time-- hr	SRSI	MSI	ETC	SRSI	MSI	ETC	SRSI	MSI	ETC	SRSI	MSI	ETC	
Wing cruise	1A	0.0467	0.23×10^{-5}	2.48	0.116	0.24×10^{-5}	2.34	0.117	0.24×10^{-5}	2.34	0.117	0.15×10^{-5}	2.54	0.131
	2A	0.0517	0.10×10^{-7}	2.10	0.108	0.15×10^{-7}	2.35	0.117	0.51×10^{-8}	2.34	0.117	0.22×10^{-7}	2.14	0.110
	3A	0.0517	0.11×10^{-6}	2.28	0.118	0.12×10^{-6}	2.19	0.109	0.13×10^{-6}	2.34	0.117	0.22×10^{-6}	2.34	0.124
	4A	0.0483	0.45×10^{-13}	1.17	0.056	0.33×10^{-13}	1.08	0.054	0.28×10^{-13}	1.80	0.090	0.10×10^{-11}	1.88	0.097
Wing cruise	1B	0.1017	0.58×10^{-7}	1.14	0.116				0.36×10^{-7}	1.23	0.123	0.64×10^{-7}	2.40*	0.124
	2B	0.0917	0.32×10^{-7}	1.18	0.109				0.15×10^{-7}	1.17	0.117	0.28×10^{-7}	2.29*	0.118
	3B	0.1000	0.31×10^{-8}	1.18	0.118	NOT RUN			0.83×10^{-8}	1.09	0.109	0.15×10^{-7}	2.14*	0.110
	4B	0.0983	0.27×10^{-12}	0.83	0.082				0.36×10^{-13}	1.01	0.101	0.13×10^{-11}	1.96*	0.101
	5B	0.0983	0.14×10^{-12}	0.59	0.058				0.56×10^{-12}	0.796	0.080	0.12×10^{-11}	1.88*	0.097
Wing cruise	1C	0.0900	0.14×10^{-6}	1.36	0.123				0.18×10^{-6}	2.60*	0.130	0.16×10^{-6}	2.54*	0.131
	2C	0.0483	0.19×10^{-11}	2.53	0.122	NOT RUN			0.39×10^{-12}	2.34	0.117	0.21×10^{-12}	2.23	0.115
	3C	0.0483	0.72×10^{-12}	2.10	0.102				0.29×10^{-12}	1.74	0.087	0.14×10^{-12}	1.57	0.081
	4C	0.0500	0.79×10^{-14}	1.08	0.054				0.25×10^{-15}	0.82	0.041	0.13×10^{-15}	0.62	0.032

RTH--representative time history from respective PSD

SRSI--stress rupture severity index

MSI--mechanical severity index

ETC--equivalent throttle cycles (MSI * flight time)

*Based on different flight time than raw data.

Based on average PSD from all flights. EDR 10485

Table 15.
Approach/GCA segment validation comparison.

Mission type and flight number	Flight time-- hr	Severity index levels												
		Isolated raw flight data			Isolated RTH			Average RTH			Average/average RTH			
		SRSI	MSI	ETC	SRSI	MSI	ETC	SRSI	MSI	ETC	SRSI	MSI	ETC	
Approach/GCA														
SET GCA	0.018	0.16×10^{-20}	0.610	0.011	0.22×10^{-19}	0.807	0.015	0.81×10^{-19}	0.439*	0.016	0.44×10^{-18}	0.377*	0.020	
SET GCA1 F-14	0.030	0.50×10^{-17}	0.711	0.036	0.13×10^{-17}	0.717	0.025	0.12×10^{-16}	0.823*	0.030	0.49×10^{-16}	0.687*	0.037	
SET GCA3	0.142	0.39×10^{-18}	0.236	0.033	0.37×10^{-18}	0.213	0.032	0.38×10^{-17}	0.687*	0.025	0.17×10^{-16}	0.603*	0.032	
SET GCA5 A-7	0.048	0.39×10^{-10}	2.73	0.132	0.99×10^{-9}	2.90	0.145	0.39×10^{-9}	2.61*	0.135	0.59×10^{-10}	2.56*	0.136	
SET GCA6	0.023	0.80×10^{-11}	5.96	0.139	0.51×10^{-10}	5.01	0.125	0.47×10^{-10}	2.82*	0.146	0.61×10^{-11}	2.77*	0.148	
SET GCA7 S-3A	0.037	0.48×10^{-12}	3.70	0.136	0.18×10^{-12}	3.65	0.128	0.12×10^{-13}	2.29*	0.084	0.36×10^{-13}	2.18*	0.116	
SET GCA8	0.028	0.11×10^{-14}	1.61	0.046	0.29×10^{-14}	2.67*	0.049	0.70×10^{-13}	3.09*	0.113	0.24×10^{-12}	2.58*	0.138	

First raw data case of each set.

*Based on different flight time from raw case.

In general, these results are felt to substantiate the PSD approach for defining representative tactical aircraft dynamic throttle operation when used for preliminary design (PD) engine component life assessment. It is also felt from the experience gained in examination of flight data that certain segment types, notably ground attack and air combat, do not appear adaptable to this approach but others (e.g., air refueling and terrain following) appear quite

applicable. Further, one of the basic lessons learned in this work is that the potential for any segment adaptability is fundamentally dependent on having sufficient, understandable, definitive flight data.

As discussed earlier, the use of these representative segment throttle dynamics was to enhance the steady-state training missions built up in the computer simulation. Schematically this is shown in Figure 49. An example of a training mission throttle time history trace with and without the appropriate dynamics is shown in Figure 50. This case represents a proficiency version of subsonic weapons delivery and includes dynamic throttle overlays for wingman cruise, landing approach, and air-to-air refueling. The latter segment (refuel) used wingman cruise dynamics since no air refuel was available and wingman flight was felt to approximate the close formation characteristics of air refueling. These dynamic overlays were imposed on all 136 training missions provided to DDA for engine component life assessment.

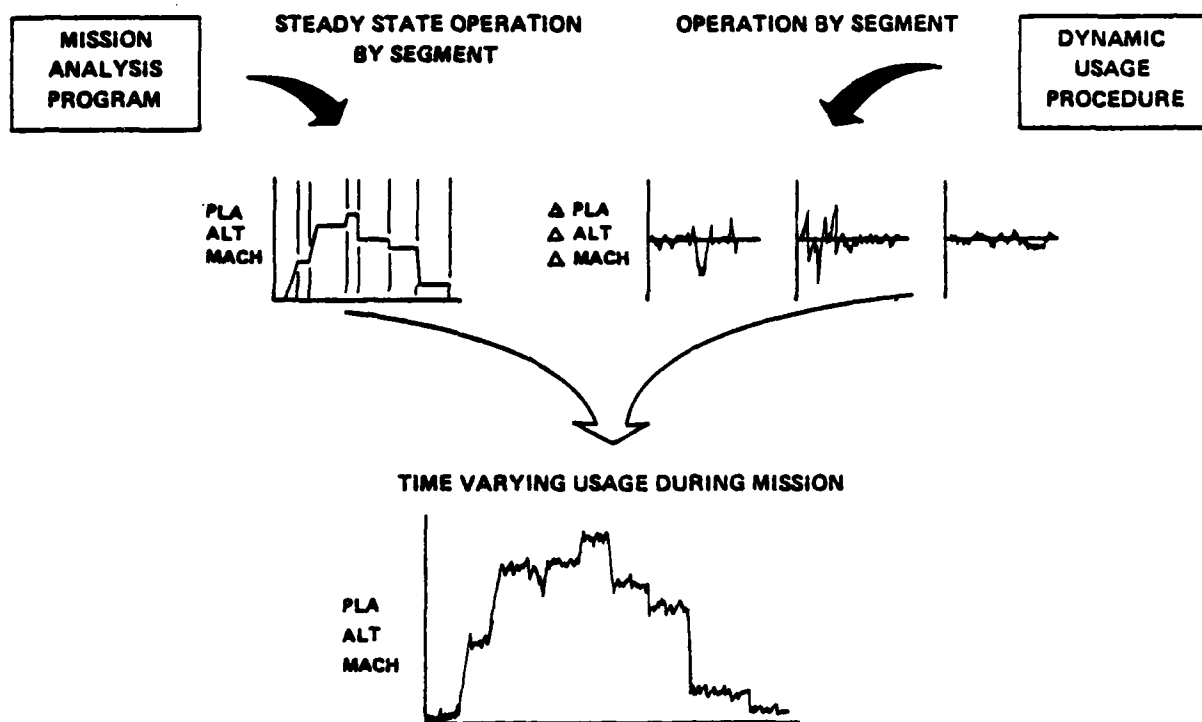


Figure 49. Mission usage definition.

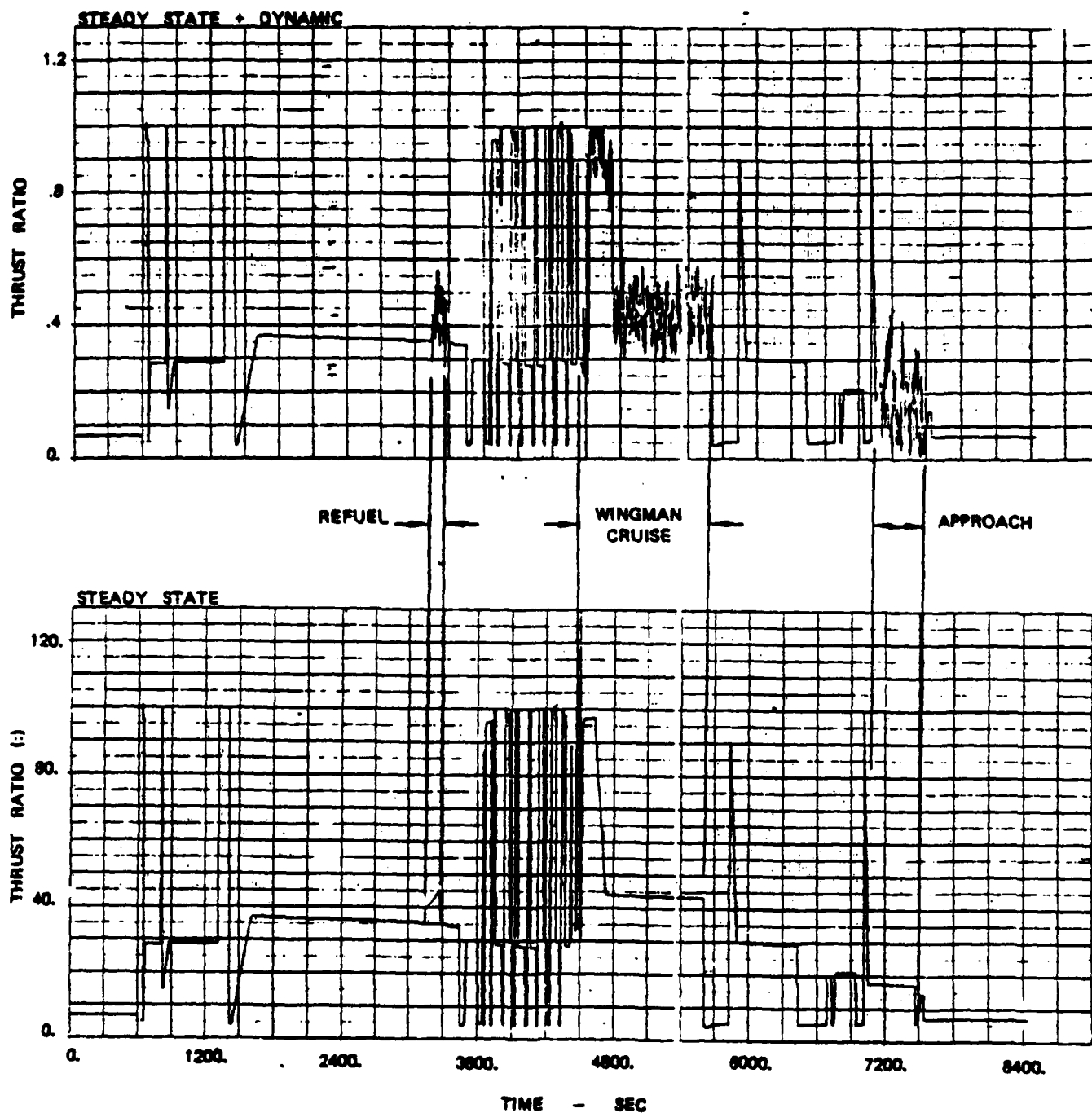


Figure 50. Sample dynamic overlay for subsonic weapons delivery/proficiency training mission.

V. TASK 3.1.4--ENGINE/AIRCRAFT INITIAL SCREENING

In this task the initial screening of aircraft and engine design variables was conducted to define wartime performance sensitivities and select the optimum performance based system. The ARES method of screening the independent design variables was used. Resultant output also allowed definition of key design variables, which defined a region of interest (ROI) for further study.

The engine concept studied in LUCID is a single-spool, nonaugmented turbojet. This class of engine is representative of the type of engine required for an advanced tactical aircraft of the 1990 time frame. A base-line configuration was a 15:1 pressure ratio, maximum temperature turbojet. The following description is for this base-line configuration around which parametric data have been based.

DDA has configured a base-line engine arrangement around the high-through-flow compressor, the high Mach number combustor, and the high-through-flow turbine. The basic engine arrangement is shown in Figure 51. The engine configuration is a modular design that can be split into seven major modules:

- o Rear bearing support and nozzle
- o Turbine rotor
- o Turbine stator
- o Diffuser/combustor
- o Compressor case halves
- o Compressor rotor
- o Front bearing support

The engine configuration includes

- o Six-stage, variable geometry compressor, high-through-flow
- o Vortex controlled diffuser
- o High Mach Lamilloy annular combustor
- o Single-stage, 3400°F rotor inlet temperature, variable vane turbine using spar and Lamilloy airfoils with modulated blade cooling
- o Lamilloy cooled exhaust nozzle
- o Variable axial load integrated device, a hydraulic piston thrust reaction mechanism with variable oil control system to react main rotor thrust
- o A two-sump, two-bearing main rotor shaft
- o Accessory gearbox front driven by a quill shaft through a compressor inlet strut from gearing at the main shaft forward end
- o Digital electronic control systems
- o Variable geometry actuation via clutches and gearing with flexible cable to ball screws at the compressor union rings and an air motor driven planocentric actuator drive at the turbine

Cooling system includes the following:

- o Stage 2 envelopment of bearing sumps for oil seal pressure balanced feed
- o Stage 5 hub bleed routed via the main shaft to the exhaust system modulation valve for duct and jet nozzle cooling
- o CDP feed via modulated swirl nozzles to the rotor blade modulation to be on/off at individual nozzles for particle separation-type flow control while swirl velocity is maintained

- o CDP feed for film/impingement cooling of turbine vane outer platform and turbine blade tip seal
- o Turbine section consisting of a single stage, with a geometrically variable vane row and a high work blade design--The vane row consists of alternate fixed and movable vanes

Selected independent variables for this screening consisted of three engine cycle variables defined in the DDA parametric cycle matching deck (PD422), four airplane parameters, and design Mach number. The range of the airplane parameters was selected to be within the design envelope of the base-line configuration and wartime mission defined in Task 3.1.2. The range of engine variables was determined by the parametric deck limits. The eight variables and their ranges were

o Engine

Overall pressure ratio (OPR)	9-18
Thetabreak (THETAB)	1.00-1.36
Turbine rotor inlet temperature (RIT)	2350-3400°F

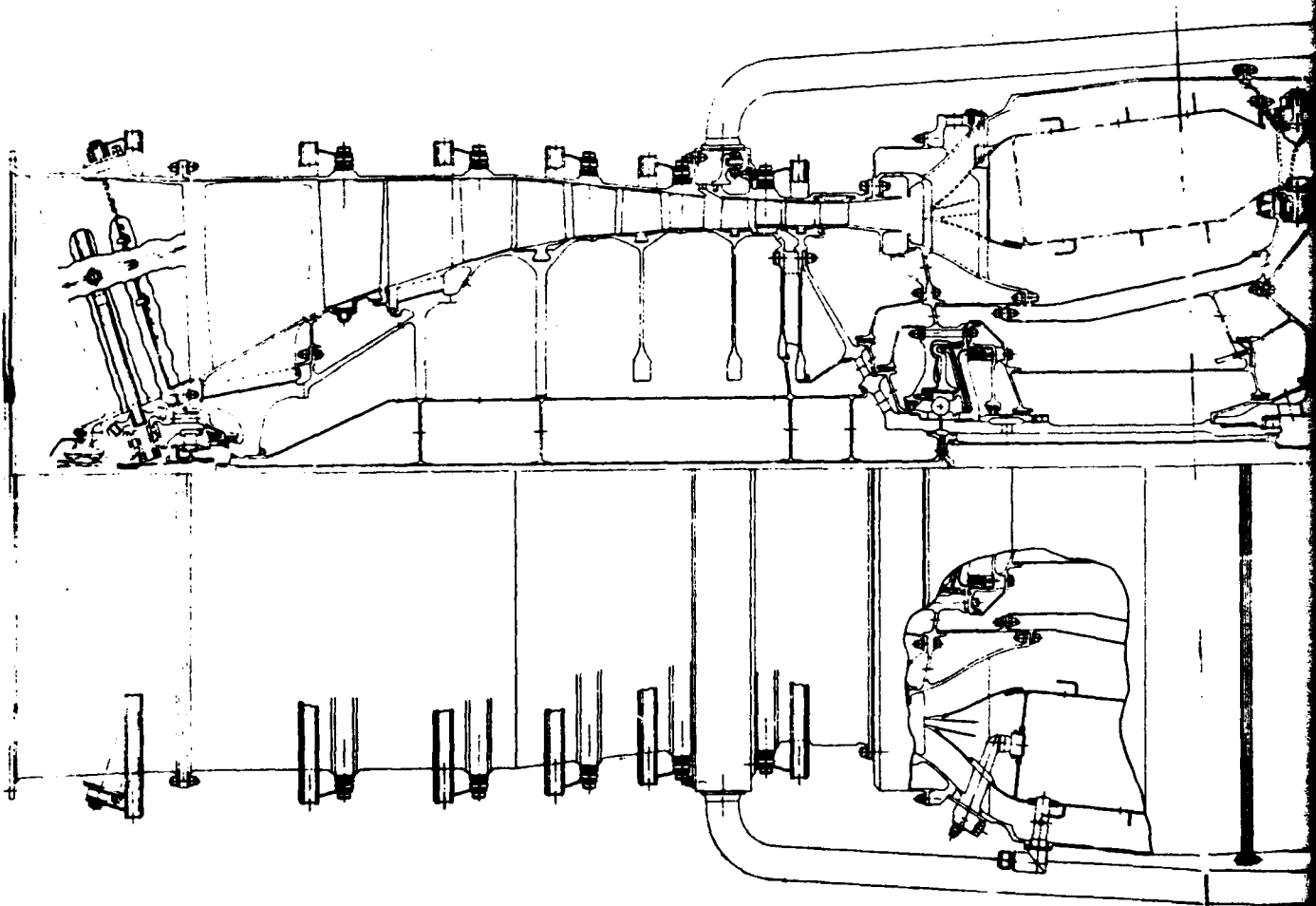
o Airplane

Thrust/weight (T/W)	0.60-1.20
Takeoff gross weight (TOGW)	40000-80000 lb
Wing loading (W/S)	60-100
Wing aspect ratio/sweep combination (AR15)	1.40-2.80

o Mission

Design cruise Mach	1.60-2.40
--------------------	-----------

The wing aerodynamic aspect ratio/sweep parameter (AR15) actually represented a wing planform variation as it varied sweep dependently with AR to hold a constant structural aspect ratio. The geometric relationship of the two parameters is shown in Figure 52. Generation of sensitivities and optima for the parametric family was conducted using the ARES method in conjunction with the Orthogonal Latin Square (OLS) design selection technique. Using the selected designs, a data base was generated using the PD422 program to calculate uninstalled engine performance and a Boeing mission simulator to define each design's mission capabilities. Next, performance trends and parameter optimizations were determined. This was accomplished by curve fitting (regressing) dependent parameters of interest as functions of the selected independent variables. Approximately 80 dependent variables were produced for possible regression. However, only 14 of these variables were regressed for use in constrained system optimizations and sensitivities. The 14 variables are listed in Table 16 along with the primary regression statistic (R^2) for each. The closer this statistic is to unity, the more confident one can be of a representative surface fit by that function. Using these regressions, the optimum system, as defined by minimum TOGW, for unconstrained (no performance requirements) and constrained (shown in Table 11) conditions, were defined. The optimum unconstrained systems as a function of Mach number are shown in Table 17, and the constrained optima are shown in Table 18. A graphic display of these results, along with an additional acceleration time constraint of 75 sec on the constrained systems is shown in Figures 53 through 55. In Figure 53, the optimum level of each independent variable is shown for the appropriate design Mach number and constraints. Engine turbine temperature was not plotted since it stayed constant at 3400°F for all optima. In Figure 54, the



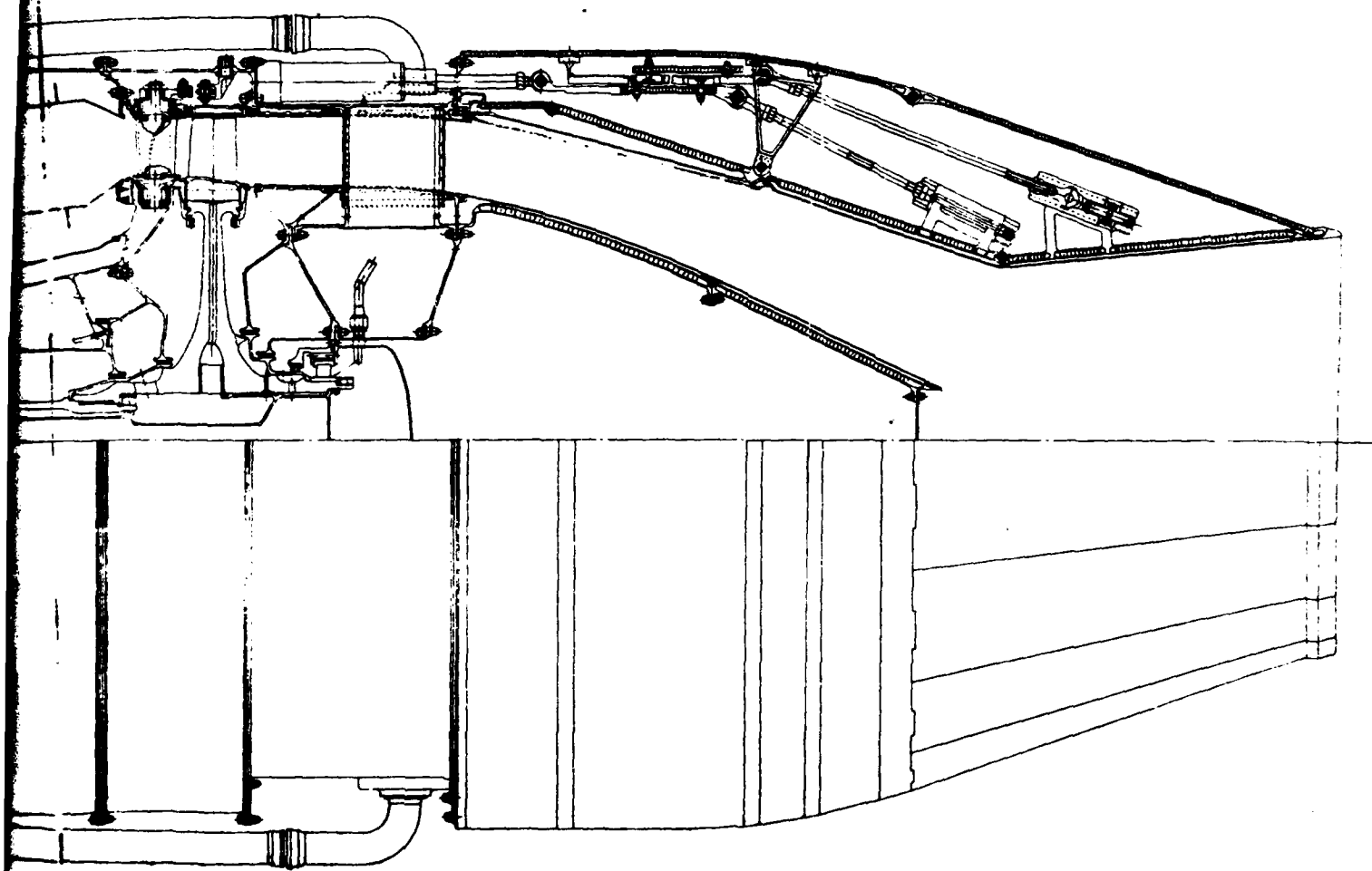


Figure 51. Preliminary engine general arrangement.

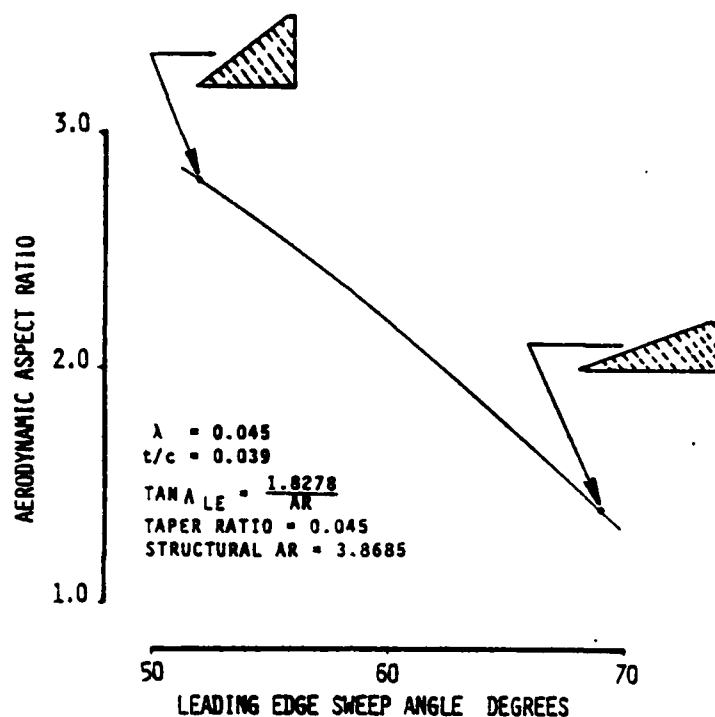


Figure 52. Wing parametric planform variation for LUCID model 987-354.

Table 16.
Dependent variable regression accuracy for initial screening.

Dependent parameter description	Reg statistics	
	No. cases	R ²
Wing sweep angle	81	0.9999
Takeoff distance	81	0.9991
Landing velocity	81	0.9997
Landing distance	81	0.9997
Sustained combat	81	0.9989
Instantaneous combat	81	0.9953
Instantaneous avoidance	81	0.9984
Sustained avoidance	81	0.9909
Acceleration time	93	0.9812
Cruise out altitude	93	0.9728
Cruise out power setting	93	0.9922
Cruise turn sustained	93	0.9838
Cruise out SFC	93	0.9741
Mission radius	122	0.9846

Table 17.
Initial screening unconstrained optimal system definitions.

Design Mach number, M_N	Airplane thrust/weight, T/W	Airplane wing loading, W/S	Aspect ratio parameter, AR	Takeoff gross weight, TOGW--lb	Overall pressure ratio, OPR	Turbine inlet temperature, RIT--°F	Engine airflow schedule, THETAB
1.60	0.60	100	1.40	39,200	15.5	3400	1.00
1.80	0.60	100	1.40	40,200	12.2	3400	1.00
2.00	0.60	100	1.40	40,600	11.2	3400	1.00
2.20	0.60	100	1.40	39,900	9.2	3400	1.00
2.40	0.60	100	1.40	39,100	9.0	3400	1.36

Table 18.
Initial screening constrained optimal system definitions.

Design Mach number, M_N	Airplane thrust/weight, T/W	Airplane wing loading, W/S	Aspect ratio parameter, AR	Takeoff gross weight, TOGW--lb	Overall pressure ratio, OPR	Turbine inlet temperature, RIT--°F	Engine airflow schedule, THETAB
1.60	0.60	64	1.78	48,700	10.0	3400	1.00
1.80	0.60	65	1.80	49,200	9.0	3400	1.36
2.00	0.60	65	1.81	49,500	9.0	3400	1.36
2.20	0.60	66	1.82	49,400	9.0	3400	1.36
2.40	0.60	67	1.83	48,900	9.0	3400	1.36

actual level of the dependent constraint parameters for each optimum are shown, and Figure 55 shows dependent performance parameters (e.g., cruise altitude and power-setting) for the various optima.

To establish credibility in the answers from the regression equations, several optima, defined for various Mach numbers and various combinations of constraints, were run back through the mission program. A comparison of answers between the regression equations and the mission validation cases is shown as symbols in Figures 54 and 55. Good agreement between mission and equation answers is shown for these cases with the average error for each well within the +5% error band normally considered acceptable.

Visibility into the influence of engine variables on minimum TOGW is shown in carpet plot form on Figures 56 through 59. In Figure 56, OPR and Mach are varied, whereas Figures 57 and 58 show OPR-RIT and OPR-THETAB, respectively, both at a constant Mach of 2.20. A fourth carpet of airplane variables, T/W and W/S at Mach 2.20, is shown in Figure 59. Each point on all these carpets represents the "best" combination of all remaining independent variables to produce the smallest (lowest TOGW) system to perform the required capabilities.

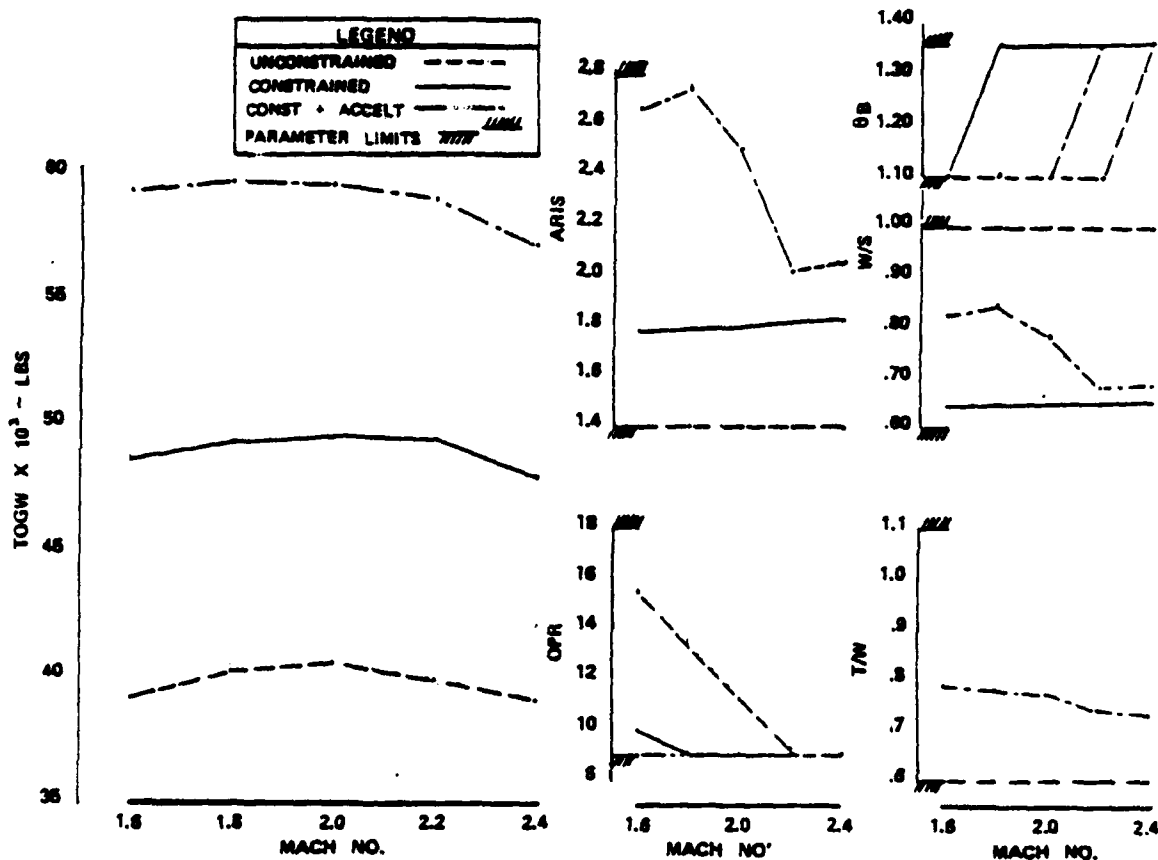


Figure 53. Optimum system definition for supersonic cruise Mach number variations for 550-nmi mission radius.

Around the Mach 2.20 constrained optimum, isolated sensitivities, Figures 60 and 61, of each independent variable were examined for their impact on system size and performance. Each independent variable was varied +15% around its optimum level or until a box limit of that variable was reached. Each variable was varied independently with no attempt at offsetting its effect with a shift in any other variable. These sensitivities are also shown for Mach 1.60 in Figure 62. From these sensitivities the following trends were noted.

The mission radius was most strongly influenced by airplane size (TOGW). Engine size (T/W) had the next most significant influence. However, at the higher Mach number (2.2) turbine temperature (RIT) was nearly as influential as T/W.

Constraint parameters were most strongly influenced by wing geometry (W/S and AR) and T/W. Supersonic avoidance capability was the exception with design Mach showing the greatest significance.

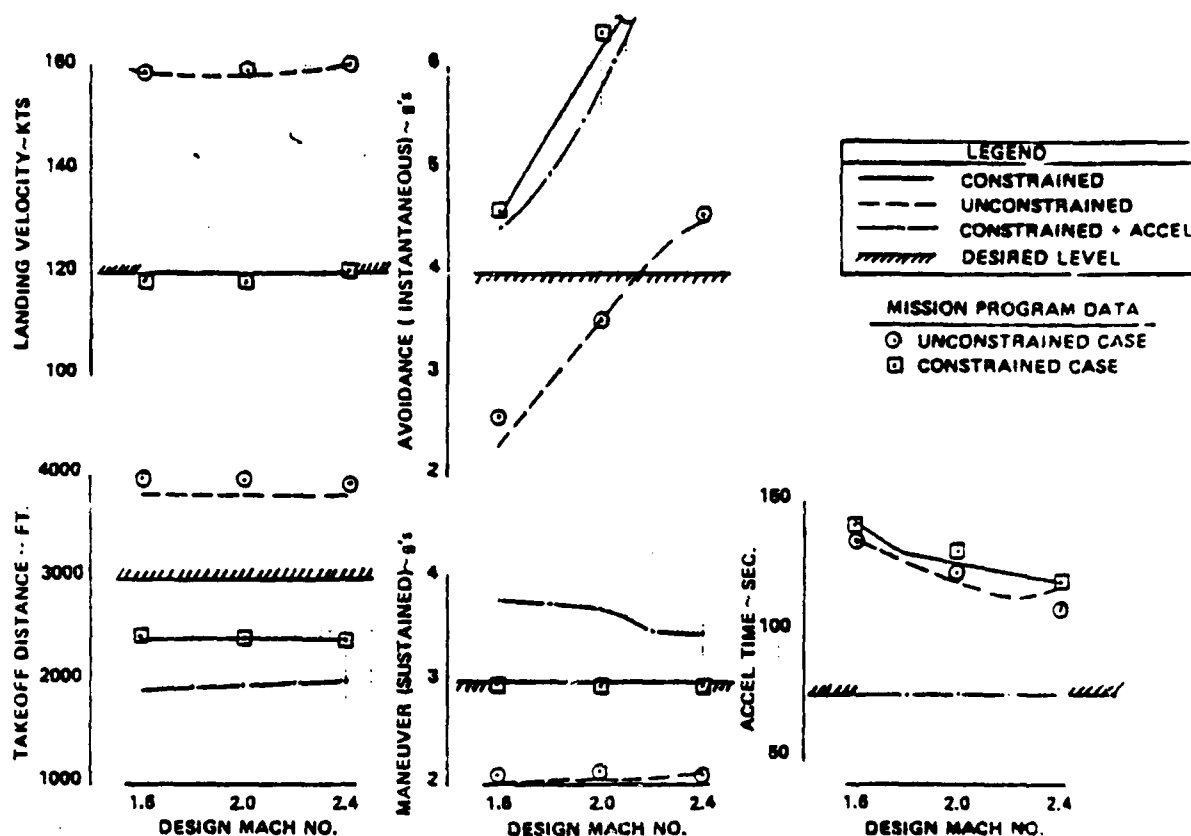


Figure 54. Impact of constraints with supersonic cruise Mach number.

Using these isolated sensitivities and the local optima carpet plots, a selection of variables and levels to represent ROI definition for Task 3.1.5 was proposed. This selection was based on the following identified characteristics. The influence of Mach number on system size and performance was found to be small for properly optimized systems; therefore, Mach number was recommended to be fixed at the original base-line level of 2.2.

From the constrained carpet a unique correlation between W/S and AR was found to exist. This relationship was independent of the other parameter levels as shown in Figure 63 and allowed the two most influential parameters on constraint levels to be compressed into one. The result provided a reduced number of ROI variables to meet the mission radius requirements and simultaneously meet all constraint requirements with the appropriate lightest TOGW.

This approach allowed the ROI variables to be selected from the remaining engine parameters without compromising overall system capability. Of the four remaining parameters, T/W and RIT were shown to have significant influence on constraints and/or the figure of merit. They also had obvious high leverage on engine operating conditions.

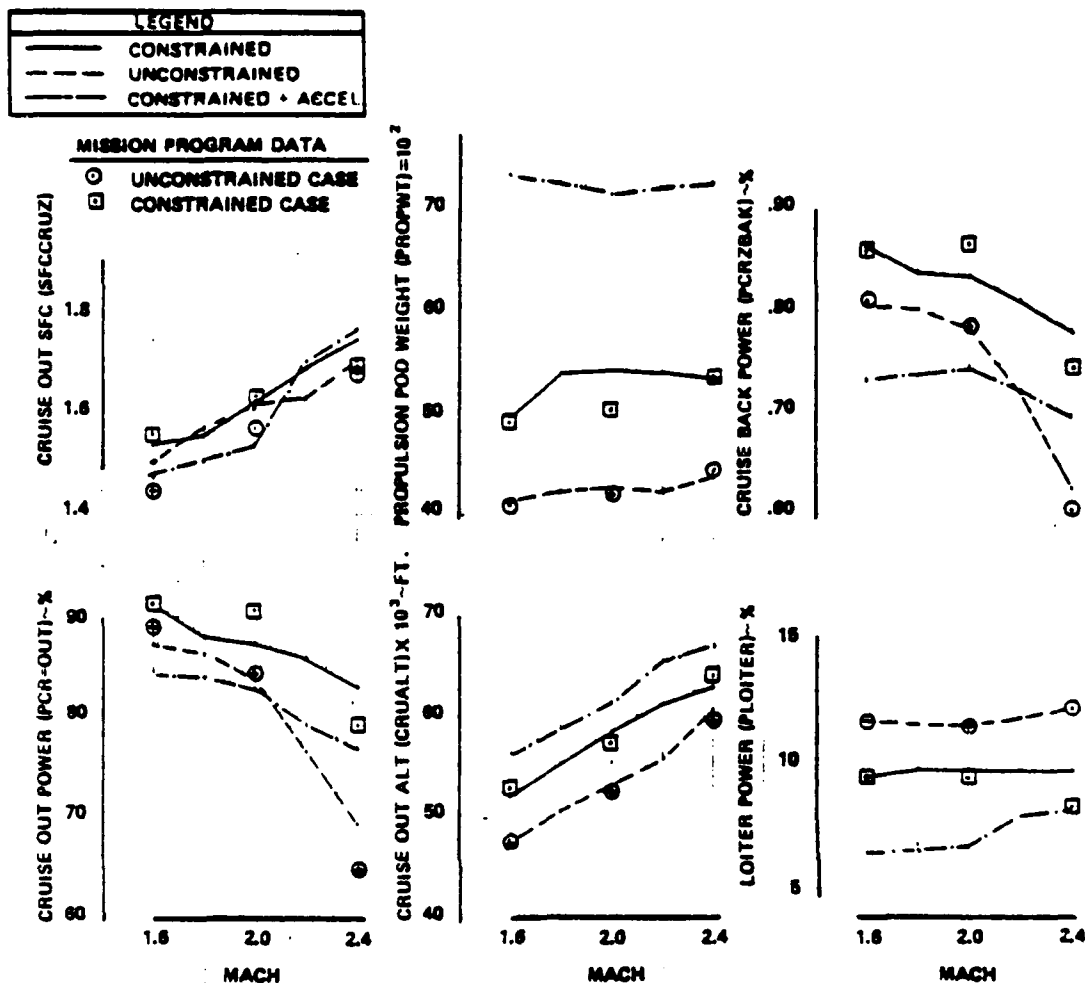


Figure 55. Performance data trends with supersonic cruise Mach number.

Of the remaining two variables (OPR and THETAB), OPR showed the most influence on combat mission capabilities. It also was felt to offer the greatest potential in affecting engine component life from training usage because of its influence on turbine cooling requirements.

In summary, the Boeing-proposed ROI variables, their ranges, and the level of other screening variables were

T/W	0.55-0.75
RIT	2800-3400
OPR	9-18
W/S - AR	Correlated and varied via regressions
THETAB	1.36
Mach No.	2.20
TOGW	Dependent (required size for 550-nmi radius)

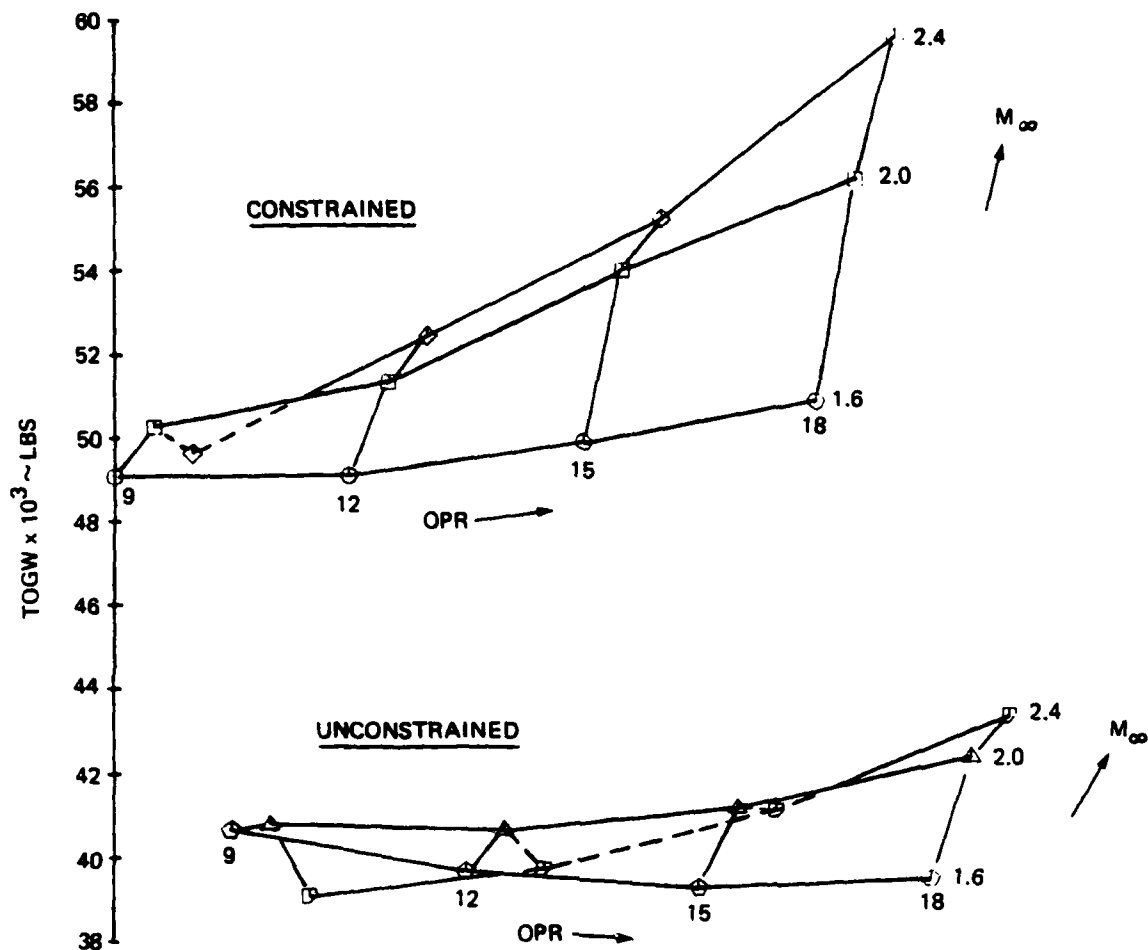


Figure 56. Initial LUCID screening--OPR and Mach number carpet plot.

Final selection of the variables was altered slightly from this list by DDA and the Air Force. The potential influence of THETAB on engine component life needed to be examined; therefore, THETAB was selected with a range of 1.00 to 1.36, and T/W was fixed at its previous box limit value of 0.60. The range of RIT variation was compatible with DDA's turbine airfoil TLEF model development for Lamilloy airfoils.

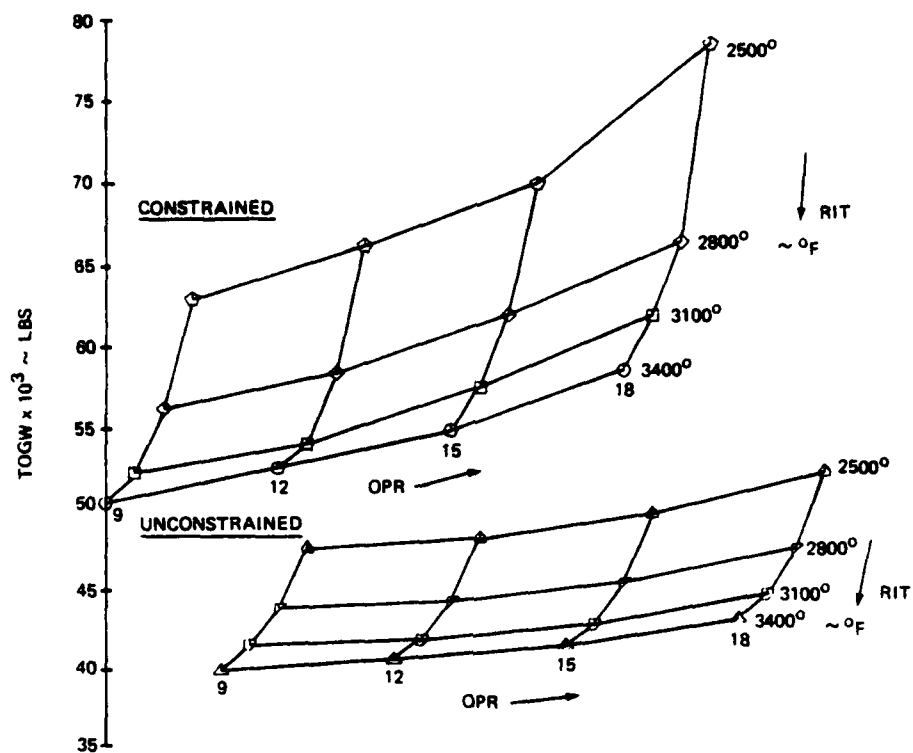


Figure 57. Initial LUCID screening--OPR and RIT carpet plot.

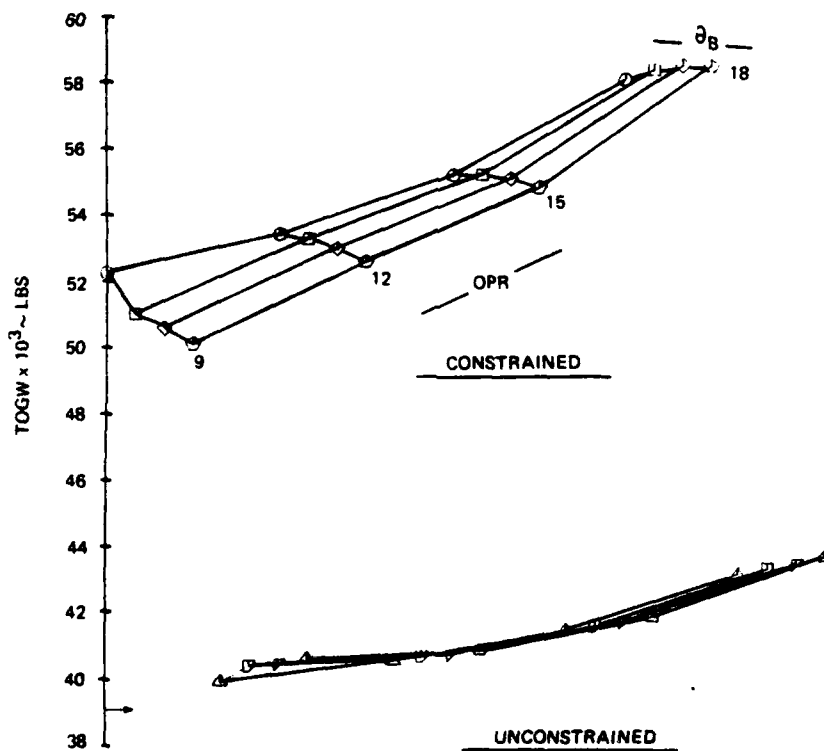


Figure 58. Initial LUCID screening--OPR and THETAB carpet plot.

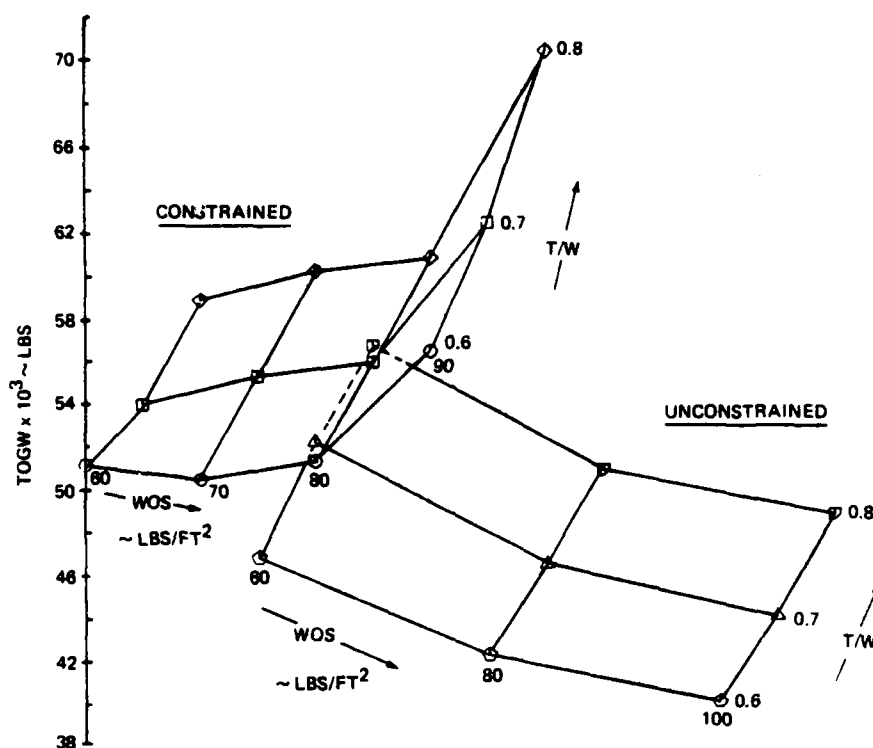


Figure 59. Initial LUCID screening--T/W and W/S carpet plot.

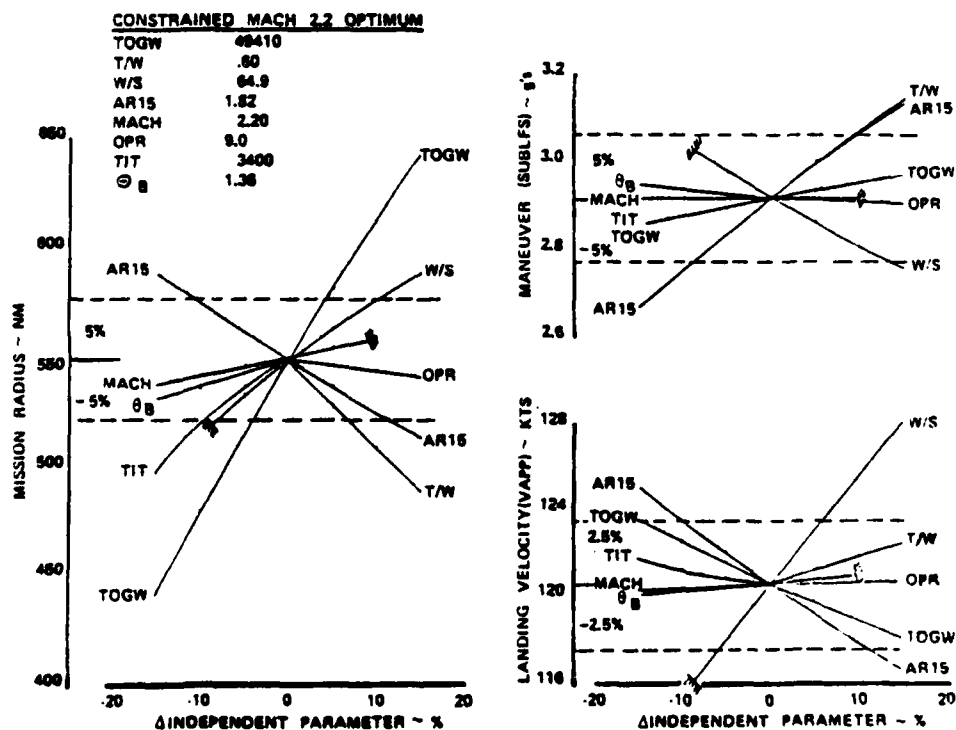


Figure 60. Independent variable sensitivity for constrained 2.2 Mn optimum design.

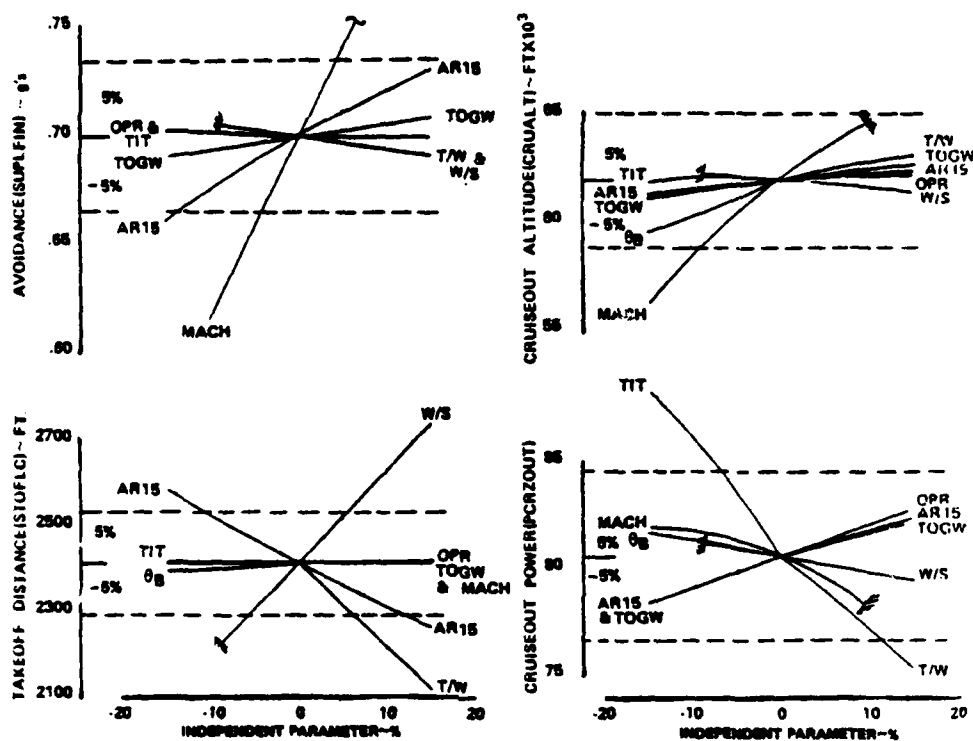


Figure 61. Independent variable sensitivity for constrained 2.2 MN optimum design.

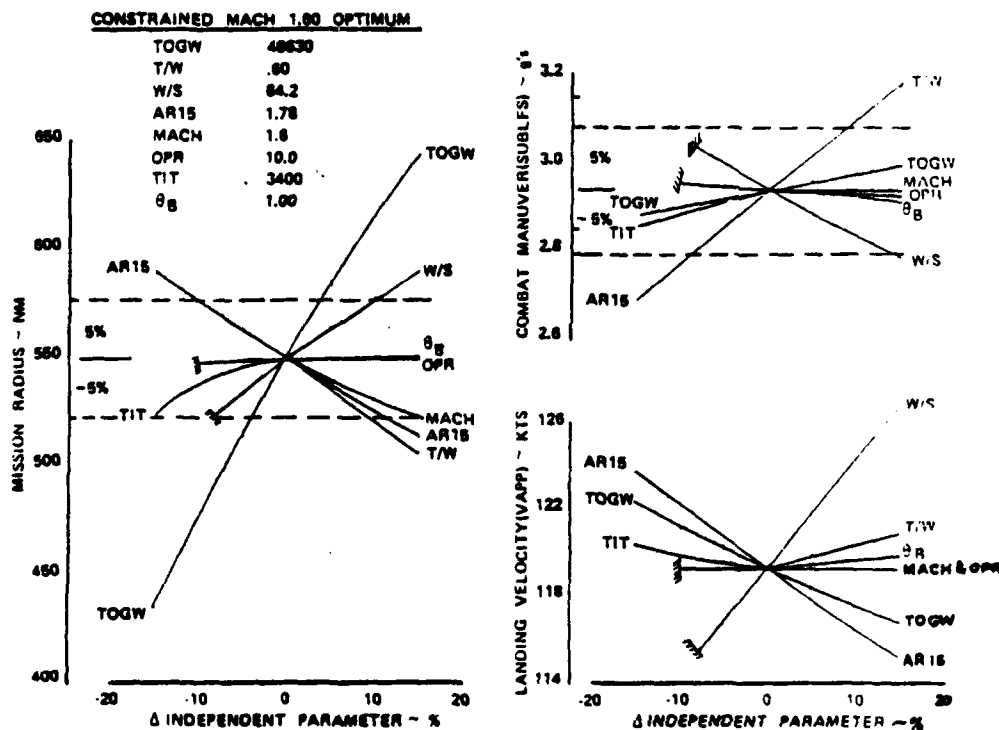


Figure 62. Independent variable sensitivity for constrained 1.6 MN optimum design.

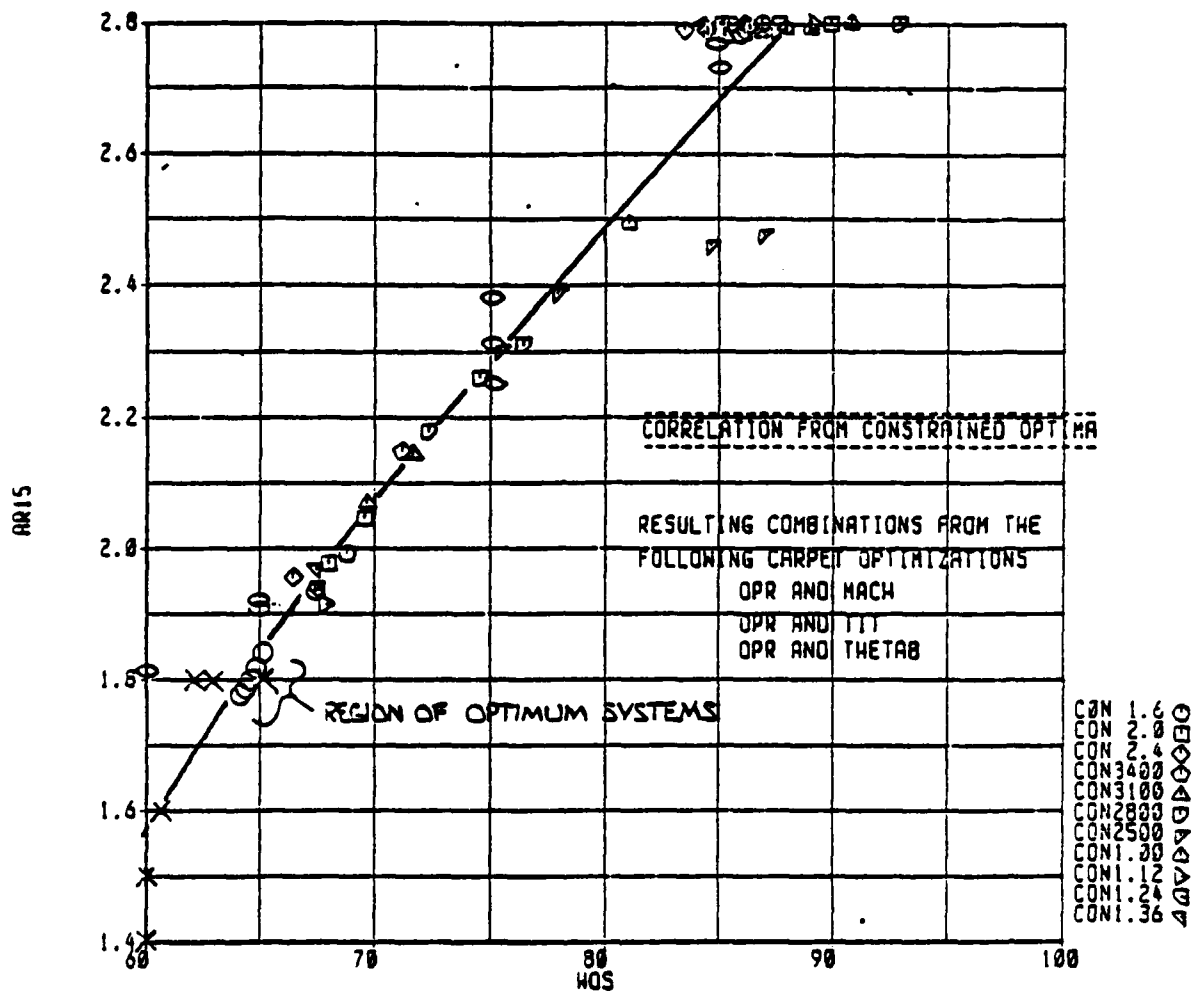


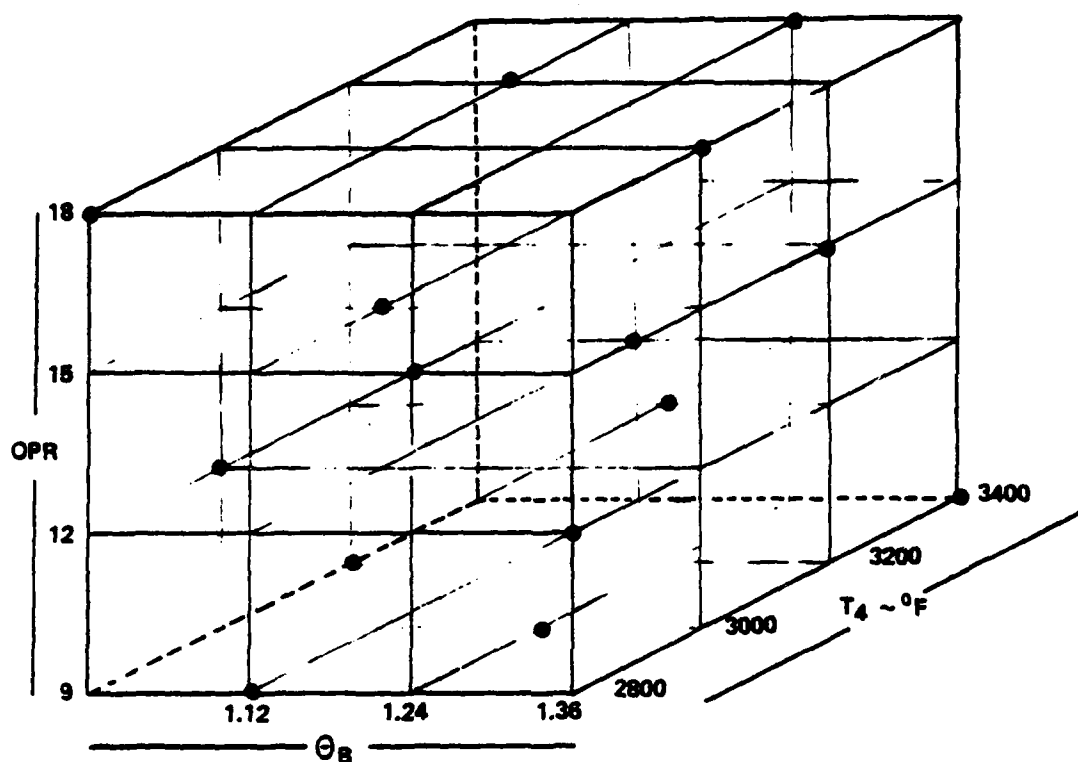
Figure 63. Initial screening--aspect ratio (AR15)-wing loading (W/S) relationship.

VI. TASK 3.1.5--REGION OF INTEREST DEVELOPMENT

In this task, the defined (from Task 3.1.4) ROI variables were run through the ARES procedure a final time for sensitivity and optimization definition around the wartime mission. Also, the same set of aircraft designs was flown on all training missions, described in Tasks 3.1.2 and 3.1.3, to define training usage characteristics.

A complete reassessment of performance for the refined ROI variables was conducted using the ARES method. Several OLS design combinations were defined to allow DDA selection based on compatibility with previous DDA engine usage studies. The selected designs are shown in Figure 64. Engine data from a slightly modified version of DDA's PD422 parametric deck were generated for a Mach, altitude, power setting matrix (Figure 65) that covered both wartime and peacetime operating envelopes. Generation of wartime performance was accomplished using the same mission simulation program used in Task 3.1.4. Unlike the initial (Task 3.1.4) data base, all cases in the ROI data base were run to meet mission constraint and radius requirements. Examination of results showed that all constraining parameters (subsonic maneuver load factor and landing approach velocity) were within 5% of the constraint requirement. The other constraint parameters--takeoff field length and supersonic load factor--were also well within the desired level.

Initial regressions of the ROI data base showed most parameters to have very poor curve fit statistics (R^2) as shown in Table 19. One such parameter was TOGW, the main variable of interest in this data base. Examination of the data showed one of the two dependent airframe variables, aspect ratio, was frequently at a limit value (2.80), thereby introducing a discontinuity that could not be picked up by the independent engine variables. To remove this problem, AR15 was fixed at its upper limit (2.80) and those cases originally with lower values were rerun. The reoptimization of these cases, using the screening regressions of Task 3.1.4, indicated only a 2% to 3% increase in TOGW from that predicted for the original designs. Regression of the revised ROI data set showed generally better R^2 ; however, that of TOGW was still unacceptable. Improvement of the ROI data base regressions was obtained with a reduced set by selectively removing two cases (No. 2, No. 12) from the full set. Then an augmented set was obtained by the addition of only two augmentation cases to the reduced set. The resultant regression statistics and standard deviation of residuals for the parameters of interest are shown in Table 19. While other important dependent variables, most notably landing velocity (VAPP), still show terrible R^2 values, improvement of these fits was not required when the range and level of the actual data were considered. The maximum and minimum values of all regressed parameters in the data base are shown in Table 20. As an example, in Table 20 VAPP is seen to range from 119 to 120 knots. Such variation is primarily a result of accuracy tolerance, truncation limits, and round-off within the mission program, causing the slight variation of the variable to appear as noise in the regression, resulting in poor fit statistics. Since the parameter is essentially a constant, its statistics are not of significance.



RUN 2 - LUCIO ROI O.L.S.

CASE	OPR	TIT	THETAB
1	18.000	2800	1.000
2	15.000	3000	1.120
3	12.000	3200	1.240
4	9.000	3400	1.360
5	15.000	3200	1.360
6	18.000	3400	1.240
7	9.000	2800	1.120
8	12.000	3000	1.000
9	12.000	3400	1.120
10	9.000	3200	1.000
11	18.000	3000	1.360
12	15.000	2800	1.240
13	9.000	3000	1.240
14	12.000	2800	1.360
15	15.000	3400	1.000
16	18.000	3200	1.120

Figure 64. ROI data cases.

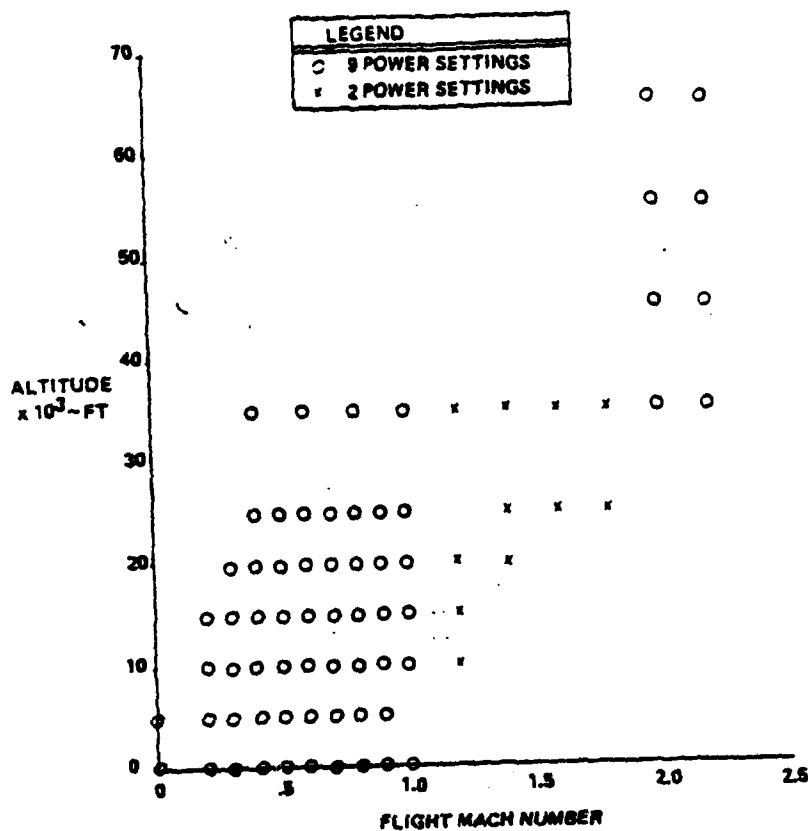


Figure 65. ROI engine data altitude/Mach matrix.

Table 19.

ROI dependent variable regression (R^2) statistic.

Variable name	Initial Regression	Revised set with constant AR15			Standard deviations for last regressions
		Full set	Reduced set	Augmented set	
No. cases	16	16	14	16	
TOGW	0.69036039	0.67715367	0.85002798	0.99343725	5.5086916×10^2
SLAND	0.37414029	0.07848228	0.00000000	0.06347429	1.7191299×10
SUPLFS	0.98967208	0.99411007	0.99482371	0.99339112	3.7950449×10^{-2}
CRUALT	0.98283877	0.98891740	0.98886008	0.98371348	5.3900788×10^2
ZLDCRUZ	0.95470324	0.98538491	0.98538415	0.96361702	6.4046149×10^{-2}
SFCCRUIZ	0.96037662	0.96006459	0.95870701	0.90364056	1.1898093×10^{-2}
PCRZDUT	0.91332643	0.94665040	0.94897350	0.99135904	3.9200423×10^{-3}
PCRZBAK	0.85645220	0.97509522	0.97800763	0.99859385	2.1721474×10^{-3}
PLOITER	0.85555339	0.81302823	0.81918844	0.81535501	1.3143126×10^{-3}
TURNLEE	0.35316345	0.41407853	0.45329175	0.66808225	2.6605235×10^{-2}
STOFLC	0.98336437	0.99409685	0.99423407	0.99907914	2.8286096
ACCELT	0.87963698	0.87594252	0.87695165	0.90347900	5.0624510
VAPP	0.06251430	0.08318982	0.06119269	0.05624803	5.6074014×10^{-1}
SUBLFS	0.64994614	0.93303688	0.97048568	0.98093790	8.3681574×10^{-3}
SUBLFIN	0.84802637	0.99049239	0.99215051	0.99588333	7.2783288×10^{-3}
WOS	0.87313483	0.92183148	0.92487520	0.99954060	7.3073127×10^{-2}

Table 20.
Range of ROI variables.

<u>Variable name</u>	<u>Data base range of variable</u>	
	<u>Minimum</u>	<u>Maximum</u>
TOGW--lb	49,100	69,100
SLAND--ft	1,898	1,963
SUPLFS--g	1.405	2.951
CRUALT--ft	47,210	61,100
ZLDCRUZ	3.676	4.798
SFCCRUIZ--lb/sec/lb	1.563	1.670
PCRZOUT	0.839	0.938
PCRZBAK	0.772	0.917
PLOITER	0.077	0.089
TURNLEE--g	1.245	1.380
STOFLC--ft	2,475	2,744
ACCELT--sec	118.1	174.5
VAPP--knots	118.9	120.4
SUBLFS--g	3.07	3.239
SUBLFIN--g	4.464	4.799
WOS--psf	84.1	92.9

Optimization of the resultant TOGW equation for minimum size airplane produced nearly the same answer in engine cycle characteristics as the original screening study. The levels of the optimum engine variables were

Overall pressure ratio	9.0
Turbine rotor inlet temperature	3400°F
Theta break	1.18

A carpet plot of the change in TOGW with engine cycle characteristics using these regressions is shown in Figure 66. The optimum THETAB and the resultant TOGW as a function of OPR and RIT are shown in Figure 67. The trend in supersonic cruise out altitude and required engine power setting for the same THETAB-optimized carpet is shown in Figure 68. These ROI characteristics and the regressions from which they were derived represent the final base for comparing training usage impact on wartime performance for constant engine peacetime life.

For the 16 engine aircraft designs and the optimum engine aircraft design, all eight training mission usage definitions were run using the procedures outlined in Tasks 3.1.2 and 3.1.3. The resultant 136 peacetime usage profiles were also run through a converter program that arranged the 12 parameters (see Table 21) of interest into a specific array and format type of transmittal to DDA. A sample of the generated time-dependent usage profiles is shown in Figures 69 through 76. These usage profiles were used in Phase II to determine engine component life, which led to subsequent readjustment of wartime system performance capabilities to provide consistent performance/life capability.

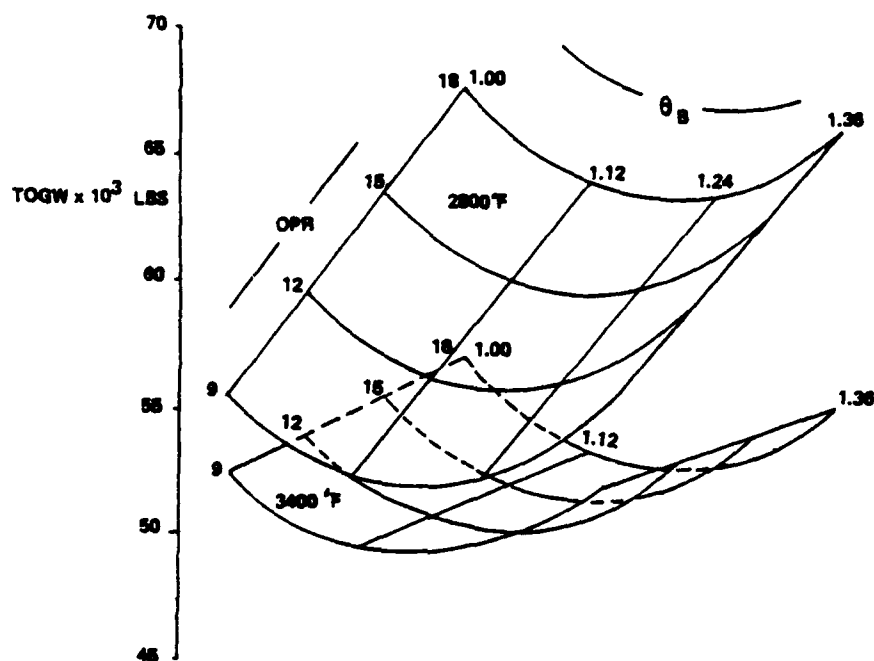


Figure 66. ROI minimum airplane size trends with engine cycle variables.

Table 21.
DDA-Defined engine utilization parameters for LUCID.

<u>Parameter</u>	<u>Units</u>	<u>Symbol</u>
Time	sec	T
Spool speed	%	XNH
Compressor discharge pressure	psia	PB3
Turbine inlet temperature	°F	T ₄
Nozzle total pressure	psia	P ₇
Inlet total pressure	psia	P _{1A}
Turbine area	%	A ₄
Free stream ambient pressure	psia	PAMBZ
Flight Mach number	---	M _N
Altitude	ft	ALT
Thrust ratio	---	F _N /F _N
Compressor discharge temperature	°F	TB3

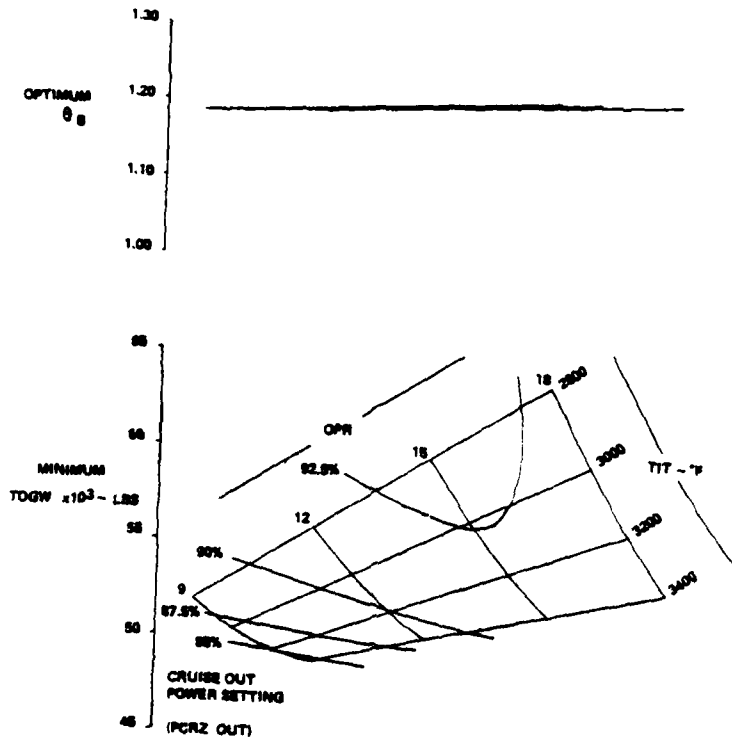


Figure 67. ROI data set optimization for minimum TOGW.

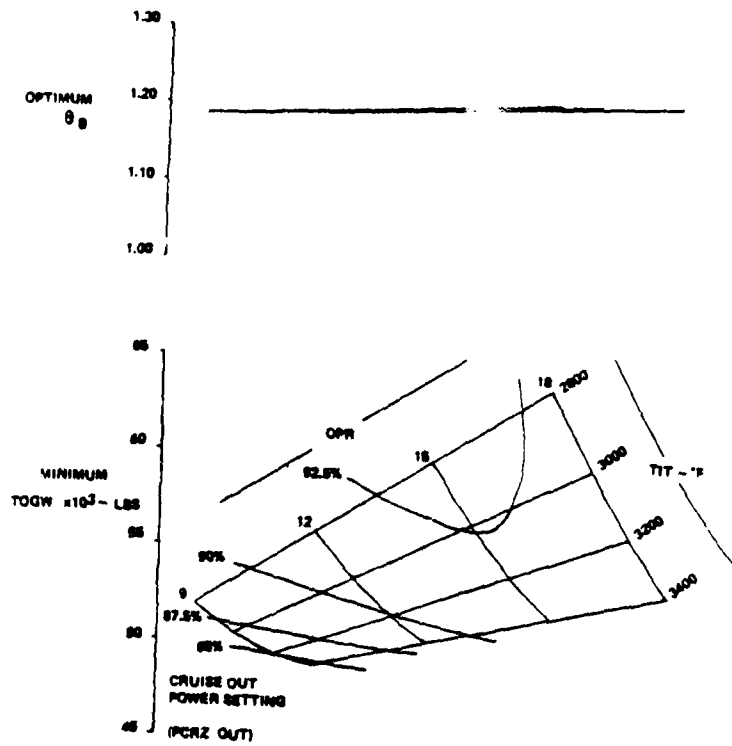


Figure 68. ROI data set optimization for minimum TOGW.

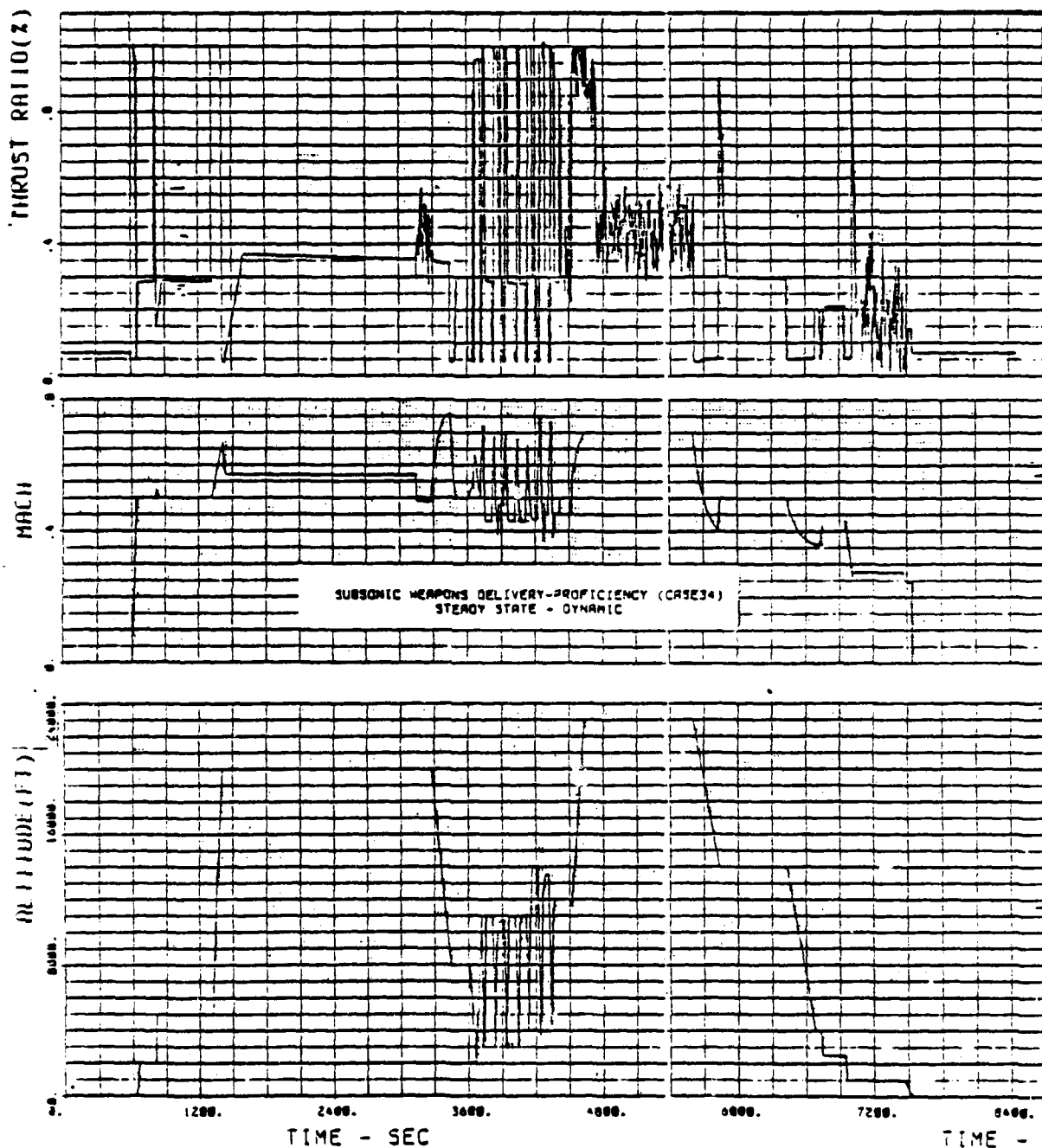


Figure 69. Time history--subsonic weapons delivery/proficiency training mission.

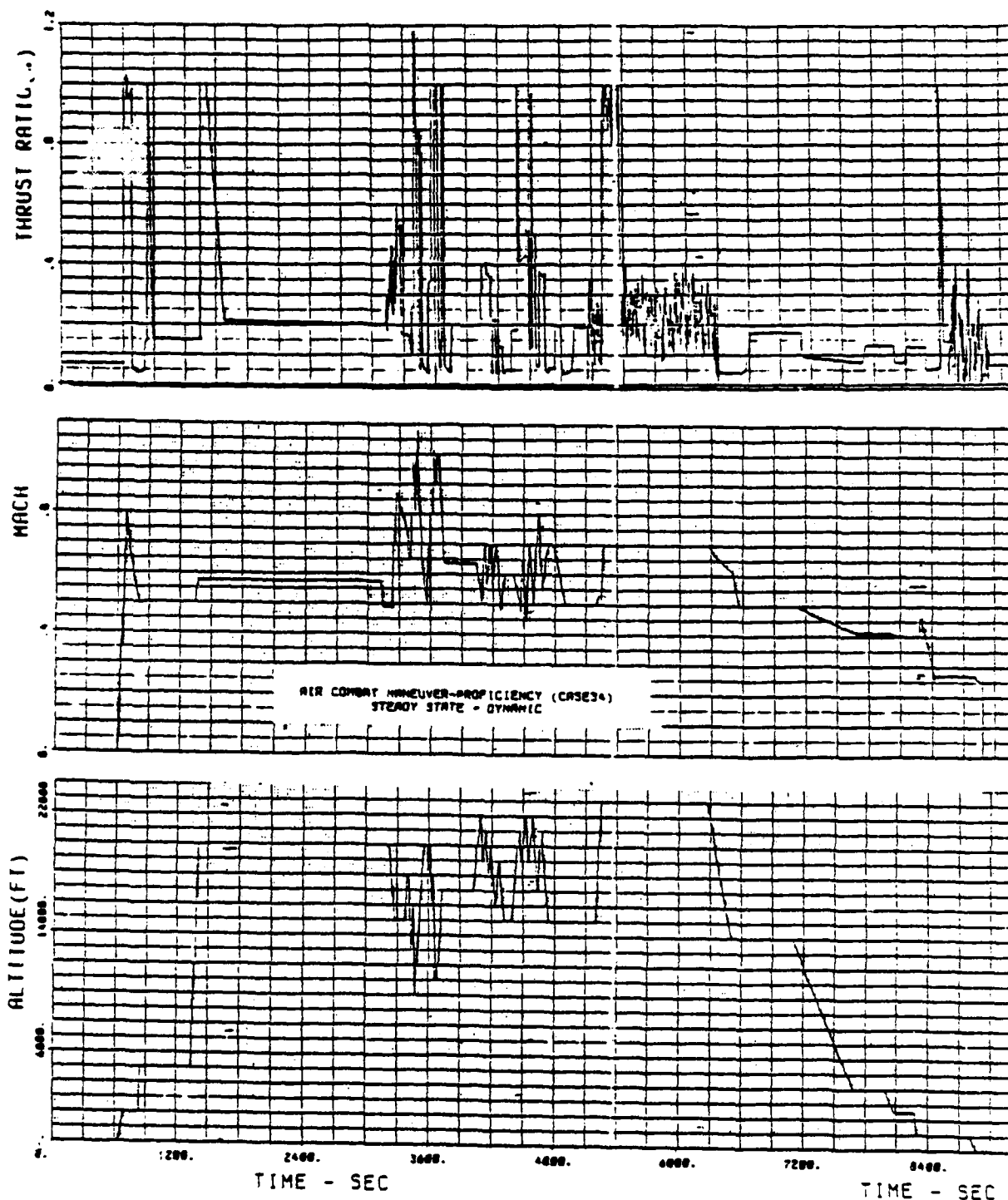


Figure 70. Time history--air combat/proficiency training mission.

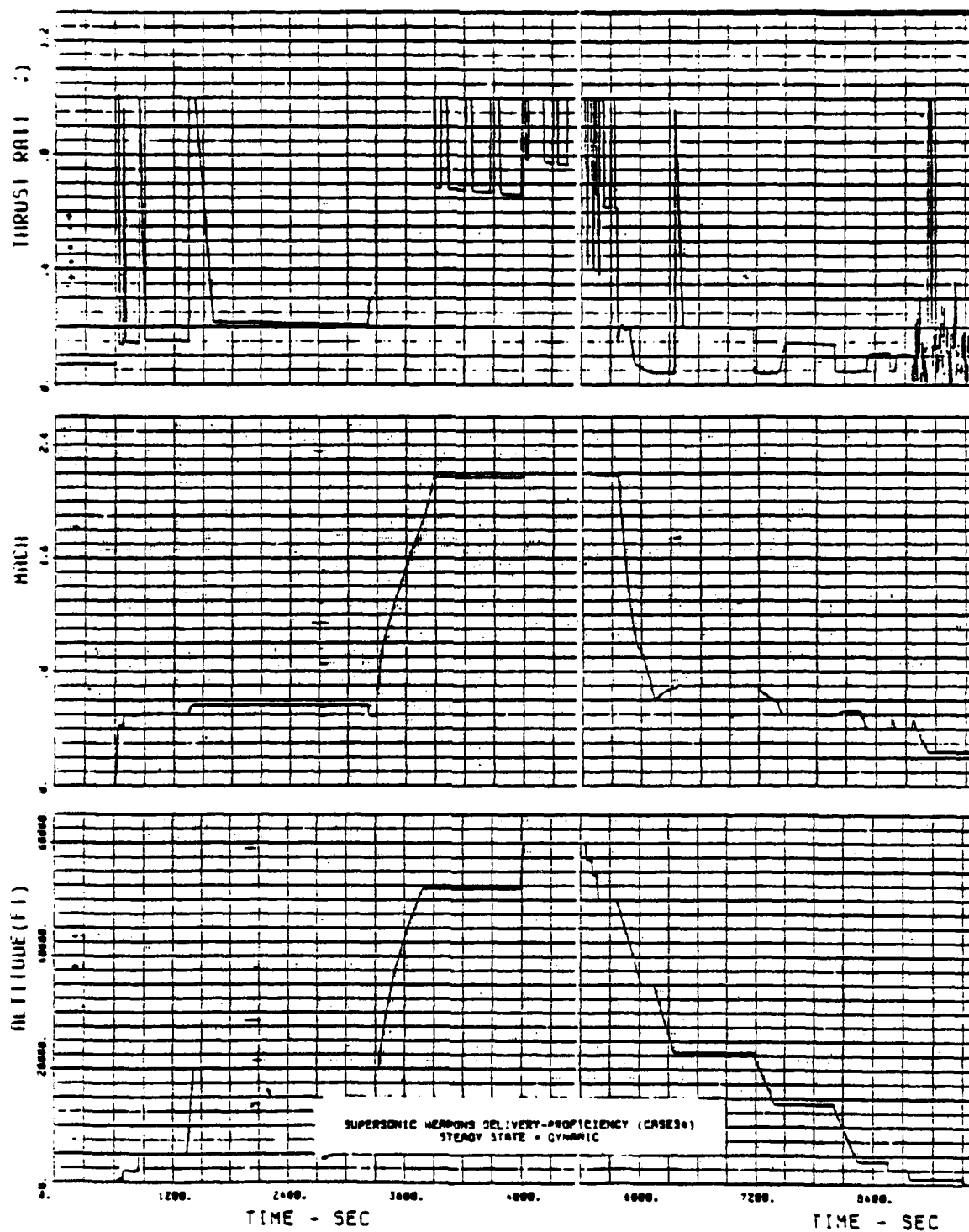


Figure 71. Time history--supersonic weapons delivery/proficiency training mission.

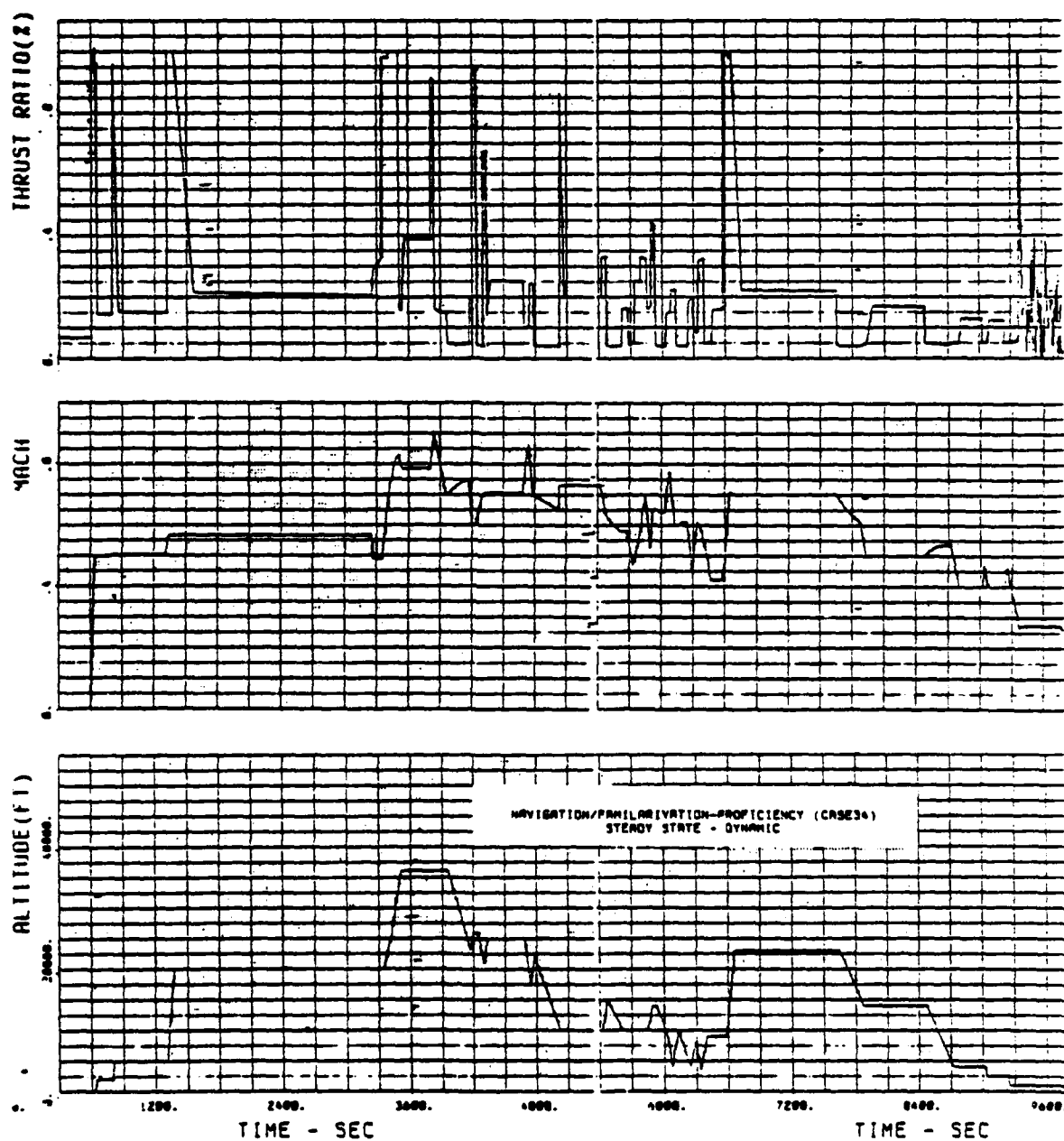


Figure 72. Time history--navigation/familiarization/proficiency training mission.

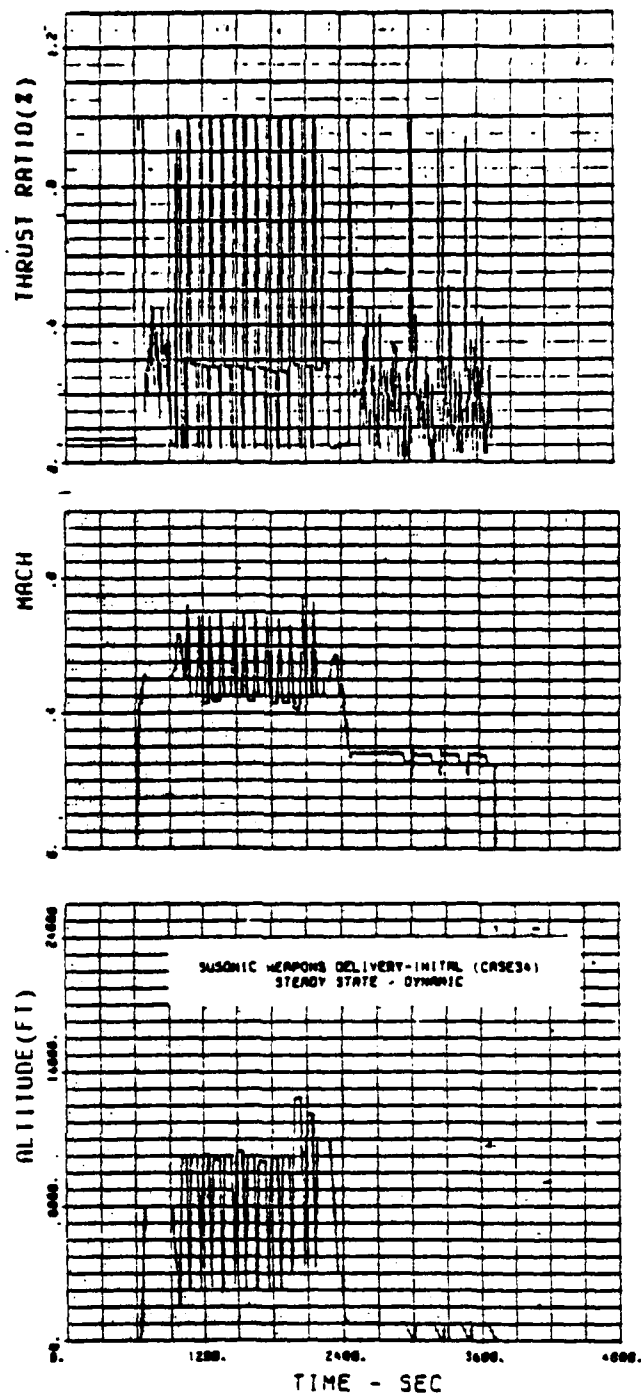


Figure 73. Time history--subsonic weapons delivery/initial training mission.

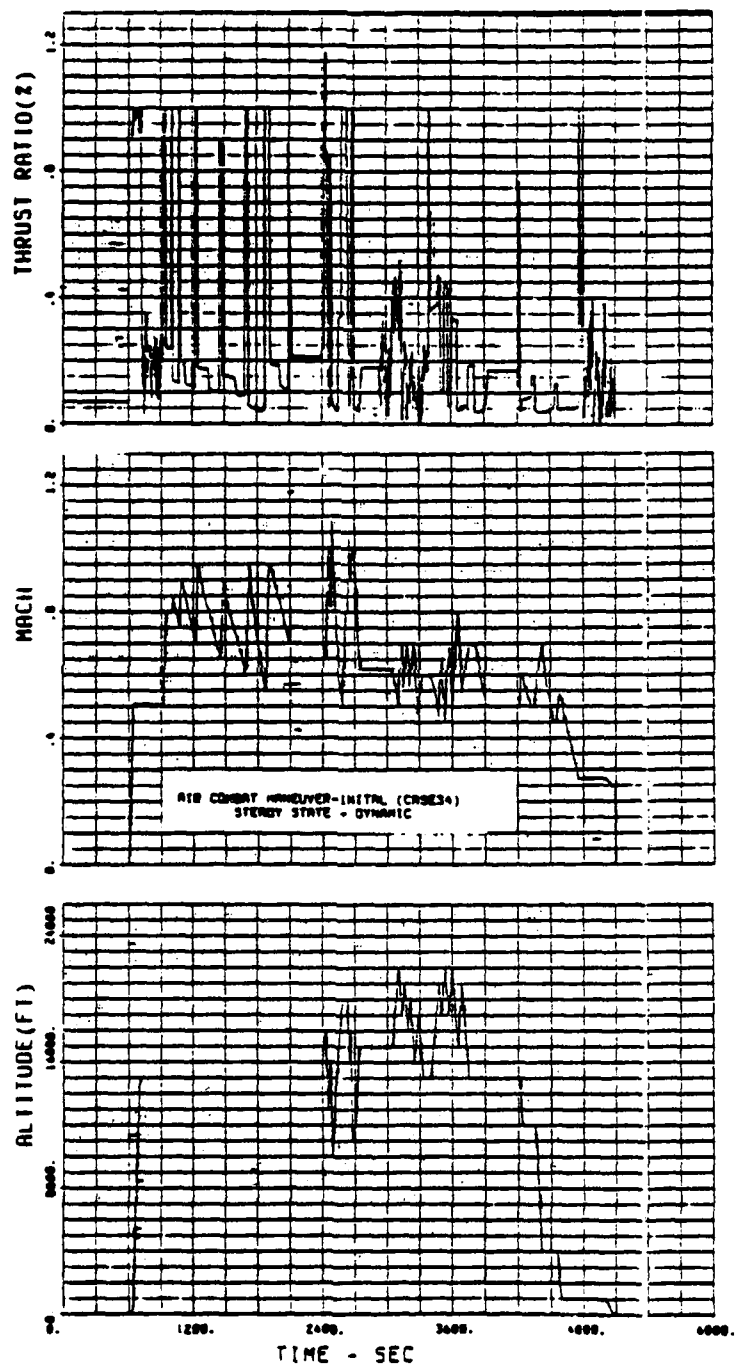


Figure 74. Time history--air combat/initial training mission.

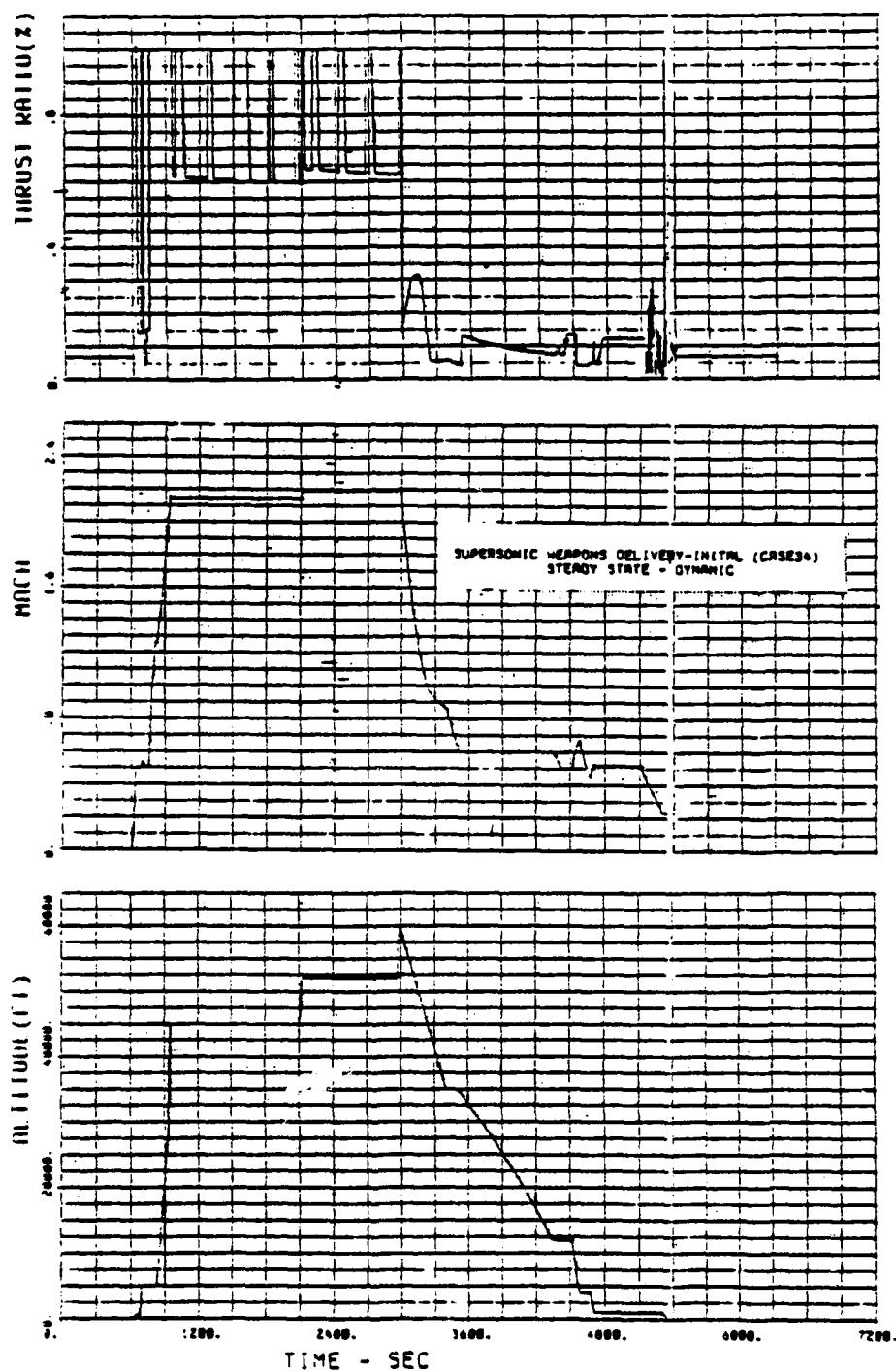


Figure 75. Time history--supersonic weapons delivery/initial training mission.

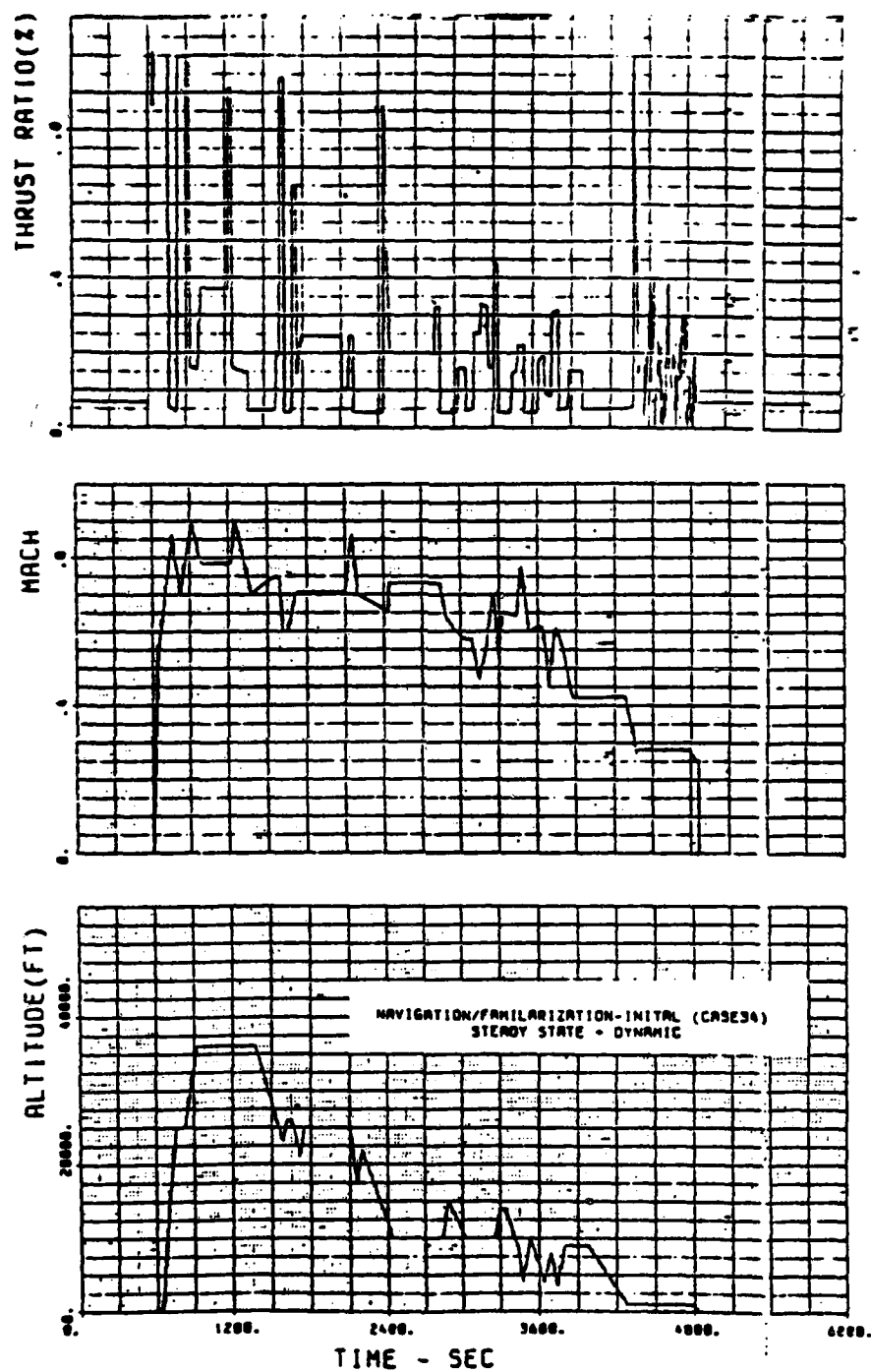


Figure 76. Time history--navigation/familiarization/initial training mission.

VII. TASK 3.1.6--VANE/TLCF SENSITIVITY STUDY

Initial evaluations of the base-line vane in the LUCID training missions revealed LUCID usage was more severe cyclically than the base-line vane had been designed to survive. This task was undertaken to identify what aspects of the base-line vane design to modify and how much change was necessary to tailor it more for the LUCID usage.

The TLCF life capability of the vane is sensitive to the local strain range and local metal temperature in the critical region of the airfoil. The strain range is a function of the stress/strain levels at the extremes of a cycle, and a simple 0-max power-0 cycle at Mach 2/60,000 ft was utilized to review the stress/strain state of the base-line design. The vane under analysis was located in the worst circumferential hot spot and only the mean radial airfoil section was examined. The strain at max power contributed the majority of the strain range, and the stress levels are predominantly thermal stresses in the critical trailing edge region. As a consequence, the vane metal temperature distribution was studied to identify where thermal gradients through the wall and around the perimeter should be reduced. A sensitivity study was conducted by arbitrarily changing the metal temperature distribution and noting the change in installed life predictions for the LUCID training missions. Upon selecting a reasonable temperature distribution as a goal, a heat transfer appraisal was made to ensure that the metal temperature changes could be accomplished and to determine the required airfoil coolant flow for this change.

INSTALLED LIFE SENSITIVITY

Two engine cases from the ROI were selected to aid in evaluating this sensitivity. The cycle definitions for those cases are as follows:

<u>Case</u>	<u>R_c</u>	<u>RIT, °F</u>	<u>θ_B</u>
34	9	3400°	1.18
35	9	2800°	1.18

The basic approach that was employed involved making changes to the base-line metal temperature distribution shown in Figure 77. The modifications were limited to the trailing edge region cooled by axial channels. The peak surface temperatures were reduced by a ΔT (see Figure 77) to the same level on both suction and pressure surfaces. Then the revised base-line temperature distribution was scaled to different average temperature levels (by varying coolant flow) to vary the vane life capability. Ideally, a design would have the highest average metal temperature with the minimum gradient to minimize the coolant requirements and still meet the TLCF criteria.

For each ΔT variant, the critical areas on the vane were relocated and found not to vary. Regressions to predict local strain for each of three critical areas were created using the same independent variables (T_m , ΔT_w , ΔT_c , P_4) and equation form developed under Task 3.1.1. A tabulation of the regression accuracy is shown in Table 22 for each of the ΔT variants. For all of the training missions, the trailing edge was the critical location for TLCF. In some cases, the pressure surface was most critical, and for other missions the

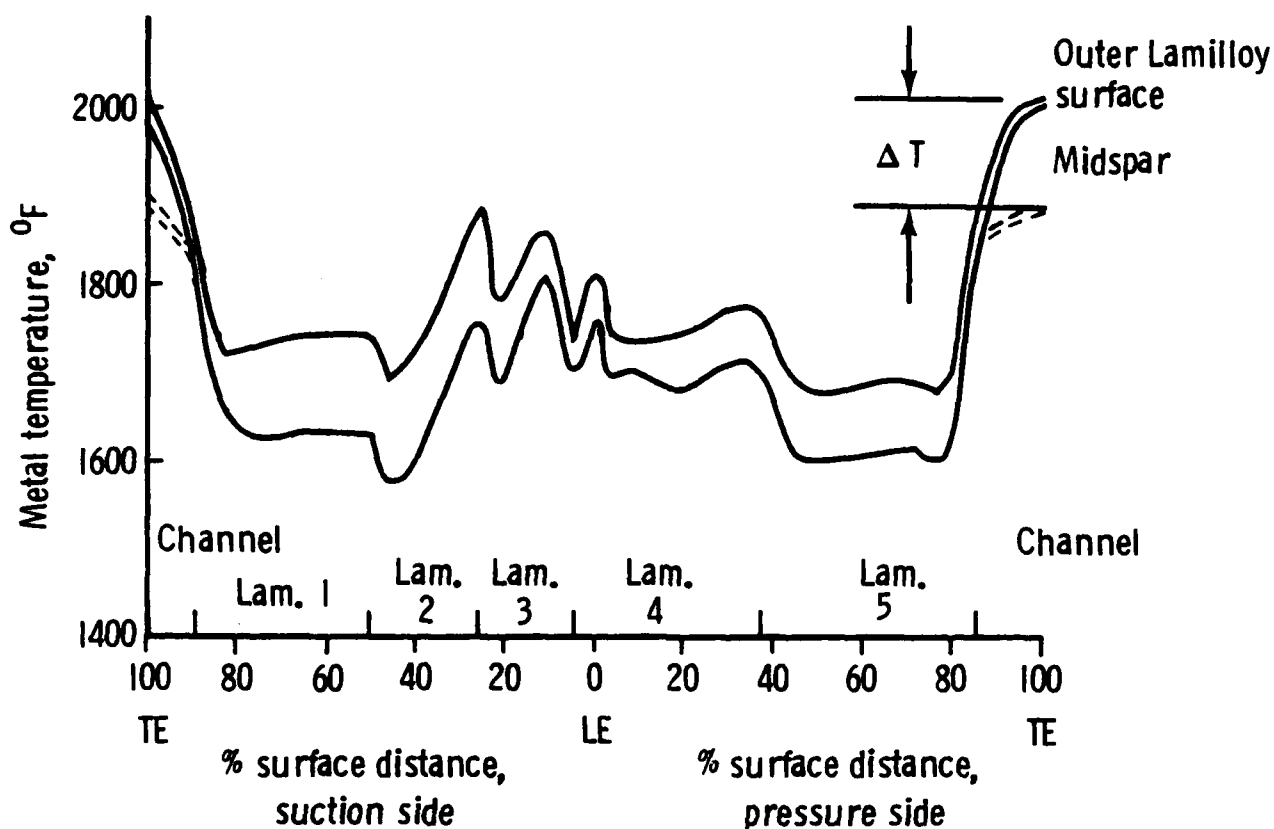


Figure 77. Vane heat transfer design point.

suction surface was most critical. For the two engine cases examined in this sensitivity study, the vane T_{LCF} life capability was selected to meet the installed life goal for the training mission mix. However, DDA noted that the resulting installed life for the wartime mission was lower than the goal. In addition, a maximum of 1700°F average metal temperature was allowed in order to meet other design criteria (corrosion, creep). Figure 78 displays the installed life trends for case 34 for the ΔT variants, while Figure 79 displays the same trends for case 35. Figure 78 shows a different trend for the wartime mission with the base-line metal temperature distribution. This unusual trend is due to the high local temperature at the trailing edge and the Mar-M246 fatigue characteristic at these temperature levels. For high strain ranges (similar to those seen in the vane trailing edge), lowering the local metal temperature actually decreases the T_{LCF} life capability. This is contrary to the normal trend of LCF fatigue data but has been observed in material test specimens. Based upon the trends shown in Figures 78 and 79, a goal metal temperature distribution was chosen that has the peak surface temperatures reduced by 80°F from the base line. This level was chosen to give reasonable average metal temperature levels for the training mission mix,

Table 22.
Vane local strain regression accuracy.

ΔT	R^2		
	TESS*	LE**	TEPS***
0	0.9518	0.9840	0.9539
-60	0.9648	0.9884	0.9630
-90	0.9680	0.9886	0.9656
-120	0.9772	0.9878	0.9703

*Trailing edge, suction surface

**Leading edge

***Trailing edge, pressure surface

to give reasonable coolant flow rates within the existing airfoil shape, and to reflect a realistic heat transfer design. For this goal temperature distribution, strain regressions were created for the three critical locations. The regression accuracy, measured in terms of R^2 , is given below:

R^2	
Trailing edge, suction surface	0.9782
Leading edge	0.9798
Trailing edge, pressure surface	0.9773

TEMPERATURE PROFILE SENSITIVITY

The goal chordwise metal temperature distribution was examined from a heat transfer viewpoint. The vane heat transfer mechanisms are shown in Figure 80. The Lamilloy portion of the base-line vane design remains basically unchanged to address the goal profile. Geometry changes are required in the axial channel region to accomplish the 80°F reduction in the trailing edge. Figure 81 shows a typical radial section through the axial channel region for a 2 sheet laminate. An analysis was performed on this channel region commensurate with preliminary design. The gas properties along the outer surface and the coolant inlet properties synthesized those of the airfoil. The channels were considered to be disconnected from the rest of the vane so that conduction between the Lamilloy and the trailing edge region was neglected. This procedure allowed the study of the effect of channel geometry on coolant flow rate and trailing edge temperature. Figures 82 and 83 chart the effect of geometry changes on coolant flow rate and metal temperature along the length of the channel. Utilizing the coolant flow trend data in Figures 82 and 83 and applying it to the baseline vane design, the goal temperature distribution could be accomplished with an additional 0.5% coolant flow by modifying the channel geometry consistent with mechanical design guidelines. Minor modifications in the Lamilloy geometry would also be required because of the additional coolant flow. However, the goal temperature profile is representative of a well-designed vane, and the airfoil coolant level is consistent with it. Since the total trailing edge thickness did not change, the turbine aerodynamic efficiency doesn't change.

The goal temperature profile has been used to determine vane/TLCF life capability requirements for each engine in the ROI. Those results are discussed in Section XI--Engine Component Life Capability.

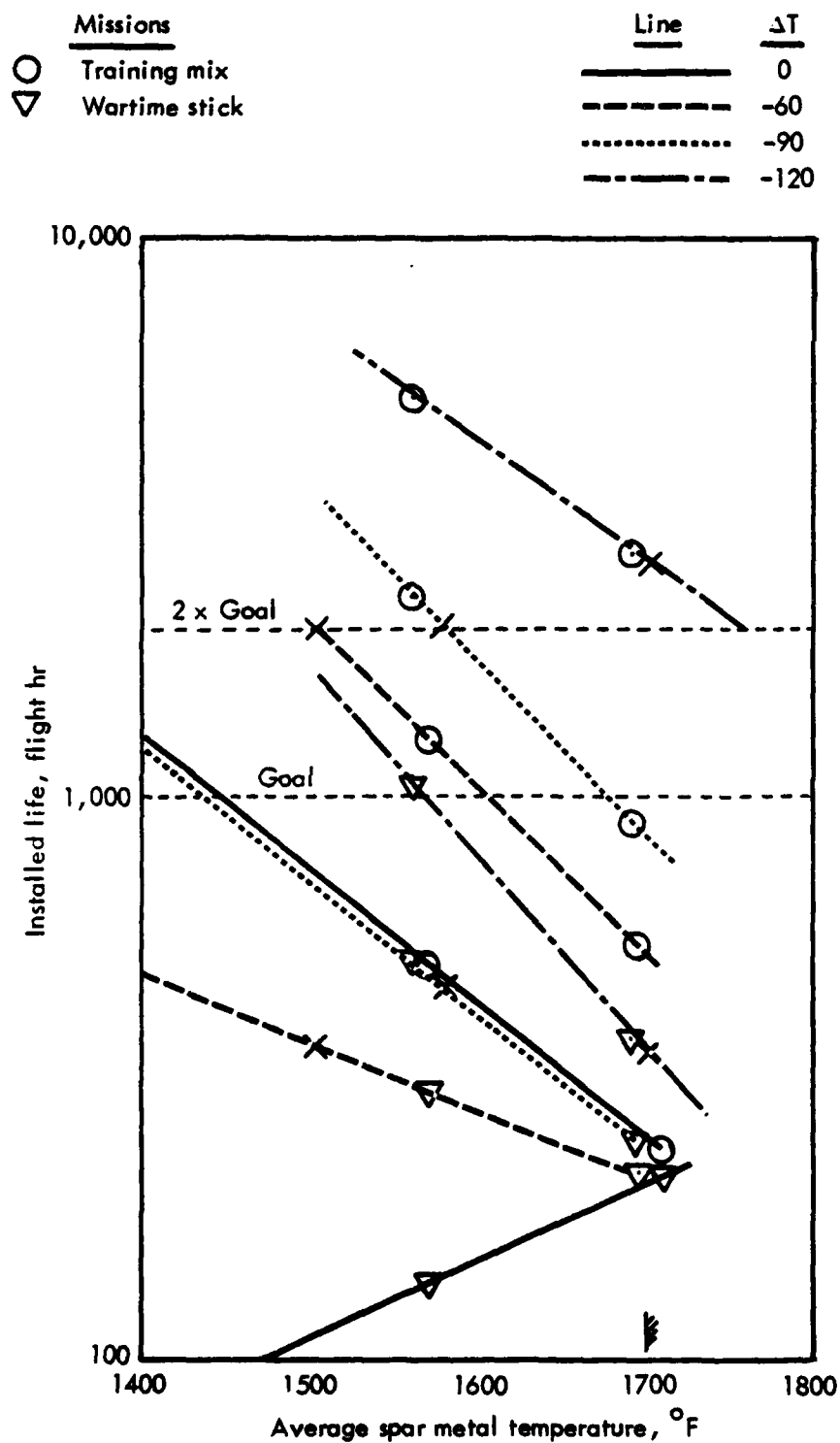


Figure 78. Case 34 installed life trends for HPT-1 vane.

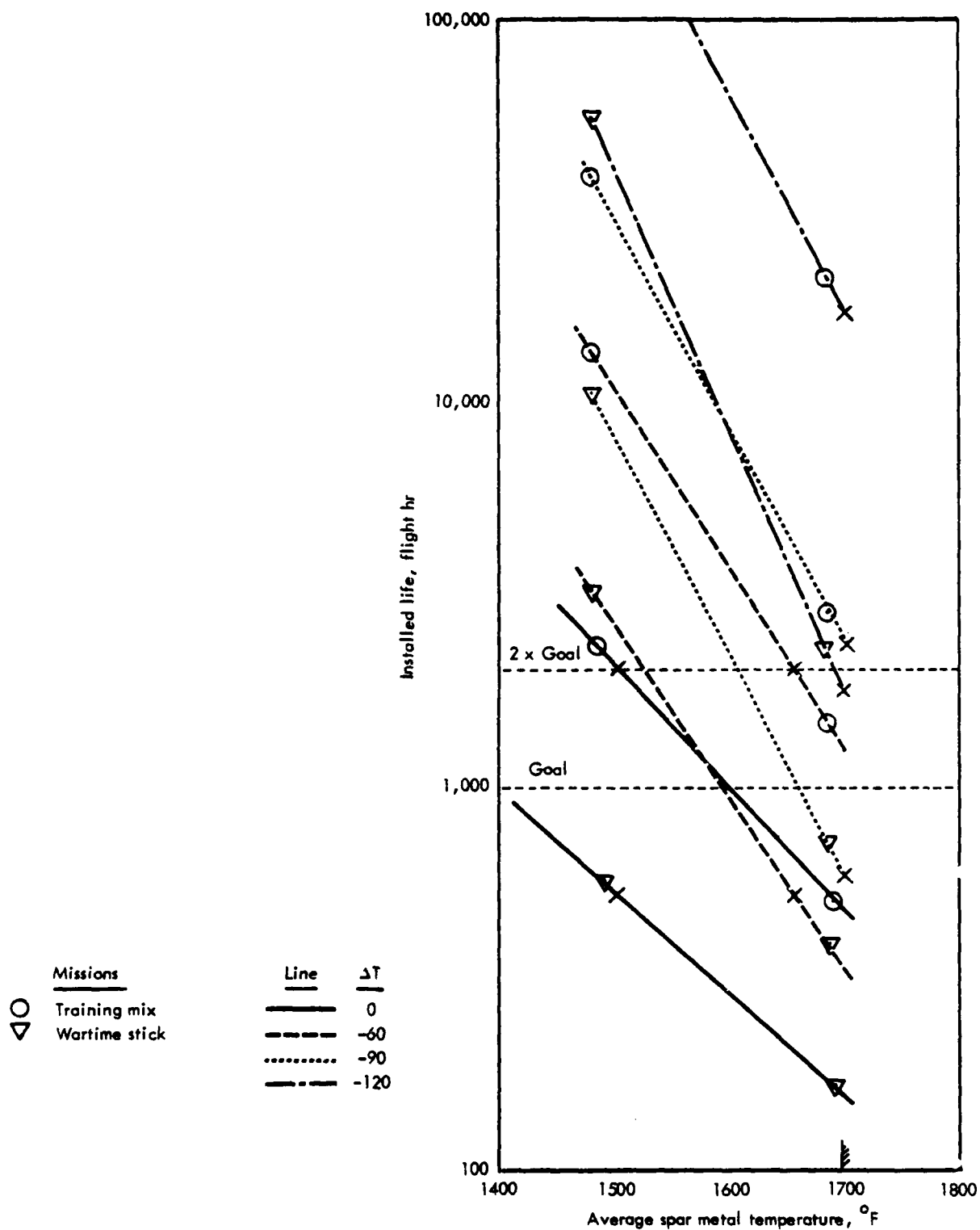


Figure 79. Case 35 installed life trends for HPT-1 vane.

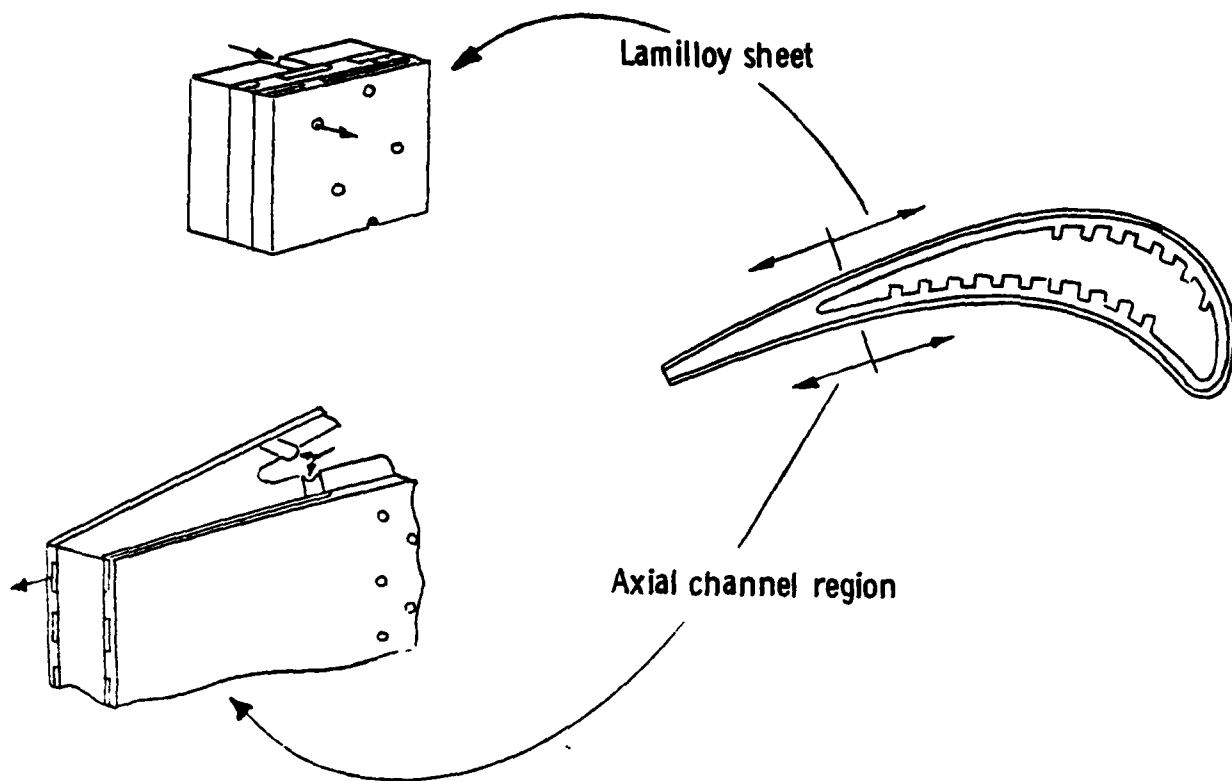


Figure 80. Heat transfer mechanisms.

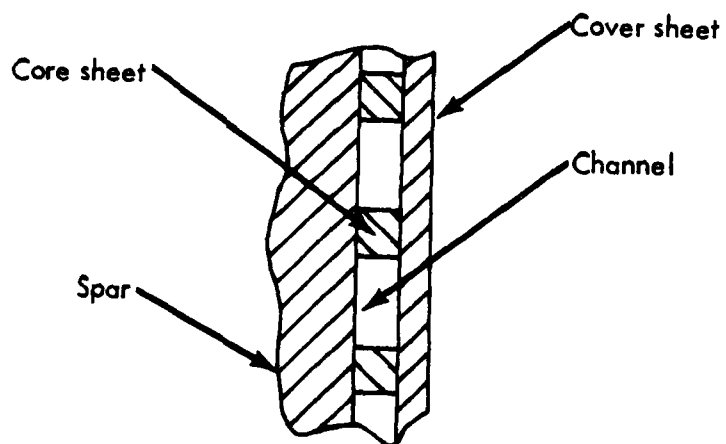


Figure 81. Axial channel region section.

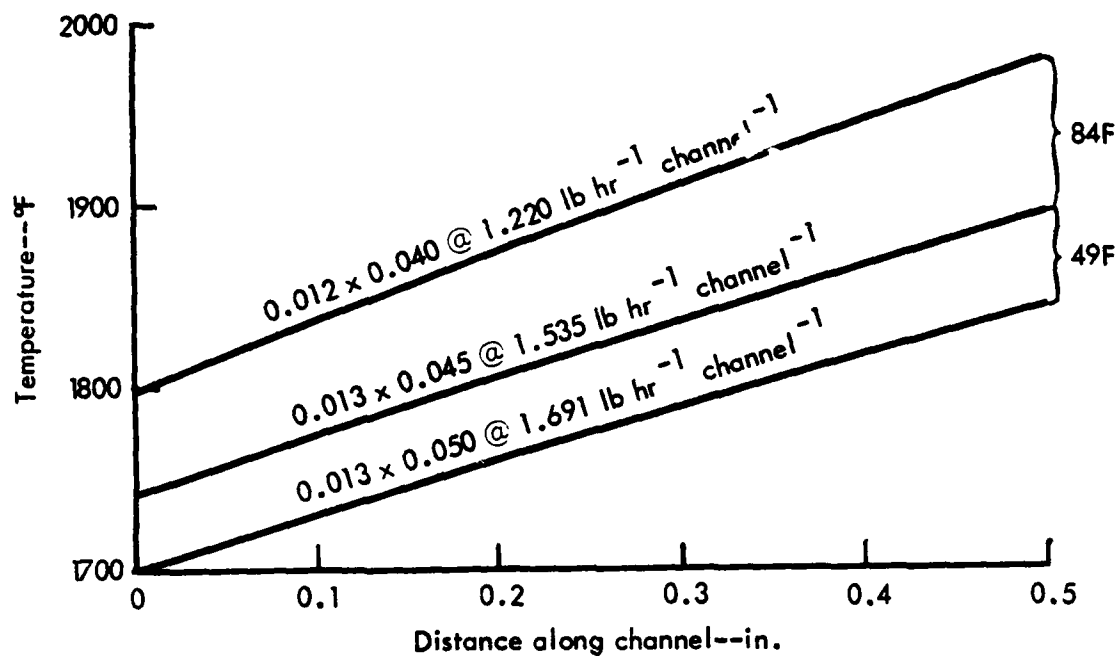


Figure 82. Surface temperatures in suction surface channel region.

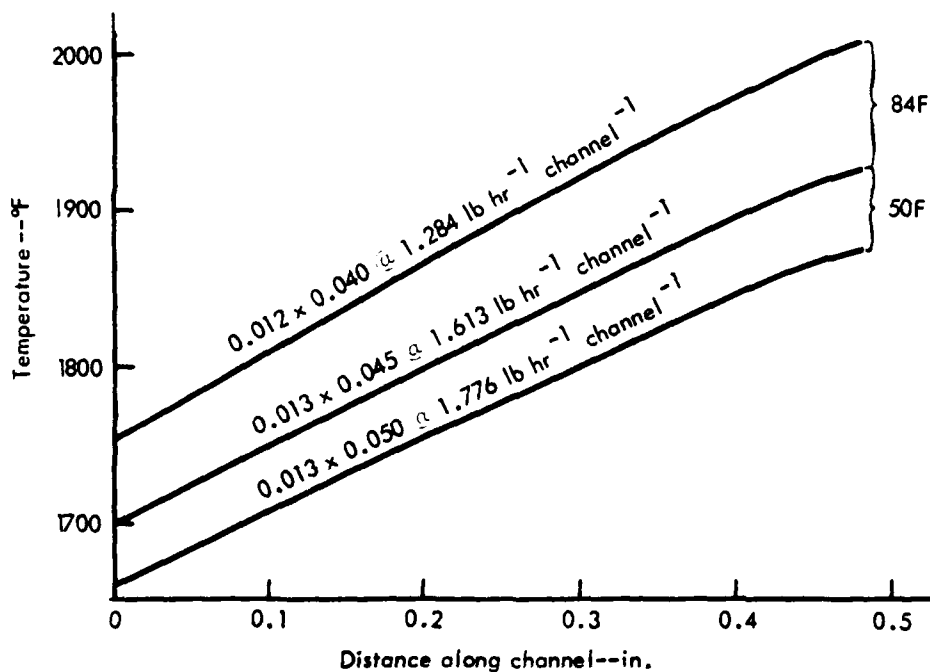


Figure 83. Surface temperatures in pressure surface channel region.

VIII. TASK 3.2.1--EFFECTS OF LIFE CAPABILITY

As a part of the LUCID approach, DDA utilizes components as indicators when modules have sufficient life capability. This section concentrates on the module changes required for different life capability levels of the indicators. These changes vary the engine weight and/or cooling flow. Tables of this adjustment data have been incorporated into the parametric engine model. Consequently, with the indicator component inputs, the parametric engine model will predict a consistent set of engine dimensions, weight, and performance.

The overall approach to the engine characteristic adjustment process is displayed in Figure 84. Shown are the weight groups for a turbojet engine with a typical percent weight for each group. Also tabulated are the indicator components and the engine weight groups that they influence. Weight adjustments can be applied to approximately 43% of the total engine weight if all indicator components require it. Also displayed in Figure 84 are the cooling flow adjustments. The turbine airfoil cooling flow is typically about 60% of the total compressor bleed flow and can be adjusted if the blade and/or vane indicators require it. The remainder of this section is organized by indicator components describing the weight and/or cooling flow adjustment data for each.

HPC-1 WHEEL

The compressor rotor is sized structurally for a myriad of design criteria including low cycle fatigue, creep, and yield/burst. Two different compressors have been sized to meet a basic set of design criteria and then re-sized for two variations in LCF life capability. This created a weight trend for the entire rotor that has been indexed to the first stage. In addition, the bearing support design changes to handle the compressor rotor weight change.

Two compressor aerodynamic designs were selected to be compatible with the matrix of engines covered by the parametric engine model. Both are 12 R_c designs with one having five stages (tip speed of 1500 ft/sec) and one having six stages (tip speed of 1300 ft/sec). They employ high-through-flow aerodynamic technology. The material selection for the mechanical design is consistent and appropriate for operation at high Mach and high altitude. An existing computer program (BA54) was used to size the compressor rotor for each set of design criteria. Figure 85 shows the type compressor rotor geometry employed for this evaluation and also shows the compressor optimization model (BA54) input. Compressor rotor weights were evaluated for both designs for 3500, 7000, and 14000 0-100-0% N cycles.

The relative weight trends are displayed in Figure 86 normalized to the 3500 cycle designs. Below 3500 cycles, the compressor would not be sized by LCF but by yield/burst. The higher tip speed design (five stages) is more sensitive to LCF requirements than the six-stage compressor. For LUCID, an average of the two cases was taken to be representative of the compressors being studied (R_c 9-18, tip speed 1000-1500 fps). Using this trend, increasing the LCF life capability by a factor of 2 increases the compressor rotor weight by 7.2% and the total engine weight by approximately 1.4%. These designs with their wheel material (AF95) are not heavily influenced by LCF. However, other materials may not have as good a LCF capability and might be more sensitive to LCF requirements. Figure 87 shows the impact of using this trend data about an engine performance cycle definition of 9 R_c , 3400°F RIT, and 1.12 θ_B .

Weight

Module	Typical % weight	Indicator components/Failure modes	Example
Forward support	3	HPCI	<p>Weight/Weight*</p> <p>HPC rotor LCF life cap</p>
Compressor case	10	Wheel/MLCF	
Compressor rotor	19	Wheel/MLCF	
Burner/Diffuser	13	HPCI/T1 Wheel/MLCF—Compressor case/MLCF	
Turbine case	12	Vane/TLCF—Compressor case/MLCF	
Turbine rotor	11	Wheel/MLCF—HPT1 blade/TLCF+SF	
Rear support	5	Wheel/MLCF—HPT1 blade/TLCF+SR	
Nozzle/Nozzle controls	15		
Accessories + Gearbox	12		
	100		

Adjustment applied to 43% total weight

Cooling flow

	Typical % HPC bleed
HPC bleed	
Cooling	
Vanes	30-35
Blades	25-30
Flowpath	
Nozzle	
Leakage	
	100

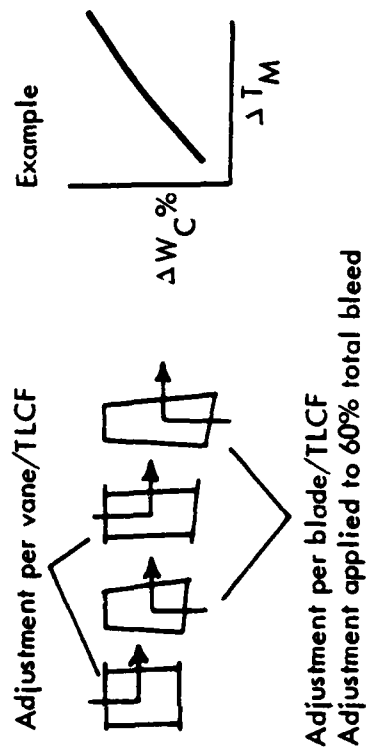
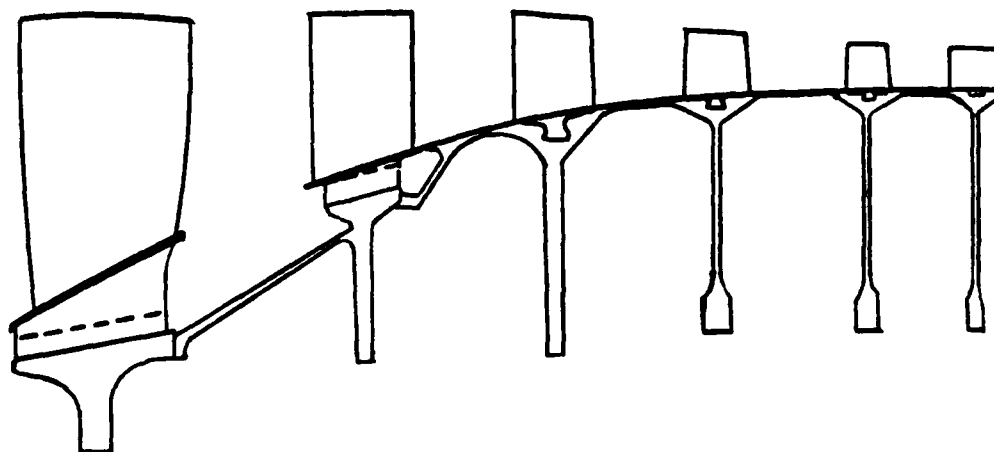


Figure 84. Engine characteristic adjustment.



Inputs

- Flow-path data
(dimensions, CF loading, rpm)
- Material selection
- Bore/Rim temperatures
- Allowable stress levels
- Attachment/Wheel type
- Geometric data
(bore radius, minimum web
thickness, platform thickness)

Output

- Minimum weight rotor
including wheels, attachments,
drive cones within geometric
and allowable stress constraints

Figure 85. BA54 compressor rotor optimization model.

COMBUSTOR CASE

The combustor outer case and the high pressure cases of the compressor and turbine are sized by burst considerations at sea level, Mach 1.2, max power. When sized for burst, the case can withstand 200,000 0-max-0 ΔP cycles for low cycle fatigue. Table 23 lists the effect on case thickness of increasing LCF life capability. Utilizing these data and extending them to engine weight, Figure 88 shows the impact on total engine weight. The burner/diffuser weight is approximately 13% of the total engine weight of which 6% is due to the outer case. Increasing the LCF life capability by a factor of 2 increases the case weight by 10% and the total engine weight by 0.6%. In addition, the impact is shown on engine cycle definitions near 9 R_c , 3400°F RIT, and 1.12 θ_B .

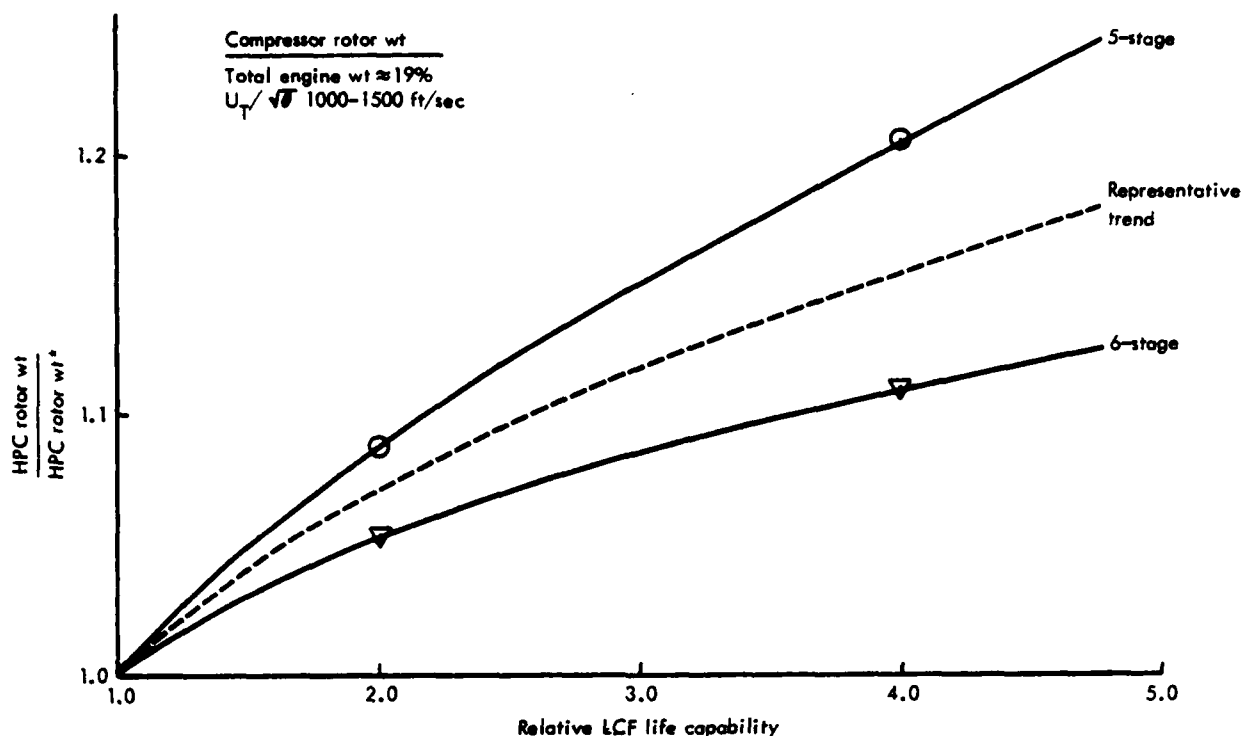


Figure 86. Compressor rotor weight trends.

Table 23.
Combustor case thickness changes with LCF requirements.

<u>LCF capability*</u>	<u>t/to</u>
200,000	1.0
400,000	1.10
800,000	1.22

* 0-max-0 ΔP cycles

HPT-1 WHEEL AND HPT-1 BLADE

The first-stage turbine wheel was used as an indicator for the rotor wheels and attachments while the first-stage blade was the index for the blades. Because these two requirements are coupled, the effect of changing LCF requirements was studied simultaneously. The two turbine designs utilized for this evaluation are identified in Table 24. An existing computer model (see Figure 89) was employed to identify the weight trends for changing the blade and/or wheel LCF requirements. Changing the stress and thus the LCF capability for either component is accomplished by changing the component weight. Results from this evaluation revealed that the blade and wheel effects were actually independent of each other over the range examined. Figure 90 shows the effect on total engine weight of changing the wheel LCF life capability. Increasing the wheel LCF life capability by a factor of 2 only increases the engine weight by 0.2%. The blade LCF and stress rupture life capability can

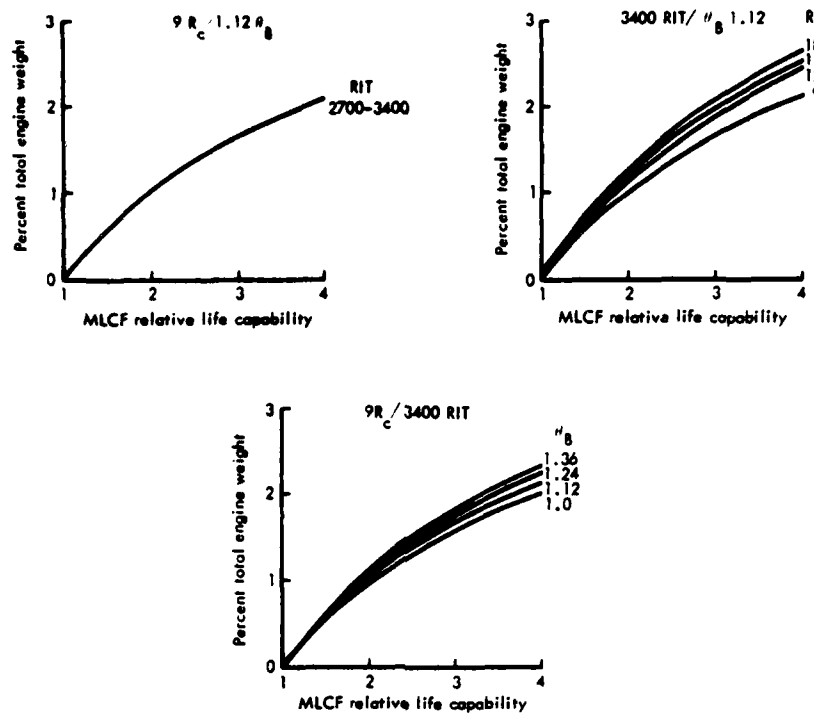


Figure 87. HP compressor rotor weight effect with changing LCF requirements.

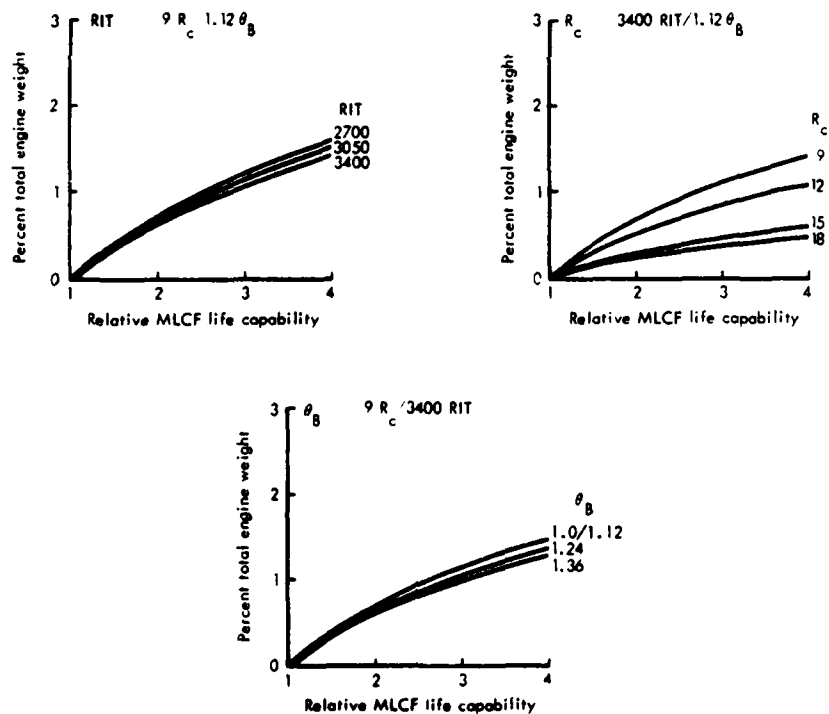
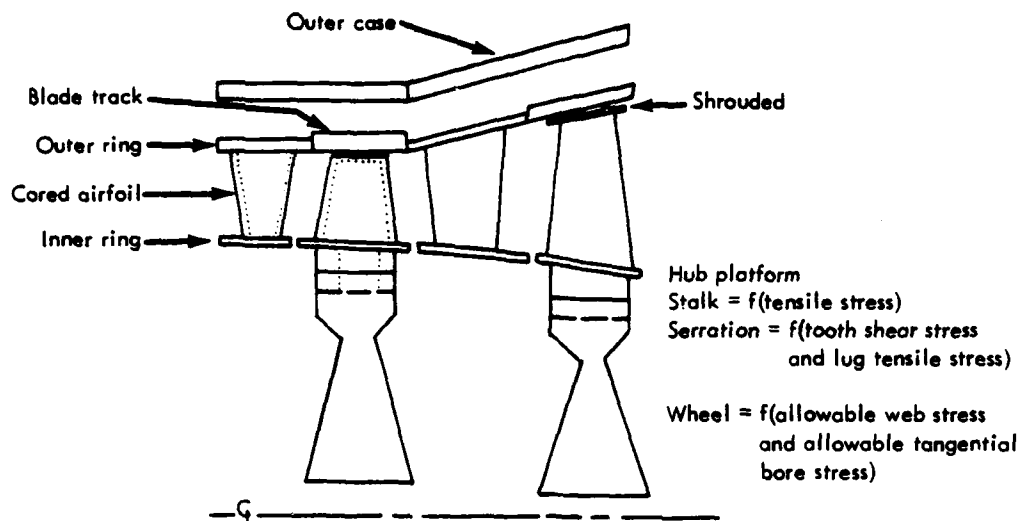


Figure 88. Burner/diffuser outer case.



Cored blade
 Wall thickness = $f(\text{stress rupture life, Larson-Miller properties, burner profile, maximum tensile stress})$

Impingement tube or Lamilloy construction

Figure 89. Turbine weight estimation.

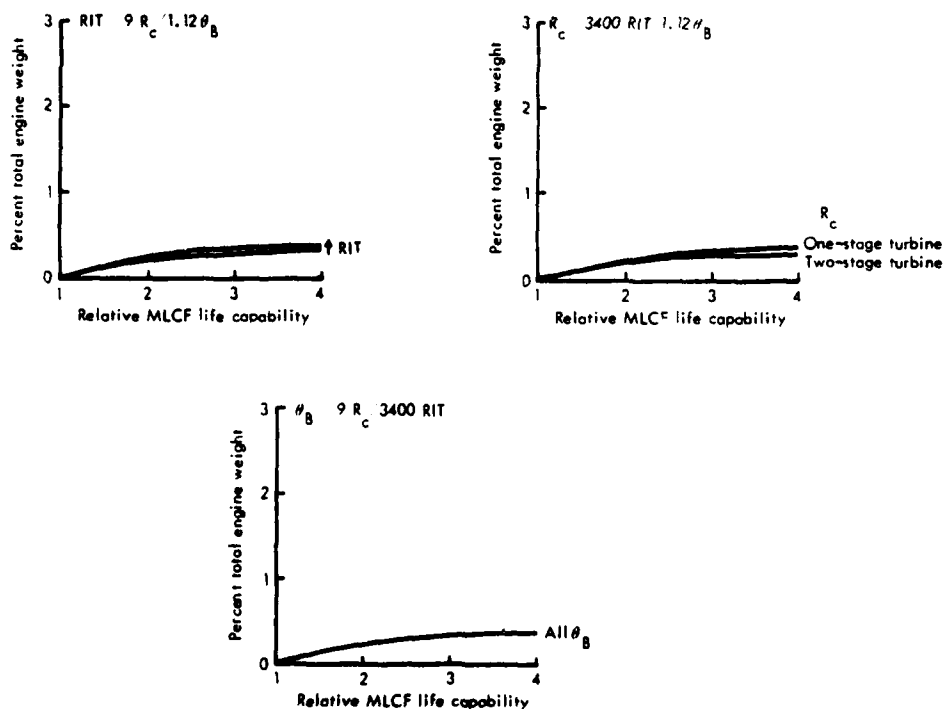


Figure 90. HP turbine wheel effects on engine weight of changing LCF requirements.

Table 24.
Turbine cycle definitions.

<u>Designation</u>	<u>PD422-4</u>	<u>PD422-12</u>
R _c	9	15
RIT, °F	3400	3400
θ_B	1.0	1.0
No. turbine stages	1	2

be changed either with the stress and/or the metal temperature. Figure 91 shows the effect on total engine weight of increasing the stress rupture life capability via stress change only. Increasing the stress rupture life capability by a factor of 2 increases the total engine weight by 0.3%.

Each engine definition originally had the same stress rupture life capability with a different nominal blade metal temperature and stress although all stress levels are less than or equal to 43 ksi and metal temperatures are greater than or equal to 1445°F at the meanline section. The basis for the parametric deck involved 64 discrete engines with different performance cycle definitions. An assessment was made for each engine, recognizing different gas and coolant properties, and predictions were made for changing the nominal blade metal temperature for both first- and second-stage blades. As an example, Figure 92 displays the coolant flow increases (from HPC discharge) required as metal temperature decreases for several engines around a 9 R_c, 3400°F RIT, and 1.12 θ_B definition. A reduction of 25°F (approx 2:1 in stress rupture life capability) requires about 1.8% additional compressor bleed for turbine blade cooling. Trend data were generated for both increasing and decreasing blade metal temperature with its impact on coolant flow.

HPT-1 VANE

The turbine vane TLCF life capability is increased by reducing the average metal temperature (increasing vane coolant flow). The vane coolant flow trend was generated in a fashion similar to the blade recognizing the different gas/coolant properties for each of the 64 base engines. Trend data were generated only for decreases in vane metal temperature since increases above the nominal level were not allowed for corrosion considerations. Figure 93 displays the trends of coolant flow for all turbine vanes with changing metal temperature. A reduction of 25°F in vane metal temperature required approximately an additional 2% coolant flow dependent upon the engine cycle definition.

Parametric Deck Update

The engine parametric deck discussed in Task 3.1.4 was updated to add the engine weight and cooling flow adjustment tables and the appropriate input data to utilize them. Table 25 lists the input index computer names and the indicator components from which the index value is determined. These updates to the parametric PD422 engine model were transmitted to Boeing along with the appropriate index values for their use in Task 3.2.5. The index values were determined by DDA during Task 3.2.4.

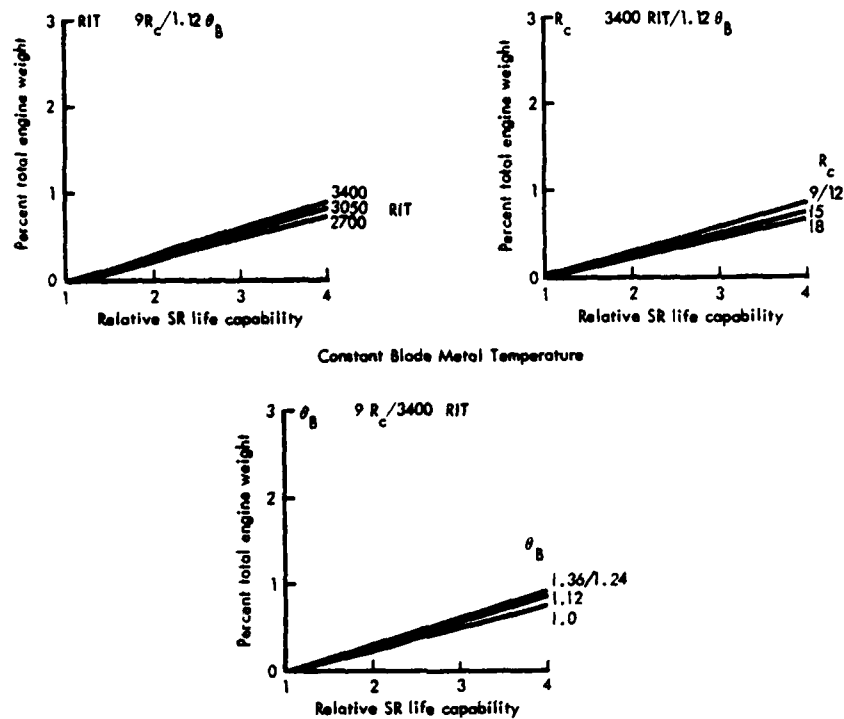


Figure 91. HPT-1 blade effects on engine weight of changing stress rupture requirements.

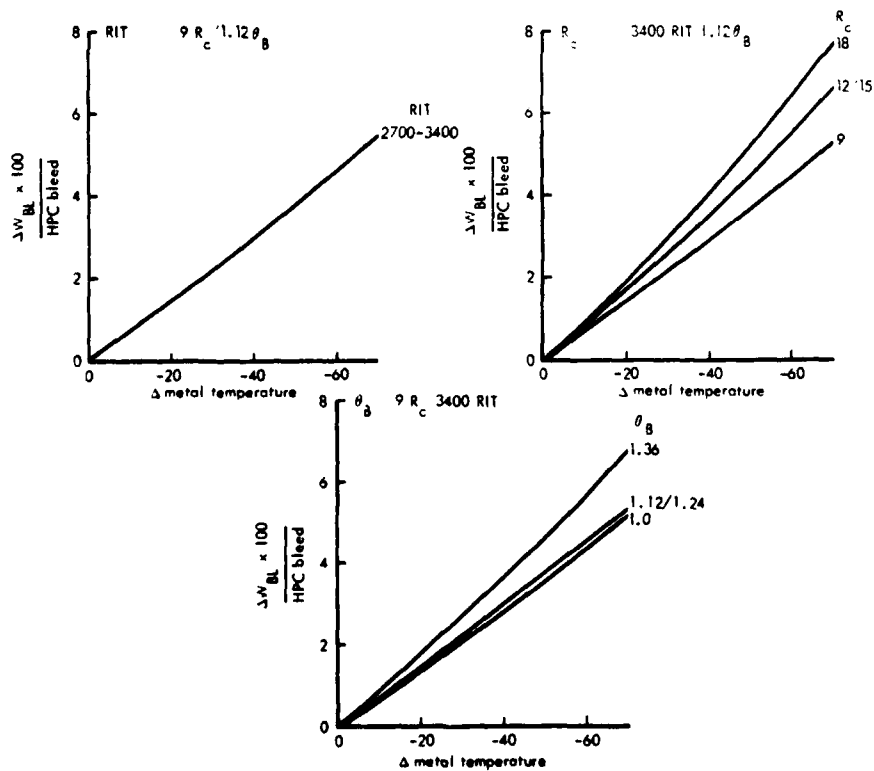


Figure 92. Rotor airfoils: Cooling flow trends with metal temperature change.

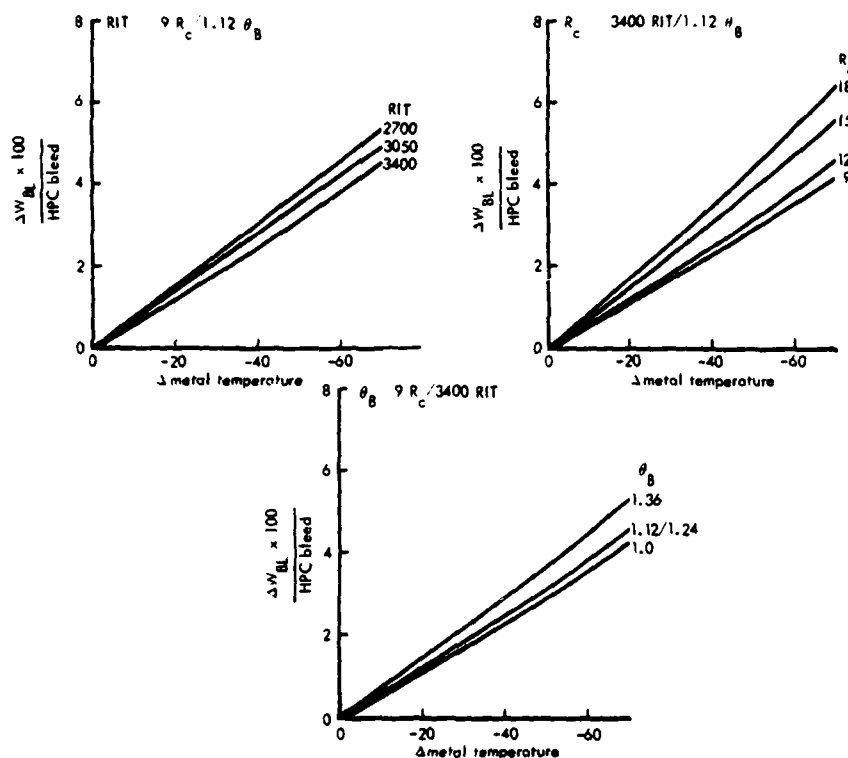


Figure 93. Vane airfoils: Cooling flow trends with metal temperature change.

Table 25.
PD422 parametric deck life index inputs.

<u>Name</u>	<u>Component/Failure mode</u>
CMLCFI	HPC-1 wheel/MLCF
BMLCFI	Combustor case/MLCF
TWMLCI	HPT-1 wheel/MLCF
TBTFI1	HPT-1 blade/TLCF + SR (ΔT_M)
TBTFI2	HPT-1 blade/TLCF + SR (Δstress)
TVTFI1	HPT-1 vane/TLCF (ΔT_M)

IX. TASK 3.2.2--REFERENCE UTILIZATION PROCEDURE

In Phase I, Task 3.1.2, a family of training missions was defined around which peacetime usage could be generated. These training missions were to be applied to specific airframe/engine combinations within the region-of-interest (ROI) of Task 3.1.5. The resultant usage time histories of each airplane on these missions represents the projected peacetime family of potential utilizations for that design over its operational life.

The intent of this task was to develop a procedure for defining an appropriate frequency of occurrence of these training missions. The resultant mix of missions based on this frequency of occurrence would be the reference aircraft utilization (RAU). The initial proposed logic for this procedure was as follows. Over the total fleet dispersion and potential operating life of an aircraft, a certain occurrence of each proposed training mission (no mission would ever be 0%) would make up the total training usage. This assumption represents the idea that once a system enters service, the original training objectives, which evolved around the original design (combat) roles, can be altered. That is, when the need arises for a system to answer "new" tactics or threat, it initially will be imposed on an appropriate aircraft in the existing inventory. The likelihood of an existing aircraft being used for the "new" objective will be dependent on its inherent design characteristics. As an example, a subsonic close air support aircraft (say an A-10 type) would have a low probability of use on an air-to-air combat mission based on its configuration, engine type, and operating envelope. Therefore, the approach of considering the total fleet dispersion of any aircraft over its potential operating life must recognize the likelihood of its training usage changing with time. The initial idea was that each aircraft would be biased into a mission mix based on the ability of its design characteristics to respond to the specific requirements of each mission. That is, each mission mix, or RAU, would vary for each discrete design in the ROI. This idea was premised on the ROI containing variation of fundamental airplane configuration variables such as thrust to weight and/or wing loading which, at a PD level, are principal factors in an airplane's capabilities. However, the final approved selection of ROI variables contained only engine parameters (OPR, RIT, THETAB). This relegated the airplane characteristics to a fixed design in the ROI.

The selection of a fixed airframe design negated the need to have a procedure for changing the RAU based on an airframe's potential application. Instead, a logical basis for defining one reference mission mix for all ROI systems was needed.

The means of determining a representative mission mix was based on current Air Force training methods. Air Force training manuals covering all current Tactical Air Command aircraft were reviewed. These various manuals (TAC 51-60, TAC 55-XX, Syllabus) provided a definition, by aircraft type, of all training missions currently in use, a frequency of occurrence of any mission to attain a specific pilot capability, details of each mission's flight operation, and the required aircraft configuration for each mission.

From these manuals, training practices for five of the most current TAC aircraft were examined in detail. The selected aircraft were F-4, F-111, F-15, F-16, and A-10. The type of data provided by these manuals is shown in Figure 94 and 95 for basic training in an F-4 aircraft.

SECTION I

GENERAL INFORMATION

1. COURSE TITLE: GAF Operational Training Course, F-4
2. COURSE Number: F4000FGB
3. Purpose: To graduate mission capable F-4 aircrews
4. Location: 35 TFW, George AFB, CA
5. Duration: 13 ground training days plus 103 flying days
6. Status Upon Completion: Upon satisfactory completion of this course, Aircraft Commander (AC) graduates will be considered mission capable. Weapon Systems Officer (WSO) graduates will be considered mission capable.

PHASES OF TRAINING

<u>Flying</u>	<u>Sorties</u>		<u>Hours</u>	
	<u>AC</u>	<u>WSO</u>	<u>AC</u>	<u>WSO</u>
Transition	13	3	19.5	4.5
Formation	4	3	6.0	4.5
Basic Fighter Maneuvers	8	6	10.8	8.6
Air Combat Maneuvers	6	6	4.8	4.8
DART	3	2	4.5	3.0
Ground Attack	11	7	15.4	9.8
Ground Attack Tactical	5	3	6.5	3.9
Ground Attack Night	4	3	5.2	3.9
Air Combat Tactics	<u>4</u>	<u>3</u>	<u>3.2</u>	<u>2.4</u>
TOTALS	58	36	75.9	45.4

Figure 94. Basic F-4 training requirements.

To simplify the understanding of TAC training variations, the various mission types were catalogued into three general classes of operation--Familiarization (FAM), Air Combat Maneuver (ACM), and Ground Attack (AG). Training missions were grouped into these three classes for each airplane type and for each training objective. Of some interest is how training objectives change with airplane type and age. The F-15 and F-16 had only one basic training format defined in the manuals, while older aircraft had several variations. Also ground attack aircraft predominately train in their role while air combat aircraft shift training emphasis between air combat and ground attack. A summary of these training missions, by airplane type, is shown in Figure 96. This figure also shows the percent split in training usage between the three objects previously outlined. This usage split shows that for relatively new airplanes, around 25%-30% of the usage is in familiarization operation and the balance is in the primary design role for which the airplane was designed.

ORDER OF TRAINING

<u>MISSION</u>	<u>HOURS PER</u>		<u>HOURS SUPPORT</u>	<u>PER STUDENT AIRCREW</u>	
	<u>PILOT</u>	<u>WSO</u>		<u>NO. HRS REQUIRED</u>	<u>NO. ACFT REQ</u>
TR-1	1.5			1.5	1
TR-2	1.5			1.5	1
TR-3	1.5	1.5		3.0	2
TR-4	1.5			1.5	1
GAN-3	1.3			1.3	1
GAN-4	1.3	1.3		2.6	2
BPM-9	1.3	1.3		2.6	2
ACT-1	.8	.4	.4	1.6	1-1/2
ACT-2	.8	.4	.4	1.6	1-1/2
ACT-3	.8	.8	.8	2.4	3
ACT-4	.8	.8	.8	2.4	3
TOTALS	75.9	45.4	13.2	116.3	92.33

TRANSITION

TR-1	Aircraft: 1	Time: 1.5
	Crew: AC/IP	Config: DO

Takeoff, departure, airwork, stab aug orientation
indexer light/aural tone orientation, approach to
stalls (1 "G" and landing configuration), straight-
in touch-and-go, normal touch-and-go's, closed
patterns, full stop landing.

FUEL/CONFIGURATION CODE

Fuel Configuration:

A - Full Internal
D - Full Internal + 2 x 370 gallon tanks full

Munitions Configuration:

0 - Clean, inboard pylons
2 - AIM-9, 1 ea captive
7 - 150 RDS TP
13- 150 RDS TP; MK-82 GP (MAU-93 fin) inert, 6 each
14- 150 RDS TP; MK-82 SE inert, 6 each
21- SUU-20 x 6 BDU-33; 1 SUU-25 x 8 MK-24 MOD 4 flares
23- 2 SUU-20 x 12 BDU-33
24- 150 RDS TP; 2 SUU-20 x 6 BDU-33 + 6 MK-106

Figure 95. Sample F-4 training details.

For older aircraft like the F-4, which have been forced into more diverse applications, a different split in training usage is more common. Nominally 50% of the training time is given to the specific training objective (e.g., ACM or AG), the balance being split between familiarization and the alternate role (AG or ACM). For basic or upgraded pilot rating on the F-4, a nearly equal split between all three areas of training occur.

From these data a mix of the three general training roles can be defined for either an air combat or a ground attack oriented aircraft. As this contract is examining a ground attack airplane and only one airframe type has been selected for the ROI, only the ground attack mix will be used in Task 3.2.3.

Reference engine utilization data were created from the reference aircraft utilization using the procedure discussed in Section IV--Utilization Prediction Procedure Development.

Air Force Syllabus Usage							
Type of aircraft	Number of sorties				Percent split		
	FAM	ACM	AG	Total	FAM	ACM	AG
F-4 BASIC	17	21	20	58	30%	36%	34%
F-4 MR	12	12	18	42	28%	28%	44%
F-4 AG	13	12	28	53	25%	23%	52%
F-4 ACM	13	27	9	49	27%	55%	18%
RF-4	18	4	--	22	82%	18%	--
F-111	1	7	17	25	5%	28%	67%
F-111A	6	--	20	26	23%	--	77%
F-111F	6	--	14	20	30%	--	70%
F-111D	2	--	10	12	17%	--	83%
F-15	4	23	--	27	15%	85%	--
A-10B	12	4	21	37	32%	11%	57%
A-10C	11	4	19	34	32%	12%	56%
A-10XA	8	--	10	18	44%	--	56%
A-10XB	7	--	--	7	100%	--	--
F-16 BASIC	6	8	8	22	27%	36%	36%

Figure 96. Current TAC aircraft usage summary.

X. TASK 3.2.3--DEFINE REFERENCE AIRCRAFT UTILIZATION AND SENSITIVITIES

As discussed in Task 3.2.2, the reference aircraft utilization was defined to be a mix of the training missions developed in Task 3.1.2. Only a single mix was required as no variation in airplane definition was made in the ROI. The primary role of the ROI airplane was air-to-ground weapon delivery from supersonic cruise. The airplane characteristics were also aligned with ground attack oriented aircraft (T/W=.60, W/S=85-90 PSF). Based on Task 3.2.2, 60% of the training should be in the ground attack role with approximately 25% spent in familiarization and 15% in air combat. However, this LUCID airplane was designed as a dedicated supersonic cruise tactical design. It is therefore assumed that a reasonable level of supersonic operation would be required. Unfortunately, no current TAC inventory aircraft provides a basis for defining what level of supersonic operation should be used. It was arbitrarily decided to split the 60% ground attack training into 35% supersonic weapon delivery practice and 25% conventional subsonic ground attack practice. One other consideration was required for the LUCID training mix. Two classes of training had been defined in Task 3.1.2: initial and proficiency. The split between these two classes of usage is very dependent on the capability of other inventory aircraft to perform similar operations. Because of the dependence on supersonic cruise of the airplane, no alternate airplane was seen as a likely replacement to eliminate or minimize either class of training. Therefore a 50-50 split between the two classes was selected. The resultant training mission mix for the ROI reference utilization is shown in Figure 97 for all four mission types and each mission class.

In the initial proposal of this task, the ROI was to be represented by only a few (possibly 3 to 4) selected system designs. These designs were to have all training usage profiles defined by appropriate segmented mission time histories. Around these selected designs, usage sensitivities were also to be generated. From these sensitivities a general usage impact over the complete ROI was to be made. This approach to Task 3.2.3 was revised prior to performing the work. It was mutually agreed by the Air Force, DDA, and BMAC to examine all cases making up the ROI (17 cases) and use the ARES method to examine the usage impact. Both system performance and engine component usage were evaluated with this method. Results from this work are presented in Task 3.2.5.

One set of sensitivities was required by DDA to allow adjustment of engine characteristics to attain consistent life levels. This was the sensitivity of airplane takeoff gross weight to engine weight and to mission segment SFC. These sensitivities were generated around the optimum engine/airplane configuration from the initial ROI results. The resultant sensitivities are shown in Figure 98. These data were available to guide design modifications for different life capability requirements when more than one avenue for change was available (i.e., turbine blade--where either stress or metal temperature could be charged).

Mission Type	Percent Mission Split	
	Mission Class	
	Initial	Proficiency
Familiarization	12.5%	12.5%
Air combat	7.5%	7.5%
Subsonic ground attack	12.5%	12.5%
Supersonic weapon delivery	17.5%	17.5%
Subtotal	50.0%	50.0%
Total	100%	

Figure 97. Training mission mix for reference aircraft utilization.

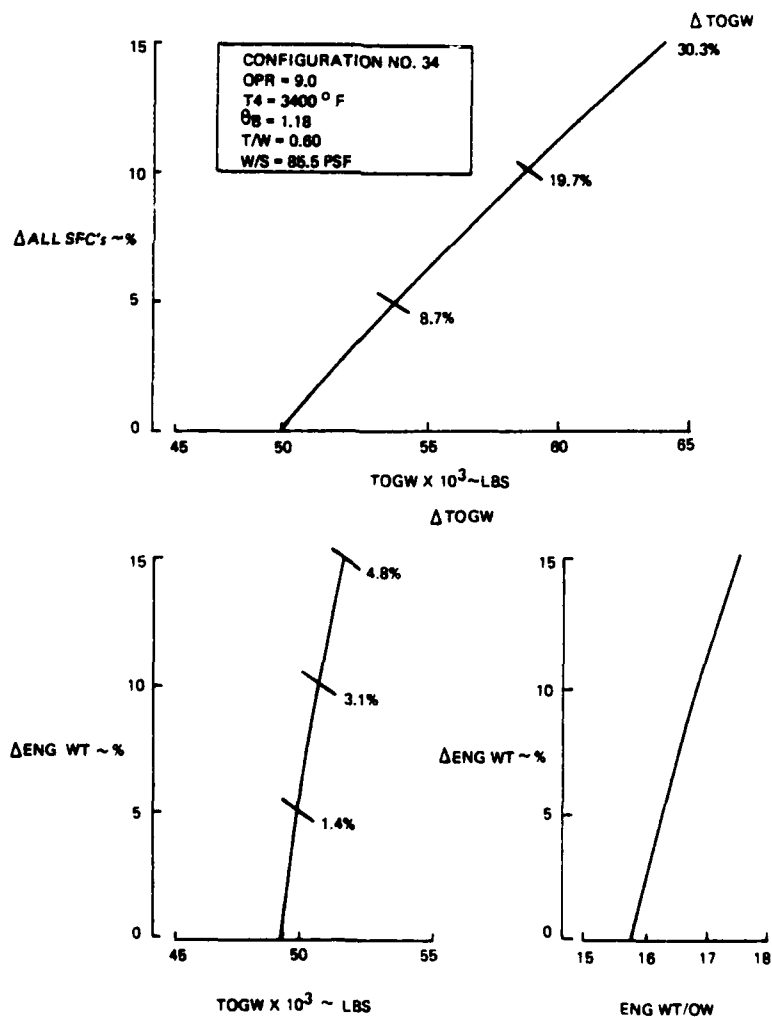


Figure 98. Wartime mission sensitivity to engine weight and SFC--Configuration 34.

XI. TASK 3.2.4--ENGINE COMPONENT LIFE CAPABILITY

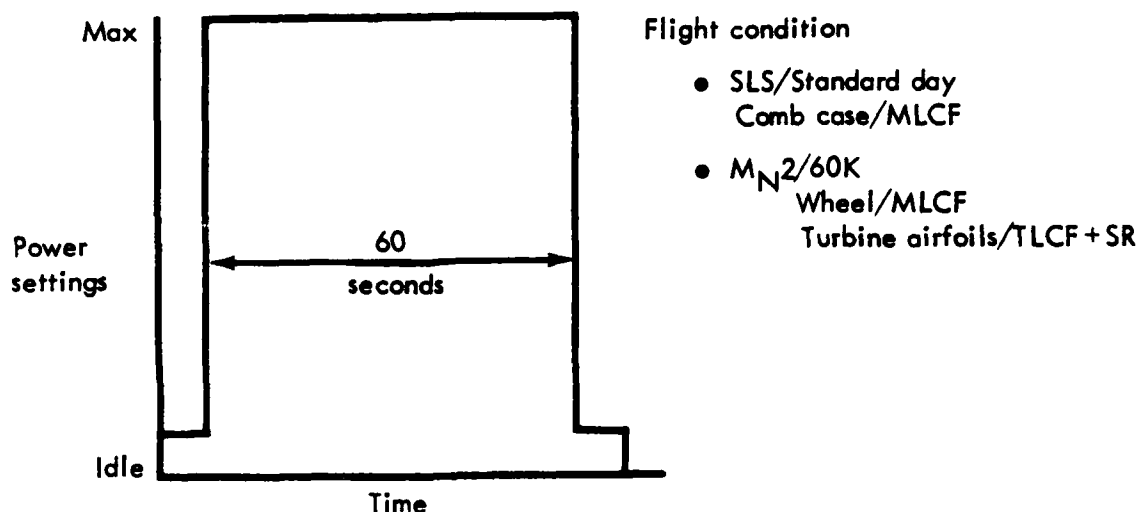
The life capability requirements were determined for each of the indicator components for each of the 17 engine cases in the ROI. The requirements were selected to meet the installed life goals listed in Table 26 for the training mission mix. Damage accrual from events happening during pre- and post-flight ground operation was included while the time was not included in addressing the installed life goals (flight hours versus engine operating hours). Worst case material properties (-3σ) were utilized in this selection process. Generally, several life capabilities of each component were evaluated for the appropriate usage, and a graphical solution selected the life capability requirements and the indication of the damage done per flight of a mission relative to a 0-max power-0 cycle at a reference flight condition (see Figure 99). The reference flight condition is M_N 2/60,000 ft for all components except the combustor case where it is sea level static, standard day. The reference cycle was selected as a unit of measure for relative damage and as a consequence has a reasonable amount of damage for the failure modes being considered. Each life capability was evaluated for all eight training missions, the wartime mission (stick mission without PLA dynamics), and two reference 0-max power-0 cycles. The mission mix discussed in Section X--Reference Utilization Definition was used to compute a weighted average life consumption rate and installed life. The balance of this section discusses the results for each component concluded with the input to the parametric deck for all components.

Table 26.
Installed life goals.

Turbine airfoils	1000 flt hr
Other hot section parts	2000 flt hr
Cold section parts	4000 flt hr

HPC-1 AND HPT-1 WHEELS

First-stage compressor and first-stage turbine wheels were evaluated for the MLCF failure mode. Both wheels have AF95 material with the compressor wheel operating at 390°F and the turbine wheel operating at 850°F. The critical location examined on each wheel was the bore. The wheel life capabilities were varied by changing the average tangential stress in the bore, which requires modifying the shape of the wheel in the bore region. The base-line life capabilities for the original PD422 parametric series of engines were 7000 and 3500 0-100-0% N cycles for the compressor and turbine wheels respectively. Table 27 lists the required life capabilities to meet the installed life goal for the training mission mix for both wheels. The compressor wheel for engine case 14 was the only exception, since it was sized for yield/burst considerations rather than for MLCF. DDA requested Boeing to create a time history for the wartime mission for potential stress rupture sizing for the turbine blades. The PLA time history did not contain all of the throttle movements that would be expected for this mission. Even so, some of the wheel designs sized for the training mission mix did not meet the installed life goals for the wartime stick mission. Discussions with USAF personnel led to the decision not to size the wheels for cyclical requirements for the wartime mission. This decision was based on program funding and schedule considerations.



Purpose

- Unit of measure for relative damage/life capability
- Reasonable level of damage

Figure 99. Severity index reference cycles.

Tables 28 and 29 list the mission severity indexes for the compressor and turbine wheels, respectively. The severity index is based on the damage done per flight. The initial training versions of the ground attack mission or supersonic weapons delivery mission are the most damaging missions since they have the highest damage rate. The proficiency versions of the navigation/familiarization mission or supersonic weapons delivery mission are the least damaging missions since they have the lowest damage rate.

Based on observation of the required life capability levels, the engines with low Thetabreak require more LCF capability. Thetabreak is an airflow scheduling parameter that indicates the lowest engine inlet total temperature where the mechanical speed at max power is 100%. The training missions, for the most part, occur in a portion of the flight envelope where engine inlet temperatures are approximately 5°F-110°F. Therefore, for low Thetabreak engines, the maximum mechanical speed during a training mission is 100% while high Thetabreak engines never get up to 100% N during the training mission. Both versions of the supersonic weapons delivery missions are the exception. During these missions, high inlet temperatures are encountered supersonically, and all engines, regardless of Thetabreak, reach 100% N during a flight. Consequently, it is not surprising that low Thetabreak engine require more 0-100-0% N cycles since during every training mission 100% N is achieved.

Table 27.
HPC-1, HPT-1 wheel/MLCF results.

Engine Case	R _C	RIT	θ_B	HPC-1 life capability**	HPT-1 life capability**
1	18	2800	1.0	9345	7290
3	12	3200	1.24	4350*	3120*
4	9	3400	1.36	3280*	2380
5	15	3200	1.36	3280*	2400*
6	18	3400	1.24	4765*	3494
7	9	2800	1.12	6393*	4620
8	12	3000	1.0	8620	6800
9	12	3400	1.12	6470*	4819
10	9	3200	1.0	8130	6370
11	18	3000	1.36	3270*	2300
12	15	2800	1.24	4290*	3140*
13	9	3000	1.24	4340*	3080
14	12	2800	1.36	3250* ¹	2290*
15	15	3400	1.0	9910	7637
16	18	3200	1.12	7373	5410
34	9	3400	1.18	4995*	3710
35	9	2800	1.18	5118*	3647

* Less than 4000/2000 hr for wartime stick mission

**0-100-0% N cycles

¹ Sized for burst/yield considerations

Table 28.
Severity index summary HPC-1 wheel/MLCF.

Case	Air combat		Ground attack		Nav/Fam		Sup weapon delivery		Training mix	Wartime	Ref cycle	
	Init	Prof	Init	Prof	Init	Prof	Init	Prof			SLSS	MN2/60 K
1	1.984	1.737	2.724+	2.057	1.326	1.432	1.371	1.459-	2.151	1.0	1.0	1.0
3	0.913	0.823	0.867+	0.686	0.397	0.419-	1.079	1.103	0.940	1.0	0.253	1.0
4	0.546	0.493	0.483	0.365	0.229	0.242-	1.107+	1.124	0.722	1.035	0.150	1.0
5	0.541	0.492	0.536	0.423	0.242	0.259-	1.096+	1.100	0.733	1.036	0.150	1.0
6	1.016	0.876	1.079+	0.826	0.418	0.456-	1.123	1.147	1.047	1.0	0.251	1.0
7	1.353	1.249	1.504+	1.067	0.747	0.781-	1.299	1.437	1.401	1.0	0.467	1.0
8	1.847	1.630	2.309+	1.875	1.314	1.402	1.263	1.361-	1.932	1.0	1.0	1.0
9	1.595	1.414	1.559+	1.240	0.763	0.808-	1.158	1.225	1.414	1.0	0.475	1.0
10	1.643	1.487	2.042+	1.653	1.247	1.325-	1.241	1.331	1.765	1.0	1.0	1.0
11	0.536	0.486	0.565	0.427	0.242	0.258-	1.104+	0.988	0.732	0.647	0.15	1.0
12	0.899	0.808	0.885+	0.709	0.427	0.432-	1.091	1.087	0.952	1.0	0.256	1.0
13	0.851	0.800	0.830+	0.592	0.375	0.396-	1.159	1.120	0.930	1.0	0.355	1.0
14	0.495	0.451	0.455	0.372	0.230	0.241-	1.077+	1.081	0.687	1.035	0.150	1.0
15	2.138	1.757	2.866+	2.208	1.398	1.524	1.358	1.476-	2.233	1.0	1.0	1.0
16	1.787	1.539	1.973+	1.509	0.824	0.894-	1.236	1.280	1.632	1.0	0.471	1.0
34	1.001	0.929	1.113+	0.853	0.525	0.557-	1.137	1.209	1.089	1.0	0.353	1.0
35	0.919	0.873	1.151+	0.780	0.514	0.540-	1.263	1.393	1.129	1.0	0.352	1.0

+ Highest damage rate
- Lowest damage rate

Table 29.
Severity index summary HPT-1 wheel/MLCF.

Case	Air combat		Ground attack		Nav/Pam		Sup weapon delivery		Training mix	Wartime	Ref cycle	
	Init	Prof	Init	Prof	Init	Prof	Init	Prof			SLSS	MN2/60 K
1	3.395	2.656	4.907+	3.544	1.717	2.046	1.738	1.986-	3.389	1.001	1.0	1.0
3	1.352	1.111	1.461+	1.085	0.488	0.556-	1.266	1.268	1.288	1.004	0.247	1.0
4	0.848	0.708	0.877	0.616	0.297	0.346-	1.474+	1.307	1.024	1.038	0.155	1.0
5	0.858	0.711	0.981	0.725	0.318	0.373-	1.470+	1.289	1.060	1.048	0.154	1.0
6	1.590	1.261	1.928+	1.390	0.551	0.656-	1.366	1.349	1.531	1.002	0.259	1.0
7	2.124	1.760	2.644+	1.776	0.931	1.052-	1.466	1.642	2.000	1.0	0.476	1.0
8	3.164	2.500	4.364+	3.280	1.712	1.988	1.589	1.849-	3.078	1.0	1.0	1.0
9	2.493	2.009	2.793+	2.056	0.963	1.108-	1.368	1.487	2.087	1.0	0.474	1.0
10	2.849	2.286	3.930+	2.917	1.620	1.893	1.553	1.796-	2.802	1.0	1.0	1.0
11	0.863	0.713	1.044+	0.741	0.323	0.376-	1.258	1.112	1.011	0.690	0.156	1.0
12	1.438	1.165	1.653+	1.228	0.559	0.617-	1.287	1.228	1.388	1.006	0.267	1.0
13	1.334	1.143	1.549+	1.034	0.498	0.570-	1.304	1.272	1.318	1.001	0.268	1.0
14	0.792	0.653	0.844	0.634	0.302	0.346-	1.365+	1.228	0.961	1.041	0.156	1.0
15	3.462	2.622	4.959+	3.646	1.794	2.124	1.694	1.979-	3.382	1.001	1.0	1.0
16	2.783	2.174	3.612+	2.466	1.036	1.224-	1.477	1.567	2.410	1.003	0.469	1.0
34	1.625	1.360	2.899+	1.486	0.688	0.799-	1.356	1.545	1.640	1.003	0.366	1.0
35	1.473	1.259	2.891+	1.359	0.674	0.769-	1.392	1.634	1.623	1.0	0.365	1.0

+ Highest damage rate
- Lowest damage rate

COMBUSTOR CASE

The outer combustor case was evaluated for the MLCF failure mode for all 17 engines in the ROI. The case material is IN706 and operating at 975°F. All of the parametric PD422 engines employed outer combustion cases nominally sized for burst considerations, which yielded a LCF capability of 200,000 0-max-0ΔP cycles. Results of the training mission evaluations showed that this nominal life capability was more than sufficient to meet the 4000 flt hr installed life goal. Table 30 lists the severity indices for all missions and engines in the ROI. The initial training version of the supersonic weapons delivery mission was the most damaging because it had the highest damage rate. The proficiency versions of the navigation/familiarization and supersonic weapons delivery missions were the least damaging since they had the lowest damage rate. The initial training variant of the supersonic weapons delivery mission had a significantly higher severity index so that an examination was conducted to determine the reason. Table 31 lists the peak ΔP across the case wall occurring during a mission normalized to the ΔP used to size the combustor case for burst for engine case 34. The peak ΔP is significantly higher for this mission. The flight path is different for this mission in that an acceleration occurs at 5000 ft from 0.5 Mach to about 1.2 Mach. The high flight velocity at low altitude explains the high ΔP for this mission. All of the other missions either don't go as fast or don't go as fast until they reach a higher altitude.

Table 30.
Severity index summary combustor case/MLCF.

Case	Air combat		Ground attack		Nav/Fam		Sup weapon delivery		Training mix	Wartime	Ref cycle	
	Init	Prof	Init	Prof	Init	Prof	Init	Prof			SLSS	MN2/60 K
1	14.0	11.8	22.0+	15.0	3.58	5.15	26.2	4.12-	17.6	12.7	1.0	0
3	18.1	15.7	24.6	16.1	3.71	5.46	232.0+	5.52-	68.7	14.1	1.0	0
4	17.7	15.8	24.5	16.0	3.69	5.51-	231.0+	10.3	70.4	10.9	1.0	0
5	16.5	14.6	24.6	16.1	3.70	5.46-	210.0+	9.66	63.7	11.9	1.0	0
6	17.8	15.2	24.7	16.2	3.76	5.41-	196.0+	5.50	59.8	14.9	1.0	0
7	20.6	17.4	25.4	16.2	4.09	6.17-	127.0+	8.31	43.9	20.3	1.0	0
8	14.9	12.5	21.2	14.8	3.60	5.19	42.9+	5.09-	21.4	12.9	1.0	0
9	20.6	18.0	25.4	16.9	4.11	6.15-	110.0+	9.09	40.2	20.9	1.0	0
10	15.8	13.3	22.3	15.8	3.59	5.33-	80.9+	5.65	31.8	12.9	1.0	0
11	17.0	14.1	24.6	16.0	3.67	5.44-	193.0+	5.48	60.01	11.8	1.0	0
12	17.9	15.0	25.0	16.3	3.82	5.52	223.0+	5.53-	65.4	15.5	1.0	0
13	18.9	16.1	24.6	16.1	3.77	5.52-	144.0+	9.78	48.3	13.5	1.0	0
14	16.4	14.2	24.4	15.9	3.66	5.47-	235.0+	9.79	68.1	11.6	1.0	0
15	14.7	12.5	21.6	14.8	3.65	5.25	76.5+	5.19-	30.8	13.3	1.0	0
16	19.8	16.9	26.6	18.1	4.17	6.11	88.4+	5.10-	35.1	21.1	1.0	0
34	18.0	16.3	24.9	16.4	3.93	5.53-	134.0+	1.2	44.3	20.3	1.0	0
35	17.7	15.3	24.8	16.2	3.92	5.51-	184.0+	10.1	44.3	20.3	1.0	0

+ Highest damage rate
- Lowest damage rate

Table 31.
Combustor case ΔP --case 34 (9/3400/1.18).

Mission	Max $\Delta P/\Delta P^*$
Air combat, initial	0.503
Air combat, proficiency	0.654
Ground attack, initial	0.528
Ground attack, proficiency	0.527
Navigation/Familiarization, initial	0.506
Navigation/Familiarization, proficiency	0.535
Supersonic weapon delivery, initial	0.945
Supersonic weapon delivery, proficiency	0.495
Wartime	0.780
Ref cycle, SLSS	0.439
Ref cycle, $M_N2/60K$	0.214

5K accel
0.5 \rightarrow 1.25 M_N

* ΔP = 267.2 psia ($M_N1.2$ /SL/max power)

HPT-1 BLADE

The first-stage turbine blade was evaluated for the thermal low cycle fatigue (TLCF) and stress rupture failure modes. The airfoil is a Lamilloy design with Mar-M246 spar material and a HA188 two-ply laminate. The critical location is either the trailing edge on the pressure surface or the leading edge of the spar depending on the mission. Each turbine blade in the parametric PD422 series has a consistent stress rupture life capability at the meanline radius location. As can be seen from Figure 100, an infinite number of combinations of stress and metal temperature will give that stress rupture life capability. The last turbine stage has a blade stress at max power of 42.5 ksi or less due to an aerodynamic guideline. Consequently, the single stage turbines all have the same nominal stress and metal temperature. The two-stage turbine designs have a nominal stress and metal temperature for the first-stage blade in a region indicated in Figure 100. The mission evaluations indicated that a blade design TLCF life capability was most sensitive to the blade average stress level. Consequently, the approach taken to determine the blade life capability requirement was to reduce the blade stress from its nominal level to satisfy the training mission mix accounting for damage from both failure modes. Subsequently, the metal temperature was raised from its nominal level until the wartime mission installed life met the goal accounting for only stress rupture damage.

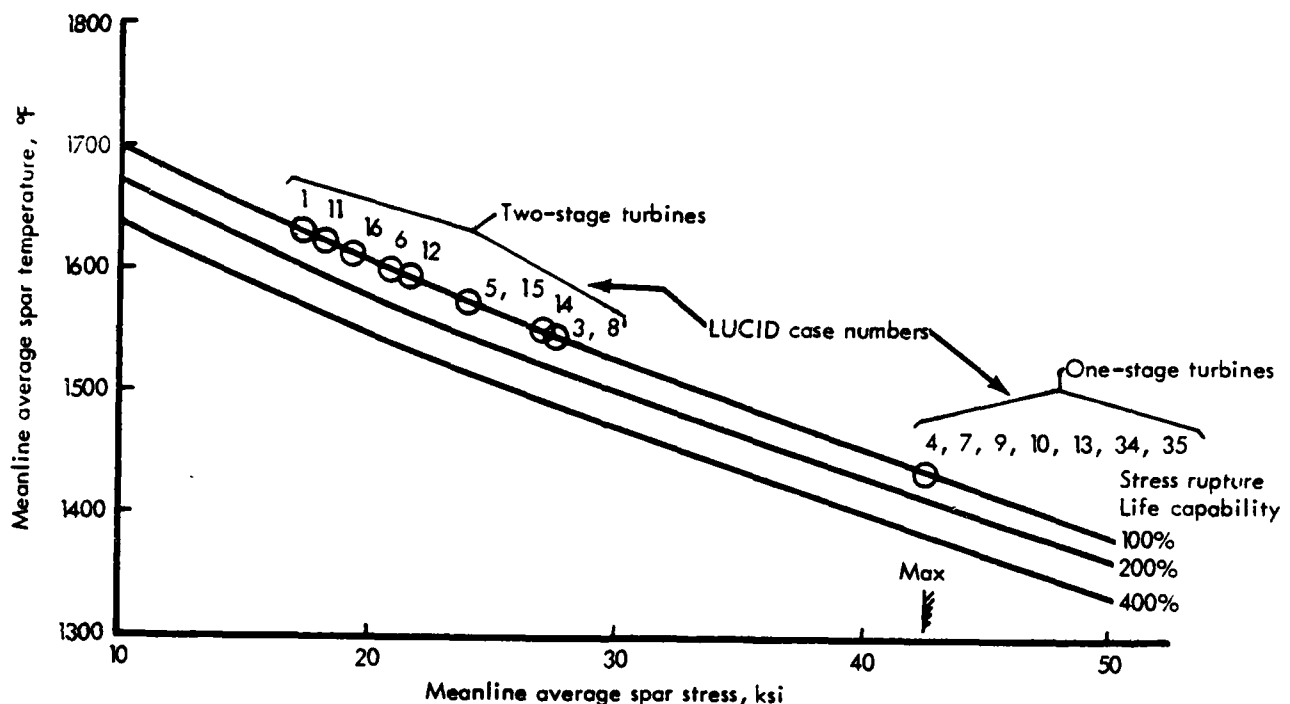


Figure 100. HPT-1 blade nominal designs.

The simplified turbine blade/TLCF model scaled the base-line design metal temperature distribution to a different average temperature level via airfoil coolant changes at the Mach 2/60,000 ft/max power condition. This revised distribution was then used to compute local and average metal temperatures for each time slice of a mission. The terms in the local strain regressions for centrifugal stress were scaled to allow for different stress levels at the same flight condition (Mach 2/60,000 ft/max power). These revised coefficients were then used to assess local strain for each mission time slice (different speeds, local metal temperatures, etc.). This approach allowed the damage assessments for both TLCF and stress rupture for varying turbine life capabilities. Table 32 lists the base life capability for each engine case along with the required life capability to meet the installed life goal. These life capabilities are expressed in terms of a nominal stress and metal temperature due to the evaluations for two failure modes.

Table 32.
HPT-1 blade/TLCF + SR results.

Engine case	R _C	RIT	θ_B	Life capability	
				Base	TR mission mix/Wartime SR
1	18	2800	1.0	17.0/1630	17.0/1650
3	12	3200	1.24	27.5/1542	23.9/1551
4	9	3400	1.36	42.5/1445	20.6/1581
5	15	3200	1.36	23.0/1578	23.0/1551
6	18	3400	1.24	20.5/1600	20.5/1547
7	9	2800	1.12	42.5/1445	26.4/1542
8	12	3000	1.0	27.5/1543	23.0/1588
9	12	3400	1.12	42.5/1445	19.7/1583
10	9	3200	1.0	42.5/1445	16.3/1643
11	18	3000	1.36	18.0/1618	18.0/1641
12	15	2800	1.24	21.5/1594	21.5/1571
13	9	3000	1.24	42.5/1445	25.8/1540
14	12	2800	1.36	27.0/1550	27.0/1529
15	15	3400	1.0	24.0/1571	18.7/1625
16	18	3200	1.12	19.0/1608	19.0/1604
34	9	3400	1.18	42.5/1445	16.6/1637
35	9	2800	1.18	42.5/1445	25.5/1550

*Spar average stress (ksi)/metal temp (°F) @ M_N2/60K/max power

NOTE: A) Stress set for min wall thickness or training mission mix/TLCF+SR

B) Temperature set for wartime mission/SR

The mission severity indexes based on damage done per flight for the HPT-1 blade are listed in Table 33. Either the initial training version of the ground attack mission or the proficiency training version of the supersonic weapons delivery mission is the most damaging mission. The least damaging mission is the proficiency training variant of the navigation/familiarization mission.

Table 33.
Severity index summary HPT-1 blade/combined TLCF + SR.

Case	Air combat		Ground attack		Nav/Fam		Sup weapon delivery		Training mix	Wartime	Ref cycle	
	Init	Prof	Init	Prof	Init	Prof	Init	Prof			SLSS	MN2/60 K
1	0.732	0.694	1.373+	0.979	0.420	0.502-	1.665	1.743	1.310	3.654	0.301	1.0
3	0.684	0.592	0.873	0.673	0.355	0.404-	1.139	2.537+	1.087	2.811	0.193	1.0
4	0.918	0.782	1.253+	0.911	0.435	0.529-	1.218	1.96	1.220	2.917	0.225	1.0
5	0.322	0.287	0.419	0.321	0.195	0.213-	1.125	2.618+	0.839	3.311	0.101	1.0
6	0.355	0.318	0.441	0.362	0.233	0.246-	1.157	2.803+	0.888	3.850	0.117	1.0
7	0.877	0.719	1.091+	0.762	0.426	0.485-	1.296	3.089	1.299	2.598	0.316	1.0
8	0.857	0.707	1.079+	0.840	0.459	0.505-	1.234	1.933	1.155	2.288	0.250	1.0
9	1.098	0.914	1.387+	1.071	0.568	0.661-	1.191	2.739	1.418	2.678	0.269	1.0
10	0.823	0.689	1.054	0.800	0.386	0.469-	1.070	3.657+	1.299	2.583	0.198	1.0
11	0.173	0.143	0.213	0.152	0.006	0.008-	0.796	3.209+	0.705	2.780	0.005	1.0
12	0.332	0.276	0.412	0.295	0.155	0.164-	1.533	3.881+	1.059	4.178	0.009	1.0
13	0.760	0.651	1.015+	0.714	0.391	0.453-	1.277	2.442	1.173	2.689	0.270	1.0
14	0.337	0.287	0.404	0.320	0.186	0.206-	1.267	2.611+	0.878	3.148	0.121	1.0
15	0.664	0.564	0.854+	0.681	0.377	0.423-	0.926	2.346	1.010	2.092	0.151	1.0
16	0.356	0.305	0.468	0.330	0.196	0.208-	1.263	2.930+	0.916	2.921	0.009	1.0
34	1.270	0.765	1.450+	1.112	0.473	0.614-	1.856	2.662	1.564	2.607	0.238	1.0
35	0.611	0.506	0.824	0.560	0.294	0.338-	1.806	3.523+	1.294	2.931	0.210	1.0

+ Highest damage rate
- Lowest damage rate

For the required life capability level, Table 34 lists a quantity called failure mode ratio (FMR) for each of the 17 engine cases. FMR is defined to give an indication of the TLCF damage done per flight relative to the stress rupture damage done per flight for a given mission. From observing Table 34, the following missions have hardly any stress rupture damage: both training variants of the air combat mission, the ground attack mission, and the navigation/familiarization mission and the reference cycle at sea level static on a standard day.

This is due to a Reynolds number characteristic of a Lamilloy cooled airfoil. As Reynolds number decreases (i.e., with increasing altitude), a given percentage coolant flow loses effectiveness. Therefore, the turbine airfoils are designed for metal temperature levels representative of high altitudes. For LUCID, the heat transfer design point is max power at Mach 2/60,000 ft. During the training missions, the flight profile never gets above 30,000 ft altitude except for the supersonic weapons delivery training missions and the wartime mission. Consequently, the turbine blades do not spend any time at high enough metal temperatures to accumulate much stress rupture damage for most of the training missions.

HPT-1 VANE

The first-stage turbine vane was evaluated at the meanline radial location for TLCF. The vane is a Lamilloy-spar design utilizing Mar M246 material for the spar and MA956 material for the two-ply laminate. The most critical location for TLCF is at the trailing edge on the suction surface of the spar. The parametric PD422 series has nominal turbine vane designs where the average spar metal temperature is 1700°F at max power, Mach 2/60,000 ft. The approach taken for determining the required life capability for the turbine vane was to satisfy the installed life goal for the training mission mix.

Table 34.
HPT-1 blade failure mode ratio summary.

Case	Air combat		Ground attack		Nav/Fam		Sup weapon delivery		Training max	Wartime	Ref cycle	
	Init	Prof	Init	Prof	Init	Prof	Init	Prof			SLSS	M2/60 K
1	7860	11033	23149	17875	12570	11815	0.65	0.45	2.54	0.182	68700	2.68
3	2.2x10 ⁶	2.8x10 ⁶	8.4x10 ⁶	7.6x10 ⁶	7.8x10 ⁶	8.7x10 ⁶	7.65	1.43	5.71	0.974	5.3x10 ⁷	21.2
4	1.1x10 ⁷	1.3x10 ⁷	4.2x10 ⁷	3.3x10 ⁷	2.2x10 ⁷	2.4x10 ⁷	12.3	2.55	11.3	1.15	1.6x10 ⁸	17.5
5	6.6x10 ⁶	8.1x10 ⁶	3.4x10 ⁷	3.4x10 ⁷	4.4x10 ⁷	5.3x10 ⁷	5.14	1.11	3.25	0.80	3.2x10 ⁸	19.9
6	3.0x10 ⁶	3.4x10 ⁶	1.8x10 ⁷	2.0x10 ⁷	2.7x10 ⁷	3.1x10 ⁷	5.63	1.07	3.33	0.65	2.2x10 ⁸	31.2
7	74441	97121	1.8x10 ⁵	1.4x10 ⁵	1.3x10 ⁵	1.3x10 ⁵	4.29	0.77	3.43	0.80	8.4x10 ⁵	12.4
8	62228	73039	1.4x10 ⁵	1.0x10 ⁵	82796	69411	3.40	0.53	4.27	0.64	4.2x10 ⁵	10.2
9	1.1x10 ⁶	1.4x10 ⁶	3.5x10 ⁶	3.1x10 ⁶	2.6x10 ⁶	2.8x10 ⁶	6.70	1.02	5.05	0.86	1.6x10 ⁷	16.4
10	44266	43572	95314	63861	31307	27506	4.80	0.52	2.67	0.70	2.1x10 ⁵	7.65
11	2.3x10 ⁵	2.7x10 ⁵	8.9x10 ⁵	8.2x10 ⁵	7.1x10 ⁵	8.6x10 ⁵	1.13	0.33	0.23	0.82	7.4x10 ⁶	3.90
12	1.5x10 ⁵	1.8x10 ⁵	4.5x10 ⁵	3.9x10 ⁵	2.0x10 ⁵	4.2x10 ⁵	1.43	0.50	1.31	0.38	2.3x10 ⁶	9.25
13	7.7x10 ⁵	9.8x10 ⁵	2.7x10 ⁶	2.2x10 ⁶	1.8x10 ⁶	1.9x10 ⁶	6.30	1.30	5.30	1.01	1.5x10 ⁷	16.3
14	1.3x10 ⁶	1.7x10 ⁶	4.6x10 ⁶	4.6x10 ⁶	5.4x10 ⁶	6.0x10 ⁶	4.16	1.00	2.83	0.77	3.8x10 ⁷	17.9
15	1.7x10 ⁵	2.8x10 ⁵	5.5x10 ⁵	4.3x10 ⁵	3.4x10 ⁵	3.1x10 ⁵	6.98	1.13	5.31	0.73	1.6x10 ⁶	10.9
16	1.1x10 ⁵	1.4x10 ⁵	4.4x10 ⁵	3.8x10 ⁵	4.5x10 ⁵	4.8x10 ⁵	2.12	0.81	2.19	0.41	2.8x10 ⁶	10.7
34	5.0x10 ⁵	4.9x10 ⁵	9.6x10 ⁵	6.7x10 ⁵	3.7x10 ⁵	3.8x10 ⁵	6.92	1.01	4.76	0.91	2.4x10 ⁶	9.04
35	96255	1.2x10 ⁵	2.4x10 ⁵	1.9x10 ⁵	1.6x10 ⁵	1.5x10 ⁵	4.29	0.83	3.11	0.78	1.1x10 ⁶	13.0

Due to design considerations for other failure modes (such as corrosion), the maximum average vane metal temperature was limited to 1700°F. In a manner similar to the blade life capability, the vane life capability was varied by scaling the goal metal temperature distribution (determined in Task 3.1.6) to different average levels at the Mach 2/60,000 ft/max power condition. This scaled distribution was then used to evaluate local metal temperatures during a given mission. Table 35 lists the life capability requirements for the HPT-1 vane for all 17 engines in the ROI. Generally, as the design RIT increases, the HPT-1 vane average metal temperature decreased in order to satisfy the installed life goal for the training mission mix. In addition, none of the vane designs in Table 35 satisfy the installed life goals for the wartime stick mission. Per the decision with the USAF, none of the component designs were sized for LCF for the wartime mission.

Table 36 shows the turbine vane mission severity indices based on life consumption per flight. One of the training variants of the supersonic weapons delivery missions is the most damaging training mission. The wartime mission is the most damaging usage. The proficiency training variant of the navigation/familiarization mission is the least damaging mission.

PARAMETRIC DECK INPUTS

DDA took the results of the failure mode evaluations of the indicator components and defined the appropriate values for input into the parametric PD422 engine model. These inputs used the engine characteristic adjustment data defined in Task 3.2.1. Table 37 lists those inputs for each of the 17 engines in the ROI using the computer names defined in Table 25. Boeing regenerated engine performance, weights, and dimensions using these adjustments to perform Task 3.2.5. In addition, DDA transmitted to Boeing the various component mission severity indexes and required life capability levels for potential trending with regression of the engine independent variables.

Table 35.
HPT-1 vane/TLCF results.

Engine case	R _C	RIT	θ_B	Life capability	
				Base	TR mission mix
1	18	2800	1.0	1700	1700
3	12	3200	1.24	1700	1626
4	9	3400	1.36	1700	1607
5	15	3200	1.36	1700	1632
6	18	3400	1.24	1700	1665
7	9	2800	1.12	1700	1700
8	12	3000	1.0	1700	1700
9	12	3400	1.12	1700	1587
10	9	2100	1.0	1700	1650
11	18	3000	1.36	1700	1696
12	15	2800	1.24	1700	1700
13	9	3000	1.24	1700	1689
14	12	2800	1.36	1700	1700
15	15	3400	1.0	1700	1581
16	18	3200	1.12	1700	1505
34	9	3400	1.18	1700	1564
35	9	2800	1.18	1700	1699

*Average spar temperature °F @ M_N2/60K/max

Table 36.
Severity index summary HPT-1 vane/TLCF.

Case	Air combat		Ground attack		Nav/Fam		Sup weapon delivery		Training mix	Wartime	Ref cycle	
	Init	Prof	Init	Prof	Init	Prof	Init	Prof			SLSS	MW2/60 K
1	0.050	0.036	0.071	0.045	0.017	0.018-	0.764+	0.282	0.248	0.745	0.008	1.0
3	0.052	0.041	0.063	0.040	0.013	0.014-	1.006+	1.427	0.453	1.417	0.003	1.0
4	0.043	0.033	0.051	0.034	0.011	0.013-	0.768+	1.162	0.364	1.490	0.003	1.0
5	0.020	0.016	0.026	0.016	0.006	0.006-	0.890+	1.340	0.394	1.396	0.002	1.0
6	0.031	0.024	0.034	0.019	0.009	0.009-	0.259	1.403+	0.249	1.381	0.004	1.0
7	0.072	0.049	0.093	0.063	0.018	0.021-	0.734+	1.286	0.378	1.177	0.003	1.0
8	0.085	0.063	0.120	0.079	0.025	0.027-	0.974+	0.507	0.350	1.072	0.007	1.0
9	0.048	0.034	0.061	0.040	0.013	0.015-	0.910+	1.400	0.421	1.495	0.004	1.0
10	0.078	0.058	0.097	0.066	0.021	0.025-	0.769+	1.276	0.396	1.122	0.005	1.0
11	0.018	0.015	0.021	0.014	0.006	0.006-	0.732+	1.058	0.322	0.873	0.003	1.0
12	0.047	0.036	0.062	0.040	0.014	0.014-	0.274	1.371+	0.260	1.255	0.004	1.0
13	0.065	0.047	0.077	0.052	0.015	0.018-	0.828+	1.238	0.396	1.280	0.003	1.0
14	0.041	0.029	0.053	0.035	0.011	0.012-	0.795+	1.278	0.382	1.374	0.003	1.0
15	0.034	0.026	0.053	0.033	0.012	0.012-	0.942+	1.332	0.418	1.051	0.005	1.0
16	0.013	0.010	0.016	0.010	0.004	0.004-	0.874+	1.505	0.396	1.263	0.002	1.0
34	0.052	0.042	0.077	0.052	0.017	0.021-	1.446+	1.573	0.566	1.555	0.004	1.0
35	0.055	0.039	0.076	0.052	0.015	0.018-	1.321+	1.456	0.517	1.259	0.003	1.0

+ Highest damage rate
- Lowest damage rate

Table 37.

PD422 parametric deck input summary for consistent installed life level.

<u>Eng case</u>	<u>CMLCFI</u>	<u>BMLCFI</u>	<u>TWMLCI</u>	<u>TVTFL1</u>	<u>TBTFI1</u>	<u>TBTFI2</u>
1	1.335	1.0	2.083	0.1	+20	1.0
3	0.621	1.0	0.891	-74	+7	15.0
4	0.469	1.0	0.680	-93	+106	63.7
5	0.469	1.0	0.686	-68	-27	1.0
6	0.681	1.0	0.998	-35	-53	1.0
7	0.913	1.0	1.320	0.1	+103	17.3
8	1.231	1.0	1.943	0.1	+45	17.0
9	0.924	1.0	1.377	-113	+138	80.7
10	1.161	1.0	1.820	-50	+203	185.4
11	0.467	1.0	0.657	-4	+13	1.0
12	0.613	1.0	0.897	0.1	-23	1.0
13	0.620	1.0	0.880	-11	+95	21.9
14	0.464	1.0	0.654	0.1	-21	1.0
15	1.416	1.0	2.182	-119	+54	30.5
16	1.053	1.0	1.546	-105	0	1.0
34	0.714	1.0	1.060	-136	+192	164.2
35	0.731	1.0	1.042	0.1	+105	21.9

XII. TASK 3.2.5--SYSTEM PERFORMANCE SENSITIVITY

In this task, two separate items were addressed. First, DDA supplied engine life severity indices for each engine component on each peacetime mission. Regressions were generated for each level. These regressions were to be used to show engine component sensitivity to the various training usages and the reference aircraft utilization. Second, DDA also supplied engine component life coefficients as new inputs to the PD422 engine program. A new ROI mission data set was generated with these new engines. Using this new data set, airplane performance parameters were regressed and optimized (as in Task 3.1.5) to find the minimum airplane size.

Figures 101 through 106 show the regression statistic, R^2 , for all engine component severity indexes on each type of training mission. The results generally were below acceptable standards. Only the compressor and turbine wheel produced acceptable R^2 values. None of the combustor, blade (stress), or vane R^2 values exceeded 0.9 and several returned values of 0, which indicated complete randomness. The Blade Failure Mode Ratio regressions gave reasonable values, above 0.9 for all missions except the Ground Attack and Navigation Training missions.

Several attempts were made to improve the correlation coefficients (R^2) of the various components. First, the regression results were searched for cases which showed consistently bad predictions (residual/standard deviation) for the missions under a particular component. (For example, Figure 104 shows that case 8 exhibits this behavior for blade stress.) These cases were dropped, and the remaining data were regressed again. But the new results showed little if any improvement over the old. Then, cases 34 and 35 were added to the data base. These cases were originally planned for use as validation checks on regression answers; however, because of the poor fits they were included in the regression set of cases. Once again, there was little improvement. In conversations with DDA about the poor results, it was suggested that the cases could be divided up according to the number of turbine stages (1 or 2) used for a particular case. This was tried for the supersonic missions of the turbine wheel component. Figure 103 shows an improved R^2 for the Initial and Proficiency Supersonic missions (HPT-8 and HPT-9) which had cases with two-stage turbines, but poor results occurred with the single-stage cases.

After having little success with improving the various R^2 , it was decided to proceed with the equation coefficients from the first set of regressions. The equations with R^2 values greater than 0.9 were evaluated using the OPR, RIT, and THETAB of the validation cases (34 and 35). Figure 107 shows the comparison of predicted and actual data for case 34. The equations generally showed their predictions to be within about 10% of the actual values.

Using the compressor and turbine wheel regressions, the type of training (e.g., ground attack, air combat, initial, proficiency, etc.) impact on component life consumption was examined for several engine cycle combinations. These comparisons also included the reference aircraft utilizations. Two levels of OPR (9 and 15) and RIT (3000 and 3400) and one level of THETAB (1.18) were considered. The THETAB level was based on where the optimum value was found to occur in subsequent work.

HIGH PRESSURE COMPRESSOR COMPONENT					
VARIABLE NAME	DDA NAME	STATISTICAL COEFFICIENT R^2	HIGH VALUE RESIDUAL STD. DEV.		R^2 WITHOUT CASE 6
HPC 2	Air to Air Initial (A/I)	0.980	-		0.994
HPC 3	Air to Air Proficiency (A/P)	0.981	-		0.989
HPC 4	Air to Ground Initial (G/I)	0.973	-		0.997
HPC 5	Air to Ground Proficiency (G/P)	0.997	-		0.999
HPC 6	Navigation Familiarization Initial (NF/I)	0.997	-		0.999
HPC 7	Navigation Familiarization (NF/P)	0.999	-		0.999
HPC 8	Supersonic Initial (S/I)	0.790	0.94 Case 6	function of θ_B & θ_B^2	0.785
HPC 9	Supersonic Proficiency (S/P)	0.805	0.997 Case 6	function of θ_B & θ_B^2	0.802
HPC 10	Wartime (W)	0.235	-2.77 Case 10	constant except No. 10	0.297
HPC 12	Training Mix (RAU)	0.993	-		

Figure 101. HP compressor severity index regressions.

For the OPR=9, RIT=3000 case, maximum HPC life consumption per flight occurred during supersonic weapon training. However, air combat and subsonic ground attack were nearly as high. The reference utilization proved to be more severe than all but the supersonic training. For the turbine, life consumption was most severe for initial subsonic air to ground training, with air combat a close second. Supersonic weapons training was noticeably below both of the former missions. The RAU was more severe than all but the initial air to ground training. Figure 108 shows these results. With increased RIT (3400), only small shifts in all the life consumptions were observed for the low OPR case. With increased OPR (15) and 3000 RIT, a change in the HPC life consumption was observed. Supersonic weapon, air combat, and subsonic ground attack training were all about equal consumers of life (see Figure 109). For the HPT both the air combat and the subsonic ground attack showed a noticeable increase over the lower OPR case. When RIT was increased to 3400 again, some small increases in the life consumption rates were noticed for each training mission, but the RAU took a noticeable increase as seen in Figure 110.

COMBUSTOR					
VARIABLE NAME	DDA NAME	R ²	HIGH RESID. CASE NO.		
CCM 2	A/I	0.149	6, 8, 14, 15		
CCM 3	A/P	0.232	6, 8, 14, 15		
CCM 4	G/I	0.768	15		
CCM 5	G/P	0.130	7, 8, 14, 15		
CCM 6	NF/I	0	1, 6, 8, 15		
CCM 7	NF/P	0	1, 6, 7, 18, 15		
CCM 8	S/I	0.890	-		
CCM 9	S/P	0.692	2, 8		
CCM 10	W	0.663	15, 12, 8, 2		
CCM 12	RAU	NOT RUN			

Figure 102. Combustor case severity index regressions.

HIGH PRESSURE TURBINE COMPONENT					
VARIABLE NAME	DDA NAME	R ²	COMMENTS		
HPT 2	A/I	0.990			
HPT 3	A/P	0.982			
HPT 4	G/I	0.997			
HPT 5	G/P	0.991			
HPT 6	NF/I	0.998			
HPT 7	NF/P	0.999			
HPT 8	S/I	0.775	function of θ_B & θ_B^2	R ² single stage 0	R ² two stages 0.871
HPT 9	S/P	0.937	function of θ_B & θ_B^2	0.810	0.971
HPT 10	W	0.211	constant values of data except for no. 10		
HPT 12	RAU	0.894			

Figure 103. HPT wheel severity index regressions.

These results provided some insight into training usage impact on component life. However, many of the regressions on which these results were based are statistically poorer than desired. Also, no extra set of cases was available around which validations could be made. Further, most components considered for life assessment could not be examined because of the unacceptable regression fit. All these areas point out where follow-on work holds the potential for a better understanding of how usage impacts component life.

BLADE - STRESS RUPTURE					
VARIABLE NAME	DDA NAME	R ²	HIGH RESID. CASE NO.	R ₂ NO CASE 8	
SRR 3	A/I	0.781	8	0.768	
SRR 4	A/P	0.750	1, 13, 8	0.739	
SRR 5	G/I	0.871	1, 13, 8	0.866	
SRR 6	G/P	0.740	1, 13, 8	0.860	
SRR 7	NF/I	0.753	1, 13, 8	0.736	
SRR 8	NF/P	0.740	1, 13, 8	0.727	
SRR 9	S/I	0.414	1, 13, 8	0.419	
SRR 10	S/P	0	1, 13, 8	0	
SRR 11	W	0.501	1, 13, 8	0.465	
SRR 13	RAU	0.713	1, 13, 8	0.731	

Figure 104. HPT blade severity index regressions.

BLADE - FAILURE MODE RATIO					
VARIABLE NAME	DDA NAME	R ²	HIGH RESID. CASE NO.		
SRR 25	A/I	0.949			
SRR 26	A/P	0.950			
SRR 27	G/I	0.935			
SRR 28	G/P	0.618	4, 10		
SRR 29	NF/I	0.512	4, 10		
SRR 30	NF/P	0.491	4, 10		
SRR 31	S/I	0.959			
SRR 32	S/P	0.970			
SRR 33	W	0.986			
SRR 35	RAU	0.925			

Figure 105. Blade failure mode severity index regressions.

In the second part of Task 3.2.5, new engines were generated on the PD422 parametric engine program. These engines had the same cycles as those in Task 3.1.5. They also contained the new component life coefficients. Each engine was "flown" on the same mission as its Phase I predecessor, and regressions of the same mission variables were generated. Figure 111 shows the R² levels for the first regression tried on mission cases 1, and 3-16. Note that case 2 was not used as it had been eliminated in the original ROI screening. The TOGW value R² (which is the primary parameter of interest) was notably low, so a second regression was tried on the same final set of mission cases used in Phase I (cases 1, 3-11, 13-16, 34-35). This improved the results somewhat, but the TOGW correlation was still poor.

VANE					
VARIABLE NAME	DDA NAME	R ²	HIGH RESID. CASE NO.		
VNN 2	A/I	0.871	5, 7, 15		
VNN 3	A/P	0.782	5, 7, 15		
VNN 4	G/I	0.839	5, 7, 15		
VNN 5	G/P	0.863	7, 15		
VNN 6	NF/I	0.767	5, 7, 15		
VNN 7	NF/P	0.804	7, 15		
VNN 8	S/I	0.147	2, 11		
VNN 9	S/P	0.271	1, 3, 7, 15		
VNN 10	W	0.851	10, 13		

Figure 106. HPT vane severity index regressions.

Then, a third regression was tried in which cases 4 and 9 were selectively dropped. Again the R^2 value improved (Figure 111), but it was still not as high as desired. In all these TOGW regressions, THETAB was not included by the regressor program as an independent variable in the equation. Therefore, another regression was made on cases 1, 3-11, 13-16, 34, and 35 with all 10 combinations of OPR, RIT, and THETAB forced to appear in the output. This resulted in the best R^2 for TOGW (Figure 111).

This equation for TOGW was chosen for the minimum airplane size optimization. The equations for the other parameters were chosen from the second regression attempt. While several of these parameters also exhibited low R^2 values, inspection of their minimums and maximums showed that their ranges were quite small. For instance, Figure 111 shows that VAPP (approach velocity) has an R value of 0.468. Its minimum and maximum values, however, are 118.4 and 121.4, respectively. This variation is probably due to accuracy tolerances, truncation limits, and round-offs within the mission program. It appears as noise to the regressor and causes a poor fit.

Figure 112 is a carpet plot of the change in TOGW with engine cycle characteristics and component life coefficients. Two of the surfaces represent the data of constant performance and component life at RITs of 2800°F and 3400°F. The other one is the constant performance only surface that was generated at a RIT of 3400°F in Task 3.1.5. The plot shows that at the high OPRs the airplane grew in size by 7-8% because of engine modifications for constant component life. At the low OPRs the increase is only about 2-3%.

The optimum Thetabreak as a function of OPR and RIT for changes in engine cycle characteristics and component life coefficients is shown in Figure 113. The resultant TOGW versus OPR and RIT for constant performance and constant life is shown in Figure 114. Along with it is the constant performance only

Predicted versus Actual for $R^2 > 0.90$
Case No. 34

Missions	High-Pressure Compressor Disk (HPC)			High-Pressure Turbine Disk (HPT)			Turbine Blade (FMR)		
	Predicted	Actual	Percent error	Predicted	Actual	Percent error	Predicted*	Actual	Percent error
A/I	1.163	1.001	16%	1.792	1.625	10%	3.8×10^6	0.5×10^6	--
A/P	1.056	0.926	14%	1.500	1.360	10%	3.8×10^6	0.5×10^6	--
G/I	1.109	1.113	0.3%	1.873	2.099	11%	9.9×10^6	0.9×10^6	--
G/P	0.817	0.853	4%	1.413	1.486	5%	--	--	--
NF/I	0.543	0.525	3%	0.688	0.688	--	--	--	--
NF/P	0.537	0.557	4%	0.740	0.799	7%	--	--	--
S/I	--	--	--	--	--	--	9.359	6.930	35%
S/P	--	--	--	1.399	1.545	9%	1.634	1.010	62%
W	--	--	--	--	--	--	0.925	0.911	2%

*These poor predictions are a result of how the failure mode ratio is calculated. In cases where the denominator is very small (a large ratio), a small error in the prediction of the denominator results in a poor final result.

Figure 107. Comparison of predicted versus actual severity index levels.

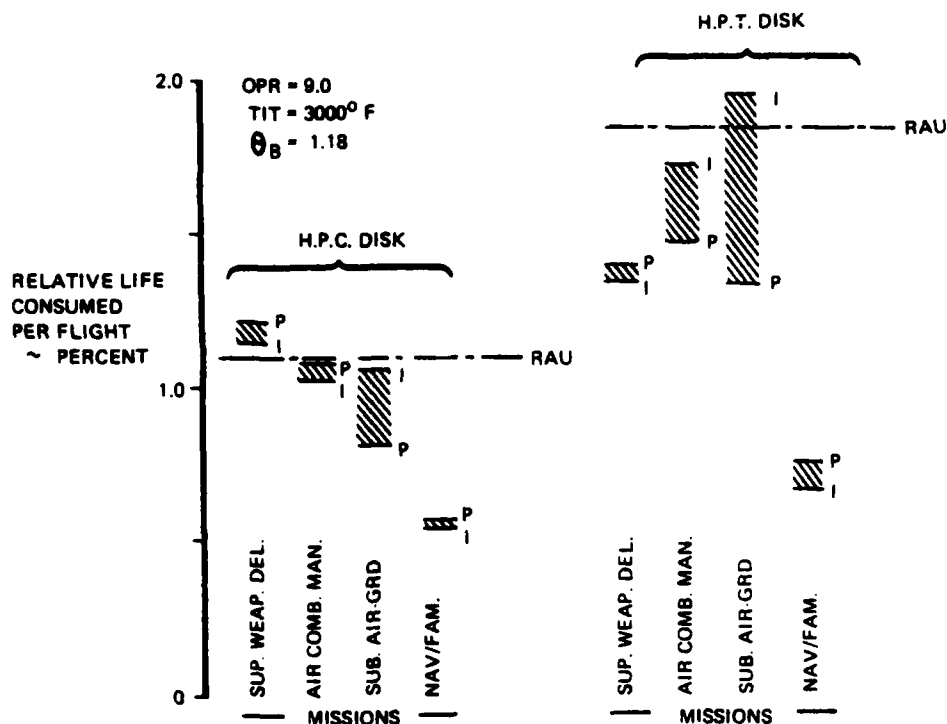


Figure 108. Engine component life consumption versus training mission--
OPR=9, RIT=3000°F.

surface from Task 3.1.5. Again, at the low OPRs the increase is about 3%, while at the high OPRs it ranges from 2% at RIT=2800 to 8% at RIT=3400. From the constant performance-constant life surface on Figure 114, the cycle characteristics for the minimum airplane size are as follows:

Overall pressure ratio	9
Turbine rotor inlet temperature	3200°F
Thetabreak	1.173 (from Figure 113)

This cycle is different from the Task 3.1.5 constant performance optimum. Both a small decrease in Thetabreak (down from 1.18) and a decrease in RIT of 200°F (down from 3400°F) have occurred. The constant performance constant life surface shows that the OPR=9, RIT=3400 point also gives a minimum airplane size. But since the same minimum size and component life are retained at the OPR=9, RIT=3200°F point, it was chosen because the decrease in RIT represents a decrease in risk.

To gain a better understanding of how the component life inputs to the engine parametric deck were changing with cycle, regressions were tried on several of them. Table 37 shows the engine inputs, and Figure 115 lists the R^2 values. Two of the life inputs (compressor wheel and turbine wheel) showed excellent fits to OPR, RIT, and THETAB. For the other parameters which exhibited a poor fit or obvious discontinuities in the data (turbine vane LCF for vane metal

temperature, turbine blade LCF for blade metal temperature, and turbine blade LCF for blade metal thickness), plots of their variation with OPR, RIT, and THETAB were made. The idea was to spot trends and possibly adjust cases that did not follow the trend. Several cases were found to be in need of adjustment based on these plots. However, in discussions with DDA, they pointed out that there were other factors present during the original processing of the engine life inputs (such as the fact that some cases used a single-stage turbine and others used two stages) that could have caused wide spread in the data. Therefore the attempt was not pursued further.

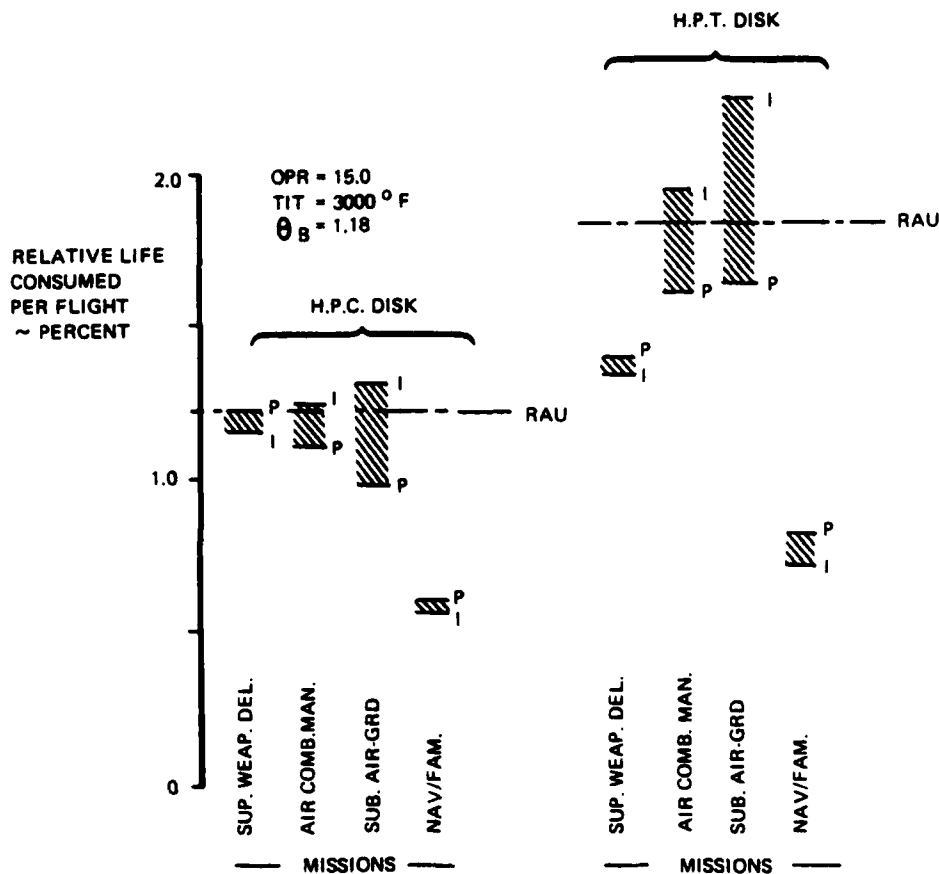


Figure 109. Engine component life consumption versus training mission--OPR=15, RIT=3000 °F.

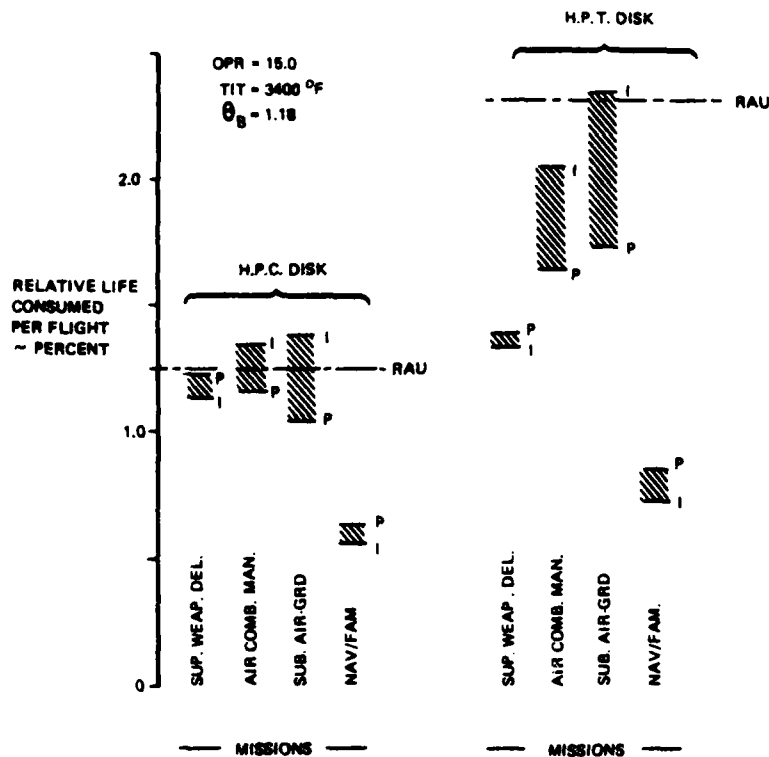


Figure 110. Engine component life consumption versus training mission--OPR=15, RIT=3400 °F.

Variable Name	Regression Statistic (R^2)			
	Cases 1,3-16	Cases 1,3-11,13-16,34,35	Drop Case 4,9	Forced (Set 2)
TOGM	0.782	0.845	0.930	0.948
SLAND	0.555	0.475	--	--
SUPLFS	0.995	0.995	--	--
CRUALT	0.996	0.984	--	--
LDCRUZ	0.988	0.966	--	--
SFCCRUZ	0.902	0.907	--	--
PCRZOUT	0.983	0.974	--	--
PCRZBAK	0.987	0.982	--	--
PLOITER	0.813	0.923	--	--
TURNLEE	0.617	0.637	--	--
STOFLC	0.999	0.999	--	--
ACCELT	0.877	0.899	--	--
VAPP	0.552	0.468	--	--
SUBLFS	0.974	0.971	--	--
SUBLFIN	0.995	0.997	--	--
WOS	0.925	0.999	--	--

Figure 111. ROI mission performance regressions.

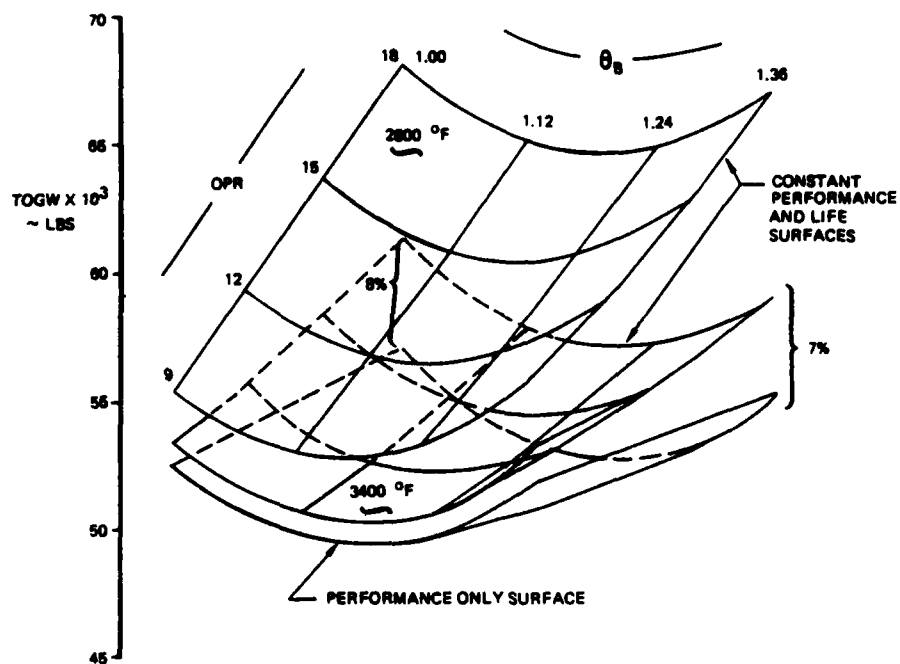


Figure 112. ROI engine cycle impact on TOGW.

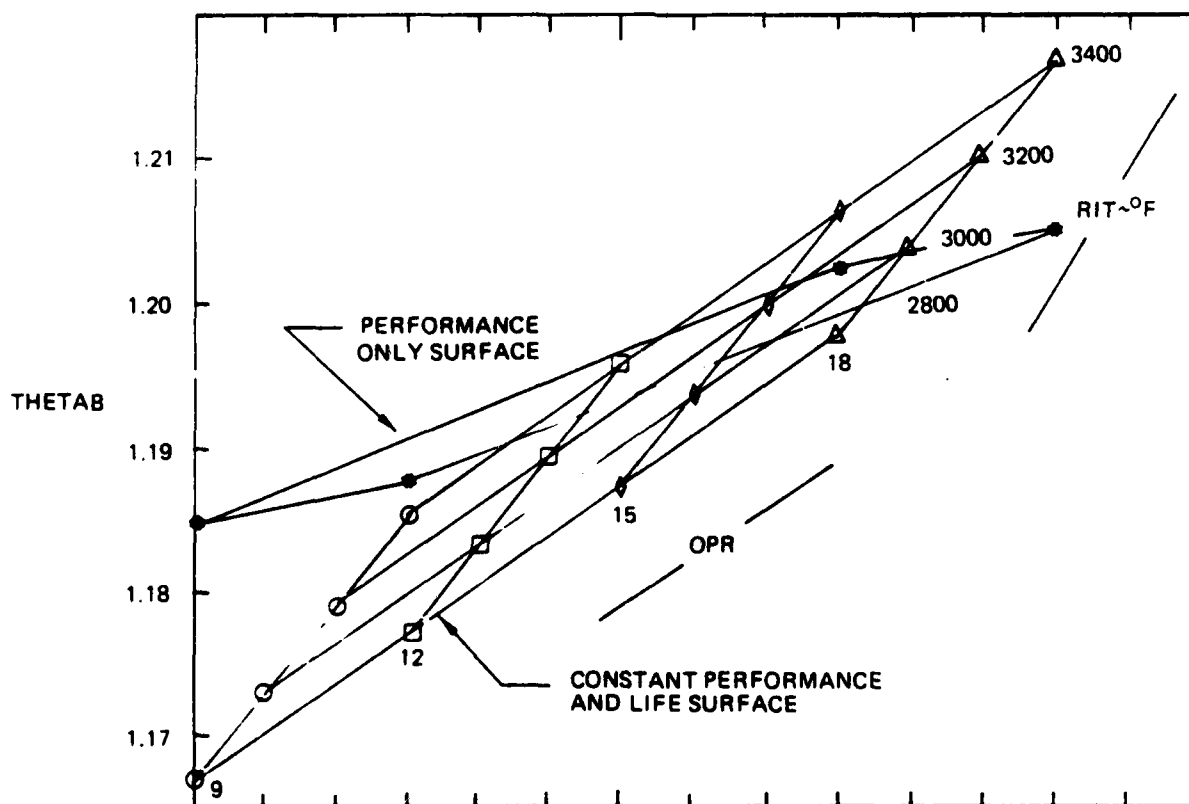


Figure 113. Comparison of optimum THETAB.

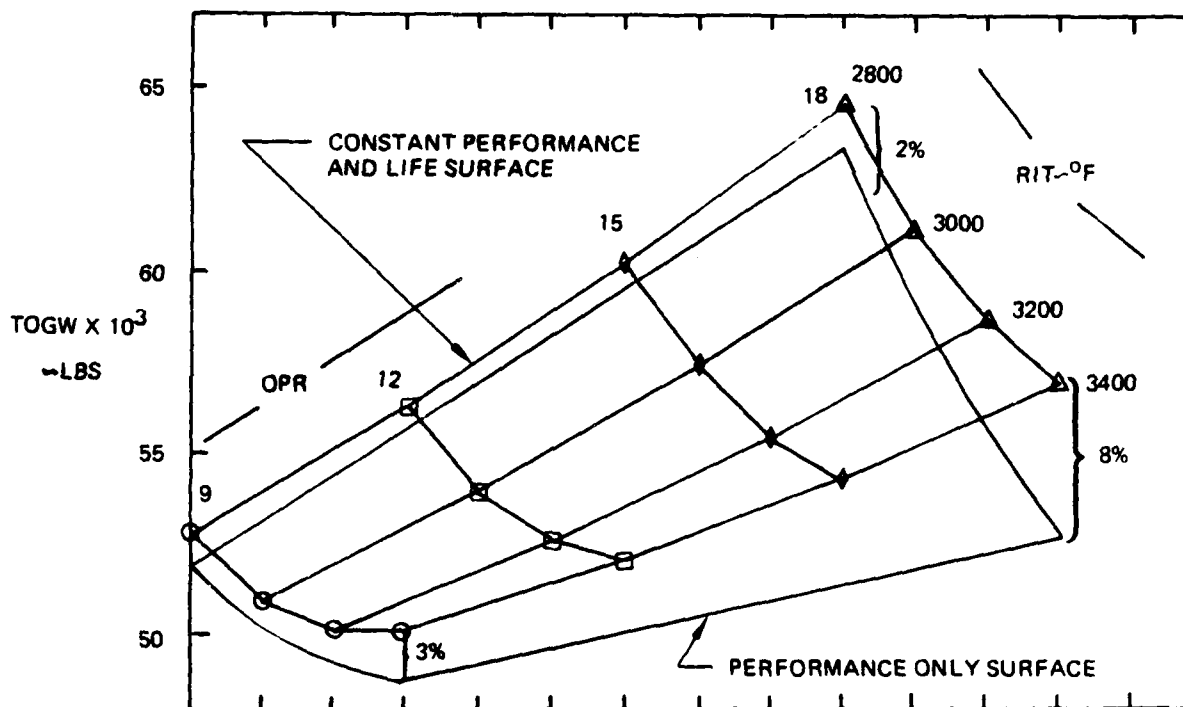


Figure 114. Minimum TOGW versus engine OPR and RIT.

Variable Name	Regression Statistic ~ R^2	Comments
CMLCFI	0.994	--
TWMLCI	0.991	--
TBTFI1	0.727	--
BMLCFI	--	Constant @ 1.0
TVTFI1	--	Discontinuous @ 0.1
TVTFI2	--	Constant @ 1.0
TBTFI2	--	Discontinuous @ 1.0

Figure 115. Regression of engine life parameters.

XIII. TASK 3.2.6--ENGINE AND AIRCRAFT DESIGN SELECTION

The selection of the optimum (minimum TOGW) system naturally follows Task 3.2.5. This selection reflects a set of consistent installed life goals and life capability requirements for the reference utilization (training mission mix). The following design variables identify this optimal system:

Engine	
R _c	9
RIT	3200°F
θ_B	1.17
Aircraft	
TOGW	50,100 lb
T/W	0.6
W/S	87
AR	2.8

The influence of the consistent life and usage criteria did impact the system selection in terms of the optimal engine definition. The Thetabreak definition was only slightly affected while the RIT selection was affected by a 200°F reduction due to a flattening of the TOGW trend with RIT. A higher RIT did not have any TOGW advantage for RITs above 3200°F. For this advanced tactical fighter system, the inclusion of consistent life and usage criteria was somewhat significant. The most important output would be the definition of the usage data and the life capability requirements with which to initiate a possible follow-on engine design.

XIV. TASK 3.2.8--DATA AND DATA FORMAT DEFINITION

Task 3.2.8 addresses the data and data format (DDF) required to start a systematic method of considering engine structural life and performance in a preliminary design tactical aircraft. The goal is to provide guidance to the Air Force in the type and level of data needed to conduct future studies of advanced engine usage and life. The DDF description that follows is broken down into engine and aircraft company inputs.

The engine company inputs for the DDF address definition of engine installed life goals, determination of life capability requirements, and engine sensitivity to the life capability requirements. Engine installed life should probably be expressed in terms of flight hours and relative to airframe structural life. Key ideas include whether on a design basis some or all engine modules are replaced (consumption of all available life capability) prior to the consumption of all of the airframe life. Therefore, engine installed life goals should be defined for all modules which have different life goals from those of the basic engine.

Realistic usage projections are extremely important for a reliable engine design to be created. Usage includes not only types of missions flown and power setting variations for each but also damaging events required for the maintenance and operation of the engine and airframe. Typical events include engine control trim operation and aircraft navigation system initialization. These events may or may not be damaging depending upon the engine/aircraft design. Another aspect of usage that is important is how engine life capability requirements are defined. Components can be designed to meet installed life goals for the least damaging usage, for the most damaging usage, or for some mix (average) usage. The wisdom of which usage design philosophy is best is dependent upon the diversity of the anticipated usage, the sensitivity of the engine design to the life capability levels, and the confidence associated with accurately predicting usage for the aircraft at the PD level. In addition, the confidence level of accurately predicting engine installed life for a complex mission also impacts the usage design philosophy.

As a guide for both the engine company and military customer, engine sensitivity data to different life capability levels could be used to assess appropriateness of engine life capability requirements. The military should participate in this judgment in the performance of a study and/or engine design. The resulting engine life capability requirements would then be available with which to initiate a follow-on engine detailed design.

The airframe company has a major responsibility for developing realistic projections of peacetime training and responsive definitions of usage characteristics for those missions.

It should be noted that a wartime (design) mission usage definition may also be required for engine life assessment. This mission can dictate turbine requirements for creep/stress rupture due to time spent at maximum power settings. However, this mission is fundamental in sizing the airplane, and its flight profile will always be available. Usage projections would have to be developed for the wartime mission.

Development of realistic peacetime training for an advanced system fundamentally requires a good understanding of how past and present training of tactical aircraft has occurred. This must include how peacetime roles of specific aircraft change with time and how such change in usage is selected. With such data a systematic approach can be taken to project an advanced tactical airplane's probable peacetime role. The data which define current usage practices already exist in a usable format. Several Air Force training manuals are in use and available which define the types of missions required to achieve desired pilot proficiencies and levels of combat capability. These manuals cover every tactical aircraft by type in the inventory. They include such information as the number of sorties in each specific mission, what the mission consists of, and how long each sortie is to be flown. The documents which cover this data are TAC 51-60, TAC 55-XX, and Syllabus. Another important source of data is actual statistical usages of aircraft by Air Force base. Such data provide insight into how operational aircraft are used versus the use of the same aircraft from training oriented bases. To better understand the details of training real time recordings of fundamental airplane characteristics are required. The minimum parameters necessary from such recordings to allow an understanding of the flight are altitude, Mach (or air speed), engine power setting, and airplane load factor. Recording rate of such parameters should be at a 1 to 2 second per point rate. This rate is generally more than adequate for understanding the mission makeup but is necessary for analyzing actual usage levels. Another extremely important piece of data which needs to accompany every recorded usage is some form of pilot report or debriefing. This piece of data is mandatory for understanding how the mission was actually flown. As an example, basic information like whether he was lead or wing in a formation, if and when terrain following occurred, when and how long an air-to-air engagement occurred, and what format was used for passes at ground targets allows a more complete use of inflight recorded data. It prevents or minimizes the guesswork that occurs in examining the time trace. The specific questions to be addressed are dependent on the type of mission being flown. A possible aid to this would be inclusions of an event marker on the recordings which would be pilot initiated (directly or indirectly) when key events occurred in the mission.

Because of the potentially large number of training missions which may be needed to adequately define peacetime usage over an airplane's life, a reference utilization needs to be defined. This reference allows a common point around which comparisons can be conveniently made as engine cycle and airplane characteristics are varied. The reference is recommended to be represented as a percentage mix of all missions which define peacetime operation. The specific percentage mix, however, is application and configuration dependent and cannot be arbitrarily defined. The method used in this contract (Task 3.2.3) provides one approach.

As mentioned earlier, inflight recordings also aid in projecting representative usages for each mission. How such data is used to build projected usages can be very engine company dependent. The format of such representative usage which is ultimately supplied to the engine company is very dependent on what the engine company's life assessment method is based on. The approach taken in this LUCID contract is probably the most universal in defining engine usage. In this contract a complete usage time history of key parameters, from engine startup to shutdown, was defined for each mission. This data format provided each parameter level on an interval of one second per point. Such a rate was felt adequate by the engine company and was supported by available

flight data. Another important factor is the tolerance level used for each parameter. Three parameters were key: altitude, Mach number, and powersetting. Each had a different accuracy level used. The range of each parameter is again in response to engine company needs. From the LUCID work with DDA, the following tolerance levels were found adequate: altitude ± 2000 ft., Mach number $\pm .03$, power setting $\pm 1\%$.

The buildup of discrete usage time histories for each training mission is recommended as the standard means of providing usage characteristics from the airframe company to the engine company. While this is more detailed than required by some engine companies, it contains all the information needed for any engine life assessment method. The specific means of building up usage time histories should be left to individual airframe company methods. However, the data should provide more than just a stick mission step-function definition of the key parameters. Some form of dynamic response, particularly of engine throttle usage, must be incorporated into appropriate segments of the missions. An example of the type of usage definition generated in this contract is provided in Tasks 3.1.4 and 3.1.5.

XV. CONCLUSIONS AND RECOMMENDATIONS

The LUCID approach to conceptual design is significant in that the minimum TOGW system definition was influenced by including an assessment of consistent life/utilization goals as well as performance goals. This process identifies life and performance tradeoffs very early in the engine design process and allows the engine designer to address both when maximum design flexibility exists. In addition, realistic usage projections are then available for follow-on detailed design efforts.

The following recommendations for potential follow-on programs are appropriate for the conceptual design arena. They incorporate utilization and life capability considerations that represent expansions of the basic LUCID approach.

- o Update methodology for turbine airfoil/TLCF models that is appropriate for Lamilloy airfoils. DDA currently has work under way to revise the TLCF methodology for Lamilloy airfoils and has plans to verify it. Upon completion of these activities, it would be appropriate to adapt this work into the LUCID framework.
- o Examine at a preliminary design level an increased number of components whose design may be influenced by engine utilization. The intent would be to address all additional important failure modes (creep) and other components from other engine modules (i.e., combustor liner/LCF).
- o Expand turbine airfoil/TLCF model data to address other base-line designs that utilize other types of cooling schemes. Some of this has already been done for the Advanced Technology Engine Studies (ATES) contract where turbine airfoil input was put together based on XT701 turbine blade and vane designs. Other blade designs are available (such as first-stage T56) to expand the range of gas temperatures covered by these base-line designs.
- o Review continuously recorded engine data as they become available to expand aircraft utilization prediction capability. LUCID addressed wingman cruise and approach mission segments, and a data base for other type mission segments needs to be created and analyzed for future predictive purposes.
- o Examine technology impact on engine characteristic trends with varying life capability. Identify which technology aspects are most sensitive to life capability variations by examining several typical materials, life capability levels, and aerodynamic designs.
- o Assess impact on optimal engine/aircraft definition due to different reference utilization. Select most damaging mission (or least damaging) as reference utilization, recompute aircraft TOGWs, and note differences in optimal system selection.
- o Expand region-of-interest to address an aircraft parameter (such as thrust loading) and assess impact of engine life/utilization on optimal airplane/engine definition. The reference aircraft utilization will thus vary within the region of interest.

- o Assess sensitivity of an engine/aircraft definition to types of changes typically encountered during a development program (such as aircraft weight growth requiring higher steady-state power settings). Modifications of the engine design to address development problems introduce life/performance tradeoffs within a limited flexibility to respond.